A HUMANIZED MODEL OF BREAST CANCER METASTASIS TO BONE REVEALING UNIQUE ROLES FOR THE PRIMARY TUMOR AND BONE MICROENVIRONMENT

A Dissertation

Submitted by

Robert Howard Goldstein

In partial fulfillment of the requirements
for the degree of

Doctor of Philosophy

in Genetics

TUFTS UNIVERSITY

Sackler School of Graduate Biomedical Sciences

May 2010

ADVISER: Michael Rosenblatt, MD

Acknowledgements

I would like to thank my advisor and mentor, Michael Rosenblatt, for his support, encouragement and guidance. I am so lucky to have learned from such an exemplary scientist and physician and I am grateful for the opportunities that I have received while in his lab. Additionally, I'd like to thank my thesis committee members Charlotte Kuperwasser, Phil Hinds, David Kaplan and Naomi Rosenberg for their guidance and advice during my graduate school years. In particular, Naomi has been a constant resource and has profoundly shaped my scientific and academic career. I also thank all of the members of the Rosenblatt lab, past and present, who have made the lab a great place to work and have made me a better scientist. I would also like to acknowledge David Kaplan and all of the members in his lab, especially Michaela Reagan, for the highly educational and productive collaboration that we have had over the past three years. I appreciate the support of the students, faculty and staff of the Genetics Graduate Program, Physiology Department and MD/PhD Program, as well as the many other students and faculty who have been instrumental in my graduate education. Finally, I want to thank my parents, my sister, and Ryan for their love, support, patience, understanding and encouragement. Together we have accomplished the work that follows.

Abstract

Approximately 200,000 new cases of breast cancer and 40,000 breast cancer deaths occur annually in the U.S., making breast cancer the most common malignancy and second leading cause of cancer death in women. Metastasis of breast cancer cells from the primary neoplasm to the bone marrow has been shown to occur in up to 70% of breast cancer cases and development of this spread to clinically detectable macrometastases signals an incurable progression of the disease. Many mechanisms behind the metastatic process still remain unclear, particularly the roles of surrounding supportive tissue, but strong evidence of a central role for stromal cells from distant locations such as the bone marrow is building. Additionally, the contribution of specific genetic changes within primary tumor cells has been studied in the context of metastasis. Recent reports have demonstrated the ability of bone marrow-derived mesenchymal stem cells (BMSCs) to diversely affect tumors of various origins, including the breast. The influence of exogenously supplied human BMSCs (hBMSCs) on tumorigenesis, proliferation, and metastasis has been extensively described, but, to our knowledge, no model has accurately demonstrated the effect of a physiologic level of hBMSCs on cancer cells. Nor have any xenograft models studied the contribution of BMSCs from a humanized bone microenvironment. Herein is demonstrated, for the first time, that hBMSCs from the bone environment can home to orthotopically implanted human breast cancer tumors and alter tumor cell proliferation and visceral and skeletal metastasis frequency. This work develops a novel model system to study the role of bone-derived cells on primary tumor growth and migration and suggests that cancer cells with different

tissue tropisms and metastatic frequencies respond uniquely to hBMSC stimulation. Additionally, using a humanized model of breast cancer metastasis to bone we have identified that over-expression of *il-17br* can serve as a marker of skeletal metastasis, and along with it's ligand, *il-17b*, can possibly mediate the response of breast cancer cells to hBMSCs and lead to increased migration and metastasis.

Table of Contents

List of Figures

List of Tables

List of Third Party Copyrighted Material

Parts of the introduction and discussion sections are based on:

Goldstein, R.H., Weinberg, R.A. & Rosenblatt, M. Of mice and (wo)men: Mouse models of breast cancer metastasis to bone. *Journal of Bone and Mineral Research* **25**, 431-436 (2010).

List of Symbols and Abbreviations

hBMSC; human bone marrow-derived mesenchymal stem cell

PTHrP; parathyroid hormone-related protein

RANKL; receptor activation of NF-κB ligand

ECM; extracelleullar matrix

TGF-β; transforming growth factor-β

BMP; bone morphogenetic proteins

FGF; fibroblast growth factor

PDGF; platelet-derived growth factor

OPN; osteopontin

RANK; Receptor activation of NF-κB

MMTV; mouse mammary tumor virus

Prkdc; DNA-dependent protein kinase catalytic subunit

CTGF; connective tissue growth factor

MMP; matrix metallo-proteinase

IL; interleukin

VEGF; vascular endothelial growth factor

HUNK; human neu-associated kinase

TNF; tumor necrosis factor

SDF-1; stromal-derived factor-1

MCP-1; monocyte chemoattractant protein-1

LL-37; leucine, leucine-37

ERα; estrogen receptor alpha

EMT; epithelial-to-mesenchymal transition

IFN-β; interferon beta

TRAIL; TNF-related apoptosis-inducing ligand

TEB; tissue engineered bone

cDNA; complimentary DNA

qRT-PCR; quantitative reverse transcription polymerase chain reaction

BCC; breast cancer cell

NOD/Scid; non-obese diabetic/severe combined immunodeficient

GFP; green fluorescent protein

H&E; hematoxylin and eosin

FACS; fluorescence-activated cell sorting

CTC; circulating tumor cell

DTC; disseminated tumor cell

Preface

The “Introduction” section is based on a review written with Dr. Robert Weinberg and Dr. Michael Rosenblatt, published in *The Journal of Bone and Mineral Research*. Chapters 2 and 3 (“Results”) are based on a submitted manuscript written with Michaela Reagan, Dr. Kristen Anderson, Dr. David Kaplan and Dr. Michael Rosenblatt. Creation of the SUM1315-BP2 breast cancer cell line and the gene array studies presented in the “Introduction,” “Results,” and Appendices A, B and C were done by Dr. Kristen Anderson prior to me joining the lab. The gene array is presented here for further understanding and was used as a base for the genetic studies presented. The work involving hBMSCs in the primary and metastatic microenvironments was done in collaboration with Dr. David Kaplan and Michaela Reagan. All of these experiments were designed and performed jointly, with Dr. Kaplan’s lab focusing on tissue-engineered bone creation and hBMSC manipulation and the Rosenblatt lab focusing on *in vivo* modeling and molecular biology analyses.

Chapter 1

Introduction

Clinical Aspects of Breast Cancer Metastasis

Approximately 200,000 new cases of breast cancer and 40,000 breast cancer deaths occur each year in the U.S. (Jermal et al., 2009). For the most aggressive breast cancers, metastasis to the bone marrow is a common endpoint; spread of breast cancer cells from the primary neoplasm to the bone marrow has been shown to occur in up to 70% of breast cancer cases (Manders et al., 2006). In many respects, metastasis to the bone is a more serious problem than the original tumor and the discovery of clinically detectable skeletal metastases signals an incurable progression of the disease (Mundy, 2002). Long before death, however, numerous other complications, both skeletal and otherwise, threaten the patient's well-being and quality of life, including fractures, disability, pain and hypercalcemia (Rubens, 1992).

Breast cancer is not unique in its tropism, nor its preference, for the skeleton. Prostate cancer, renal cell carcinoma, and multiple myeloma all have a high rate of skeletal progression. Many important discoveries have been made that have advanced our understanding and treatment of the these primary malignancies, but relatively little progress has been made in understanding the pathogenesis and effective treatment of the disseminated metastases. As of this writing, very few validated therapeutic targets have been identified in skeletal metastases, precluding efforts to discover metastasis-specific therapies. In addition to therapy for the primary neoplasm, including chemotherapy, radiation and surgical excision, patients harboring bone metastases undergo palliative measures to help alleviate any pain or disability that may arise. These treatments, which include radiotherapy, radiopharmaceuticals, bisphosphonates, and other anti-resorptive

drugs, are rarely curative and have been linked to only modest increases in time to skeletal progression and skeletal-related adverse events (i.e. increases of 6-7 months) (Coleman, 2000).

Within the skeleton, metastatic lesions are often found to correlate with the activity of the bone marrow (Kufe et al., 2003). The axial skeleton, which contains the active hematopoietic marrow, is the most common site for skeletal metastases, while relatively few metastatic foci are localized to the comparatively avascular fatty marrow. At autopsy, 70% of patients who die with underlying cancer have detectable skeletal metastases, although the majority of these are clinically silent micrometastases. Skeletal metastases from breast cancers are usually classified as osteolytic, resulting in a net loss of bone. In contrast, metastatic lesions from prostate cancer are usually described as osteoblastic and demonstrate a marked increase in bone formation. Some metastatic lesions, including those from breast cancers, have areas of both bone resorption and bone formation and are classified as mixed, or osteolytic osteoblastic, metastases.

Breast Cancer and Bone Have Many Similarities

Rather than resorbing bone directly, breast carcinoma cells within the bone must subvert the normal physiologic resorptive machinery, more specifically, the resident osteoclasts (Yoneda, 2000; Rodan, 2003; Yoneda & Hiraga, 2005). Osteoclasts, along with bone-forming osteoblasts, are involved in continuous remodeling of mineralized bone. Activation of the bone resorption process depends on the ability of breast cancer cells to secrete factors that perturb the normal interaction between osteoclasts and

osteoblasts (Webe et al, 2000; Goltzman, 2001). The resulting osteolysis releases a number of growth factors and cytokines that are normally sequestered in the collagenous matrix of the bone. This release can further stimulate the growth and survival of disseminated breast cancer cells. The breast cancer cells can themselves stimulate ever-increasing numbers of osteoclasts, resulting in a self-perpetuating "vicious cycle" (Käkönen & Mundy, 2003). Breast cancer cells secrete parathyroid hormone-related protein (PTHrP), enabling them to recruit a "shell" of osteoblasts around a metastatic colony (Yoneda, 2000; Yoneda & Hiraga, 2005; Hunt et al., 2001). The osteoblasts, by releasing receptor activation of NF-κB ligand (RANKL), stimulate the maturation of nearby osteoclast precursors into osteoclasts. The osteoclasts then resorb mineralized bone, mobilizing factors previously sequestered in the organic extracellular matrix (ECM) of the bone, among them growth factors such as transforming growth factor-β (TGF-β); TGF-β in turn stimulates PTHrP release by the tumor cells, fueling the "vicious cycle" mentioned above (Käkönen & Mundy, 2003; Chirgwin & Guise, 2000; Lindemann et al., 2001). In addition to the growth factors involved in the "vicious cycle", the dissolution of the collagenous bone matrix releases a series of trapped mitogenic and trophic factors, notably bone morphogenetic proteins (BMPs), fibroblast growth factors (FGFs) and platlet-derived growth factor (PDGF).

Stromal interactions are important and distinctive for breast cancer osteotropism. Breast cancer cells display cell surface adhesion molecules, such as the $\alpha_v\beta_3$ integrin, that bind to bone matrix proteins. Osteopontin (OPN) is an abundant component of the bone stroma, and binding and signaling of OPN through $\alpha_v\beta_3$ integrins on breast cancer cells

can block apoptosis, providing a survival advantage to breast cancer cells in the bone marrow (Sloan & Anderson, 2002; Noti, 2000). Additionally, breast cancer cells decorate themselves with bone matrix proteins, such as bone sialoprotein and OPN, enabling bone stromal cells expressing integrins to trap them and increase bone homing of breast cancer cells (Bäuerie et al., 2005; Waltregny et al, 2000; Ibrahim et al., 2000).

There are similarities between the microenvironments of primary mammary tumors and that of the bone marrow, which may contribute to the ability of breast cancer cells to survive and proliferate within the bone. Both microenvironments contain conserved stromal and basement membrane components (i.e. collagen type-I, laminin and fibronectin), as well as distinctive components; for example, many breast carcinomas express, OPN (Bellahcéne & Castronovo, 1997). Receptor activation of NF-κB (RANK) signaling is essential for both osteoclasts and mammary epithelial cells during mammary gland development (Fata et al., 2003). The transcription factor Runx2, involved in osteogenesis, is also present during breast cancer tumorigenesis (Javed et al., 2005; Barnes et al., 2004; Shore, 2005). Moreover, within the bone marrow, disseminated breast cancer cells encounter additional mitogens and other factors that normally support hematopoiesis and adult stem cells. Together, these factors in the bone environment present the disseminated carcinoma cells with an array of chemokines, growth factors, and anti-apoptotic factors, too numerous to list here, that support colonization and thus the development of macroscopic, clinically detectable, metastases (Yoneda, 2000; Yoneda & Hiraga,, 2005; Sloan & Anderson, 2002; Guise, 2000; Boyce et al., 1999; Goltzman et al., 2000; Roodman, 2003; Vogelstein & Kinzler, 2004).

Dissemination of Primary Breast Cancer Cells to the Bone

A major impediment to research on bone metastasis has been the complexity of this multi-step process. In order to disseminate from their site of origin, primary carcinoma cells must invade through the adjacent stroma and enter the blood stream or lymphatic vessels; a process termed intravasation. Hematogenous spread, which is responsible for the vast majority of life-threatening metastases, results in the deposition of cells in the microvasculature of diverse tissues throughout the body. Specific adhesion of carcinoma cells to the luminal surfaces of endothelial cells may occur in some tissues. However, a more common mechanism of dissemination and arrest likely involves the mechanical trapping of 20-30 μm diameter cancer cells in the ~8 μm-wide capillaries (Goldstein et al., 2010).

Once lodged in these vessels, carcinoma cells may begin to form a colony intraluminally and eventually rupture the microvessel around them. Alternatively, cancer cells can invade through the endothelium into the adjacent tissue parenchyma. Following this extravasation, the breast cancer cells experience a novel and quite foreign microenvironment to which they must adapt. Some may survive to form micrometastatic colonies, but very few of these will ever succeed in growing into macroscopic metastases, which, as mentioned above, herald the life-threatening phase of the disease. As many as one-third of breast cancer patients, upon clinical presentation, carry many thousands of micrometastases in their marrow, but only half of these will ever develop clinically relevant metastatic disease. This provides dramatic indication that colonization is a

highly inefficient process (Aslakson & Miller, 2002; Chambers et al., 2002; Fidler, 2003; Pantel et al., 2008).

The first observation that dissemination and subsequent growth of metastases was tissue-specific and inefficient was described by Dr. Stephen Paget in 1889 (Paget, 1989). Dr. Paget noted a nonrandom distribution of metastasis on autopsy of cancer patients, suggesting that tumor cells, "the seeds," have an affinity for the environment of certain organs, "the soil." While complicated pathways and innumerable steps have been implicated in the mechanisms of cancer cell metastasis, the basic tenant of Dr. Paget's "seed and soil hypothesis" still drives much of cancer metastasis research today.

Animal Models of Breast Cancer Metastasis to Bone

Syngeneic Models

One barrier to identifying the mechanisms of osteotropic metastasis, and thus metastasis-specific treatments, has been the lack of animal models that reflect the complex biology of skeletal metastasis in humans (Parsons et al., 2002). While some rodents develop spontaneous mammary tumors, these tumors rarely metastasize to the skeleton or resemble the human histopathology seen in breast carcinoma development. In certain strains of laboratory mice, spontaneous mammary tumors are often the result of retroviral integration of the mouse mammary tumor virus (MMTV) provirus. Despite the identification of MMTV-like sequences in clinical samples from breast cancer patients, a causal role for retrovirus integration in human mammary tumor pathogenesis has not been demonstrated (Lawson et al., 2010). Regardless, the MMTV promoter along with

other mouse mammary-specific promoters have proven to be useful experimental tools that can be used to drive tissue-specific expression of oncogenes, including genes known to be responsible for human malignancies (e.g. *erbb2/neu*, *ras*, *myc*) and other oncogenes (e.g., *pyMT*, *SV40 LT antigen*). The resulting transgenes cause rapid tumor development and, in some cases, distant metastases (Guy et al., 1992; Liney et al., 2003; Maroulakou et al., 1994; Nielsen, 1992; Sinn et al., 1987). While these models provide a platform to study oncogene-induced carcinogenesis and soft tissue metastasis within a mouse model, some rely on oncogenes that are rarely or never involved in human breast cancers (e.g., *pyMT, SV40 LT antigen*) and all of the resulting mammary tumors generate skeletal metastases at a low frequency, if at all (Hüseman & Klein, 2009).

In addition to oncogene-induced carcinogenesis and ensuing metastasis, radiation and applied carcinogenic chemicals have been used to drive mammary tumor formation and dissemination. BALB/c mice have a known polymorphism in the DNA-dependent protein kinase catalytic subunit (*Prkdc*) that, in the context of a p53 mutation, renders them susceptible to mammary tumors following ionizing radiation exposure (Yu et al., 2001; Mori et al., 2003; Backlund et al., 2001). Similar to MMTV-driven tumorigenesis, these models rarely metastasize to distant sites and almost never disseminate to the skeleton. Additionally, these models share few similarities with the clinical course or histopathology of breast cancer in humans, in part because they activate oncogene expression in inappropriate cells-of-origin in the mammary gland and express these oncogenes at supraphysiologic levels.

The 4T1 mouse model of breast cancer development and metastasis was originally

identified as a spontaneous breast cancer model in the BALB/c mouse strain (Miller et al., 1983). When implanted in syngeneic hosts, the system has been used repeatedly over the past two decades as an experimental model to study tumor development and metastasis to various organs. The parental 4T1 cell line, when injected orthotopically (i.e., into the mammary fat pad) is capable of limited and infrequent metastasis to local lymph nodes, lung, liver, brain and the skeleton, while sublines of the 4T1 line (e.g. 4T1.2 and 4T1.13) have been developed that are highly metastatic and have tropisms to specific organs, including the skeleton (Eckhardt et al., 2005). These sublines have been used to identify gene expression signatures from different stages of tumor development and metastasis. Moreover, study of the gene expression signature of 4T1 tumor cells relative to other closely related mammary tumors led to the identification of Twist, a transcription factor that serves as an important mediator of the metastatic dissemination of breast cancer cells (Yang et al., 2004).

The utility of the 4T1 and other syngeneic models as models of breast cancer pathogenesis derives in part from the fact that these tumors can be studied in immunocompetent hosts. The immunocompetence of the host mouse allows an understanding of the interactions among tumor cells, cells of the immune system, and stromal cells within the bone marrow. Recent work has demonstrated, for example, the important role of immune cells, namely T lymphocytes, dendritic cells and macrophages, in tumorigenesis and cancer progression (Siveen & Kuttan, 2009; Gabrilovic, 2004; Gallimore & Godkin, 2008; DeNardo & Coussens, 2007). Consequently, these fully competent models are useful in elucidating the functions of novel pharmacologic agents

and anti-tumor vaccines under development, and in the future, they may enable study of the contribution of various immunocytes to osteotropic metastasis (Quaglino, 2008). Unfortunately, none of these systems of studying autochthonous breast tumor formation in mice provide a robust skeletal metastasis phenotype. Further, as highlighted above, these tumors rarely resemble breast carcinomas that are commonly encountered in the clinic.

Xenograft Models

In an effort to develop models that more closely mimic breast carcinoma in humans, mouse xenograft models have been developed that use human breast cancer cell lines within an immunocompromised animal host. While these experimental models do not recapitulate all of the interactions between cancer cells and the host tissue microenvironment and immune system, their relative ease, short time to metastasis and histopathologic similarities to corresponding human tumors make them attractive models to study tumor development and bone metastasis. Initial xenograft models of skeletal metastasis utilized direct inoculation of cancer cells into the skeleton of immunocompromised mice (Wang & Chang, 1997). These models result in near 100% frequency of development of these "experimental metastases" and have been used to assess efficacy of therapeutic agents under development; such agents have been assessed, more specifically, for their ability to block breast cancer growth within the bone and breast cancer-mediated bone resorption (Neuder et al., 2003). They have also provided an *in vivo* system in which human cancer cells can be passaged through a bone

microenvironment, aiding the development of breast cancer cells that have been selected for their osteotropism and thus, generate reproducible and efficient osteotropic metastasis during subsequent rounds of growth in mice. Such cells can be used to study the genetic changes that are required for survival and proliferation of cancer cells within the bone environment (described in detail below), as well as the changes within the bone microenvironment induced by the disseminated cancer cells (Nannuru et al., 2010).

More recently, xenograft models of skeletal metastases have utilized intracardiac injection of human breast cancer cells (Kang et al, 2003). By injecting MDA-MB-231 human breast cancer cells into the left cardiac ventricle, researchers are able to circumvent trapping of cancer cells in the lung microvasculature, allowing efficient seeding of bone metastases. This model has led to the identification of novel genes that are crucial for efficient growth of tumors within the bone marrow, including *tgf*-β, *ctgf*, *cxcr4*, various matrix metallo-proteinases (MMPs), and *il-11*, all of which will be discussed in detail below (Kang et al, 2003, Yoneda et al., 1997). Additionally, the intracardiac injection model has been exploited as a laboratory model of breast cancer skeletal metastasis that is especially useful in testing novel therapeutic and even diagnostic strategies, such as the *in vivo* imaging of signaling pathways active in disseminated cancer cells (Peyruchaud et al., 2001; Canon et al., 2008; Korpal et al., 2009).

In addition to intracardiac or direct skeletal injection of breast cancer cells, some xenograft models of breast cancer pathogenesis use orthotopic injection of cancer cells, resulting in fully developed primary tumors that give rise to metastases (Price et al.,

1990). Both MDA-MB-231 and MDA-MB-435 human cancer cell lines can be injected into the mammary fat pad and give rise to metastatic breast cancers, with increased frequency of detection in the lungs, liver and lymph nodes (Li et al., 2002). MDA-MB-435 tumor tissue from these animal models, or tumor explants comprised of human cancer cells and mouse stroma, can be implanted orthotopically and have been shown to develop skeletal metastases at a near 100% frequency [1] (Hoffman, 1999). These data suggest that there are important tumor-stroma interactions at the primary tumor site that may promote metastasis to specific organs and emphasize the importance of studying orthotopic growth of cancer cells.

As useful as they are, these experimental models may fail to recapitulate more subtle aspects of the tumor-bone marrow interaction that operate in human patients. First, certain signaling interactions between cancer cells and host stromal cells may not occur properly because of inter-species signaling incompatibilities, i.e., interactions of ligands of one species with receptors of the other. Second, in the case of intracardiac and skeletal injection models, because these cancer cells do not originate from primary tumors growing in the orthotopic site, they may not undergo certain biologic modifications that metastasizing tumor cells undergo in response to signals received from the activated stroma in these tumors (Karnoub et al., 2007).

Humanized, Xenograft Models

---

[1] Recent work has shown that the MDA-MB-435 cancer cell line was originally derived from a human melanoma (Lacroix, 2009) and not human breast cancer as previously thought. Regardless, these studies demonstrate the importance of orthotopic implantation and tumor-stroma interactions in contributing to metastasis.

A model of prostate cancer skeletal metastasis was developed that was instructive for the development of comparable breast cancer models. Using intravenous administration of prostate cancer cells and an implanted human bone xenograft, researchers were able to demonstrate that human prostate cancer metastasizes to bone in both a species- and a tissue-specific manner (Nemeth et al., 1999; Shtivelman & Namikawa, 1995; Yonou et al., 2001). Similar to the intracardiac and intraskeletal models described above, the cells that metastasize to human bone in this model are not required to execute the earlier steps of the invasion-metastasis cascade, but they must express genes necessary to home specifically to human bone.

Building off the successful humanized models developed for prostate cancer, researchers have used similar techniques to develop useful breast cancer metastasis models (Kuperwasser et al., 2005; Yang et al., 2007). This novel model of breast cancer metastasis is used in our lab and utilizes subcutaneous implantation of human bone fragments followed by orthotopic injection of human breast cancer cells to monitor migration of human cancer cells from the primary tumor environment to a human bone environment (Kuperwasser et al., 2005; Figure 1-1). This model more closely follows the natural pathology of metastasis development from primary tumor growth and extravasation to homing at a distant site, and thus provides a platform to study paired tumor samples (i.e., the primary tumor and subsequent metastasis) in a controlled laboratory setting.

Additional modifications of the humanized model performed within our lab have shown that a tissue-engineered bone construct can be used as a metastasis target

following orthotopic cancer injection (Moreau et al., 2007). Using silk fibroin protein sponges as scaffolds, human bone marrow-derived mesenchymal stem cells can be seeded and differentiated towards an osteoblast lineage *in vitro*, creating a biocompatible and three-dimensional porous, silk-based, human bone-like structure (Kim et al., 2004). The silk fibroin used to create the scaffolds can be coupled with various growth factors (e.g., BMPs and VEGF) and the bone marrow-derived mesenchymal stem cells can be fluorescently-labeled for tracking or genetically manipulated to assess the contribution of specific factors within the bone microenvironment (Li et al., 2006).

In addition to recent advances in humanizing and manipulating the metastatic microenvironment described above, new findings have shown that the primary tumor stromal environment can also be at least partially humanized (Kuperwasser et al., 2004). By implanting human mammary stromal cells from reduction mammoplasties, the mouse mammary fat pad can be converted into a more humanized microenvironment, comprised of mouse and human stromal cells; these in turn should create a more hospitable microenvironment for the subsequent implantation of human mammary epithelial cells, including those of neoplastic origin. Further modifications of this model may eventually allow the complete humanization of the stromal microenvironment. While, as of this writing, this model has not been used to study skeletal metastasis, it suggests the possibility of studying the full cascade of steps required in epithelial transformation, tumorigenesis and metastasis in a fully humanized system.

A.

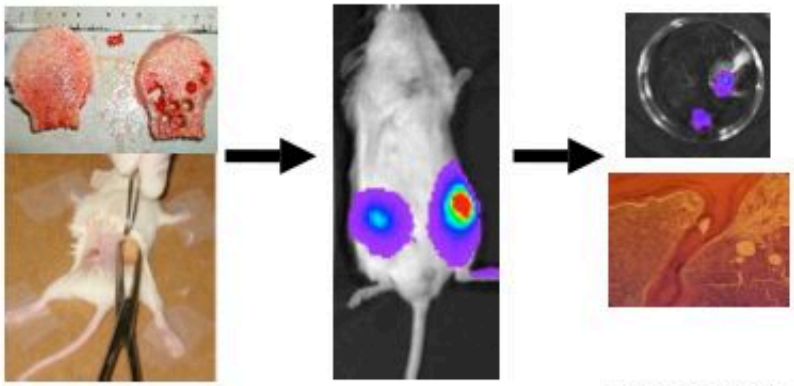

Human bone cores implanted into NOD/Scid females at 6 weeks

500K BrCa cells tagged with luciferase injected orthotopically at 10 weeks

Remove bone cores and mouse limbs to visualize metastasis by bioluminescence and histology (+10 weeks)

B.

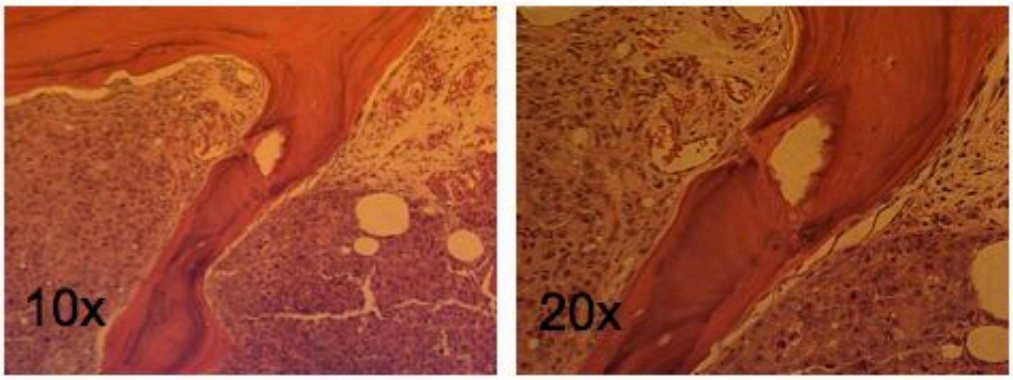

Figure 1-1. Humanized mouse model of breast cancer metastasis to bone. (A) Discarded human femoral heads from hip replacement surgeries are obtained and sliced 1-cm thick. 0.5-cm x 1-cm cores are punched out using a surgical harvester. Cores are implanted subcutaneously into the backs of 6-7 week old NOD/Scid female mice. 4-weeks later, 500,000 luciferase-tagged breast cancer cells are injected into the right and left 4th mammary fat pads. 8-12 weeks later tumor growth and metastasis are analyzed using bioluminescence and histology. (B) 10x and 20x H&E histology of a human bone core containing MDA-MB-231 breast cancer cells. Tumor cells are seen infiltrating human bone trabeculae.

Genetic Changes Involved in Skeletal Metastasis

Several efforts have been made to identify gene signatures that are prognostic of breast cancer's natural history. Using microarray analysis of tumor tissue from breast cancer patients, researchers have identified so-called "poor prognosis" signatures that identify cancers that are more likely to metastasize (van de Vijver et al., 2002; van't Veer et al., 2002). The idea that cancer cells inherently express a metastasis signature challenges the traditional model of metastasis, and suggests that the early oncogenic events that give rise to primary tumors also confer metastatic potential, rather than a later accumulation of genetic hits leading to greater instability and subsequent metastases (Weigelt & van't Veer, 2004).

In the traditional multistep model of cancer progression, only a small subset of cancer cells possess the ability to invade the surrounding tissue, intravasate into the blood-stream, survive in the circulation, extravasate at and seed a secondary site, and subsequently proliferate into a metastasis. Thus, tissue-specific metastases would arise only from a rare cell possessing a highly specific set of mutations conferring both metastatic capability and tissue tropism for a specific organ. Given that over 50% of patients with advanced cases of breast cancer have metastatic disease, this traditional explanation is less likely (Yin et al., 2005). These observations may be more easily explained by the "seed and soil" hypothesis, proposed by Stephen Paget in 1889 and described above (Paget, 1989). The specific microenvironments of the colonized organs may confer a selective advantage to certain cell types by providing a supportive niche of growth factors and chemokines.

Animal models of cancer metastasis have been used to identify conserved genetic changes that direct tissue specific metastasis of breast cancer cells. By introducing breast cancer cells via intracardiac and intravascular injections, researchers have discovered gene signatures for skeletal, lung, and brain metastasis (Kang et al., 2003; Minn et al., 2005; Bos et al., 2009). This work has demonstrated that breast cancer cells require conserved and unique gene sets in order to efficiently colonize secondary sites. Additionally, these animal model studies have confirmed some genes within the "poor prognosis" signatures discovered in human samples, as well as other prognostic gene signatures, while giving functional significance to specific genetic changes.

With respect to bone, Kang et al. isolated four genes, which appear to help shape the metastatic phenotype observed: *interleukin-11* (*il-11*), *connective tissue growth factor* (*ctgf*), *matrix metallo-proteinase 1* (*mmp-1*), and the chemokine receptor *cxcr4*. When these genes were co-expressed, individually or in concert, along with *osteopontin* (*opn*) within the MDA-MB-231 human breast cancer cell line, an increase in the metastatic phenotype was observed. The five genes described above fall into four functional classes: (i) homing (*cxcr4*), (ii) invasion (*mmp-1*), (iii) angiogenesis (*ctgf*), and (iv) osteolysis (*il-11, opn*). Kang et al. proposed that the elevated expression of genes within these distinct classes enables tumor cells to invade, colonize and destroy the bone matrix, releasing stored growth factors, such as TGF-β, and establishing a positive feedback cycle. TGF-β has been demonstrated to be the central factor in the vicious cycle of bone metastasis, as described above (Guise et al., 2006).

Using the humanized model of breast cancer metastasis to human bone, a similar

genetic analysis revealed genes that are up-regulated in human breast cancer cells cultured within human bone. The human SUM1315 breast cancer cell line was used to create a human bone-passaged subline, SUM1315-BP2 (Figure 1-2). Using microarray analysis, four metastasis-related genes were identified: *interleukin-17b* (*il-17b)* and its receptor *interleukin-17b receptor* (*il-17br*), *human neu-associated kinase* (*hunk*), and *matrix metallo-proteinase-13* (*mmp-13*) (Figure 1-2; Table 1-1; Appendices A, B and C). While unique in identity from the genes discovered using the intracardiac injection model and the MDA-MB-231 human breast cancer cell line, these genes fall within the functional classifications outlined above, i.e., invasion (*mmp-13*), angiogenesis (*hunk*), and homing and osteolysis (*il-17b, il-17br*).

Each of the genes identified in the above microarray analyses can be implicated in osteotropic breast cancer homing and expansion. Along with PTHrP and other interleukins, IL-11 plays an important role in stimulating osteoclast development and driving bone resorption (Manolagas, 1995). It is difficult to tease out the specific role of IL-11 in the context of other physiologically relevant stimulators (e.g. IL-1, IL-6, PTHrP, and TNF), but in the context of metastatic breast cancer cells within an intracardiac injection model, over-expression of *il-11* along with *opn* significantly increases the frequency of metastasis, possibly through an increase in osteolysis (Kang et al., 2003). Similarly, IL-17B, the ligand for IL-17BR, has a documented role in bone resorption and osteoclast development, and has been linked to tumor progression (Yago et al., 2009; Jung et al., 2009).

The growth factor CTGF is a member of the CCN gene family of growth factors

that is activated by a variety of microenvironment signals, including TGF-β (Moussad & Brigstock, 2002). Through its role in remodeling the extracellullar matrix, CTGF is able to drive neovascularization and tumor progression. Similarly, HUNK was identified as a SNF1-related protein kinase that plays a role in mammary gland development and is required for efficient breast cancer metastasis, possibly through it's ability to remodel the extracellular matrix and promote motility (Gardner et al., 2000; Wertheim et al., 2009).

Matrix metallo-proteinases (MMPs) are capable of degrading extracellular matrix proteins and, through their degradation products, can induce cancer cell growth, differentiation, and migration as well as angiogenesis (Egebald & Werb, 2002). Of the more than twenty eight different MMPs, MMP-1 and MMP-13 share a large amount of similarities. Both MMP-1 and MMP-13 are collagenases, capable of breaking down the abundant extracellular protein within the bone matrix. Additionally, their transcription is repressed by the tumor suppressor p53, and can be dysregulated in the context of cancer growth (Sun et al., 1999; Sun et al., 2000).

Chemokines were first discovered in the context of leukocyte and hematopoetic cell trafficking, but have subsequently been shown to play a large role in cancer cell homing (Müller et al., 2001). The chemokine receptor *cxcr4* is highly expressed in breast cancer cells, and its ligand, CXCL12, is found in the sites of breast cancer cell dissemination, including bone. Among other roles in tumor progression, CXCR4 has a well documented role in breast cancer metastasis (Burger & Kipps, 2006). Neutralization of this cascade can block metastasis, and over-expression of the *cxcr4* receptor leads to an increase in metastasis frequency (Müller et al, 2001; Kang et al., 2003).

OPN is a secretory protein that is found in the bone marrow and matrix and, as described above, can stimulate breast cancer cells and signal through integrins, blocking cell death and providing breast cancer cells with a growth advantage while in the bone marrow (Sloan & Anderson, 2002; Noti, 2000). Additionally, breast cancer cells express OPN, allowing them to be trapped by receptor-expressing cells within the bone matrix and mediating tumor-cell homing to the bone (Bäuerie et al, 2005; Waltregny et al, 2000; Ibrahim et al., 2000). In combination with some of the genes described above, over-expression of *opn* drives metastasis and increases the incidence of skeletal metastases within an intracardiac injection model (Kang et al, 2003).

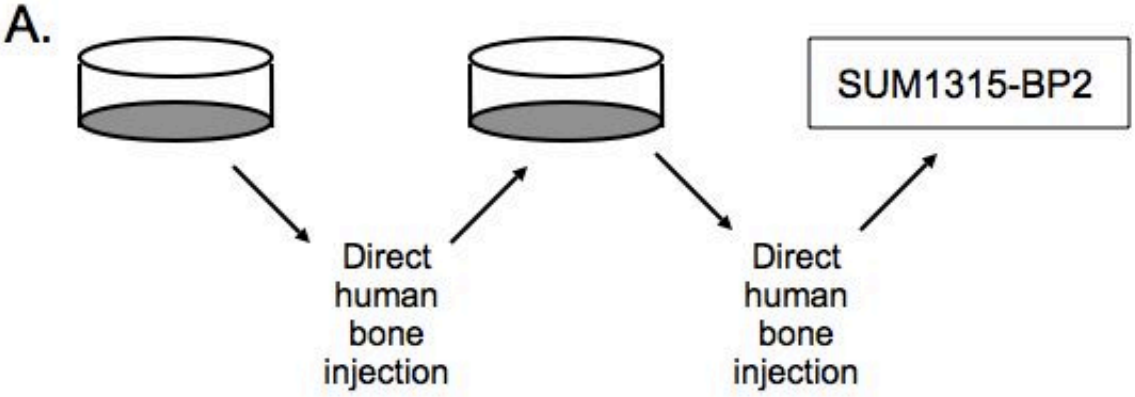
A.
SUM1315-BP2
Direct human bone injection
Direct human bone injection

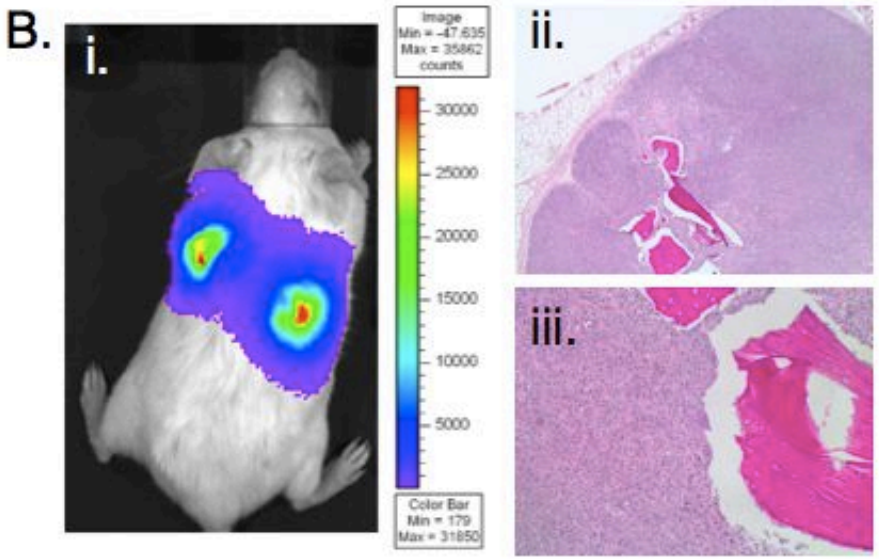
B.
i.
ii.
iii.
Image
Min = -47.635
Max = 35862
counts
30000
25000
20000
15000
10000
5000
Color Bar
Min = 179
Max = 31850

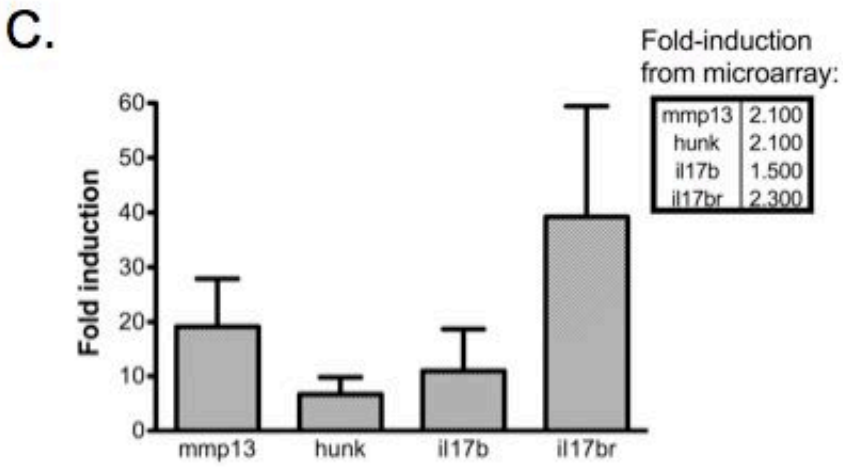
C.
Fold-induction from microarray:
mmp13 2.100
hunk 2.100
il17b 1.500
il17br 2.300
Fold induction
60
50
40
30
20
10
0
mmp13
hunk
il17b
il17br

Figure 1-2. Creation of the SUM1315-BP2 human bone-passaged breast cancer cell line. (A) SUM1315 cells were directly injected into human bone cores implanted subcutaneously into the flanks of NOD/Scid female mice. The cells were allowed to grow for 12 weeks, isolated, cultured *in vitro* and expanded. This "SUM1315-BP1" line was again directly injected into human bone implanted into the flanks of NOD/Scid female mice and allowed to grow for 12 weeks. The resulting cells were named SUM1315-BP2. (B) i. Xenogen imaging of luciferase-expressing bone-residing tumor from direct-injection of SUM1315 human breast cancer cells into human bone implant; ii. 40x, iii. 100x H&E stains of SUM1315-BP2 cells within the human bone cores. Tumors were allowed to grow for 12 weeks before removal, and tumors outgrowing bone implant area were used for microarray analysis. (C) Four genes were confirmed for over-expression from the RNA used for gene array analysis between mammary fat pad residing SUM1315 breast cancer cells and bone residing SUM1315-BP2 cells. Data are represented as mean ± SEM. Inset table references fold-induction found on microarray analysis comparing SUM1315-BP2 and SUM1315 cells (see Table 1; Appendix A).

Table 1-1

Down-Regulated (Fold)	Up-regulated (Fold)
VAV2 (1.4)	MMP13 (2.1)
RAD51C (1.4)	MAPKKKK4 (1.4)
MAPKKK3 (1.5)	AGT (1.5)
RAB27A (1.4)	FGB (1.9)
MAPK-activated protein 2 (1.5)	Caspase 7 (1.4)
DLK (1.4)	Cathepsin F (1.4)
HSPA5 (1.8)	TNFAIP6 (1.6)
ST5 (2.5)	Integrin Alpha X (1.7)
FGFRL1 (1.6)	FOXH1 (1.9)
COL1A2 (1.9)	Thrombospondin 3 (1.8)
Cathepsin W (1.4)	EpoR (1.5)
PAX6 (1.6)	MUC1 (1.4)
TRADD (1.4)	CEBPB (2.5)
SENP3 (1.6)	HUNK (2.1)
ABL1 (1.7)	IL17B (1.4)
WNT-1 (1.6)	IL17BR (2.3)
WIT-1 (1.4)	FGF (1.4)

Table 1-1. Candidate genes related to breast cancer cell growth and bone metastasis. Genes were found in gene array comparing primary SUM1315 breast cancer cells from the mammary fat pad with SUM1315-BP2 breast cancer cells from the bone environment. Fold up- or down-regulated is in parenthesis.

Role Of Bone-Derived hMSCs In Breast Cancer Metastasis

Many mechanisms behind the metastatic process still remain unclear, including the genetic alterations that may signal or lead to metastasis, but strong evidence is beginning to accumulate that shows a central role for stromal cells from distant locations, such as the bone marrow, in driving breast cancer metastasis (Karnoub et al., 2007; Rhodes et al., 2009; Molloy et al., 2009). Human bone-derived mesenchymal stem cells (hBMSCs) are pluripotent adult stem cells that are able to differentiate into pericytes, chondrocytes, osteoblasts and adipocytes (Lazennec & Jorgensen, 2008). Through interactions with hematopoietic stem cells, hBMSCs are able to promote differentiation and hematopoiesis, as well as immunosuppression; these functions may lead to the ability of hBMSCs to direct tumor growth and metastasis (Majumdar et al., 2000; Lazennec & Jorgensen, 2008).

Initial studies of hBMSCs were done in healthy animals and demonstrated that hBMSCs can home randomly to many organs and are rapidly cleared (Lazennac & Jorgensen, 2008; Kidd et al., 2009). When introduced into an experimental system harboring cancer or chronic inflammation, hBMSCs demonstrated disease-specific homing (Zappia et al., 2005; Houghton et al., 2004). Further work has demonstrated that this site-specific homing is found for many types of cancers, including breast carcinomas (Karnoub et al., 2007). The above experiments have relied on inoculation of large amounts of hBMSCs within the experimental system, either though direct subcutaneous injection or intravascular introduction, and it has been difficult to document efficient specific migration in human subjects (Lazennec & Jorgensen, 2008). No unique, universal label has been identified for hBMSCs and it is unclear if the cells retain their

pluripotent phenotype and cell surface characteristics once they arrive at the primary tumor, or if they differentiate into tumor-associated fibroblasts or myofibroblasts as they interact with cancer cells and other stromal factors (Lazennec & Jorgensen, 2008; Spaeth et al., 2009). Tagging of hBMSCs with fluorescent proteins, luciferase expression vectors, and other labels has allowed detection of these cells within experimental systems, but detection within human subjects and samples remains a challenge (Kidd et al., 2009; Loebinger et al., 2009).

While repeated studies have shown that hBMSCs can migrate to primary tumors *in vivo*, the chemotactic or attracting factors have not been fully defined. In these settings, hBMSCs can migrate in response to stromal-derived factor-1 (SDF-1), platelet-derived growth factor (PDGF), monocyte chemoattractant protein-1 (MCP-1), and interleukin 8 (IL-8), among others (Lin et al., 2008). It is possible that different breast tumors recruit hBMSCs at different frequencies due to their ability to secrete these, and other, chemotactic factors. MDA-MB-231 and MCF7 breast cancer cells secrete both vascular endothelial growth factor (VEGF) and fibroblast growth factor 2 (FGF2), which may interact with the VEGF- and FGF2-receptors present on hBMSCs. Blockade of these growth factors abrogates *in vitro* migration of hBMSCs towards breast cancer cells (Ritter et al., 2008). Additionally, MDA-MB-231 cells secrete cyclophilin B and hepatoma-derived growth factor, two chemotactic peptides that promote hBMSC migration to breast cancer cells *in vitro* (Lin et al., 2008). Some ovarian cancer and breast cancer cells secrete leucine, leucine-37 (LL-37), a known chemotactic factor. *In vivo* studies have shown that neutralization of this protein can block hBMSC migration to

ovarian tumors. Further, LL-37 stimulation of hBMSCs leads to increased angiogenesis *in vivo*, suggesting a possible dual role for LL-37 in mediating hBMSC chemoattraction and stimulation (Coffelt et al., 2009).

Once at the primary tumor, the affect of hBMSCs on breast cancer tumors is mixed. While some reports have shown little or no affect of hBMSCs on breast cancer cell growth both *in vitro* and *in vivo*, recent reports have identified a significant proliferative response of breast cancer cells to hBMSC co-culture (Lazennac & Jorgnesen, 2008). Further, proliferative responses appear to vary when analyzed *in vitro* and *in vivo*, in 2- or 3-dimension culture, or depending on the hormone-receptor status of the breast cancer cells (Ramasamy et al., 2007). For example, estrogen receptor alpha (ERα) positive breast cancer cells respond to hBMSC-derived IL-6 and activate STAT3 phosphorylation driving proliferation; no STAT3 activation or increase in proliferation was observed for ERα negative breast cancer cells (Sasser, 2007). Other factors may also contribute to the growth kinetics observed with hBMSC and breast cancer co-culture, including immunosuppressive and pro-angiogenic factors secreted by hBMSCs. For example, hBMSCs secrete VEGF decoy receptor, tsFlk-1. Truncation of this protein abolishes the proliferative affect of hBMSCs on lymphoma cells (Kyriakou et al., 2006).

Beyond their role in affecting tumor growth, hBMSCs have been reported to influence other tumor characteristics. Cancer cells respond to hBMSC stimulation *in vitro* with increased motility and invasion and, recently, it was shown that hBMSC co-culture *in vivo* can increase breast cancer metastasis to the lung (Dittmer et al., 2009; Karnoub et al, 2007). MDA-MB-231 breast cancer cells co-injected with hBMSCs

demonstrated a significant increase in lung metastasis frequency that was mediated by secretion of Rantes (CCL5) from hBMSCs and stimulation of the receptor CCR5 on breast cancer cells (Karnoub et al., 2007). Strikingly, this pro-invasive stimulation was not permanent; when metastatic MDA-MB-231 breast cancer cells were re-introduced into the mouse without hBMSC co-inoculation, no sustained increase in metastasis was observed. Additionally, the hBMSCs did not migrate with the breast cancer cells and were not found in the lung metastases, suggesting that their influence is transient and limited to the primary microenvironment. hBMSCs have also been shown to induce an epithelial-to-mesenchymal transition (EMT) of breast cancer cells in a cell-contact dependent manner (Martin et al., 2010). EMT induction may be yet another way that hBMSCs drive metastasis of breast cancer cells.

Because of their ability to home to tumors, hBMSCs have been utilized as a method for therapeutic delivery. The first study to use hBMSCs as a therapeutic used adenoviral expression of human interferon beta (IFN-β) to slow the growth of MDA-MB-231 breast cancer cells and A375SM melanoma cells (Studeny et al., 2004). IFN-β-expressing hBMSCs were able to decrease tumor growth and increase overall survival. Further studies showed that hBMSCs can be engineered to express TRAIL and IL-12 and can slow tumor progression and metastasis (Chen et al., 2008; Loebinger et al., 2009). Given the mixed interactions of hBMSCs with breast cancer cells presented above and the potential for stimulation of cancer growth and dissemination, it will be important to use caution before proceeding with further clinical applications of hBMSCs as therapeutics.

Chapter 2

Materials and Methods

Cell Culture

All cells were cultured as described previously or according to the ATCC (Moreau et al., 2007; Kuperwasser et al., 2005; Liu et al., 2009; Kang et al., 2003). All breast cancer cell lines expressed the firefly-luciferase reporter gene. SUM1315 cells were obtained from S. Ethier and used to create the SUM1315-BP2 cell line. Both were cultured in Ham's F12 (Gibco) supplemented with 5% FBS, 5 μg/ml Insulin (Sigma), 10 ng/ml epidermal growth factor (Sigma) and 100-units/ml penicillin/streptomycin (Gibco). MDA-MB-231 and BoM2 cells were obtained from J. Massagué and cultured in RPMI 1640 (Gibco) supplemented with 10% FBS and 100-units/ml penicillin/streptomycin (Gibco). MCF7 cells were obtained from M. Forgac and grown in DMEM (Gibco) supplemented with 10% FBS and 100-units/ml penicillin/streptomycin (Gibco). Human bone marrow-derived mesenchymal stem cells were isolated from healthy adult males and cultured in DMEM (Gibco) supplemented with 10% FBS, 0.1 mmol/L non-essential amino acids (Gibco), 1 ng/ml basic fibroblast growth factor (Sigma) and 100-united/ml penicillin/ streptomycin (Gibco). Human bone marrow endothelial cells (hBME) were grown in DMEM (Gibco) supplemented with 10% FBS and 100-units/ml penicillin/streptomycin (Gibco). Human pre-osteoblast cells (hFOB1.19) were obtained from the ATCC and cultured in 1:1 Ham's F12 without phenol red (Gibco) supplemented with 10% FBS, 2.5 mM L-glutamine (Sigma), 0.3 mg/ml G418 (Invitrogen) and 100-units/ml penicillin/ streptomycin (Gibco). hFOB1.19 are cultured at 33.5°C to accelerate proliferation; the temperature is raised to 37°C to induce osteoblast differentiation. Human pre-osteoclast cells (FLG 29.1) were derived from a culture of bone marrow cells collected from a

patient with acute monoblastic leukemia (Gattel et al., 1992). The cells are cultured in RPM1 1640 (Gibco) supplemented with 10% FBS, 300 μg/ml L-glutamine (Sigma), 50 μg/ml G418 (Invitrogen) and 100-units/ml penicillin/streptomycin. Differentiation into mature osteoclasts was achieved by addition of 10 μM TPA (Sigma).

Humanized Model of Breast Cancer Metastasis to Human Bone

The Tufts University Department of Laboratory Management and Institutional Animal Care and Use Committee approved all animal experimental procedures. Experimental procedures for the humanized model of breast cancer metastasis to bone, including bioluminescent imaging of primary tumors and organs harboring metastases, were similar to the methods described previously (Kuperwasser et al., 2005; Moreau et al., 2007; Liu et al., 2009) (Figure 1-1). All human bone tissue was obtained from the New England Baptist Hospital or Tufts Medical Center and was done in compliance with NIH and institutional guidelines, including Institutional Review Board approval. Human bone was isolated from discarded femoral heads from unidentified patients undergoing total hip replacement surgery. Bone was cut into 1-cm discs on a table-top bone saw. A bone harvester (MiTek) was used to core 1 x 0.5-cm bone fragments, which were implanted into the right and left dorsal flanks of an anesthetized 6-8 week old female NOD/Scid mouse. The bone implants were allowed to engraft for 4 weeks prior to tumor inoculation into the mouse.

Orthotopic injection of breast cancer cells was performed on anesthetized mice. 500,000

breast cancer cells were resuspended in diluted Matrigel 1:3 (BD Biosciences) and injected in a volume of 20 µl/mammary fat pad (4th, right and left). Tumors were monitored twice weekly and animals were sacrificed when tumors reach >1.5 cm in diameter, or 10 weeks after initial tumor inoculation.

Primary tumors and metastases were detected via bioluminescent imaging using the Xenogen 2000 and IVIS software. Mice were given intraperitoneal injections of luciferin (100 µl of 1 mg/ml; Molecular Probes). After 10 minutes, animals were anesthetized and imaged. At the conclusion of the experiment mice were euthanized (CO_2 inhalation) and implanted bone fragments, lungs, livers and mouse hind limbs were removed for imaging and detection of metastasis. All images were standardized through IVIS software to photons/second/cm_2.

SUM1315-BP2 Creation and Isolation

A bone variant of the parental SUM1315 breast cancer cell line was generated through *in vivo* serial passage by injection into human bone grafts implanted in female NOD/Scid mice, as depicted in Figure 1-2. One million SUM1315 BCCs in a volume of 50 µl of growth medium were injected directly into the cylindrical fragments of human trabecular bone implanted subcutaneously into NOD/Scid mice using a 22-gauge needle attached to a Hamilton syringe. Bone grafts were harvested at 3-4 months, or after tumor became palpable, outgrowing the bone implant. Tumor cells were isolated either manually or through collagenase digestion from bone tissue and cultured.

Tissue Engineered Bone Constructs

Hexa-fluoro-isopropanol silk fibroin scaffolds (17% wt/wt) were created and seeded with hBMSCs as previously reported (Moreau et al., 2007) with the following modifications. Silk scaffolds were sized 8-mm in diameter and 4-mm in height, contained pores of 500-600 μm, and were autoclaved for sterilization. Scaffolds were soaked overnight in hBMSC media in 6-well plates before seeding, then aspirated until moist, and seeded with 20 μL of single cell suspensions. Scaffolds received 1 million P2-hBMSCs for an initial 2 weeks of static, *in vitro* differentiation in osteogenic media. Scaffolds were then seeded with 1 million freshly labeled P3-hBMSCs from the same bone marrow donor. For each seeding, cells were allowed to adhere to the moist, absorbent scaffolds for 1-2 hours before fresh hBMSC growth media was applied to cover the scaffolds. The day following the second seeding, tissue engineered bone samples were implanted.

Osteogenic differentiation media has been previously described (Moreau et al., 2007) and consists of high glucose DMEM supplemented with 10% FBS, 0.1 mmol/L NEAA, 100 units/mL penicillin/streptomycin, 100 nmol/L, dexamethasone, 0.05 mmol/L ascorbic acid-2-phosphate, and 10 mmol/L β-glycerophosphate. BMSC adipogenic differentiation media used has also been previously described (Mauney et al., 2005). Briefly, this consists of high glucose DMEM, 10% FBS, 100 units/mL penicillin/streptomycin, 0.1 mm NEAA and the following adipogenesis inducers: 0.5 mm 3-isobutyl-1-methyl-xanthine (Sigma), 1 μm dexamethasone (Sigma), 5 μg/ml insulin, and 50 μm

indomethacin (Sigma). For 2D *in vitro* validation of differentiation, hBMSCs were grown to 100% confluency and differentiated into adipocytes or osteoblasts on tissue-culture plastic for 4 weeks using the above differentiation medias. Non-differentiated, confluent hBMSCs were used as negative controls. Oil Red-O staining was performed to measure adipocyte differentiation by fixing the cells in 4% neutral buffered formalin for 12 hours, rinsing with 60% isopropanol for 30 minutes at room temperature, and staining for 30 minutes with a 0.2-μm filtered 60% Oil Red-O solution in PBS (Sigma). The stain was removed and the cells washed with PBS for 2 hours. hBMSC calcium deposition was measured using an alizarin red staining assay. Cells were fixed in 4% neutral buffered formalin for 15 minutes and then rinsed twice with water. 0.5 mL of 2% alizarin red solution (Sigma) was placed on the cells for 10 minutes and then rinsed with PBS until clear.

In Vivo Migration of hBMSCs to Primary Tumors

For *in vivo* migration of hBMSCs (Figure 2-1), 0.5 million breast cancer cells in 20 μl of a 1:2 (vol:vol) Matrigel (BD Biosciences):PBS mixture were injected into the right and left 4th mammary fat pad of 10-week old NOD/Scid female mice. Mice were anesthetized during the procedure using isofluorane inhalation. Tissue engineered bone (TEB) constructs (described above) were implanted subcutaneously over the left shoulder 2-weeks later through a dorsal incision of ~7 mm. Animals were monitored daily over the course of 10 days. 2-weeks after TEB implantation, mice were sacrificed and the primary tumors and engineered bone fragments were removed for confocal imaging or

FACS analysis.

Histology

Bone implants, hind limbs, lungs, livers, primary tumors, and other samples were preserved for histology either in 10% neutral-buffered formalin or frozen in OCT at -80°C. Formalin fixed samples were transferred to cassettes. Calcified bone samples were decalcified in 8% formic acid solution for 48-hours. All formalin fixed samples were stored in 70% ethanol until paraffin embedding. Paraffin embedding and cross-section cuts were performed by Tufts Medical Center. Samples were stained with H&E, Masson's Trichrome, von Kossa or antibodies to GFP and mounted for light microscope visualization. Primary tumor and engineered bones used for confocal imaging were frozen and embedded in OCT (Tissue-Tek). Samples were stored at -80°C until cut into 10-50 μm sections on a Reichert-Jung Cryocut 1800. Samples were placed on SuperFrost Ultra Plus adhesion slides (ThermoScientific) and incubated in a 100 μM DAPI (Invitrogen) solution for 30 minutes and rinsed before imaging.. Confocal imaging and multiphoton imaging of DiI, DiD and DAPI was done using a Leica DMIRE2 confocal microscope and image merging was done using Leica Confocal Software Lite.

Primary Tumor Digestion and FACS Analysis

Primary tumors were removed from mice and put in sterile PBS on ice until ready for digestion. Tumors were minced with a razor, resuspended in DMEM:F12 supplemented with 5% FBS, 5 μg/ml insulin, 1 μg/ml hydrocortisone (Sigma), 10 ng/ml epidermal

growth factor (Sigma), 100 units/mL penicillin/streptomycin, 1.5 mg/ml collagenase (Sigma), and 20 µg/ml DNase (Roche), and rotated for 3 hours at 37°C. Cells were pelleted and resuspended in RBC lysis buffer (Sigma) for 2 minutes. Cells were then re-pelleted and suspended in Trypsin-EDTA (0.05%) (Gibco) for 10 minutes at 37°C. Finally, cells were filtered through a 70-µm nylon strainer and resuspended in sterile PBS. FACS analysis was performed on a Moflo Cell Sorter (Beckman-Coulter). Data was analyzed using FloJo Software v. 7.5.4.

RNA Isolation, Gene Microarray Analysis and qRT-PCR

Total RNA was extracted from frozen tumor tissues and bone fragments by homogenization in TRIzol reagent (Invitrogen) according to manufacturer's instructions. RNA was quantified using NanoSpec (ThermoFisher) and stored at -20°C until use. For gene microarray analysis, complementary DNA (cDNA) was synthesized and hybridized at the Tufts Medical Center Microarray Core to an Operon 70-mer 2.1 with 2.1 upgrade human genome set array chip, consisting of 27-mer oligos of 26,791 human genes. Transcriptional profiles were analyzed using GeneSpring. ANOVA was run using a parametric test with the p- value cutoff 0.05 to select for genes that were significantly up- or down-regulated by greater than 1.4-fold.

Gene expression was confirmed using qRT-PCR analysis. Primers were designed using PrimerBank (Harvard Medical School; http://pga.mgh.harvard.edu/primerbank/) (Table 2-1). cDNA was prepared from 100 ng RNA using the iScript cDNA Synthesis Kit

(BioRad). The qRT-PCR assays were performed on the iCycler iQ Real-Time PCR Detection System using the iQ-SYBR Green Supermix (BioRad) according to manufacturer's instructions.

Western Blots

Cells were cultured to confluence, pelleted, and stored at -80°C until use. Whole cell extracts were obtained using M-Per (Pierce) and cytoplasmic and membrane fractions were obtained using Mem-Per (Pierce), according to the manufacturer's instructions. Protein quantification was done using a Bradford Assay (Bio-Rad) and a fresh standard curve was created for each assay with BSA. Protein was denatured at 80°C for 20-40 minutes with β-mercaptoethanol and 4x loading dye. Denatured protein was run on a 4-12% Bis-Tris Gel (Invitrogen). Proteins were transferred to PVDF membranes. Membranes were blocked in 4% powdered milk in TBS-T. All antibodies were diluted into 2% powdered milk in TBS-T. Antibodies used are presented in Table 2-2.

Collection of Conditioned Media

Conditioned medias were derived by culturing cells to 80% confluence in growth media and then switching to serum free media (CellGro Complete Media; Mediatech). Cells were cultured for 48- or 72- hours and the conditioned media was removed and spun at 2000 RPM for 10 minutes to pellet cells. Conditioned media was decanted from the pellet and stored at -80°C until use. For breast cancer cell response to bone cell conditioned media assays, breast cancer cells were cultured in 96-well plates (4000 cells/

well) for 24-hours in growth media and then changed to conditioned media from different bone-derived cell types for 48-hours. Cell proliferation was measured using an MTT-based assay (Roche) as described below.

Cell Proliferation Assays

Cells were grown to 80% confluence and then serum-starved for 18-24 hours in CellGro Complete Media (Mediatech). Cells were harvested and plated in 96-well plates (4,000 cells/well). Cells were grown in either growth media, conditioned media, or media supplemented with rh-IL-17B. Cell proliferation was measured using an MTT-based proliferation assay (Roche) according to the manufacturer's protocol.

Cell Migration Assays

Cancer cells or hBMSCs were grown to 80% confluence and then serum-starved for 18-24 hours. Cells were either serum starved in CellGro Complete Media (Mediatech) or serum-free conditioned media. Cells were harvested and plated on the top well of transwell plates (Neuroprobe, Corning, Millipore or Trevigen/Cultrex) and migration was assessed according to the manufacturer's protocol. Cells were allowed to migrate for 6-hours towards conditioned media or media supplemented with 10% FBS, depending on the assay. Migration was quantified either by cell staining (DiffQuick; IMEB) or fluorescence (Cultrex).

TGF-β1 and IL-17B Stimulation, Inhibition, and Quantification

For TGF-β1 stimulation, 32 ng/ml of recombinant human TGF-β1 (R&D Systems) was added to the bottom well to attract migration. For TGF-β1 inhibition, 60 µg/ml of polyclonal α-TGF-β1(R&D Systems) was incubated at room temperature with samples for 30 minutes before samples were added to bottom wells and migration was initiated. Total TGF-β1 levels in BCC conditioned media were measured by ELISA (eBioscience) according to the manufacturer's instructions. For migration and proliferation assays involving IL-17B stimulation, recombinant human IL-17B (R&D Systems) was diluted according to the manufacturer's directions and was added to the breast cancer cells at a concentration of 10, 20, 50, or 100 ng/mL prior to cell seeding.

***il-17br* Over-Expression**

A plasmid containing the IL-17BR cDNA was obtained from PlasmID (Harvard Medical School; http://plasmid.med.harvard.edu/PLASMID/). The cDNA was cloned into pLenti6.2/V5-DEST (Invitrogen), used to create lentivirus particles and infect SUM1315 and MDA-MB-231 breast cancer cells according to the manufacturer's directions. Briefly, the pLenti6.2/V5-DEST plasmid was cotransfected with ViraPower Lentiviral Gateway Packaging Vectors (Invitrogen) into 293FT cells using Lipofectamine (Roche). pLenti6.2/V5-DEST containing no cDNA insert was used as a mock infection control. Viral supernatant from the 293FT cells was collected after 72-hours and filtered through a sterile 0.4-µm filter onto 60% confluent SUM1315 and MDA-MB-231 cancer cells with polybrene (Sigma). After 4-hours, the viral supernatant was removed and replaced with growth media. After 48-hours selection of infected cells was performed using blasticidin

(Invitrogen). A canary plate was used to monitor cell death. The resulting cell lines were assessed with qRT-PCR and Western blot for IL-17BR over-expression.

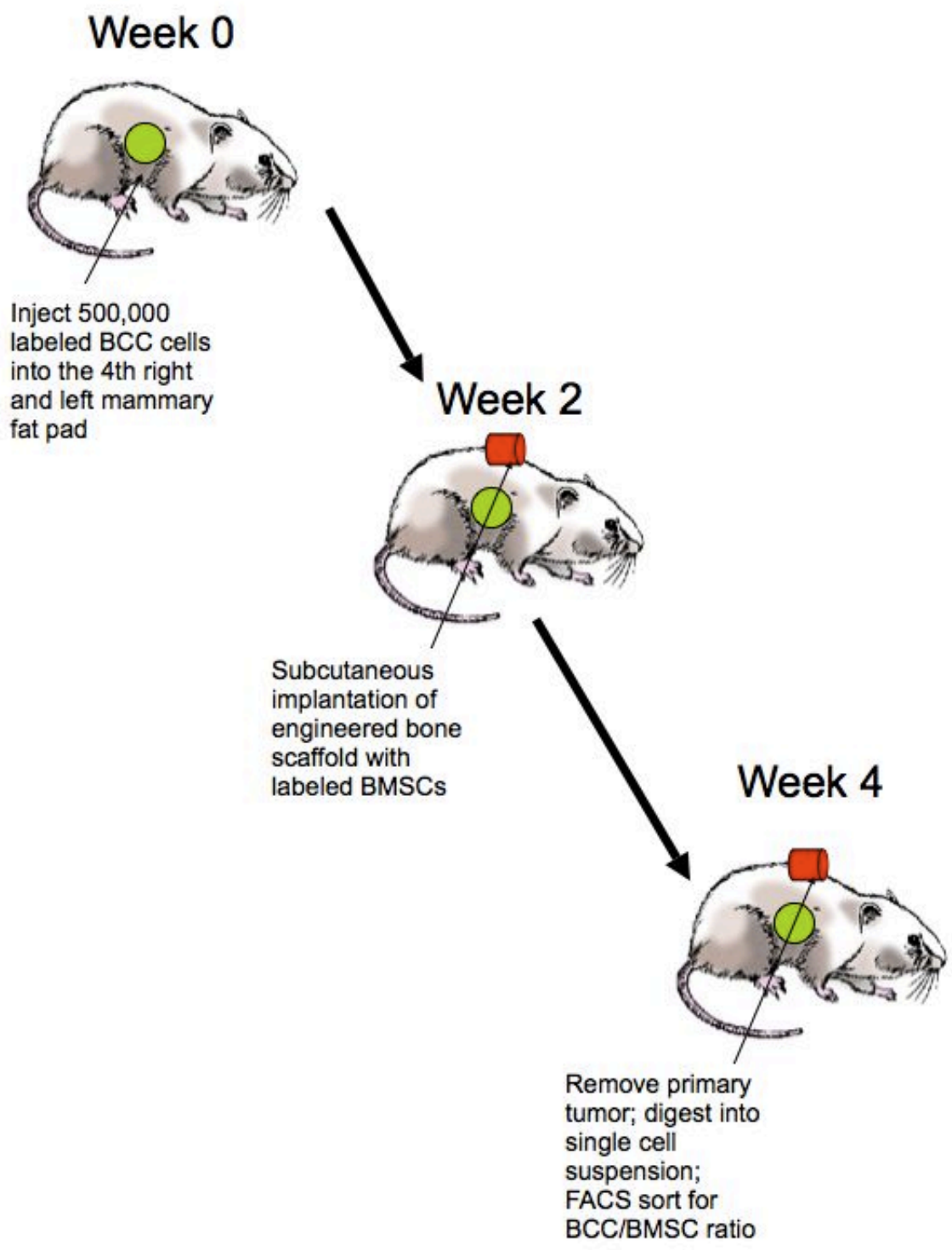

Figure 2-1. A schematic of the *in vivo* design for modeling hBMSC migration from the bone environment to primary breast cancer tumors.

Table 2-1

Gene	Sequence	
il-17br	GCCCTTCCATGTCTGTGAAT	F
	CAGGGGAGTGGTTGTGAAGT	R
il-17	GACCTGGTGTCACGGATGAAA	F
	CCTCGATGTTCCTCTCATACTCC	R
mmp13	GGTCCAGGAGATGAAGACC	F
	GGAAGTTCTGGCCAAAATGA	R
mmp1	TCTGGGGTGTGGTGTCTCA	F
	GCCTCCCATCATTCTTCAGGTT	R
hunk	ATGCTCATCGGCAGCAGGAAG	F
	CCAAAGAAATCCTGTTGGGA	R
ctgf	CCGTACTCCCAAAATCTCCA	F
	GTAATGGCAGGCACAGGTCT	R
cxcr-4	GAAGCTGTTGGCTGAAAAGG	F
	TGGAGTGTGACAGCTTGGAG	R
opn	ACTCGAACGACTCTGATGATGT	F
	GTCAGGTCTGCGAAACTTCTTA	R
gapdh	GAGTCAACGGATTTGGTCGT	F
	GATCTCGCTCCTGGAAGATG	R
beta-actin	CATGTACGTTGCTATCCAGGC	F
	CTCCTTAATGTCACGCACGAT	R

Table 2-2

Protein	Supplier	Catalog Num.
α-*IL-17RB*	Santa Cruz Biotechnology, Inc.	SC-52925
α-*GAPDH*	Santa Cruz Biotechnology, Inc.	SC-47724
α-*IL-17B*	R&D Systems	AF1789
α-*TGF-β1*	R&D Systems	AB-101-NA
rhIL-17B	R&D Systems	1248-IB/CF
rhTGF-β1	R&D Systems	240-B/CF

Table 2-1. List of PCR primers used. Primers were designed using PrimerBank (Harvard Medical School; http://pga.mgh.harvard.edu/primerbank/)

Table 2-2. Antibodies and proteins used for Western blotting and functional studies.

Chapter 3

Results

Validation of the Humanized Model of Breast Cancer Metastasis to Human Bone

Detailed Description of the Humanized Model of Breast Cancer Metastasis to Bone

As described above, previous work established the humanized model of breast cancer metastasis to human bone as a reproducible model of breast cancer dissemination from the orthotopic location to subcutaneously implanted human bone fragment (Kuperwasser et al., 2005; Moreau et al., 2007). The model is presented below and in Figure 1-1 for greater understanding. Unidentified (e.g., age, gender, disease status, etc.) femoral heads are obtained from discarded tissue samples from total hip replacement surgeries. Within 4-hours of removal, the femoral head is cut into 1-cm thick slices on a bone saw using a diamond blade to ensure smooth edges and the bone slices are used to core 1-cm by 0.5-cm bone fragments using a bone biopsy trephine cutter. The bone fragments are washed in PBS and placed on ice until implanted into mice. 6-8 week old NOD/Scid female mice are anesthetized and an approximately 0.8-cm incision is made bilaterally on the lower backs of the animals. Using hemostats, bone fragments are placed subcutaneously on the flanks of the animal over the right and left shoulder blade.

Four weeks after bone implantation, the animal is again anesthetized and 500,000 luciferase-tagged breast cancer cells (BCCs) are injected into the right and left 4th mammary fat pads. The BCCs are injected in a 1:2 mixture of Matrigel and sterile PBS. The mice are monitored for 10-weeks, specifically for tumor growth, signs of metastatic disease and general health. Throughout the experiment, bioluminescent imaging is used to analyze primary tumor growth and distant metastasis. Because the primary tumors are so large by the end of the experiment and produce a saturating bioluminescent signal, it is not possible to visualize *in vivo* metastasis. Thus, mice are sacrificed and the human

bone cores and other organs (e.g., mouse hind limbs, lungs, livers, spleen, kidney) are removed to image separately. Positive metastases detected by bioluminescence can be confirmed with histology, as well as PCR detection of human- or cancer-specific genes (e.g. *luciferase*).

In addition to using native human bone fragments cored from femoral head slices, the humanized metastasis model has been modified to incorporate tissue engineered bone (TEB) (Moreau et al., 2007). As described above, using silk fibroin protein sponges as scaffolds, human bone marrow-derived mesenchymal stem cells can be seeded and differentiated towards an osteoblast lineage *in vitro*, creating a biocompatible and three-dimensional porous, silk-based, human bone-like structure (Kim et al., 2004). These TEB structures can serve as efficient targets of breast cancer metastasis from the orthotopic location, with equal frequency as native human bone. Additionally, to enhance *in vivo* differentiation of TEB, bone morphogenetic protein-2 (BMP-2) can be coupled to the silk scaffold and drive osteoblast development following hBMSC seeding (Li et al., 2006). BMP-2-coupled scaffolds demonstrated the highest frequency of breast cancer metastasis, possibly relating to their ability to prime the metastatic niche with bone marrow stem cells and to promote *in vivo* osteoblast differentiation (Moreau et al., 2007).

Maintenance of a Fully Human Environment in the Human Bone Fragment

The initial report of the humanized model of breast cancer metastasis to human bone elegantly described the viability of the human bone fragments (Kuperwasser et al., 2005). After 12-weeks of implantation, the human bone cores remain viable and

populated with normal, human cells: fibroblasts, adipocytes, endothelial cells, osteoclasts, and bone marrow cells. In addition, bone remodeling continues to take place; newly synthesized bone was clearly present in histologic sections. Remarkably, after 12-weeks *in vivo*, the human bone fragments demonstrated neoangiogenesis. Blood vessels within and around the bone implant were demonstrated to be a hybrid of mouse host- and human-derived endothelial cells, indicating that the bone was able to recruit the mouse vasculature and form an anastamosis of mouse and human blood vessels.

In addition to viability and bone morphology, Kuperwasser et al. studied the functionality of the human bone fragments within the humanized metastasis model. Human hematopoietic cells were observed within the mouse host. Premature B-lymphocytes form within the bone marrow and then home to the spleen to complete differentiation. Human B cells were found within the spleens of mice engrafted with human bone cores, demonstrating that the human bone marrow retains the ability to create fully functional lymphocytes.

To support these results and to understand whether host cells were able to penetrate the human bone core, we carried out the following experiment: human bone fragments were implanted into NOD/Scid female mice universally expressing green fluorescent protein (NOD/Scid-GFP). After 10-weeks, the human bone fragments were removed along with the host mouse hind limbs, kidneys, spleen, gut, and lung (Figure 3-1 and data not shown). Sections of each organ were stained with H&E and anti-GFP to distinguish mouse- vs. human-derived cells. Remarkably, the center of the human bone fragment was devoid of any mouse-derived cells. The stromal cells, osteoblasts,

osteocytes and osteoclasts within the bone fragment were all human. Mouse osteoblasts and osteocytes were observed within the mouse hind limb, and mouse stromal cells were seen throughout the various organs examined. These data suggest that metastatic breast cancer cells encounter a human-derived bone remodeling environment within the bone fragment. This finding further supports the use of the humanized breast cancer metastasis model as a method to study human breast cancer and human bone interactions, as well as human-specific pathways involved in skeletal metastases and also validates the use of the model to study therapeutic targets in human disease.

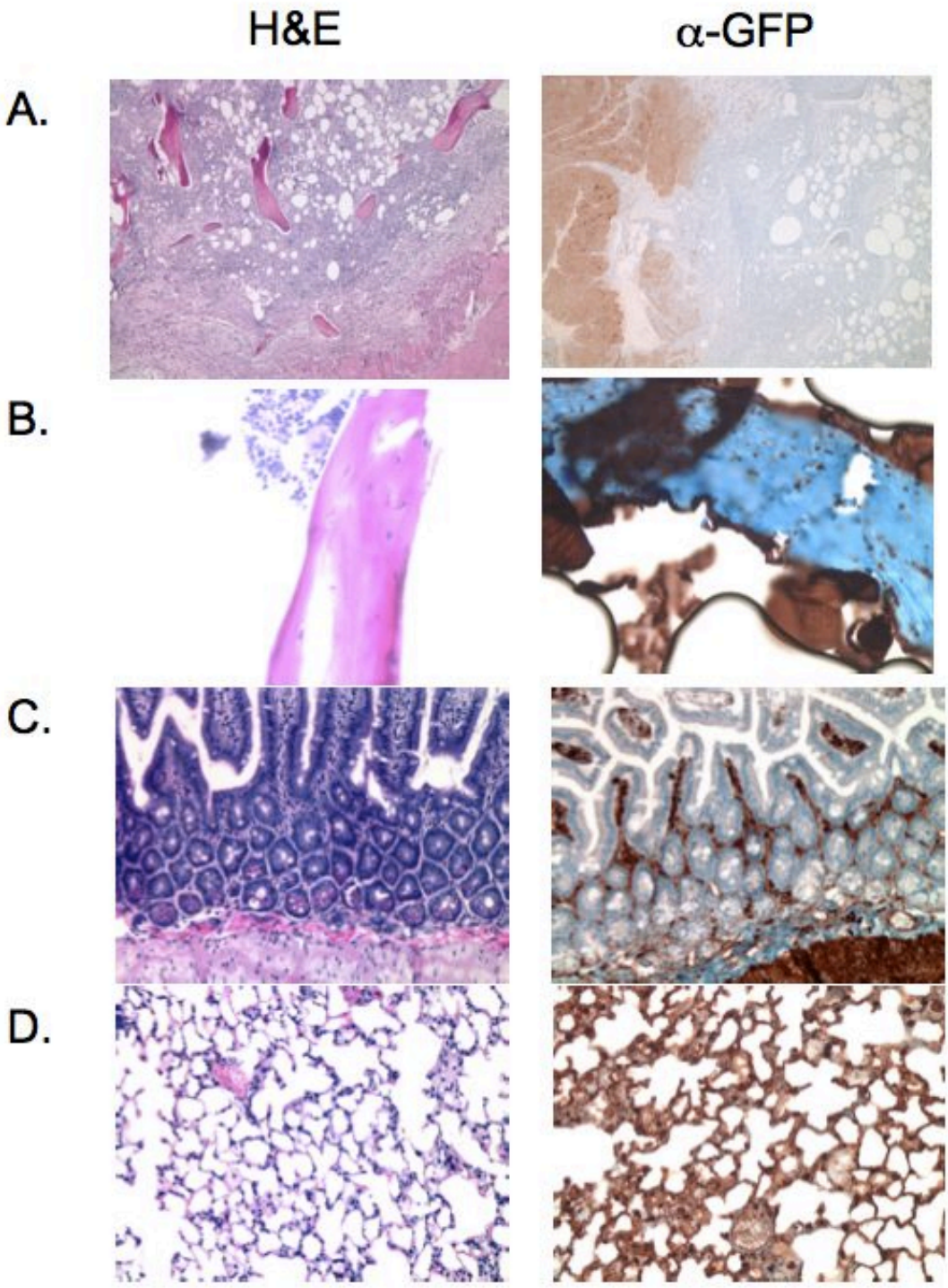
H&E
α-GFP
A.
B.
C.
D.

Figure 3-1. The human bone core remains completely comprised of human cells. A GFP-expressing NOD/Scid female mouse was implanted with human bone cores. After 14-weeks *in vivo*, the bone cores (A), mouse bones (B), mouse gut (C) and mouse lung (D) were removed and sectioned for histology. H&E (left) and anti-GFP (right) staining show that the human bone core does not contain any mouse (GFP-expressing cells) after 14-weeks *in vivo*. Images are representative of the 3 mice used in the experiment and 10 serial sections of each organ that were visualized.

Increased Sensitivity Leads to Increased Metastasis Detection

Kuperwasser et al. chose 12 different human breast cancer cell lines to study in their original publication of the humanized breast cancer metastasis model. Only the SUM1315 breast cancer cell line was able to form bone metastases when implanted orthotopically in NOD/Scid female mice. Additionally, the SUM1315 metastases were only observed in the human bone fragments; no metastasis to the mouse skeleton was observed. Metastasis was determined by radiography and histologic analysis of serial sections of the human- and mouse-bone samples. Novel bioluminescent imaging techniques that rely on expression of the firefly *luciferase* gene have introduced a more sensitive method of detecting micro- and macrometastases within the experimental model (O'Neill et al., 2010). Given the increased sensitivity, it was important to re-evaluate the model and see whether more than just the SUM1315 BCC line could efficiently metastasize.

Two human-derived BCC lines and their respective bone-passaged sublines were tagged with a firefly-luciferase vector and analyzed *in vitro* and *in vivo*: SUM1315 and SUM1315-BP2, MDA-MB-231 and BoM2 (SUM1315-BP2 and BoM2 will be discussed in greater detail below). The sublines demonstrated significantly decreased proliferation and migration compared to their parental line, *in vitro* (Figure 3-2). When used in the humanized model of breast cancer metastasis to human bone, all four BCC lines demonstrated metastasis to the human bone fragments, as assessed by bioluminescent imaging (Figure 3-3). Remarkably, the frequency of metastasis to human bone fragments was not significantly different between parental and bone-passaged sublines, suggesting

that *in vitro* and *in vivo* migration characteristics are different, especially in the context of orthotopic implantation. This observation is supported by many reports that show the importance of the microenvironment in tumor growth and metastasis (Joyce & Pollard, 2009). Also, all four human BCC lines metastasized to the mouse skeleton, albeit at widely varying frequencies. Of note, the SUM1315-BP2 BCC line demonstrated the lowest frequency of mouse skeletal metastasis, suggesting that passaging the cell line through human bone decreased its ability to home to non-human bone.

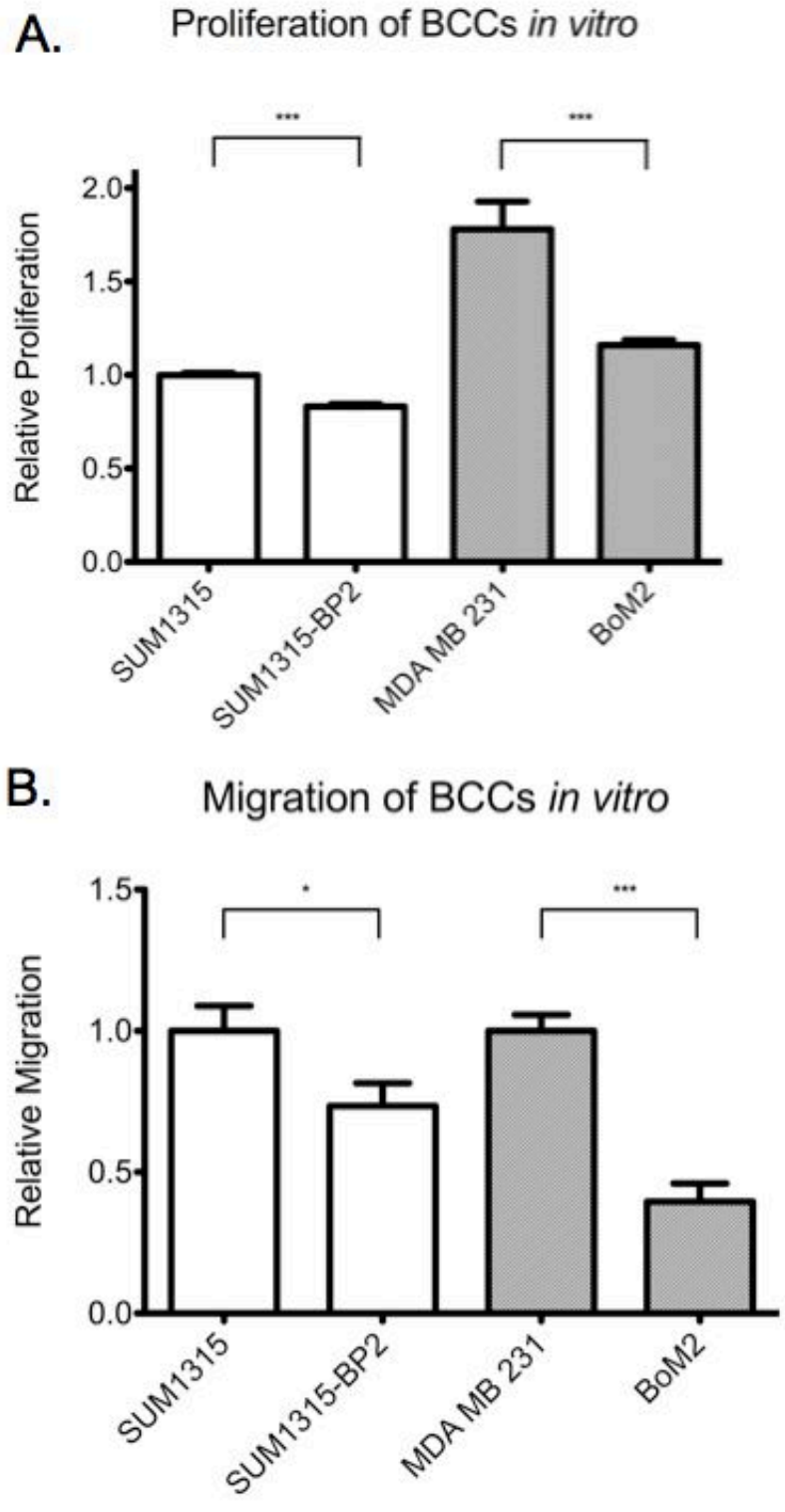
A.
Proliferation of BCCs *in vitro*
***
***
Relative Proliferation
2.0
1.5
1.0
0.5
0.0
SUM1315
SUM1315-BP2
MDA MB 231
BoM2
B.
Migration of BCCs *in vitro*
*
***
Relative Migration
1.5
1.0
0.5
0.0
SUM1315
SUM1315-BP2
MDA MB 231
BoM2

Figure 3-2. Bone-passaged breast cancer cell lines have decreased proliferation and migration when compared to their parental line. (A) Serum-starved SUM1315, SUM1315-BP2, MDA- MB-231 and BoM2 BCCs were seeded in replicate wells of a 96-well plate (4,000 cells/ well). Cells were cultured in growth medium for 48-hours and proliferation was measured using an MTT-based assay (Roche). Proliferation of BCCs is normalized to SUM1315 and was analyzed using a two-sided Student's T-test. Data are represented as mean ± SEM. ***, $p<0.001$. (B) Serum-starved SUM1315, SUM1315-BP2, MDA-MB-231 and BoM2 BCCs were plated in equal numbers (30,000) on the top well of a 96-well transwell migration assay (Millipore) and allowed to migrate for 6-hours towards DMEM supplemented with 10% FBS. Migration was measured according to the manufacturer's instructions. Migration of SUM1315-BP2 is normalized to SUM1315. Migration of BoM2 is normalized to MDA-MB-231 and was analyzed using a two-sided Student's T-test. Data are represented as mean ± SEM. *, $p<0.05$; ***, $p<0.001$.

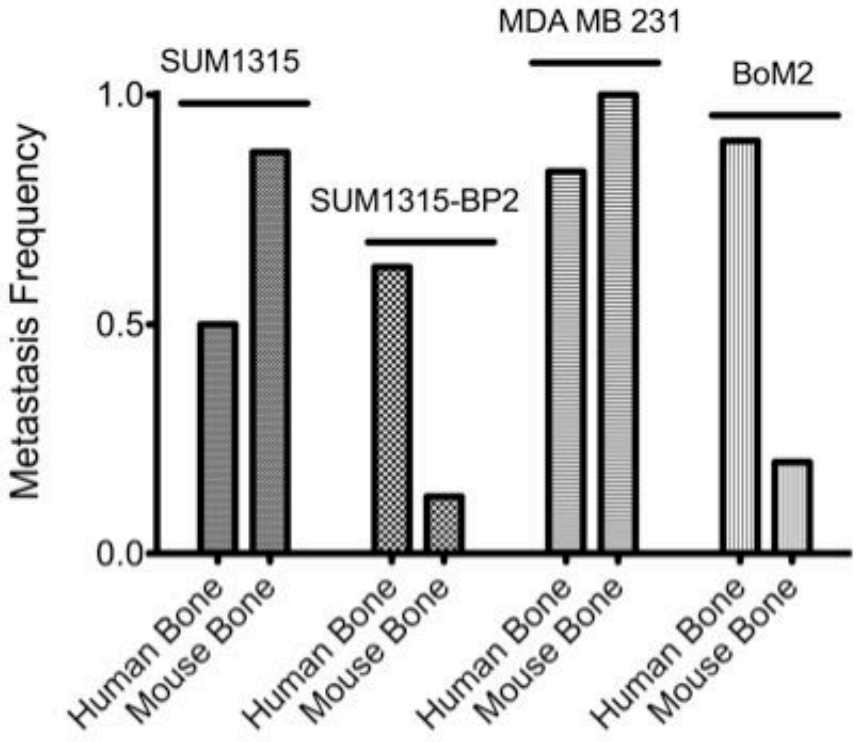

Figure 3-3. Metastasis frequencies from different breast cancer cell lines. 500,000 breast cancer cells were injected into the right and left 4th mammary fat pad of NOD/Scid mice harboring human bone fragments. After 10 weeks of growth *in vivo* the mice were sacrificed, and the frequencies of metastasis to the implanted human bone fragments and mouse femurs were calculated. Metastasis was analyzed using bioluminescent imaging of human bone fragments and mouse hind limbs. Metastatic samples were counted and frequency was calculated by dividing number of metastatic samples by total samples analyzed. N=10 bone fragments for all cell lines.

Chapter 4

Results

Primary Tumor Genetic Changes Affect Metastasis Frequency

Comparison of Two Gene Signatures of Metastasis

As described above, animal models of cancer metastasis to bone have been used to identify genes that are important for efficient skeletal metastasis. An intracardiac injection model of breast cancer metastasis to the mouse skeleton identified *il-11*, *mmp-1, ctgf, cxcr4* and *opn* as major contributors to the metastatic phenotype observed, while use of the humanized model of breast cancer metastasis to human bone focused on *il-17br, mmp-13,* and *hunk* as critical genetic components of human-specific metastasis (Kang et al. 2003). Both of these gene "signatures" were identified with the help of serial bone passaging of human breast cancer cell lines.

Kang et al. utilized an intracardiac injection model of breast cancer metastasis and the MDA-MB-231 human BCC line. Parental MDA-MB-231 BCCs were directly injected into the left cardiac ventricle of an immunocompromised mouse, resulting in metastasis to the mouse tibia (frequency: approximately 1/4). Metastatic cells were isolated from the mouse bone, expanded *in vitro*, and re-injected into the left cardiac ventricle, resulting in more efficient metastasis to the mouse tibia (frequency: approximately 9/10). The metastatic cells were again isolated from the mouse bone and used for microarray profiling, comparing the gene expression of the highly bone metastatic subline, BoM2, with the parental BCC line, MDA-MB-231 (Figure 4-1).

In a similar experiment, SUM1315 BCCs were passaged through human bone (Figure 1-2; Figure 4-1). SUM1315 BCCs were directly injected into subcutaneously implanted human bone fragments. The cells were allowed to grow within the bone for 12-weeks, and were then isolated and cultured *in vitro*. The expanded cells were re-

injected directly into the human bone fragments and again allowed to grow for 12-weeks. The twice passaged cells were collected and used for microarray profiling, comparing the gene expression of the bone residing SUM1315-BP2 cells with SUM1315 BCCs grown in the mammary fat pad of a mouse (Figure 4-1).

The gene expression signature of SUM1315-BP2 BCCs is enriched for genes that may promote tumor growth and metastasis (Table 1-1; Appendices A, B, and C). Four genes that have documented roles in metastasis were confirmed to be over-expressed based on qRT-PCR analysis of RNA from mammary fat pad-residing SUM1315 BCCs and bone-residing SUM1315-BP2 BCCs: *mmp-1, hunk, il-17b,* and *il-17br* (Figure 1-2). While these genes were different in identity than those isolated from comparison of the MDA-MB-231 and BoM2 BCC lines, the genes fit into the same functional classifications identified by Kang et al., i.e. homing, invasion, angiogenesis and osteolysis (Figure 4-1). We hypothesized that the two gene signature may represent species-specific "tool boxes" for skeletal metastasis. As such, we expected that the human signature (*mmp-13, hunk, il-17br/il-17b*) would be up-regulated in metastases within human bone fragments and the mouse signature (*mmp-1, cxcr4, ctgf, il-11*) would be up-regulated in metastases to the mouse skeleton, independent of the BCC line used to form the primary tumor.

A.

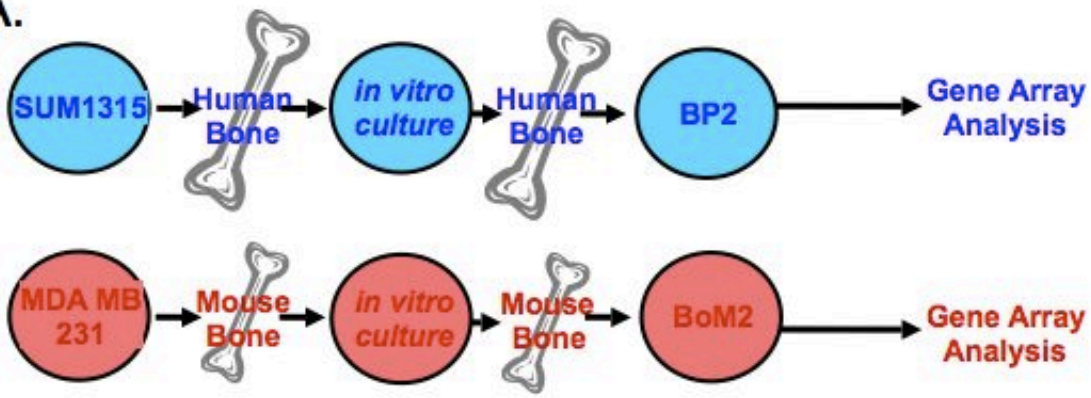

B.

Function	Gene	Target	Role in Bone Metastasis
Homing	CXCR4	Mouse Skeleton	Known homing signal used by the bone marrow environment
Invasion	MMP1	Mouse Skeleton	Promotes osteolysis via cleavage of collage in matrix
	MMP13	Human Bone	Plays a key role in bone remodeling and tumor invasion
Blood Supply	CTGF	Mouse Skeleton	Known mediator of local angiogenesis induced by breast cancer
	HUNK	Human Bone	Function in tumorigenesis and tumor formation
Osteolysis	IL-11	Mouse Skeleton	Potent inducer of osteoclast formation from progenitor cells
	IL-17BR	Human Bone	Potent inducer of osteoclast formation from progeneitor cells
	OPN	Both Targets	Stimulates osteoclast adhesion to bone matrix

Figure 4-1. Comparison of two bone metastasis gene signatures. (A) SUM1315 and MDA-MB-231 BCCs were passaged twice through human and mouse bone, respectively. The resulting sublines (SUM1315-BP2 and BoM2) were used for gene array analysis. (B) The two gene arrays were compared and four gene functions were identified and conserved: homing, invasion, blood supply and osteolysis. Genes in red (CXCR4, MMP1, CTGF, IL-11) were isolated from the BoM2-based gene array. Genes in blue (MMP13, HUNK, IL-17BR) were isolated from the SUM1315-BP2-based gene array. OPN was up-regulated in both gene arrays.

Neither Proposed Gene Signature Correlates With *in vivo* Expression

To test our hypothesis, we analyzed the gene profiles of all four BCC lines in the context of the humanized metastasis model. As described above, the four cell lines have different *in vitro* proliferation and migration profiles, as well as differences in *in vivo* metastasis frequency to human bone fragments when injected orthotopically (Figure 3-2; Figure 3-3). Additionally, the four cell lines were injected into the left cardiac ventricle of an immunocompromised mouse with subcutaneous human bone implants and resulted in equivalent metastasis frequencies (frequency: 2/2). Human and mouse bone samples containing breast cancer metastases, both from intracardiac and orthotopic injections, were used for RNA isolation and analysis. The mouse or human bone was frozen on dry ice immediately after imaging and complete RNA was extracted using TRIzol reagent (Invitrogen). The expression of *il-11, mmp-1, cxcr4, ctgf, opn, il-17br, mmp-13* and *hunk* was quantified using qRT-PCR and is summarized in Figures 4-2. The expression of each gene was normalized to 18S RNA, *β-actin*, and *gapdh*, and is represented as relative expression compared to matched primary tumors.

Interestingly, neither the human nor mouse gene signature was consistently up-regulated in human or mouse bone, respectively (Figure 4-2). While, neither "tool box" was found to be conserved, four genes did demonstrate interesting patterns of expression when looked at across different BCC lines and metastatic sites. *mmp-1* was consistently over-expressed across all cell lines and metastatic sites, most likely as a result of its critical role in extravasation and collagen degradation. *opn* expression was mixed, with all mouse skeletal metastases exhibiting highly over-expressed levels of *opn* and all

human bone metastases exhibiting highly down-regulated levels of *opn*. Osteopontin has been implicated in cancer metastasis and as a serum-marker of disease progression in patient samples, but its expression pattern in this study suggests that it may not be an essential gene for growth within the human bone environment (Shevde et al., 2010).

Hunk is a novel SNF-1-related kinase, discovered for its role in mammary gland development (Gardner et al., 2000). It has recently been shown that *hunk* expression is crucial for breast cancer metastasis to the lung; *hunk*-deficient tumors failed to escape the mammary fat pad and efficiently extravasate into the circulation in an autochthonous model of breast cancer metastasis resulting in a significant decrease in lung metastases (Wertheim et al., 2009). Conversely, over-expression of *hunk* in a derivative of the MDA-MB-231 human BCC line decreased *in vitro* migration, cytoskeletal rearrangement, and lymph node metastasis from the orthotopic location (Quintela-Fandino et al., 2009). Thus, it was not surprising that *hunk* expression was mixed in SUM1315, SUM1315-BP2, MDA-MB-231 and BoM2 metastases in human and mouse bone (Figure 4-2).

A.

	SUM1315		MDA MB 231		BoM2		BP2
	Mouse Bone	Human Bone	Mouse Bone	Human Bone	Mouse Bone	Human Bone	Human Bone
MMP1	↑↑↑	↑↑	↑↑↑	↑↑↑	↑↑	↑↑↑	↑↑↑
CXCR4	↓	↓	↓↓↓	↓↓↓	↑	↑↑↑	↓
CTGF	↑↑↑	↑↑	↑	↓↓↓	↑↑↑	↑↑↑	↑↑
OPN	↑↑↑	↓↓↓	↑↑↑	↓	↑↑↑	↓↓↓	↓↓
IL17BR	↑	↑↑	-	-	↑	↑↑↑	↑↑↑
MMP13	↓↓	↓↓↓	↓	↓↓↓	↑	↓	↓↓↓
HUNK	↑	-	-	↓↓	↑	↓↓	↑

B.

	SUM1315	MDA-MB-231	BoM2	BP2
	Human Bone	Human Bone	Human Bone	Human Bone
MMP1	↑↑↑	↑↑↑	↑↑	↑↑↑
CXCR4	↓	↓↓↓	↑	-
CTGF	↑↑↑	↓↓↓	↑↑↑	↑↑
OPN	↓↓↓	↓	↓↓	-
IL17BR	↑↑↑	-	↑↑↑	
MMP13	↓↓↓	↓↓↓	↓↓	↓↓
HUNK	↑	↓	↓	-

Figure 4-2. Genetic profiling of metastatic breast cancer cells from orthotopic (A) and intracardiac (B) injection. RNA was isolated from human bone cores and mouse femurs containing metastases by mechanical grinding and Trizol extraction. Total RNA was used in qRT- PCR analysis for *mmp1, cxcr4, ctgf, opn, il-17br, mmp13*, and *hunk*. Expression of each gene was normalized to *18S* RNA, *gapdh,* and *β-actin* and reported in fold expression relative to matched primary tumors. Data are representative of N=3 samples for all cell lines, except SUM1315-BP2 (human bone) and BoM2 (mouse bone), where N=2. No arrows, <2 fold; one arrow, 2-5 fold; two arrows, 5-10 fold; three arrows, >10 fold.

il-17br Over-Expression Can Drive Metastasis

The expression of *il-17br* in primary tumors is positively correlated with good prognosis in clinical samples (Jerevall et al., 2008). Despite these clinical findings, *il-17br* was over-expressed in most metastasis samples when compared to matched primary, orthotopic tumors in our studies (Figure 4-2, Figure 4-3). Additionally, *il-17br* was consistently over-expressed in metastases from intracardiac injection of SUM1315 and BoM2 BCCs (Figure 4-3). IL-17B stimulation of IL-17BR has been linked to bone turnover and matrix degradation, and *il-17b* expression in cancer cells correlates with tumor progression (Yago et al., 2009; Jung et al., 2009). These findings, coupled with the genetic data presented above, suggest that IL-17BR may not be important in primary tumor development and aggressive behavior in the mammary fat pad, but may be activated and essential in the context of skeletal metastasis. IL-17B stimulation of BCCs over-expressing *il-17br* may promote tumor expansion within the bone or other distant sites.

To test this hypothesis we chose to over-express *il-17br* in human BCCs and assesses its effect on metastasis frequency. Over-expression of *il-17br* was done using a lentiviral vector containing the full-length cDNA for *il-17br*. Over-expression of *il-17br* was confirmed using RT-PCR and Western blot (Figure 4-4). RT-PCR demonstrated efficient over-expression of *il-17br* RNA compared to parental and mock-infected controls (Figure 4-4). To confirm protein overexpression and proper localization of IL-17BR we used Western blotting of whole cell lysates (“WCE”), membrane proteins and cytoplasmic proteins. We noticed that whole cell lysates of parental, mock-infected

and over-expression cell lines had nearly equivalent levels of IL-17BR protein (Figure 4-4, "WCE"). Subsequent fractionation of protein extracts into membrane and cytoplasmic fractions showed that while parental and mock-infected BCCs express IL-17BR protein, the expression is limited to the cytoplasmic protein fraction. Over-expression of IL-17BR protein drives expression of IL-17BR on the cell membrane, where it can interact with its ligand, IL-17B (Figure 4-4).

Over-expression of *il-17br* had no affect on proliferation of BCCs *in vitro* or *in vivo*, but did significantly increase migration of SUM1315 and MDA-MB-231 cells *in vitro* (Figure 4-5, Figure 4-6). When used in the humanized model of breast cancer metastasis, SUM1315 and MDA-MB-231 BCCs over-expressing *il-17br* resulted in increased frequencies of metastasis compared to mock-infected controls (Figure 4-6). While no difference was seen in the frequency of human bone metastasis, both cell lines demonstrated a significant increase in lung metastases, and SUM1315 cells over-expressing *il-17br* had an increased frequency of liver metastasis. Together, these data support a role for *il-17br* in affecting metastasis and growth within a distant site, while having little affect on primary tumor growth kinetics.

A. *il-17br* Expression from Orthotopic Injection

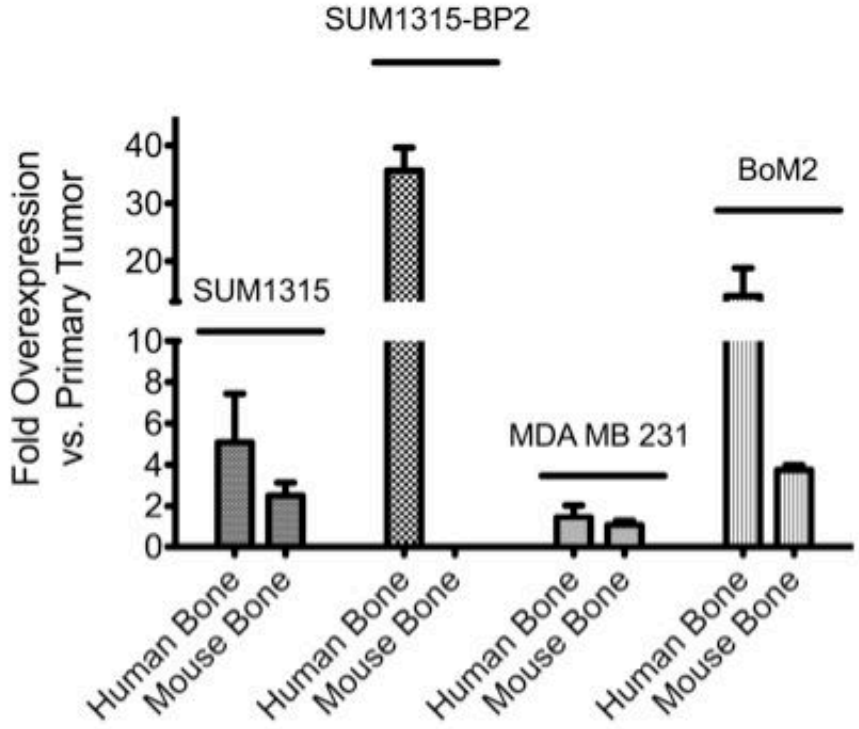

B. *il-17br* Expression from Intracardiac Injection

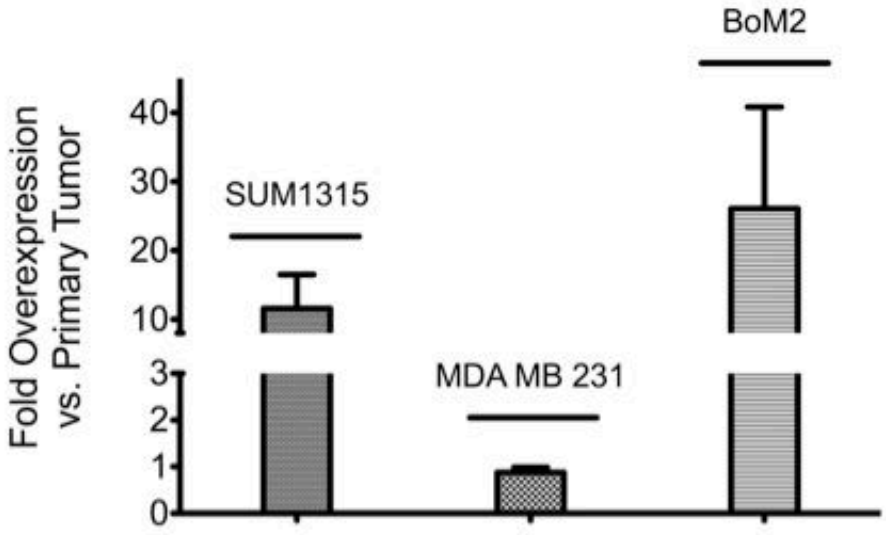

Figure 4-3. *il-17br* is over-expressed in bone metastases. Expression of *il-17br* was analyzed using qRT-PCR. Metastatic cells from orthotopic (A) and intracardiac (B) injection were compared with matched primary tumors. Except for SUM1315-BP2 (N=1) and BoM2 (N=2) mouse skeletal samples, 3 samples were analyzed for each cell line. qRT-PCR was not performed on SUM1315-BP2 mouse bone samples. Only human bone fragments were analyzed for intracardiac injection. Data are represented as mean ± SEM.

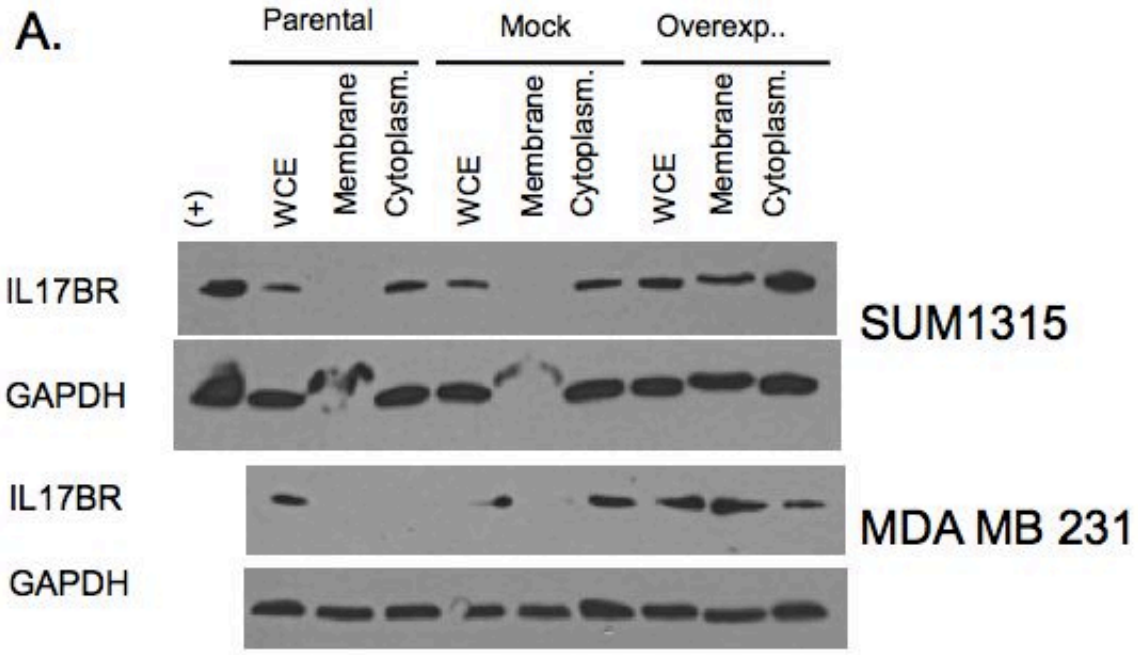
A.
Parental
Mock
Overexp..
(+)
WCE
Membrane
Cytoplasm.
WCE
Membrane
Cytoplasm.
WCE
Membrane
Cytoplasm.
IL17BR
GAPDH
SUM1315
IL17BR
GAPDH
MDA MB 231

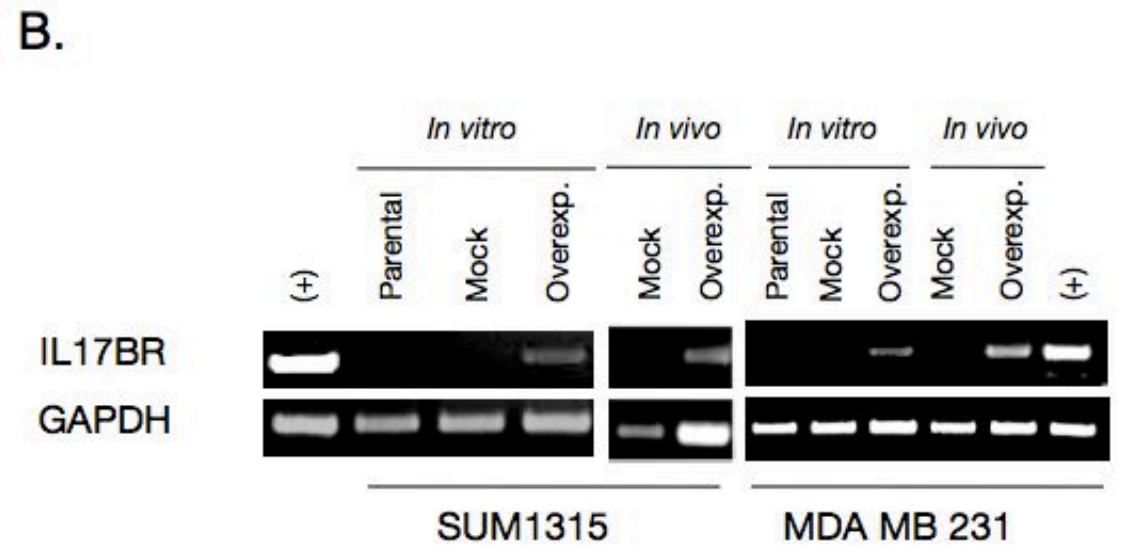
B.
In vitro
In vivo
In vitro
In vivo
(+)
Parental
Mock
Overexp.
Mock
Overexp.
Parental
Mock
Overexp.
Mock
Overexp.
(+)
IL17BR
GAPDH
SUM1315
MDA MB 231

Figure 4-4. Confirmation of *il-17br* over-expression. (A) Western blot showing efficient over-expression and membrane localization of IL-17BR protein in SUM1315 and MDA-MB-231 BCCs. *il-17br* was over-expressed in SUM1315 and MDA-MB-231 BCCs using a lentiviral vector containing the full-length cDNA. Parental and mock infected cells express IL-17BR in whole cell extracts (WCE), but the protein is limited to the cytoplasmic fraction, while over-expression of *il-17br* in BCCs causes increased membrane localized IL-17BR. (B) RT-PCR confirmation of *il-17br* over-expression of SUM1315 and MDA-MB-231 cells before orthotopic injection (*in vitro*) and after 10-weeks of growth in mice (*in vivo*).

A. Effect of *il-17br* on Proliferation *in vitro*

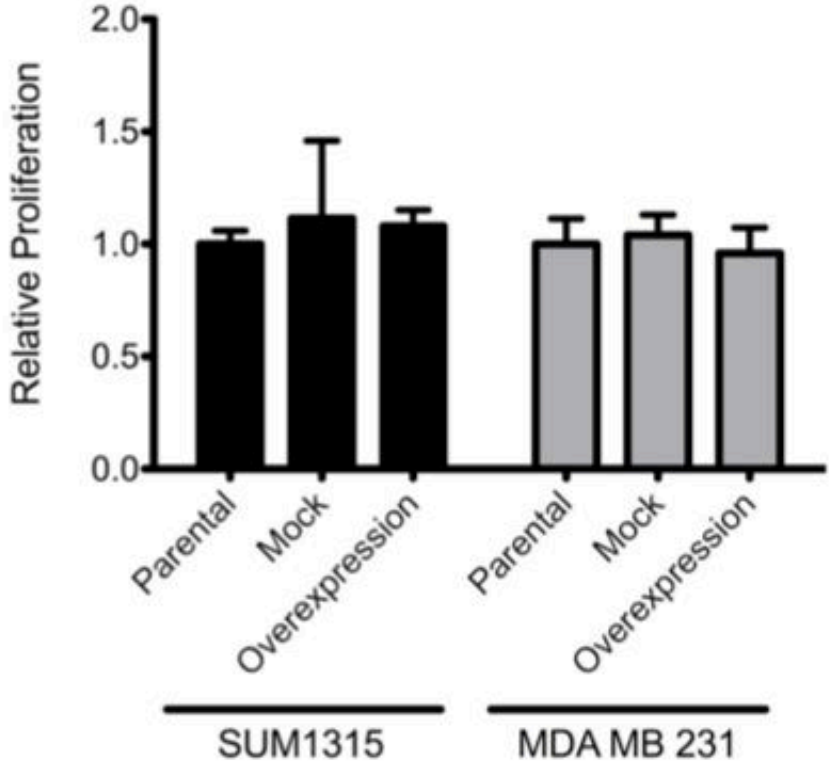

B. Effect of *il-17br* on Proliferation *in vivo*

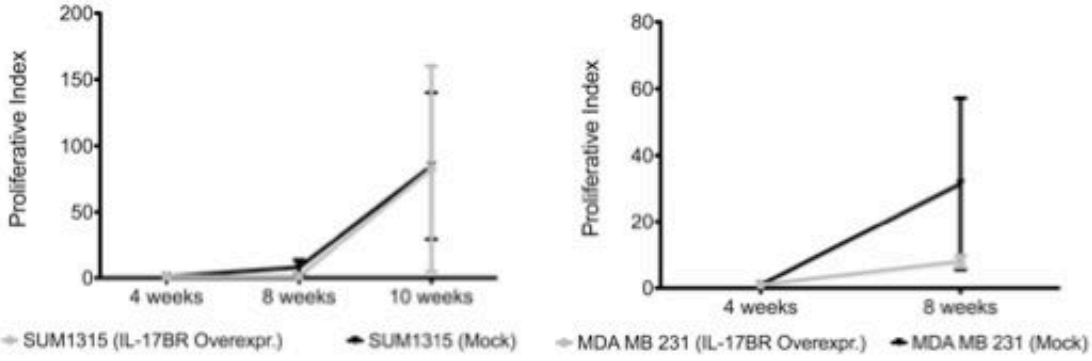

Figure 4-5. Over-expression of *il-17br* does not change breast cancer cell growth *in vitro* (A) or *in vivo* (B). *il-17br* was over-expressed in SUM1315 and MDA-MB-231 BCCs using a lentiviral vector containing the full-length cDNA. (A) Cells were seeded in equal numbers (4,000 cells/well) in replicate wells of a 96-well plate. Proliferation was measured using an MTT-based proliferation assay (Roche). No significant changes in proliferation were observed. (B) 500,000 BCCs were injected into the 4th right and left mammary fat pads of 10-week old NOD/Scid female mice containing human bone cores. Primary tumor size was measured by bioluminescence at 4, 8 and 10 weeks after injection. Primary tumor size was normalized to primary tumor size at week 4. No significant changes in proliferation were observed between mock-infected and *il-17br* over-expressing BCCs.

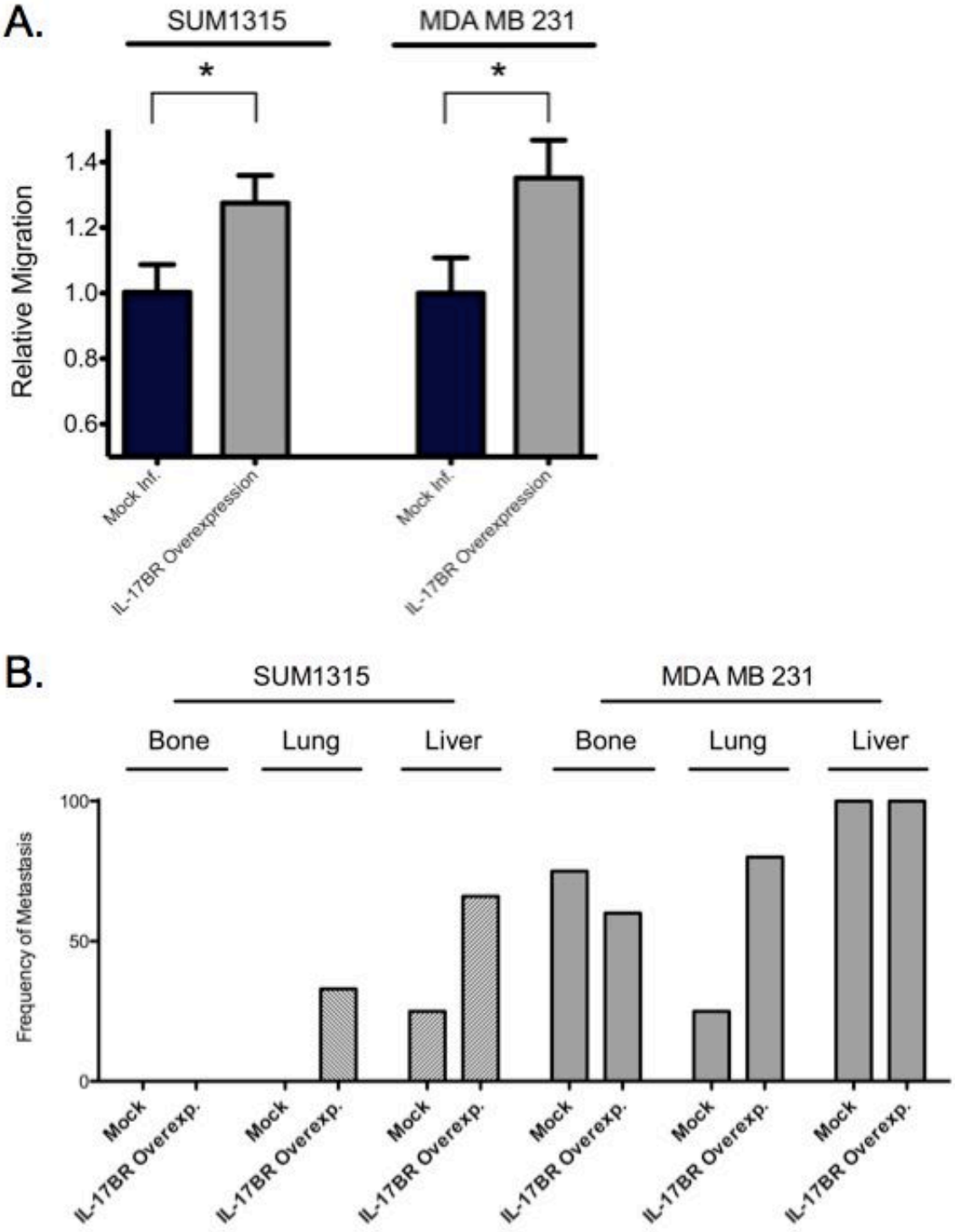
A.
SUM1315
MDA MB 231
*
*
Relative Migration
1.4
1.2
1.0
0.8
0.6
Mock Inf.
IL-17BR Overexpression
Mock Inf.
IL-17BR Overexpression
B.
SUM1315
MDA MB 231
Bone
Lung
Liver
Bone
Lung
Liver
Frequency of Metastasis
100
50
0
Mock
IL-17BR Overexp.
Mock
IL-17BR Overexp.
Mock
IL-17BR Overexp.
Mock
IL-17BR Overexp.
Mock
IL-17BR Overexp.
Mock
IL-17BR Overexp.

Figure 4-6. *il-17br* over-expression drives migration and metastasis. (A) Over-expression of *il-17br* in SUM1315 and MDA-MB-231 cells leads to increased migration *in vitro*. Serum-starved BCCs (mock infected or infected with lentivirus to over-express *il-17br* cDNA) were plated above media containing 10% FBS. Two-sided Student's t-test; *, $p<0.05$. Data are represented as mean ± SEM and normalized to mock infected samples. (B) Over-expression of *il-17br* in SUM1315 cells leads to increased metastasis to the lung and liver. Over-expression of *il-17br* in MDA-MB-231 cells leads to increased metastasis to the lung. Bioluminescent imaging of human bone fragments, lungs, and livers was used to asses metastasis frequency. Bone cores were imaged on both sides for 120 seconds. Lung and livers were imaged individually for 15 seconds.

Chapter 5

Results

hBMSCs Migrate to and Affect Breast Cancer Cell Growth and Metastasis

hBMSCs Are Pluripotent Adult Stem Cells

As described above, human bone marrow-derived mesenchymal stem cells (hBMSCs) are pluripotent adult stem cells that are able to differentiate into pericytes, chondrocytes, osteoblasts and adipocytes (Lazennec & Jorgensen, 2008). We tested the pluripotency of hBMSCs used in our studies by assessing their ability to differentiate into osteoblasts and adipocytes in 2- and 3-dimensional culture, both *in vitro* and *in vivo* (Figure 5-1). hBMSCs were obtained from healthy, adult males and differentiated *in vitro* in osteoblastic or adipogenic differentiation media as described previously (Moreau et al., 2007; Mauney et al., 2005).

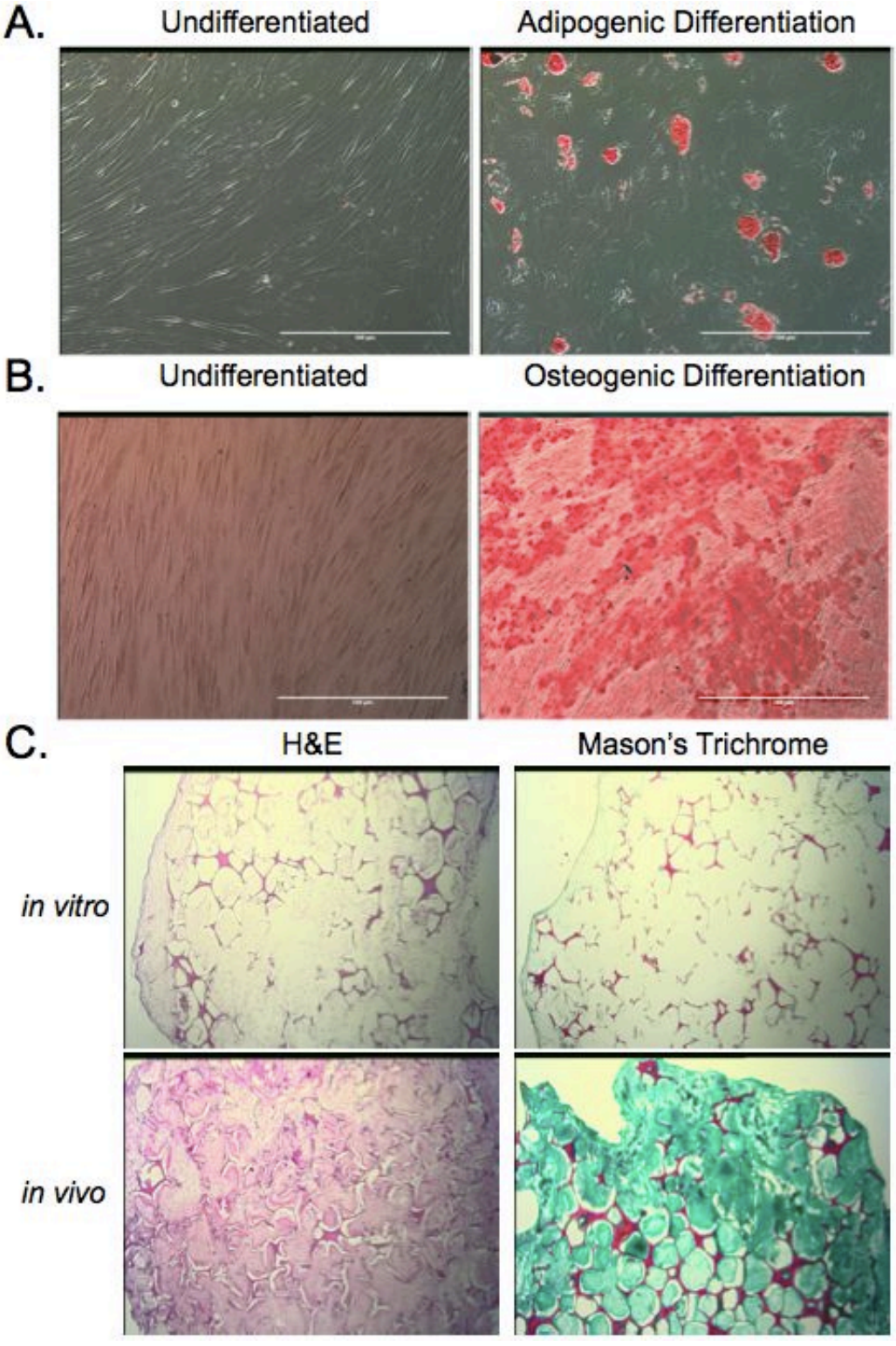
A.
Undifferentiated
Adipogenic Differentiation
B.
Undifferentiated
Osteogenic Differentiation
C.
H&E
Mason's Trichrome
in vitro
in vivo

Figure 5-1. hBMSCs are pluripotent adult stem cells. (A) Adipogenic differentiation was done in differentiation media and imaged with Oil Red O staining. (B) Osteogenic differentiation was done in osteogenic medium and assessed with Alizarin Red staining. (C) hBMSCs are seeded on silk scaffolds and differentiated towards the osteoblast lineage *in vitro* or implanted in mice. Bone characteristics were confirmed using H&E (left) and Mason's Trichrome (right) staining on scaffolds at the end of the experiment. H&E images demonstrate initial stages of bone development and presence of preliminary bone matrix. Mason's Trichrome images show collagen deposition. Scaffolds are cultured for 10-weeks *in vitro* (top) or *in vivo* (bottom).

hBMSCs Migrate to BCCs *in vitro* and *in vivo*

Previous reports have shown that hBMSCs can migrate to and affect primary tumors of various types (e.g. breast carcinomas, melanomas, neuroblastomas), possibly due to the tumor's chronic inflammation (Karnoub et al., 2007; Lazennec & Jorgensen, 2008; Kidd et al., 2009). Similar to these studies, we demonstrated that hBMSCs migrate towards conditioned medium from human breast cancer cells (BCCs) *in vitro*, with an increased affinity for highly aggressive and bone-metastatic BCCs (i.e. MDA-MB-231 and SUM1315) as compared to less aggressive BCCs (i.e. MCF7) (Figure 5-2).

To analyze the ability of hBMSCs to home from the bone environment to orthotopic (i.e. in the mammary fat pad) human tumors *in vivo*, we incorporated our previously developed tissue-engineered bone (TEB) into a novel hBMSC-tumor homing model (Moreau et al., 2007). Seeding and osteogenic differentiation of hBMSCs on silk fibroin sponges results in biocompatible, biodegradable, porous, mineralized TEB after 2-weeks of *in vitro* differentiation (Figure 5-3). These constructs have previously been shown to function as targets of BCC metastasis in a modified version of the humanized animal model of breast cancer metastasis, as described above (Moreau et al., 2007). In this experiment, TEB was seeded with fluorescently-labeled hBMSCs and implanted subcutaneously in the flanks of NOD/Scid mice (Figure 2-1). From this location, hBMSCs migrated to orthotopically implanted breast cancer tumors as assessed by fluorescence and confocal microscopy, as well as fluorescence-activated cell sorting (FACS) (Figure 5-4; Figure 5-5). The implanted TEB retained its bone phenotype and the hBMSCs remained fluorescent until the end of the experiment (2.5 weeks post-

implantation) (Figure 5-2). *In vivo* migration of hBMSCs to primary BCC tumors paralleled what was observed *in vitro*: hBMSCs migrated towards highly aggressive and bone-metastatic BCCs (i.e. MDA-MB-231 and SUM1315) with no statistically significant migration to BCCs with weak propensity to metastasize (i.e. MCF7).

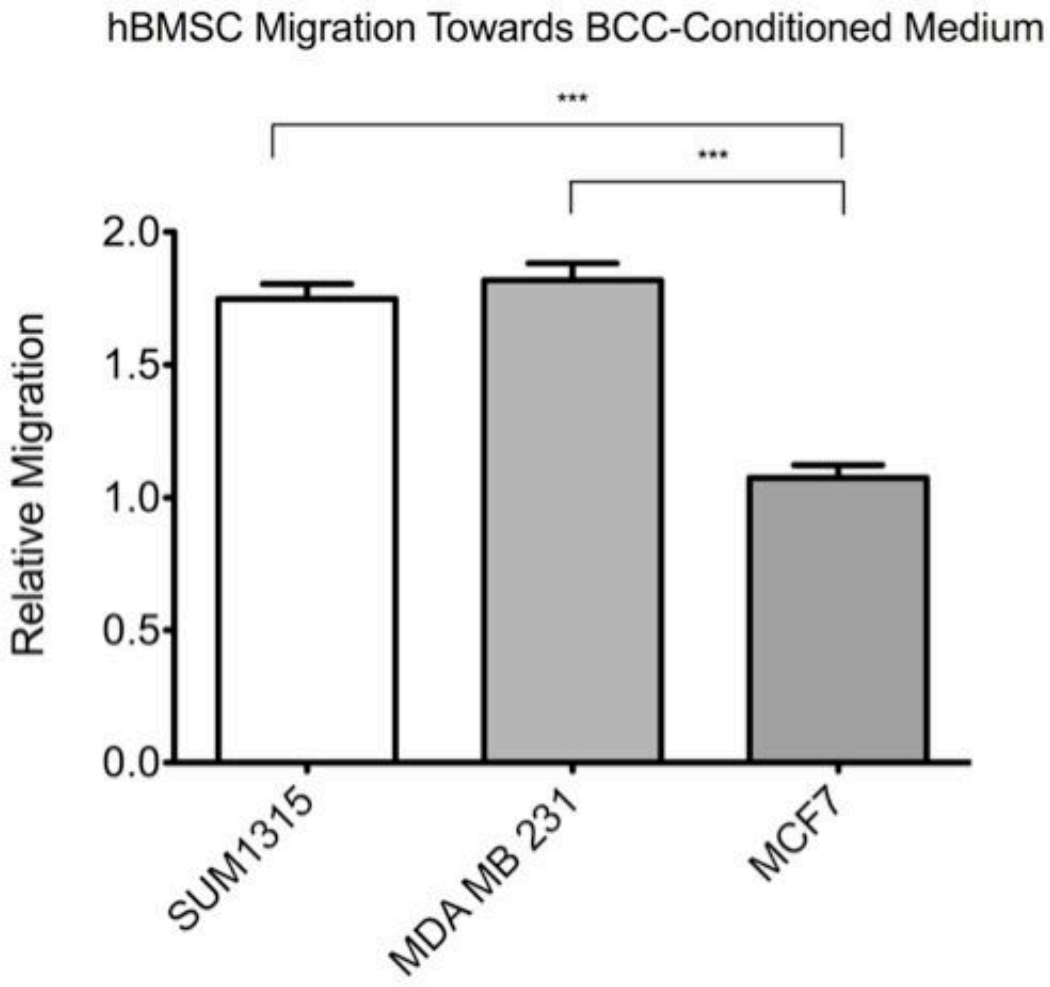
hBMSC Migration Towards BCC-Conditioned Medium
***
***
Relative Migration
2.0
1.5
1.0
0.5
0.0
SUM1315
MDA MB 231
MCF7

Figure 5-2. hBMSCs migrate towards conditioned medium from aggressive breast cancer cells. MDA-MB-231 ($p<0.0001$), SUM1315 ($p<0.0001$), and MCF7 BCCs were grown in serum free media for 48-hours. Media was collected, spun to pellet and remove extraneous cells, and plated in the receiving side of a 96-well transwell plate (Trevigen). 30,000 hBMSCs were seeded above the conditioned medium and allowed to migrate for 3-hours. After migration, calcein AM was used to quantify cell migration following the manufacturer's instructions. Values represent average number of cells/normalized to MCF7 migration and analyzed using a two-sided Student's t-test. Data are represented as mean ± SEM. N=10 for all groups.

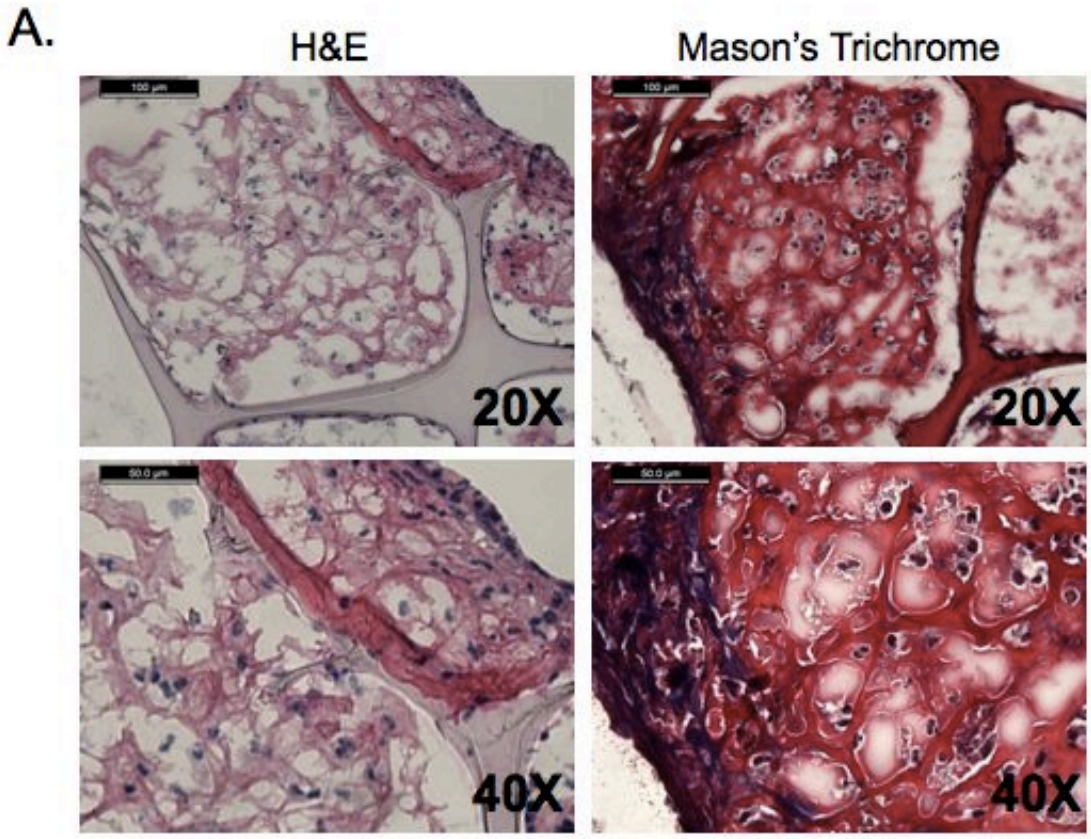
A.
H&E
Mason's Trichrome
20X
20X
40X
40X

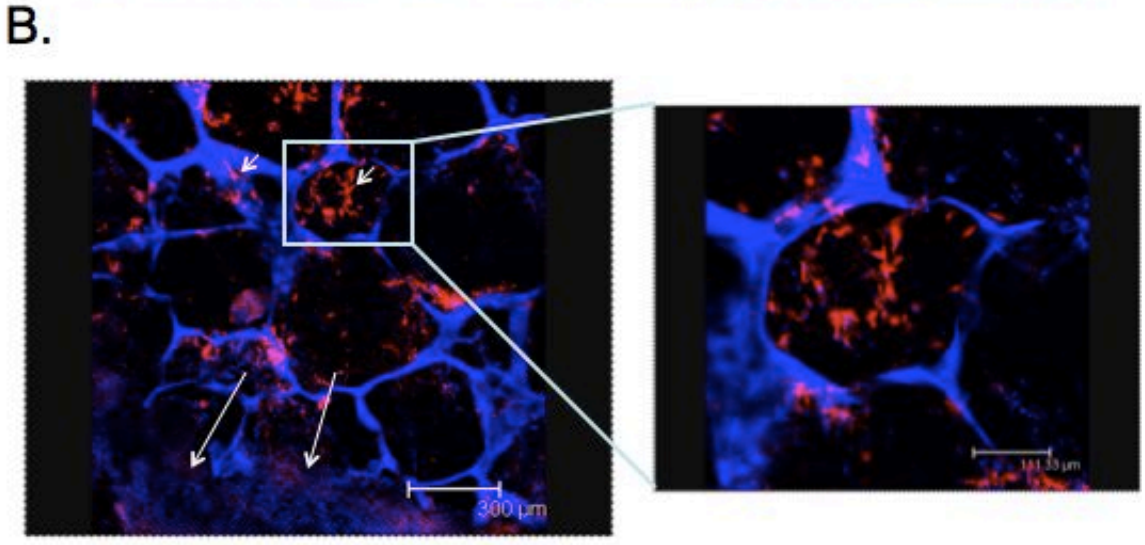
B.
300 µm

Figure 5-3. Fluorescently-labeled hBMSCs can be used to form physiologically functional tissue engineered bone scaffolds. (A) hBMSCs are seeded on silk scaffolds and differentiated towards the osteoblast lineage for 2-weeks and then implanted in mice for 10 days. Bone characteristics were confirmed using H&E (left) and Mason's Trichrome (right) staining on scaffolds at the end of the experiment. 20x (top) and 40x (bottom) views are shown. Scale bar is equivalent to 500 μm for 20x images and 50 μm for 40x images. H&E images demonstrate initial stages of bone development and presence of preliminary bone matrix. Mason's Trichrome images show collagen deposition, mostly towards the edge of the scaffold. (B) After 2.5-weeks *in vivo*, hBMSCs retain cell-tracker dye fluorescent label (red). Confocal image of OCT-embedded engineered bone constructs with DiD (red) positive hBMSCs (arrow heads), surrounded by DiD-negative mouse stromal cells (arrows). DAPI (blue) counterstaining for cell nuclei and silk pores.

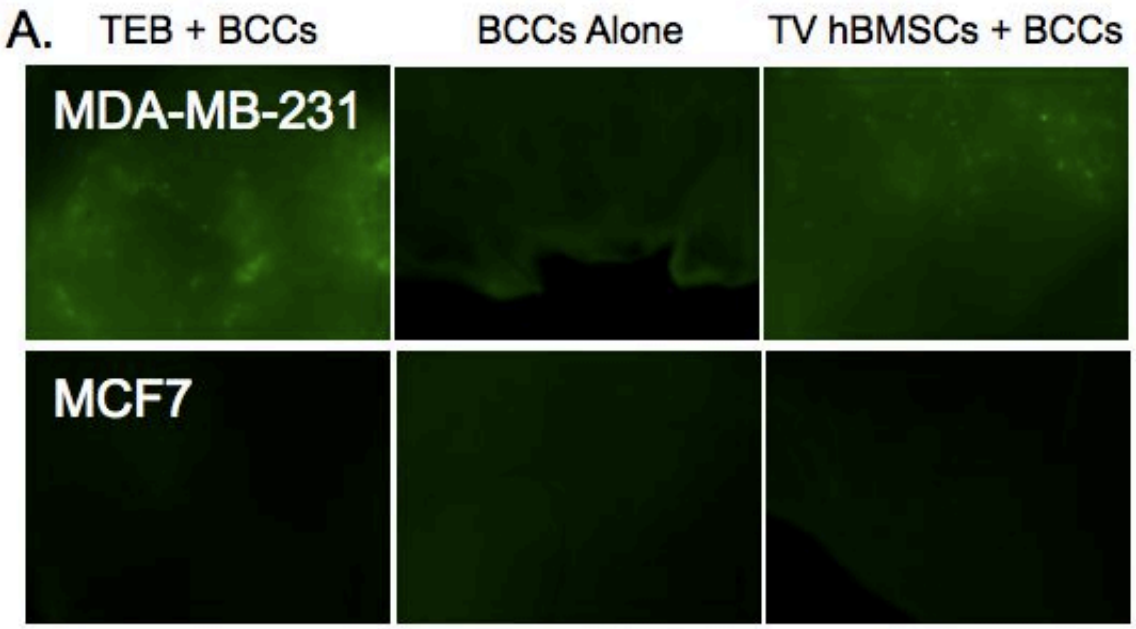
A.
TEB + BCCs
BCCs Alone
TV hBMSCs + BCCs
MDA-MB-231
MCF7

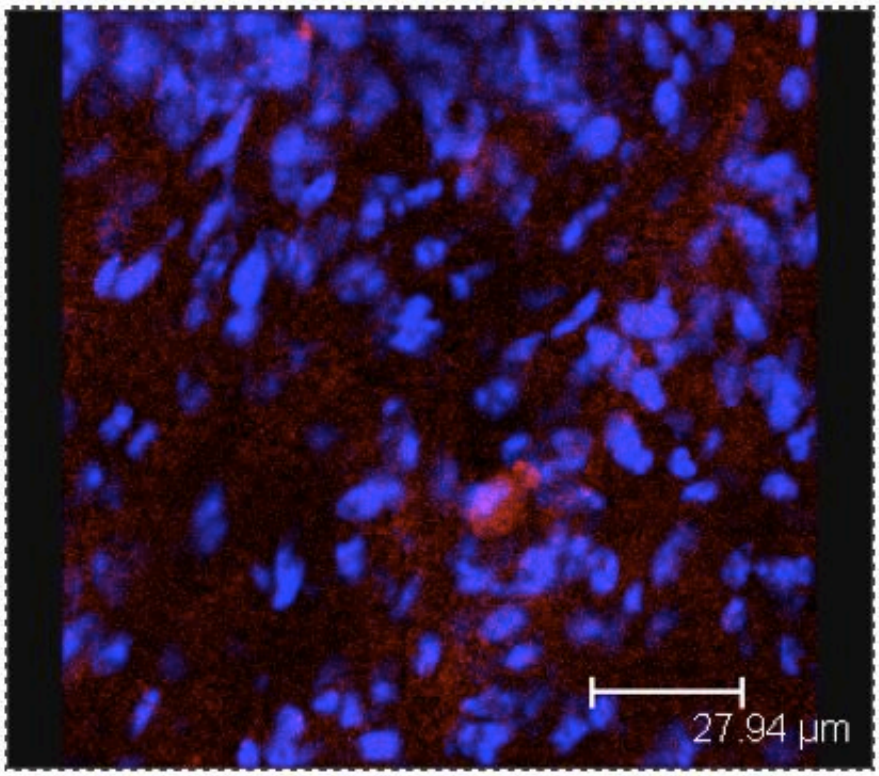
B.
27.94 µm

Figure 5-4. hBMSCs migrate to aggressive, metastatic breast cancer cell primary tumors. (A) GFP-labeled hBMSCs migrate towards MDA-MB-231 BCC primary tumors from subcutaneous TEB implantation (far left) and tail vein injection (far right), with no visible migration to MCF7 primary tumors. Primary tumors were grossly sectioned onto glass microscope slides and imaged on an upright-fluorescent microscope. Images are representative sections. For each group 3 primary tumors were sectioned into 4-5 sections. 3-4 images were taken of each section. (B) Confocal imaging of hBMSCs within primary tumors. DAPI (nuclear; blue) staining and DiD (hBMSC; red) visualization of frozen sectioned MDA-MB-231 primary tumor containing a DiD positive hBMSC. Image is representative of MDA-MB-231 primary tumors analyzed. For each group 4 primary tumors were analyzed.

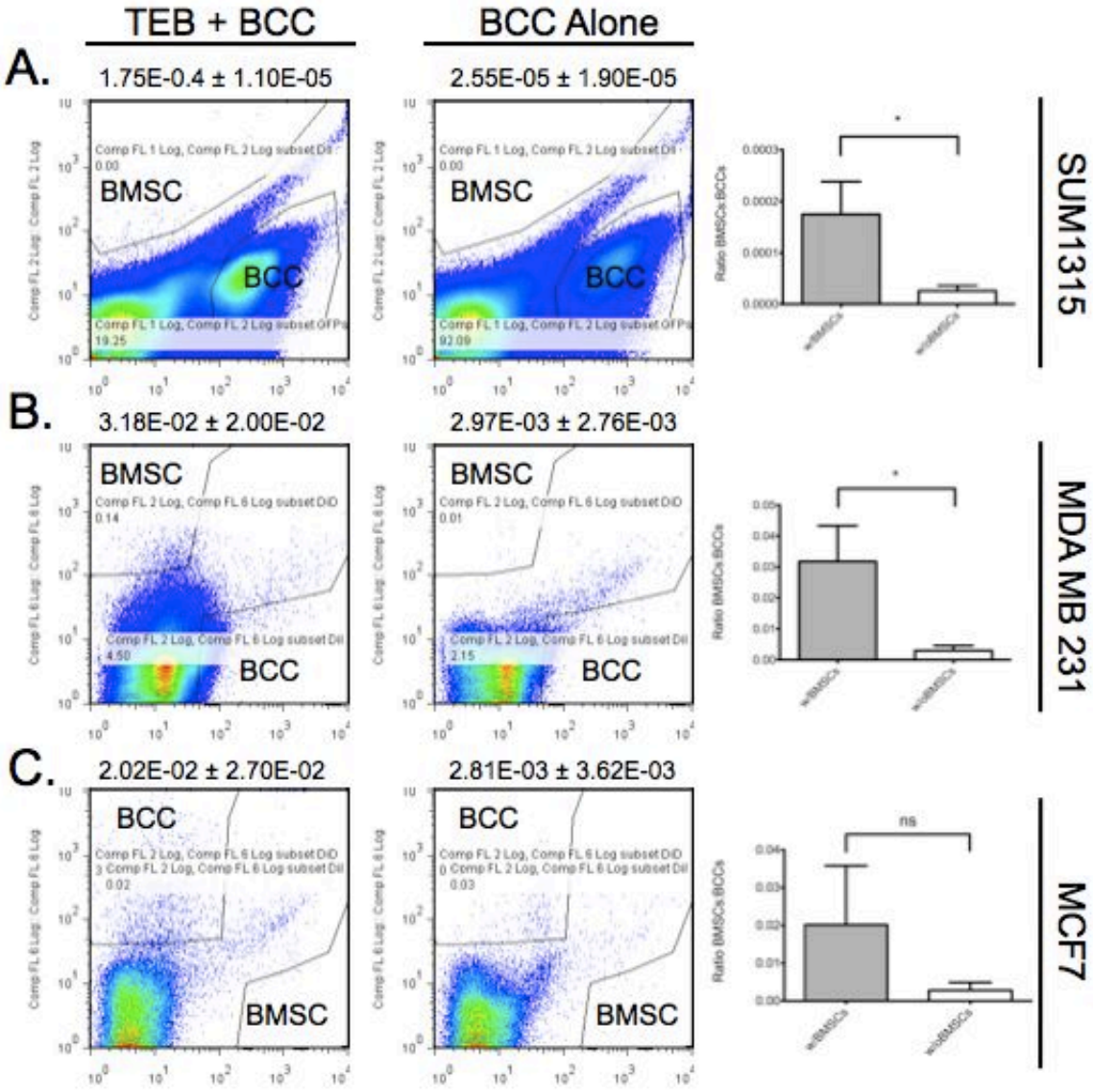
TEB + BCC
BCC Alone
A.
1.75E-0.4 ± 1.10E-05
2.55E-05 ± 1.90E-05
BMSC
BCC
SUM1315
B.
3.18E-02 ± 2.00E-02
2.97E-03 ± 2.76E-03
BMSC
BCC
MDA MB 231
C.
2.02E-02 ± 2.70E-02
2.81E-03 ± 3.62E-03
BCC
BMSC
MCF7
Ratio BMSCs:BCCs
ns

Figure 5-5. hBMSCs from the human bone environment migrate to orthotopic breast cancer cell tumors *in vivo*. Labeled hBMSCs migrate from the bone environment to SUM1315 (A) and MDA-MB-231 (B) BCC tumors, while no significant migration was observed with MCF7 BCC tumors (C). The gates used to identify positive hBMSCs and BCCs were created based on the fluorescence of positive controls (fluorescently-labeled single cell controls). The gates are presented for BCCs with engineered bone implanted (i) and BCCs without engineered bone implanted (ii), and the ratio of hBMSCs:BCCs in SUM1315 (A; $p=0.0407$), MDA-MB-231 (B; $p=0.0343$) and MCF7 (C; $p=0.1661$) primary tumors is shown (iii). Statistics performed with a one-sided Student's t-test.

TGF-β1 May Attract hBMSCs to Aggressive, Metastatic BCCs

Clinically, TGF-β1 is elevated in the plasma of breast cancer patients and has been linked to increased cancer progression and metastasis in a variety of ways (Teicher, 2001; Klopp et al., 2007). Additionally, TGF-β1 has been documented to act as a normal hBMSC chemoattractant in both *in vitro* migration assays and physiologic bone development (Tang et al., 2009). While many tumor-derived chemoattractants of hBMSCs have been discovered, we hypothesized that hBMSCs may also migrate to BCCs in response to elevated TGF-β1 levels (Lin et al., 2008; Ritter et al., 2008). Supporting this idea, MDA-MB-231 and SUM1315 BCCs that attract significant numbers of hBMSCs *in vitro* and *in vivo* secrete significantly more TGF-β1 protein when compared to MCF7 BCCs *in vitro* (Figure 5-6). Additionally, exogenous TGF-β1 can be used to attract hBMSCs in a transwell migration assay *in vitro.* Blockade of TGF-β1 in BCC- conditioned media or serum free media spiked with TGF-β1 using a neutralizing antibody significantly reduces hBMSC migration towards BCC-conditioned medium (Figure 5-6). Together, these results suggest a role for TGF-β1 secreted by aggressive cancer cells in recruiting hBMSCs to primary breast tumors.

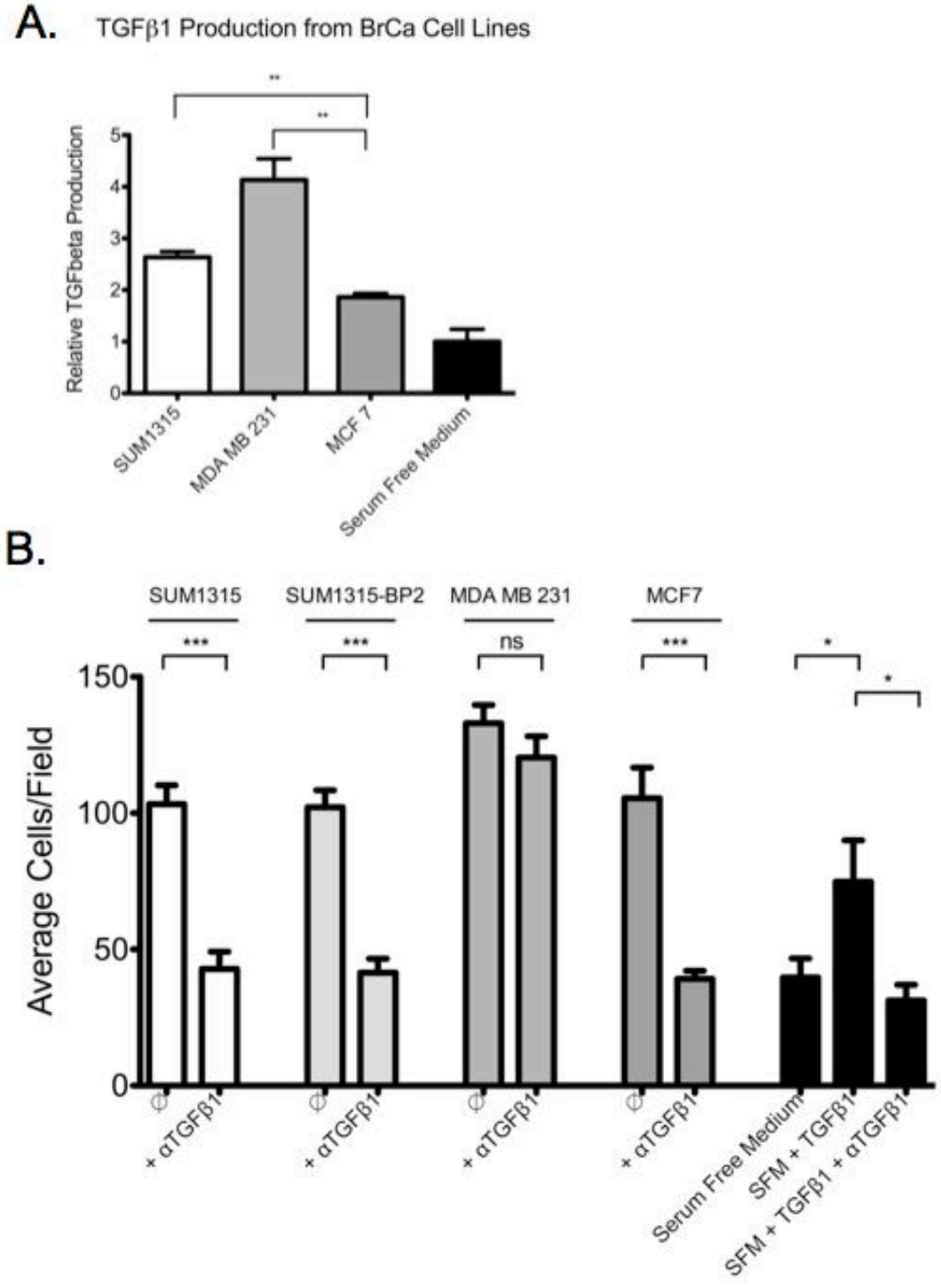
A.
TGFβ1 Production from BrCa Cell Lines
Relative TGFbeta Production
SUM1315
MDA MB 231
MCF 7
Serum Free Medium
B.
SUM1315
SUM1315-BP2
MDA MB 231
MCF7
Average Cells/Field
ns
Ø
+ αTGFβ1
Serum Free Medium
SFM + TGFβ1
SFM + TGFβ1 + αTGFβ1

Figure 5-6. TGF-β1 secretion from breast cancer cells may attract hBMSCs to the primary site. (A) Conditioned medium samples from more aggressive BCCs, i.e. SUM1315 ($p=0.0041$) and MDA-MB-231 ($p=0.0055$) contain increased levels of TGF-β1, when compared with weakly metastatic BCCs (MCF7). Conditioned medium was collected in serum free media for 48-hours from cells grown to 80% confluence (N=3 independent plates). The different media were concentrated 10X and TGF-β1 expression was quantified using ELISA (eBioscience). TGF-β1 levels are shown relative to serum free medium alone and analyzed using a two-sided Student's t-test. Data are represented as mean ± SEM. (B) Exogenous TGF-β1 can attract hBMSCs *in vitro* and a neutralizing antibody to TGF-β1 (α-TGF-β1) can block migration of hBMSCs towards BCC conditioned medium. Conditioned medium was collected in serum free medium for 72-hours from cells grown to 80% confluence. The different media were used as chemoattractants with or without α-TGF-β1 (60μg/ml). 30,000 serum-starved hBMSCs were plated above conditioned medium and allowed to migrate for 6-hours. Migration filters were fixed and stained and the number of cells migrated were counted from 3 fields of view/well and averaged. Addition of exogenous TGF-β1 (32 ng/ml) to serum free medium increases migration of hBMSCs, and this increased migration can be blocked by addition of α- TGF-β1. Analysis was done using a two-sided Student's t-test. Data are represented as mean ± SEM. N=5 or 6 for each group. *, $p<0.05$; ***, $p<0.001$.

hBMSCs Diversely Affect BCC Growth *in vitro* and *in vivo*

Many reports have shown contrasting effects of hBMSCs on the proliferation of different BCCs and other cancer cells (Karnoub et al., 2007; Sasser et al., 2007; Spaeth et al., 2009 Martin et al., 2010). We were interested in the effect of hBMSCs as well as other bone-derived cell types on the proliferation of the BCCs used in our studies. The SUM1315 human BCC line is highly aggressive and highly bone metastatic when implanted orthotopically in mice; dissemination to the lung occurs only in late stage disease, i.e. greater than 10-weeks (Kuperwasser et al., 2005; Moreau et al., 2007; Liu et al., 2009). When cultured with conditioned medium from a variety of bone-derived cell types (i.e., hBMSCs, bone marrow-derived endothelial cells, osteoblasts and osteoclasts), SUM1315 cells demonstrated increased proliferation (Figure 5-7, left). In contrast, MDA-MB-231 BCCs demonstrate widely distributed metastasis to many organs, both visceral and skeletal, when implanted orthotopically (Figure 5-8). When cultured in bone-derived cell-conditioned media no proliferative response was seen *in vitro* for MDA-MB-231 BCCs (Figure 5-7, left). The weakly metastatic MCF7 BCC line demonstrated a decrease in proliferation when cultured in hBMSC- and osteoclast-conditioned media, suggesting a unique response of BCCs to hBMSCs and other bone-derived cell types depending on their metastatic propensity and tissue tropism (Figure 5-7, left).

Unlike previous *in vivo* models using subcutaneous implantation to analyze the *in vivo* affect of hBMSCs on BCC proliferation, we utilized orthotopic implantation of BCCs and hBMSCs to assess *in vivo* proliferative changes. The local tumor environment has been well documented to affect cancer growth and progression, and accurate

modeling of tumor-stroma interactions has been shown to alter breast epithelial tumorigenesis and progression (Weaver & Bissel, 1999; Schedin & Elias, 2004; Barksy & Karlin, 2006). Consistent with our *in vitro* findings, SUM1315 BCCs co-injected with hBMSCs in the orthotopic location showed significantly increased tumor growth when compared to BCCs injected alone, whereas no differences in proliferation were found for the MDA-MB-231 BCC tumors with or without hBMSCs (Figure 5-7, right). Co-injection of hBMSCs with MCF7 BCCs *in vivo* resulted in slowed proliferation of MCF7s, which also mirrored our *in vitro* findings (Figure 5-7, right). Primary tumors were monitored by bioluminescence over 8-weeks, and primary tumor growth was normalized to week 1 luminescence. These data further suggest that bone-derived cells can influence tumor growth and may affect cancer cells differently based on their metastatic frequencies and tissue tropisms.

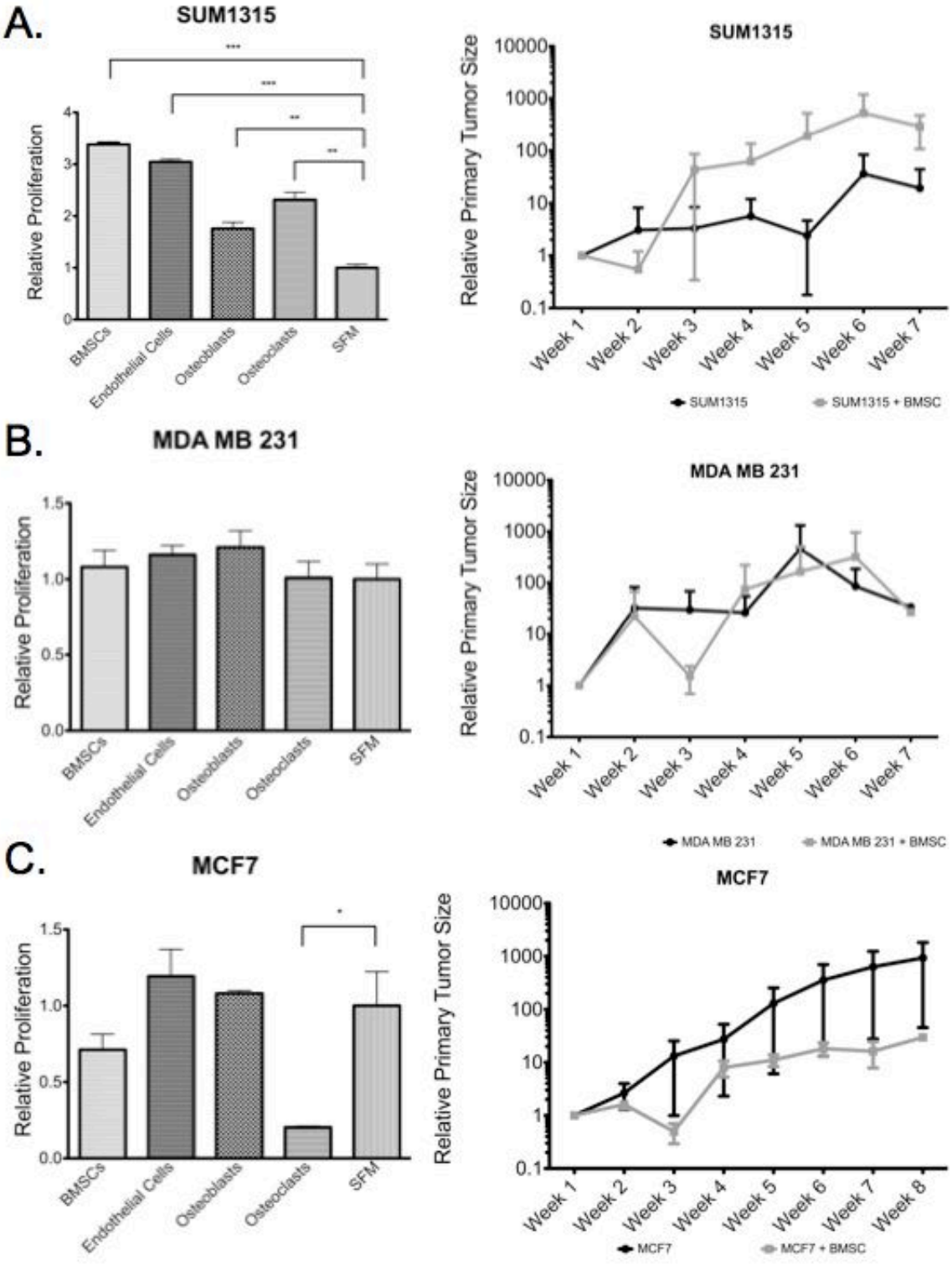
A.
SUM1315
Relative Proliferation
BMSCs
Endothelial Cells
Osteoblasts
Osteoclasts
SFM
SUM1315
Relative Primary Tumor Size
Week 1
Week 2
Week 3
Week 4
Week 5
Week 6
Week 7
SUM1315
SUM1315 + BMSC
B.
MDA MB 231
Relative Proliferation
BMSCs
Endothelial Cells
Osteoblasts
Osteoclasts
SFM
MDA MB 231
Relative Primary Tumor Size
Week 1
Week 2
Week 3
Week 4
Week 5
Week 6
Week 7
MDA MB 231
MDA MB 231 + BMSC
C.
MCF7
Relative Proliferation
BMSCs
Endothelial Cells
Osteoblasts
Osteoclasts
SFM
MCF7
Relative Primary Tumor Size
Week 1
Week 2
Week 3
Week 4
Week 5
Week 6
Week 7
Week 8
MCF7
MCF7 + BMSC

Figure 5-7. hBMSCs diversely affect BCC growth *in vitro* and *in vivo*. (A) BCCs were cultured in conditioned medium from bone-derived cells for 48-hours. Data are represented as mean ± SEM. *, $p<0.05$; **,$p>0.01$; ***, $p<0.001$.(B) SUM1315 ($p=0.0122$) and MDA-MB-231 ($p=0.9282$) BCCs were injected alone or with hBMSCs into the mammary fat pad. Tumor volume was measured with bioluminescent imaging weekly. Data are normalized to week 1 bioluminescence and represented as mean + S.E.M. N=5 for all groups. Statistics performed using 2-way ANOVA.

hBMSCs Affect Migration and Metastasis of BCCs *in vitro* and *in vivo*

Tumor growth rates are not necessarily indicative of metastatic outcomes. We were interested in understanding how hBMSCs can alter tumor cell migration and metastasis, independent of their affect on proliferation. Previous reports have demonstrated that subcutaneous co-injection of hBMSCs and MDA-MB-231 BCCs results in an increase in lung metastasis frequency and co-culture of hBMSCs with BCCs can promote *in vitro* migration (Karnoub et al., 2007; Dittmer et al., 2009). Consistent with these findings, we observed that indirect co-culture of hBMSCs with MDA-MB-231 BCCs resulted in increased migration of BCCs *in vitro*, while SUM1315 BCCs demonstrated a decrease in migration (Figure 5-8).

To assess metastasis *in vivo*, specifically to bone, we utilized the humanized model of breast cancer metastasis to bone. This model introduces a human bone microenvironment complete with human cytokines, hBMSCs and other bone cells, and incorporates the more subtle aspects of human tumor and human marrow interactions, providing a better platform to assess tumor-stroma interactions in the context of metastasis. The model revealed that co-injection of MDA-MB-231 BCCs and hBMSCs into the mammary fat pad resulted in an increased frequency of metastasis to the human bone, lung and liver (Figure 5-8). Similar to our *in vitro* results, no increase in metastasis frequency was observed for SUM1315 BCCs co-cultured with hBMSCs, despite their proliferative advantage.

As described above, the SUM1315 BCC line was passaged twice through human bone to create the SUM1315-BP2 cell line with a unique gene expression signature that

represents a “bone-educated” and, possibly, bone-dependent cell line (Figure 1-2). When co-cultured with hBMSCs, SUM1315-BP2 BCCs demonstrate similar proliferative changes to parental SUM1315 BCCs *in vivo* (Figure 5-9) and can attract hBMSCs in a TGF-β1-dependent manner, similar to SUM1315 BCCs (Figure 5-6). Indirect co-culture of SUM1315-BP2 BCCs with hBMSCs led to an increase in migration, and when co-injected with hBMSCs in the orthotopic location, SUM1315-BP2 BCCs showed an increase in skeletal metastasis frequency (Figure 5-8).

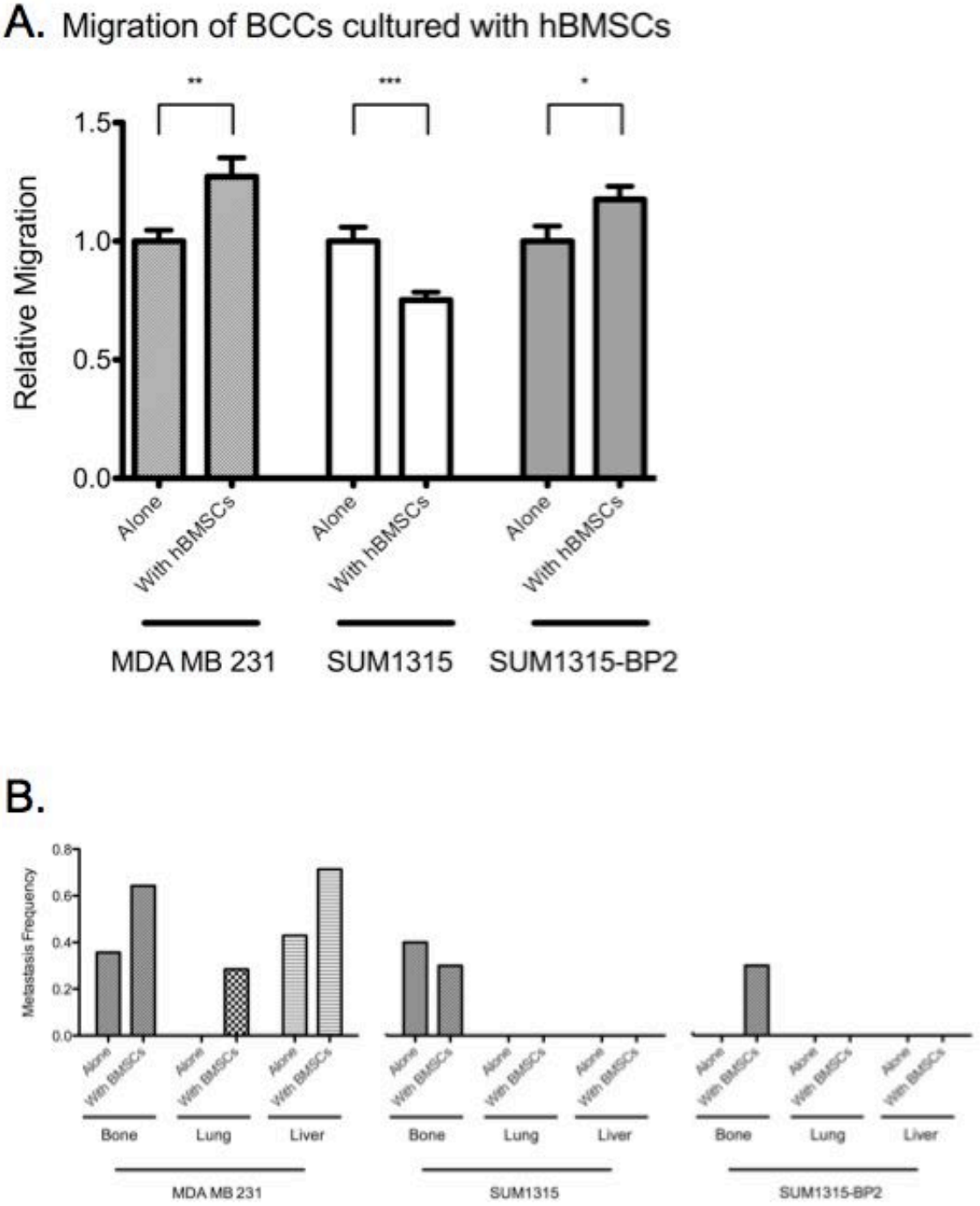
A. Migration of BCCs cultured with hBMSCs
**
***
*
1.5
1.0
0.5
0.0
Relative Migration
Alone
With hBMSCs
Alone
With hBMSCs
Alone
With hBMSCs
MDA MB 231
SUM1315
SUM1315-BP2
B.
Metastasis Frequency
0.8
0.6
0.4
0.2
0.0
Alone
With BMSCs
Bone
Lung
Liver
MDA MB 231
SUM1315
SUM1315-BP2

Figure 5-8. hBMSCs affect migration and metastasis of breast cancer cells *in vitro* and *in vivo*. (A) MDA-MB-231 (p=0.0040), SUM1315 (p=0.0005) and SUM1315-BP2 (0.0397) BCCs were grown in hBMSC serum free conditioned media for 24-hours. BCCs were allowed to migrate for 6-hours. Values represent average number of cells, normalized to cancer cell samples without hBMSCs for each BCC line. (B) BCCs were injected alone or with hBMSCs into the mammary fat pad of 10-week-old NOD/Scid female mice harboring implanted human bone cores. After 10 weeks mice were sacrificed and human bone cores, lungs and livers were analyzed for metastases using bioluminescence. Metastases were counted and frequency was calculated by dividing number of metastatic samples by total number of samples. N=7 for MDA-MB-231 groups. N=6 for SUM1315 and SUM1315-BP2 with hBMSC groups. N=5 for SUM1315 and SUM1315-BP2 alone groups.

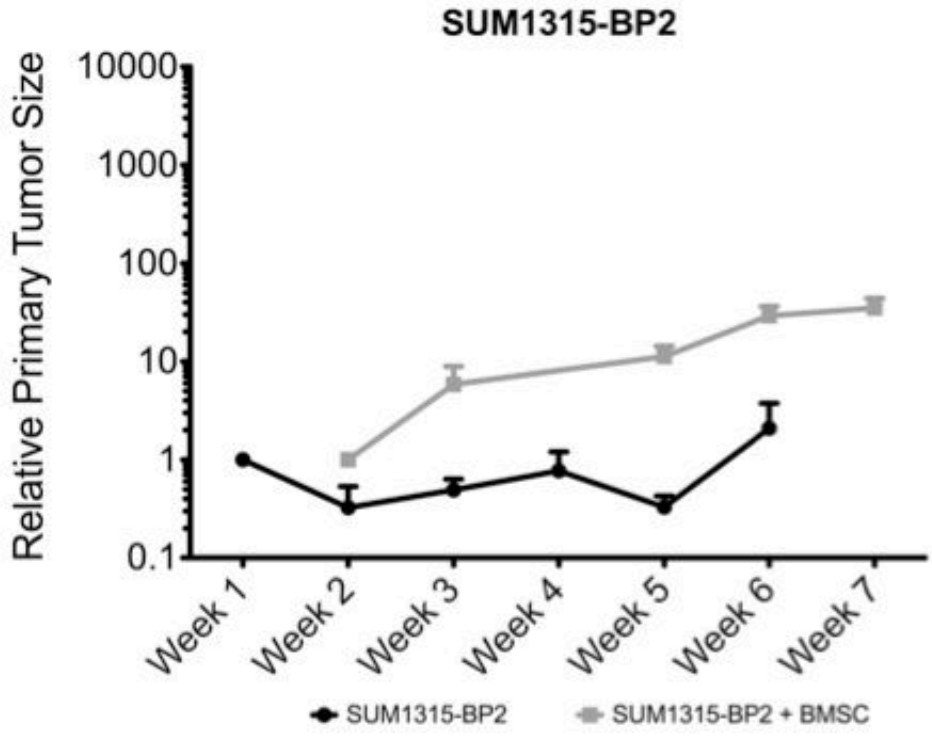

Figure 5-9. hBMSCs promote SUM1315-BP2 growth *in vivo.* 500,000 SUM1315 -BP2 BCCs were injected alone or with 1,500,000 hBMSCs into the mammary fat pad. Tumor volume was measured with bioluminescent imaging weekly. Data are normalized to week 1 bioluminescence and represented as mean + S.E.M. N=5 for all groups. Statistics performed using two-sided Student's T-test on endpoint (Week 6). p=0.0003.

IL-17B Stimulation Can Drive Migration But Not Proliferation

The gene expression signature of SUM1315-BP2 BCCs is enriched for genes that may promote metastasis (Table 1-1; described in detail above). One of these genes, *il-17br*, has been reported as a prognostic indicator of breast cancer progression and metastasis, and along with its ligand, *il-17b*, has been linked to bone turnover and degradation, as well as tumor progression (Dunn & Demichele, 2009; Jung et al., 2009, Huang et al., 2009). Of note, hBMSCs secrete IL-17B protein (Kokubu et al., 2008). We hypothesized that hBMSCs may stimulate proliferative and migratory changes in BCCs via IL-17B/IL-17BR signaling.

Using the humanized model of breast cancer metastasis to bone we showed that *il-17br* was consistently over-expressed in skeletal metastases from different BCC lines (SUM1315, SUM1315-BP2, MDA-MB-231, BoM2) when compared to their matched primary tumors, and was over-expressed greater than 10-fold in human bone core metastases from the SUM1315-BP2 and BoM2 BCC samples (Figure 4-3). These data suggest that IL-17B/IL-17BR signaling may be important in BCC interactions within the bone microenvironment, including with bone marrow-residing hBMSCs.

Stimulation of BCCs with IL-17B had no significant affect on proliferation, but did significantly increase migration of SUM1315, SUM1315-BP2 and MDA-MB-231 BCCs (Figure 5-10). Coupled with our findings that *il-17br* over-expression in BCCs increases the frequency of metastasis, these data suggest a possible mechanism by which recruited hBMSCs may stimulate different BCCs to metastasize, namely that IL-17B secretion from hBMSCs stimulates migration of BCCs through IL-17BR.

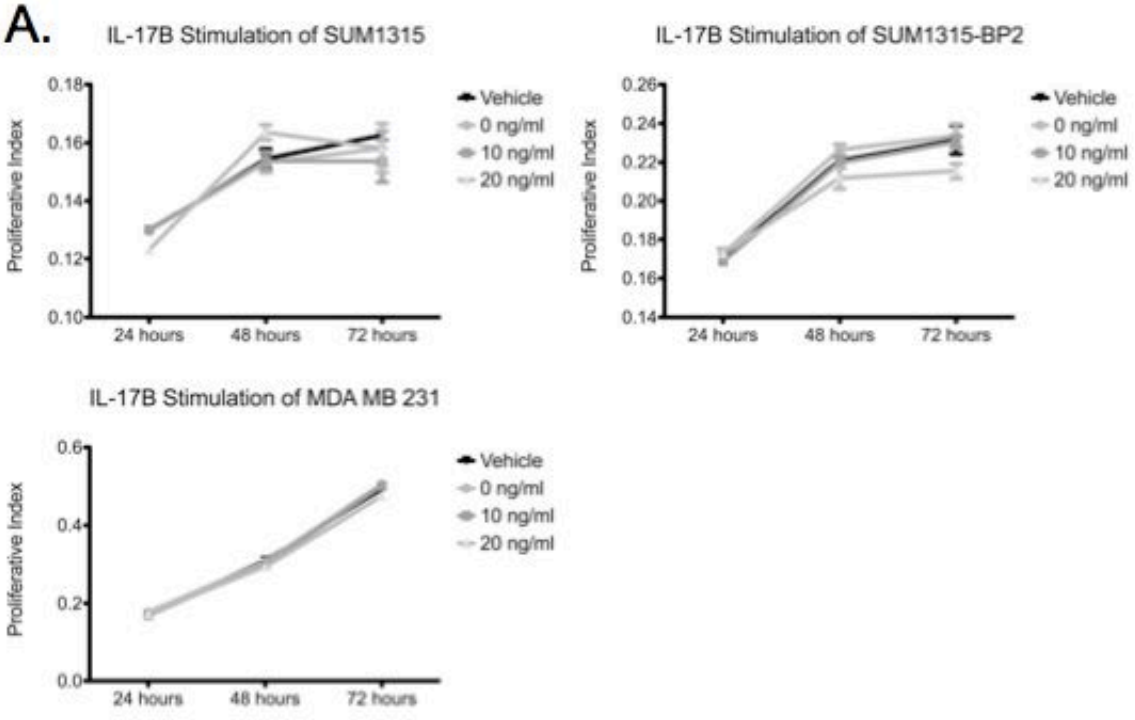
A.
IL-17B Stimulation of SUM1315
Proliferative Index
0.18
0.16
0.14
0.12
0.10
24 hours
48 hours
72 hours
Vehicle
0 ng/ml
10 ng/ml
20 ng/ml
IL-17B Stimulation of SUM1315-BP2
Proliferative Index
0.26
0.24
0.22
0.20
0.18
0.16
0.14
24 hours
48 hours
72 hours
Vehicle
0 ng/ml
10 ng/ml
20 ng/ml
IL-17B Stimulation of MDA MB 231
Proliferative Index
0.6
0.4
0.2
0.0
24 hours
48 hours
72 hours
Vehicle
0 ng/ml
10 ng/ml
20 ng/ml

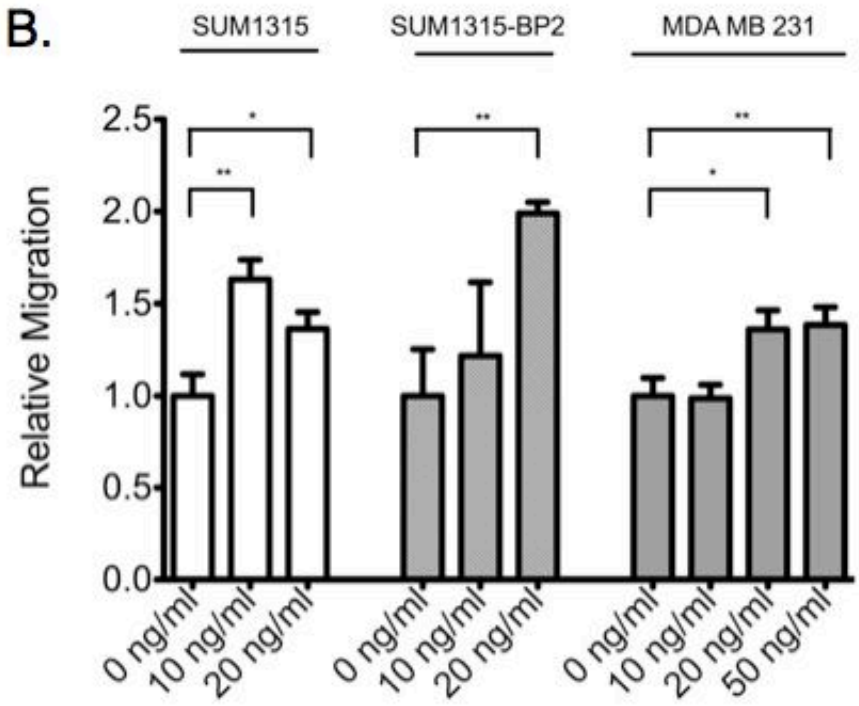
B.
SUM1315
SUM1315-BP2
MDA MB 231
Relative Migration
2.5
2.0
1.5
1.0
0.5
0.0
*
**
**
**
*
0 ng/ml
10 ng/ml
20 ng/ml
0 ng/ml
10 ng/ml
20 ng/ml
0 ng/ml
10 ng/ml
20 ng/ml
50 ng/ml

Figure 5-10. IL-17B stimulation of IL-17BR can drive migration but not proliferation. (A) SUM1315, MDA-MB-231 and SUM1315-BP2 BCCs were stimulated with 0, 10, 20, or 50 ng/ml of IL-17B (R&D Systems). Proliferation was assessed using an MTT-based assay (Roche) at 24-, 48- and 72-hours. No significant difference in proliferation was observed. (B) Serum-starved BCCs were stimulated with 0, 10, 20 or 50 ng/ml of IL-17B (R&D Systems) and allowed to migrate for 6-hours. Two-sided Student's t-test. Data are represented as mean ± SEM. *, $p<0.05$; **, $p<0.01$.

Chapter 6

Discussion

Summary of Results

The humanized model of breast cancer metastasis to bone has successfully been used to study the unique roles of the primary tumor and the bone microenvironment in breast cancer metastasis to the human skeleton. Overlapping roles for genetic changes within the primary tumor and cellular components of the bone microenvironment have been identified that link the primary tumor and metastatic niche. Preliminary studies confirmed that within the humanized model of breast cancer metastasis the human bone microenvironment remains completely humanized, with no detectable mouse-derived cell infiltration into the human bone (Figure 3-1). Additionally, by using more sensitive detection methods, it was shown that the metastasis model can be used to study multiple BCC lines and metastasis to different organs, i.e. human bone, mouse bone, mouse liver, and mouse lungs, as well as analyze genetic changes of metastases compared with matched, orthotopic primary tumor cells (Figure 3-3; Figure 4-1).

Animal models have been used to generate gene signatures representative of highly metastatic BCCs. Using the humanized mouse model, we showed that these signatures do not necessarily represent conserved genes required for efficient metastasis to both human and mouse bone (Figure 4-1). Instead, gene expression was mixed across different cell lines and within different metastatic sites. Only *mmp-1* and *il-17br* were consistently over-expressed in all metastatic sites from the different BCCs tested, independent of the method of tumor cell inoculation (i.e., orthotopic or intracardiac injection) (Figure 4-1; Figure4-2). Forced *il-17br* over-expression in BCCs leads to significant increases in migration and metastasis, with no significant change in

proliferation (Figure 4-4; Figure 4-5). Additionally, stimulation of BCCs with IL-17B, the ligand for *il-17br*, drives migration of BCCs *in vitro* (Figure 5-10).

In addition to genetic changes that affect primary tumor progression and metastasis frequency, the humanized mouse model has been used to study the influence of hBMSCs and other bone-derived cells on BCCs. hBMSCs from a human bone environment can migrate to BCCs, both *in vitro* and when implanted as orthotopic primary tumors (Figure 5-2; Figure 5-4; Figure 5-5). TGF-β1 expression from BCCs can act as a chemoattractant for hBMSCs *in vitro* (Figure 5-6). Once at the primary tumor, hBMSCs promote BCC growth and migration (Figure 5-7; Figure 5-8; Figure 5-9). hBMSCs secrete IL-17B during maturation and may stimulate BCC migration and metastasis via IL-17B/IL-17BR interactions (Figure 5-10; Figure 6-1, model).

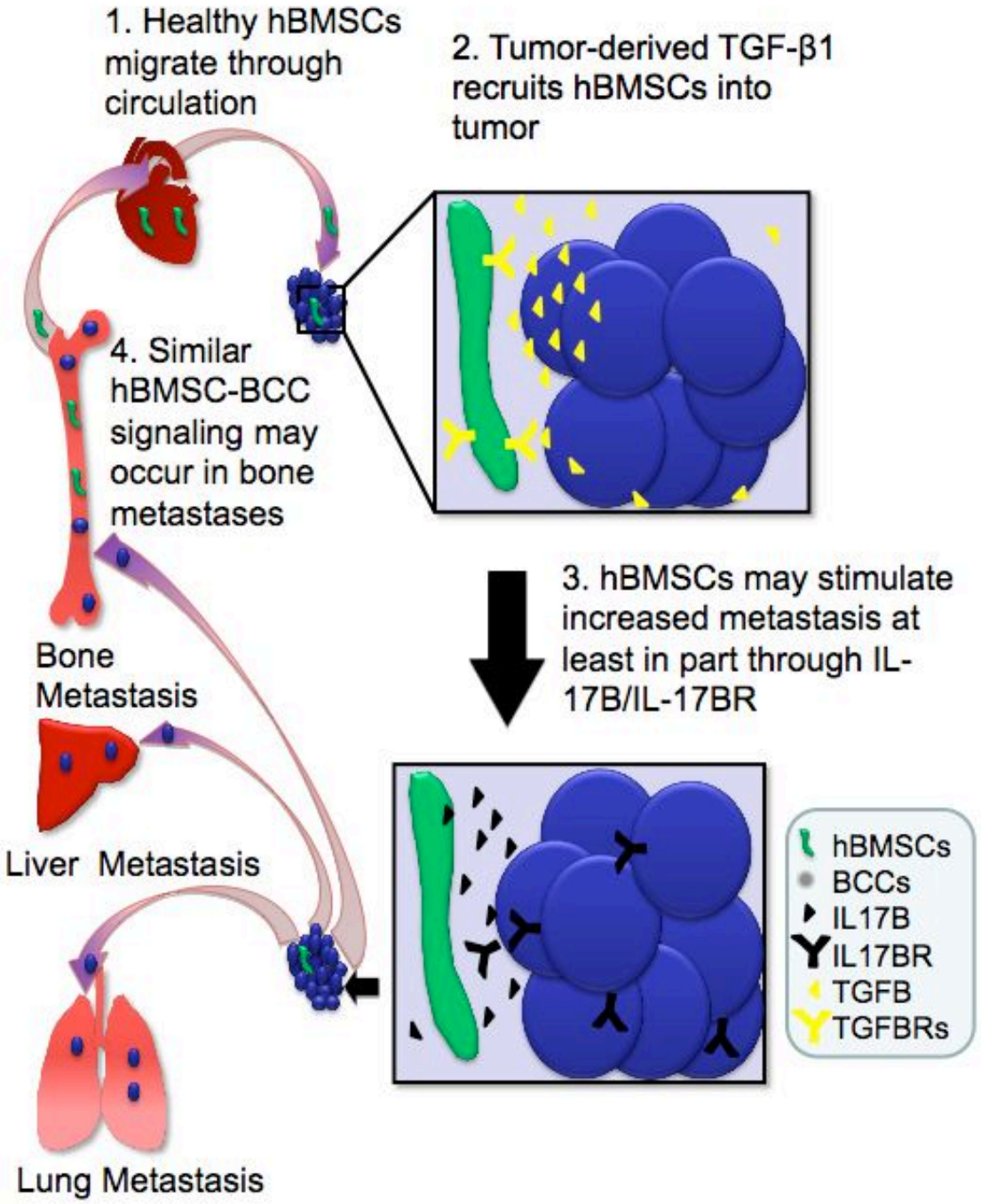
1. Healthy hBMSCs migrate through circulation
2. Tumor-derived TGF-β1 recruits hBMSCs into tumor
4. Similar hBMSC-BCC signaling may occur in bone metastases
3. hBMSCs may stimulate increased metastasis at least in part through IL-17B/IL-17BR
Bone Metastasis
Liver Metastasis
Lung Metastasis
hBMSCs
BCCs
IL17B
IL17BR
TGFB
TGFBRs

Figure 6-1. Schematic of proposed role of hBMSCs in primary breast tumor growth and metastasis. Healthy mesenchymal stem cells from the bone marrow migrate through the circulation and are attracted to breast tumors due to increased TGF-β1 secretion. Once at the primary tumor, hBMSCs secrete IL-17B into the microenvironment. BCCs with increased *il-17br* expression are stimulated to migrate, resulting in increased visceral and skeletal metastases. Similar hBMSC-BCC interactions may occur in the bone marrow, leading to increased osteolysis, metastasis expansion, and further dissemination.

Genomics of the Primary Tumor vs. the Metastasis

One advantage the humanized model of breast cancer metastasis has over other animal models used to study osteotropism is the ability to analyze matched primary tumors and metastases. Using the humanized model we showed that gene expression levels from metastatic samples rarely resemble the expression of the primary tumor, suggesting that genetic aberrations necessary for oncogenesis are not sufficient for metastasis, or that dissemination to a foreign soil results in further genetic adaptations of cancer cells. These findings are not surprising, as the primary tumor and metastatic (i.e bone) microenvironments are very different, and the processes of tumor cell detachment, homing and arrest require very different genetic tools than tumor expansion at the primary site. It is likely that subsets of primary tumor cells acquire the genetic changes necessary for metastasis to specific organs. Additionally, once the tumor "seed" reaches the metastatic "soil," cancer cells may continue to adapt and acquire additional genetic changes that enhance cell survival and proliferation within distinct stroma.

Recently, massively parallel sequencing technologies have made it easier, and more cost effective, to study genetic changes of two matched samples at increasingly higher resolutions. Analysis of a matched breast cancer primary tumor and brain metastasis from a patient revealed unique genomic changes in the metastasis in addition to the underlying oncogenic genetic triggers (Ding et al., 2010). The changes included specific genetic aberrations in genes previously linked to cancer progression, novel genetic changes that require further analysis, and whole genome rearrangements, including copy number changes, that alter the genomic profile of the metastatic cells.

Ding and colleagues also implanted the primary BCCs in an orthotopic xenograft model in immunocompromised mice and compared any genomic changes associated with mouse engraftment with the primary tumor and metastasis (Ding et al., 2010). Interestingly, the xenograft tumors retained the genetic mutations of the primary tumor, while also displaying a pattern of genomic changes resembling the metastasis, suggesting that growth in a foreign soil, whether a distant organ or different species, activates similar genetic hotspots.

The genomic changes found in the metastatic and xenograft samples still need to be functionally validated, but their discovery highlights the power of matched primary and metastatic tumors coupled with high-resolution, massively parallel sequencing technology. The report by Ding et al. relied on a single patient sample, while the humanized animal model provides nearly unlimited matched primary tumor and metastatic samples (Ding et al., 2010). Skeletal metastases are rarely surgically resected from breast cancer patients and thus, comparison with a patient's matched primary tumor is difficult. Using an animal model, whole genome comparisons can be made between primary tumors, human bone metastases and metastases to different mouse organs resulting in the confirmation and discovery of genes involved in tissue- and species-specific tropism.

Differences Between Human and Mouse Gene Signatures

Kang et al. reported four genes that enhanced the skeletal metastatic frequency of BCCs, while similar reports have identified genes implicated in lung and brain metastasis

using the same MDA-MB-231 breast cancer cell line (Kang et al. 2003; Minn et al., 2005; Bos et al., 2009). These studies support the concept that genes responsible for tissue-tropism are superimposed on a platform of genes generally responsible for an aggressive phenotype characterized by migration and invasion. By using serial passages of BCCs in mouse skeleton, brain, or lung, these reports generated subpopulations of human BCCs derived from the MDA-MB-231 line that metastasized with a high propensity to the respective organs. For example, the lung-trophic cells have an order of magnitude higher propensity to metastasize to the lung when compared to the parental cells, but no enhanced tropism for the bone or brain (Minn et al., 2005). Transcriptome profiling of these sublines revealed a small set of organ-specific genes that differ completely from a "poor prognosis" gene signature derived from the MDA-MB-231 parental line, and share little overlap with each other (Van't Veer et al., 2002).

The gene set we identified using serial passage through human bone and the SUM1315 human breast cancer cell line has no overlap with the osteotropism set identified by Kang et al. or the "poor prognosis" signature (Van't Veer et al., 2002; Kang et al., 2003). It is possible that different human tumors even of the same tissue type use different osteotropism genes. However, the functional categories represented in each set are similar: homing, invasion, angiogenesis and osteoclast-mediated osteolysis (Figure 4-1). Although the functions are similar, differences in specific genes between the two sets likely arise because of the species origin of the tissue analyzed (i.e. human vs. mouse).

Influence of hBMSCs in the Bone Environment

In addition to their role in microenvironment remodeling and supporting tumor growth, hBMSCs within the bone may be playing a larger role in tumor progression at the primary and other metastatic sites. Recently, primary tumors have been described as "conglomerates of self-metastases" or a collection of self-metastasizing cancer cells that continually shed and accumulate circulating tumor cells (CTCs) (Enderling et al., 2009). Kim et al. hypothesized that CTCs can easily colonize their tumor of origin without much adaptation (Kim et al., 2009). They demonstrated that not only can orthotopically implanted BCCs efficiently self-seed genetically identical contralateral primary tumors, but metastatic foci can release CTCs with the ability to seed a parental primary tumor; lung metastases shed CTCs that migrated to parental primary tumors in the mammary fat pad. Increased tumor self-seeding leads to increased tumor proliferation, vascularization, and recruitment of stromal cells, and has been linked with aggressive primary tumor growth, local recurrence and poor prognosis.

hBMSC stimulation of BCCs in the bone microenvironment could accelerate tumor self-seeding. We have shown that hBMSCs can migrate to primary breast cancer tumors at the orthotopic location, and that in the mammary fat pad, hBMSCs can increase BCC growth and migration (Figure 5-4; Figure 5-5; Figure 5-7; Figure 5-8). hBMSCs are a major component of the bone microenvironment. Once BCCs colonize the skeleton, they again will be surrounded by hBMSCs and can be directly influenced by them, leading to increased metastasis growth and migration of BCCs from the bone

environment back to the primary tumor. Additionally, we have demonstrated that other cellular components of the bone environment can have a direct affect on BCC growth kinetics, resulting in larger metastatic foci and an increased source of self-seeding CTCs (Figure 20).

In addition to promoting tumor self-seeding, hBMSCs may drive colonization of other distant metastases. Working with a large metastatic prostate cancer cohort, Liu et al. recently demonstrated that metastatic prostate lesions arise from a clonal index lesion (Liu et al., 2009). Using high resolution comparative genomic analyses they demonstrated the nearly identical genetic relationship between index prostate cancer lesions and metastatic foci from various organs, including the skeleton. One explanation for this gene expression pattern is direct clonal expansion of prostate cancer cells, i.e. spread from the primary prostate lesion to various organs throughout the body. Another explanation is indirect clonal expansion, or spread of a metastatic lesion to other sites throughout the body, including the initial tumor. Given the ability of hBMSCs and other bone-derived cells to promote tumor growth and migration, it is likely that this type of indirect expansion can efficiently occur in metastatic disease and lead to distant metastases that are derived from a "parental" skeletal metastasis.

Heterogeneity of the Human Bone Fragments

While the initial publication of the humanized model of breast cancer metastasis to bone, as well as other models that utilize subcutaneous implantation of human bone, detailed the viability and functionality of the different bone cores used our results

demonstrate variability between different bone samples (Nemeth et al., 1999; Kuperwasser et al., 2005; Yang et al., 2007). The frequency of metastasis to the human bone core was often different between experiments (compare Figure 4-6 and 5-8). The cells used came from similar frozen stocks, and were passaged equivalent times *in vitro* prior to inoculation. The bone cores for each experiment came from different patient samples, and most likely provide the key to the variability in these experiments.

Human femoral heads that are obtained for the humanized model vary widely in their size, disease status, vasculature and underlying genetic identity; samples are obtained without links to age, gender, patient health or reason for surgery. Visual comparison of different bone cores demonstrates their gross differences, while further molecular techniques could compare their underlying genetic and physiologic differences. It is likely that a variety of factors affect the ability of the bone core to serve as a target for metastasis.

First, the disease status and vasculature of the bone core are critical to engraftment and survival. Some bone cores are clearly affected by avascular necrosis, a disease of bone death caused by poor blood supply, and are excluded from our studies. Other bones have signs of osteoarthritis that limit blood supply to portions of the femoral head. Still other femoral heads have variable blood supply to sections of the bone, resulting from uneven distribution of blood vessels. At the time of isolation, serious efforts are taken to ensure that all bone cores isolated for each experiment come from relatively homogenous areas of vascularization, as well as mineralization, within the bone.

Second, as was previously demonstrated, the immune response from the implanted bone core limits the growth of metastatic cells (Kuperwasser et al., 2005). Irradiation of the human bone core prior to implantation increased the frequency and size of metastases detected. Each bone core will induce a different immune response to the surrounding mouse tissue and invading human breast cancer cells, resulting in differences in the frequency and size of metastases.

In addition to the blood supply and immune response, the underlying genetics of the donor patient may affect metastasis frequency. While as of this writing no study has looked at germline genetic predispositions to bone metastases, it is likely that genetic markers will be discovered that correlate with susceptibility to bone metastasis. A large number of metastatic breast cancer patients develop skeletal metastases (as detailed above), but a significant fraction of patients will never develop skeletal complications, and an even larger percentage will develop only micrometastatic disease. In the future, the humanized model of breast cancer metastasis to bone can be used to study genomic markers that may increase a patient's risk for developing metastatic disease, either through high thru-put whole genome sequencing or SNP-array analysis. Identification of markers of metastasis susceptibility will provide enormous clinical benefit, allowing targeted patient populations to receive necessary treatments, while saving others from debilitating side effects of therapeutics.

Clinical Implications: Genetic Markers of Metastasis

In addition to identification of germline genetic markers of metastasis

susceptibility, the humanized model of metastasis has provided a platform to study the gene expression changes that are associated with breast cancer metastasis to bone. Of the genes identified in both gene signatures, only *il-17br* had not been studied in the context of forced expression and *in vivo* metastasis. The remaining genes have all been confirmed either to drive metastasis via over-expression, or decrease metastatic frequency by gene knockdown. IL-11 plays an important role in stimulating osteoclast maturation from premature cells and driving bone resorption, and while the specific physiologic role of IL-11 in the context of other physiologically relevant stimulators of bone resorption (e.g. IL-1, IL-6, PTHrP, and TNF) is not completely clear, in the context of metastatic breast cancer, cells over-expressing *il-11* along with *opn* result in a significant increase in the frequency of metastasis in an intracardiac injection model (Manolagas, 1995; Kang et al., 2003).

Both MMP-1 and MMP-13 are collagenases, capable of breaking down the abundant extracellular protein within the bone matrix and their transcription is repressed by the tumor suppressor p53, resulting in dysregulation in the context of cancer growth (Sun et al., 1999; Sun et al., 2000). Over-expression of *mmp-1* has been linked with various stages of tumor progression and can drive skeletal metastasis of BCCs (Kang et al., 2003; Lu et al., 2009; Yang et al., 2009). Recently, through analysis of the tumor-bone interface in a direct skeletal injection model of bone metastasis, MMP-13 has been implicated in tumor-induced osteolysis. Knockdown of *mmp-13* in BCCs at the tumor-bone interface lead to decreased bone destruction and abrogated MMP-9, RANKL, and TGF-β signaling (Nannuru et al., 2010).

Through it's role in remodeling and stimulating the extracellullar matrix, CTGF is able to drive angiogenesis and tumor progression as well as increase the frequency of BCC metastasis. Similarly, the SNF1-related protein kinase, HUNK plays a role in mammary gland development and is required for efficient primary tumor escape and breast cancer metastasis to the lung, possibly through it's ability to remodel the extracellular matrix and promote motility (Wertheim et al., 2009). Among other roles in tumor progression, CXCR4 has a well documented role in breast cancer metastasis (Burger & Kipps, 2006). Neutralization of the CXCR4/CXCL12 cascade in mice can block metastasis, and over-expression of the *cxcr4* receptor lead to an increase in metastasis frequency (Müller et al, 2001; Kang et al., 2003).

IL-17B and its receptor IL-17BR were initially discovered in a blind screen of novel cytokines and receptors and linked to intestinal inflammation and neutrophil infiltration (Shi et al., 2000). A closely related cytokine, IL-17E, was also discovered as a ligand for IL-17BR, leading to NF-κB activation and further cytokine production (Lee et al., 2001). Tissue distribution of IL-17B, IL-17E and IL-17BR are limited, but both IL-17B and IL-17E stimulation of IL-17BR have been linked to rheumatologic disorders, specifically rheumatoid arthritis and other inflammatory disorders within joints, and IL-17B is known to stimulate IL-17BR in the context of chondrocyte maturation and bone development, suggesting that both ligands and the receptor are expressed in the skeleton under both physiologic and pathologic conditions (Hwang and Kim, 2005; Kokubu et al., 2008).

While extensive analysis has been done on the relationship of expression of

il-17br in primary breast cancer tumors with tumor progression, no studies have looked at the function of IL-17BR within a metastatic niche. Interestingly, analysis of gene profiles from women receiving adjuvant tamoxifen treatment for breast cancer revealed that decreased expression of *il-17br* in primary breast cancer tumors correlates with survival, with further work expanding these findings to early-stage and pre-treatment breast cancer patients (Goetz et al., 2006; Ma et al., 2006). Alternately, we observed that *il-17br* is over-expressed in BCCs when they encounter the bone microenvironment, both cells passaged through bone as well as metastatic cells within human bone and the mouse skeleton, and that over-expression of *il-17br* and stimulation with IL-17B can drive migration of BCCs (Figure 1-2; Figure 4-3; Figure 4-6; Figure 5-10).

It is possible that this phenotype is only relevant when BCCs encounter the bone microenvironment. In fact, consistent with the clinical data reported above, expression of IL-17BR protein in aggressive primary breast cancer cells is low and localized to the cytoplasm (Figure 4-4). Expression of *il-17br* may provide BCCs a growth advantage in the bone or when cultured with bone-derived cells (i.e. hBMSCs), where IL-17B is expressed, that is not essential or necessarily relevant in the mammary gland microenvironment, where physiologic IL-17B expression is not observed. These results, coupled with further gene expression analysis from primary and metastatic breast cancer cells, can provide refinements to the previously published "poor prognosis gene signature" and give clinicians a better tool for determining patient prognosis (van't Veer et al., 2002).

Clinical Implications: hBMSCs as Therapeutics and in Disease Relapse

As described previously, hBMSCs have been used in various therapeutic approaches to cancer, both for their ability to inhibit some tumor cell growth and to home specifically to tumor cells (Lazennec & Jorgensen, 2008). hBMSCs have been shown to stably express transgenes, making them ideal candidates to deliver anticancer drugs or molecules *in vivo* (Mosca et al., 2000). Various reports have demonstrated the ability of hBMSCs expressing chemotherapeutic transgenes to home to *in vivo* tumor cells and block growth and metastasis, including IFN-β, IL-12, and other chemokines (Lazennac & Jorgensen, 2008).

Despite their potential benefits, we have shown that caution must be taken when using hBMSCs in a therapeutic setting. Dependent on the tissue-tropism and metastatic ability, hBMSCs stimulate BCCs differently. hBMSCs can home specifically to aggressive primary tumors and promote tumor growth and metastasis (Figure 5-4; Figure 5-5; Figure 5-7; Figure 5-8). While it is possible to couple hBMSCs to therapeutic delivery, the presence of stromal-derived factors in the primary tumor microenvironment may negate any potential clinical benefit. For example, while we showed that hBMSCs negatively affect growth of MCF7 BCCs, a recent report demonstrated that hBMSC-derived osteopontin is able to enhance MCF7 migration (Koro et al., 2010). While hBMSCs may not efficiently migrate to MCF7 tumors nor accelerate their growth, the presence of hBMSCs, even in limited quantities, may promote motility and subsequent metastasis.

Further, adult mesenchymal stem cells are able to spontaneously transform, albeit

at low frequency and only after long-term *in vitro* manipulation (Rubio et al., 2005). While the rate of transformation in hBMSCs is low, it is possible to increase the rate of transformation by introducing natural oncogenes. Manipulation of hBMSCs to express chemotherapeutic transgenes may ultimately lead to transformation and clinical complications, either through long-term *in vitro* culture or induction of oncogenesis through viral infection.

Finally, hBMSCs may play a large role in disease relapse. The timing of micrometastasis seeding and growth is not clearly understood, but it is likely that CTCs are shed from tumors at a fairly early stage and clinically silent, distant micrometastases may form early during tumor development (Aguirre-Ghiso, 2007). Despite the long dormancy associated with disseminated tumor cells (DTCs) in the bone marrow, identification of DTCs at the first clinical presentation of breast cancer correlates with decreased survival (Braun et al., 2005). These small nests of cancer cells may encounter hBMSCs, either in their native bone environment or those that home to metastatic tumor cells throughout the body. hBMSC stimulation can promote disseminated tumor cell growth into clinically detectable metastasis in distant organs. This may help explain why patients often face metastatic complications long after complete surgical removal of the primary tumor (Karrison et al., 1999). Additionally, surgical resection of primary breast tumors is not always complete and inflammation is a common feature during breast reconstructions following mastectomy (Xu et al., 2009). hBMSC attraction to the remaining tumor cells and inflammation at the primary site and tumor-stroma interactions may lead to tumor relapse or metastasis.

Clinical Implications: Blockade of hBMSC Interactions

hBMSCs, a major component of the metastatic soil, play a critical role in physiologic bone development and wound remodeling. Additionally, the role of these cells in pathophysiologic tumor development and metastasis formation is currently being unraveled. It is possible that future therapeutic development may be directed at poisoning the "soil," i.e. blocking the pathophysiologic role of hBMSCs by identifying chemotactic factors and/or paracrine loops that are critical to hBMSC recruitment to, and stimulation of, cancer cells.

As described above, hBMSCs may be important in cancer cell dissemination and disease relapse. While it is likely that hBMSCs are already present in the cancer microenvironment at clinical presentation, blocking their interactions may stop further stimulation and spread of cancer cells. Additionally, hBMSCs recruitment to micrometastatic tumors may provide signals that trigger tumor growth and conversion to clinically detected metastases. Blocking homing of hBMSCs to these micrometastatic cancer islands may be a way to prevent disease relapse in the years following primary tumor removal.

Conclusions and Future Directions

Using the humanized model of breast cancer metastasis to bone, as well as variations of the model incorporating tissue-engineered bone (TEB) as a source of hBMSCs, we have identified important genetic and cellular factors in breast cancer tumor

growth and progression. While our work has been limited to human-derived breast cancer cell lines, this work could be expanded to patient samples. The work described above by Ding et al. suggests that studying patient samples in our xenograft model may help elucidate the genomic changes required of breast cancer cells to efficiently metastasize to human bone, as well as other organs.

Expansion of the model to use primary cell samples may require further modifications. The human BCC lines used in these studies grow robustly when implanted in the mammary fat pads of immunocompromised mice; primary cells may not be able to overcome the limiting pressure from the surrounding microenvironment. As reported above, in addition to recent advances in humanizing and manipulating the metastatic microenvironment, new findings have shown that the primary tumor stromal environment can also be at least partially humanized (Kuperwasser et al., 2004). By implanting human mammary stromal cells from reduction mammoplasty surgeries, the mouse mammary fat pad can be converted into a more humanized microenvironment, comprised of mouse and human stromal cells; these in turn should create a more hospitable microenvironment for the subsequent implantation of human mammary epithelial cells, including patient samples of neoplastic origin. Further modifications of this model may eventually allow the complete humanization of the stromal microenvironment. While, as of this writing, this model has not been used to study skeletal metastasis, it suggests the possibility of studying the genomic changes required for primary cells to metastasize to human bone within a controlled animal model.

In addition to global genomic changes, our work has demonstrated the correlation

of a single genetic change, over-expression of *il-17br*, with breast cancer metastasis. *il-17br* was over-expressed in all metastatic BCC samples and forced over-expression of *il-17br* increased migration and metastasis. Further, hBMSCs, a physiologic source of IL-17B have a similar affect on BCCs, i.e. increased migration and metastasis. Future studies will work to establish a mechanistic link between secretion of IL-17B by hBMSCs and increased metastasis, as well as test IL-17BR blockade as a therapeutic target. As described above, hBMSCs can stably express transgenes, including shRNA constructs to block protein translation. hBMSCs lacking IL-17B secretion can be used to test the importance of this factor in tumor progression resulting from hBMSC-BCC interactions at the primary site and TEB seeded with genetically-modified hBMSCs can be used to study the role of IL-17B/IL-17BR interactions in the metastatic niche.

Finally, we have established a novel method to track hBMSCs from a human bone environment. TEB seeded with fluorescently-labeled hBMSCs was used to study homing of stromal cells to primary breast cancer tumors. This model can be expanded to study the migration of hBMSCs to other primary tumor or metastatic niches, as well as migration of BCCs from a metastatic site back to the primary tumor or to other distant organs. In the future, the model can be used to study whether hBMSC stimulation of BCCs can promote tumor self-seeding or lead to further metastatic dissemination and disease relapse.

Chapter 7

References

1. Aguirre-Ghiso, J.A. Models, mechanisms and clinical evidence for cancer dormancy. *Nature Reviews Cancer* **7**, 834-46(2007).

2. Aslakson, C.J. & Miller, F.R. Selective events in the metastatic process defined by analysis of the sequential dissemination of subpopulations of a mouse mammary tumor. *Cancer Research* **52**, 1399-405(1992).

3. Backlund, M.G. et al. Impact of ionizing radiation and genetic background on mammary tumorigenesis in p53-deficient mice. *Cancer Research* **61**, 6577-82(2001).

4. Barnes, G.L. et al. Fidelity of Runx2 activity in breast cancer cells is required for the generation of metastases-associated osteolytic disease. *Cancer Research* **64**, 4506-13 (2004).

5. Barsky, S.H. & Karlin, N.J. Mechanisms of disease: breast tumor pathogenesis and the role of the myoepithelial cell. *Nature Clinical Practice Oncology* **3**, 138-51(2006).

6. Bellahcène, A. & Castronovo, V. Expression of bone matrix proteins in human breast cancer: potential roles in microcalcification formation and in the genesis of bone metastases. *Bulletin du cancer* **84**, 17-24(1997).

7. Bos, P.D. et al. Genes that mediate breast cancer metastasis to the brain. *Nature* **459**, 1005-1009(2009).

8. Boyce, B.F., Yoneda, T. & Guise, T.A. Factors regulating the growth of metastatic cancer in bone. *Endocrine-Related Cancer* **6**, 333-47(1999).

9. Braun, S. et al. A pooled analysis of bone marrow micrometastasis in breast cancer. *The New England Journal of Medicine* **353**, 793-802(2005).

10. Burger, J.A. & Kipps, T.J. Review article CXCR4 : a key receptor in the crosstalk between tumor cells and their microenvironment. *Blood* **107**, 1761-1767(2006).

11. Bäuerle, T. et al. Characterization of a rat model with site-specific bone metastasis induced by MDA-MB-231 breast cancer cells and its application to the effects of an antibody against bone sialoprotein. *International Journal of Cancer* **115**, 177-86(2005).

12. Canon, J.R. et al. Inhibition of RANKL blocks skeletal tumor progression and improves survival in a mouse model of breast cancer bone metastasis. *Clinical & Experimental Metastasis* **25**, 119-29(2008).

13. Chambers, A.F., Groom, A.C. & MacDonald, I.C. Dissemination and growth of cancer cells in metastatic sites. *Nature Reviews Cancer* **2**, 563-72(2002).

14. Chen, X. et al. A tumor-selective biotherapy with prolonged impact on established metastases based on cytokine gene-engineered MSCs. *Molecular Therapy* **16**, 749-56 (2008).

15. Chirgwin, J.M. & Guise, T.A. Molecular mechanisms of tumor-bone interactions in osteolytic metastases. *Critical Reviews in Eukaryotic Gene Expression* **10**, 159-78(2000).

16. Coffelt, S.B. et al. The pro-inflammatory peptide LL-37 promotes ovarian tumor progression through recruitment of multipotent mesenchymal stromal cells. *Proceedings of the National Academy of Sciences the United States of America* **106**, 3806-11(2009).

17. Coleman, R. Management of bone metastases. *The Oncologist* **5**, 463-470(2000).

18. DeNardo, D.G. & Coussens, L.M. Inflammation and breast cancer. Balancing immune response: crosstalk between adaptive and innate immune cells during breast cancer progression. *Breast Cancer Research* **9**, 212(2007).

19. Ding, L. et al. Genome remodelling in a basal-like breast cancer metastasis and xenograft. *Nature* **464**, 999-1005(2010).

20. Dittmer, A. et al. Human mesenchymal stem cells induce E-cadherin degradation in breast carcinoma spheroids by activating ADAM10. *Cellular and Molecular Life Sciences* **66**, 3053-65(2009).

21. Dunn, L. & Demichele, A. Genomic predictors of outcome and treatment response in breast cancer. *Molecular Diagnosis & Therapy* **13**, 73-90(2009).

22. Eckhardt, B.L. et al. Genomic analysis of a spontaneous model of breast cancer metastasis to bone reveals a role for the extracellular matrix. *Molecular Cancer Research* **3**, 1-13(2005).

23. Egeblad, M. & Werb, Z. New functions for the matrix metalloproteinases in cancer progression. *Nature Reviews Cancer* **2**, 161-74(2002).

24. Enderling, H., Hlatky, L. & Hahnfeldt, P. Migration rules: tumours are conglomerates of self-metastases. *British Journal of Cancer* **100**, 1917-25(2009).

25. Fata, J.E. et al. The osteoclast differentiation factor osteoprotegerin-ligand is essential for mammary gland development. *Cell* **103**, 41-50(2000).

26. Fidler, I. The pathogenesis of cancer metastasis: the 'seed and soil' hypothesis revisited. *Nature Reviews Cancer* **3**, 1-6(2003).

27. Gabrilovich, D. Mechanisms and functional significance of tumour-induced dendritic-cell defects. *Nature Reviews Immunology* **4**, 941-52(2004).

28. Gallimore, A. & Godkin, A. Regulatory T cells and tumour immunity - observations in mice and men. *Immunology* **123**, 157-63(2008).

29. Gardner, H.P. et al. Cloning and characterization of Hunk, a novel mammalian SNF1-related protein kinase. *Genomics* **63**, 46-59(2000).

30. Gattei, V. et al. Phorbol ester induced osteoclast-like differentiation of a novel human leukemic cell line (FLG 29.1). *The Journal of Cell Biology* **116**, 437-47(1992).

31. Goetz, M.P. et al. A two-gene expression ratio of homeobox 13 and interleukin-17B receptor for prediction of recurrence and survival in women receiving adjuvant tamoxifen. *Clinical Cancer Research* **12**, 2080-7(2006).

32. Goldstein, R.H., Weinberg, R.A. & Rosenblatt, M. Of mice and (wo)men: Mouse models of breast cancer metastasis to bone. *Journal of Bone and Mineral Research* **25**, 431-436(2010).

33. Goltzman, D. et al. Molecular basis of the spectrum of skeletal complications of neoplasia. *Cancer* **88**, 2903-8(2000).

34. Goltzman, D. Osteolysis and cancer. *The Journal of Clinical Investigation* **107**, 1219-20(2001).

35. Guise, T.A. et al. Basic mechanisms responsible for osteolytic and osteoblastic bone metastases. *Clinical Cancer Research* **12**, 6213s--6216s(2006).

36. Guise, T.A. Molecular mechanisms of osteolytic bone metastases. *Cancer* **88**, 2892-8 (2000).

37. Guy, C.T. et al. Expression of the neu protooncogene in the mammary epithelium of transgenic mice induces metastatic disease. *Proceedings of the National Academy of Sciences of the United States of America* **89**, 10578-82(1992).

38. Hoffman, R.M. Orthotopic metastatic mouse models for anticancer drug discovery and evaluation: a bridge to the clinic. *Investigational New Drugs* **17**, 343-59(1999).

39. Houghton, J. et al. Gastric cancer originating from bone marrow-derived cells. *Science* **306**, 1568-71(2004).

40. Huang, H. et al. IL-17 stimulates the proliferation and differentiation of human mesenchymal stem cells: implications for bone remodeling. *Cell Death and Differentiation* **16**, 1332-43(2009).

41. Hunt, N.C. et al. Cellular mechanisms of bone resorption in breast carcinoma. *British Journal of Cancer* **85**, 78-84(2001).

42. Hwang, S. & Kim, H. Expression of IL-17 homologs and their receptors in the synovial cells of rheumatoid arthritis patients. *Molecules and Cells* **19**, 180-4(2005).

43. Hüsemann, Y. & Klein, C.A. The analysis of metastasis in transgenic mouse models. *Transgenic Research* **18**, 1-5(2009).

44. Ibrahim, T. et al. Expression of bone sialoprotein and osteopontin in breast cancer bone metastases. *Clinical & Experimental Metastasis* **18**, 253-60(2000).

45. Javed, A. et al. Impaired intranuclear trafficking of Runx2 (AML3/CBFA1) transcription factors in breast cancer cells inhibits osteolysis in vivo. *Proceedings of the National Academy of Sciences of the United States of America* **102**, 1454-9(2005).

46. Jemal, A. et al. Cancer statistics, 2009. *CA* **59**, 225-49

47. Jerevall, P. et al. Exploring the two-gene ratio in breast cancer--independent roles for HOXB13 and IL17BR in prediction of clinical outcome. *Breast Cancer Research & Treatment* **107**, 225-34(2008).

48. Joyce, J.A. & Pollard, J.W. Microenvironmental regulation of metastasis. *Nature Reviews Cancer* **9**, 239-52(2009).

49. Jung, M.Y. et al. Analysis of the expression profiles of cytokines and cytokine-related genes during the progression of breast cancer growth in mice. *Oncology Reports* **22**, 1141-7(2009).

50. Kang, Y. et al. A multigenic program mediating breast cancer metastasis to bone. *Cancer Cell* **3**, 537-549(2003).

51. Karnoub, A.E. et al. Mesenchymal stem cells within tumour stroma promote breast cancer metastasis. *Nature* **449**, 557-563(2007).

52. Karrison, T.G., Ferguson, D.J. & Meier, P. Dormancy of mammary carcinoma after mastectomy. *Journal of the National Cancer Institute* **91**, 80-5(1999).

53. Kidd, S. et al. Direct evidence of mesenchymal stem cell tropism for tumor and wounding microenvironments using in vivo bioluminescent imaging. *Stem Cells* **27**, 2614-23(2009).

54. Kim, H.J. et al. Influence of macroporous protein scaffolds on bone tissue engineering from bone marrow stem cells. *Biomaterials* **26**, 4442-52(2005).

55. Kim, M. et al. Tumor self-seeding by circulating cancer cells. *Cell* **139**, 1315-26 (2009).

56. Klopp, A.H. et al. Tumor irradiation increases the recruitment of circulating mesenchymal stem cells into the tumor microenvironment. *Cancer Research* **67**, 11687-95(2007).

57. Kokubu, T. et al. Immunolocalization of IL-17A, IL-17B, and their receptors in chondrocytes during fracture healing. *The Journal of Histochemistry and Cytochemistry* **56**, 89-95(2008).

58. Koro, K. et al. Interactions between breast cancer cells and bone marrow derived cells in vitro define a role for osteopontin in affecting breast cancer cell migration. *Breast Cancer Research and Treatment* (2010).

59. Korpal, M. et al. Imaging transforming growth factor-beta signaling dynamics and therapeutic response in breast cancer bone metastasis. *Nature Medicine* **15**, 960-6(2009).

60. Kufe, D. Skeletal Metastases. *Cancer Medicine 6* 148(2003).

61. Kuperwasser, C. et al. A mouse model of human breast cancer metastasis to human bone. *Cancer Research* **65**, 6130-6138(2005).

62. Kuperwasser, C. et al. Reconstruction of functionally normal and malignant human breast tissues in mice. *Proceedings of the National Academy of Sciences of the United States of America* **101**, 4966-71(2004).

63. Kyriakou, C.A. et al. Human mesenchymal stem cells (hMSCs) expressing truncated soluble vascular endothelial growth factor receptor (tsFlk-1) following lentiviral-mediated gene transfer inhibit growth of Burkitt's lymphoma in a murine model. *The Journal of Gene Medicine* **8**, 253-64(2006).

64. Käkönen, S. & Mundy, G.R. Mechanisms of osteolytic bone metastases in breast carcinoma. *Cancer* **97**, 834-9(2003).

65. Lacroix, M. MDA-MB-435 cells are from melanoma, not from breast cancer. *Cancer Chemotherapy and Pharmacology* **63**, 567(2009).

66. Lawson, J.S. et al. Mouse Mammary Tumor Virus-like Sequences in Human Breast Cancer. *Cancer Research* (2010).

67. Lazennec, G. & Jorgensen, C. Concise review: adult multipotent stromal cells and cancer: risk or benefit? *Stem Cells* 1-15(2008).doi:10.1634/stemcells.2007-1006.Concise

68. Lee, J. et al. IL-17E, a novel proinflammatory ligand for the IL-17 receptor homolog IL-17Rh1. *The Journal of Biological Chemistry* **276**, 1660-4(2001).

69. Li, C. et al. Electrospun silk-BMP-2 scaffolds for bone tissue engineering. *Biomaterials* **27**, 3115-24(2006).

70. Li, X. et al. Optically imageable metastatic model of human breast cancer. *Clinical & Experimental Metastasis* **19**, 347-50(2002).

71. Lin, E.Y. et al. Progression to malignancy in the polyoma middle T oncoprotein mouse breast cancer model provides a reliable model for human diseases. *The American Journal of Pathology* **163**, 2113-26(2003).

72. Lin, S. et al. The isolation of novel mesenchymal stromal cell chemotactic factors from the conditioned medium of tumor cells. *Experimental Cell Research* **314**, 3107-17 (2008).

73. Lindemann, R.K. et al. Transforming growth factor beta regulates parathyroid hormone-related protein expression in MDA-MB-231 breast cancer cells through a novel Smad/Ets synergism. *The Journal of Biological Chemistry* **276**, 46661-70(2001).

74. Liu, S. et al. Inhibition of rho-associated kinase signaling prevents breast cancer metastasis to human bone. *Cancer Research* **69**, 8742-8751(2009).

75. Liu, W. et al. Copy number analysis indicates monoclonal origin of lethal metastatic prostate cancer. *Nature Medicine* **15**, 559-65(2009).

76. Loebinger, M.R. et al. Magnetic resonance imaging of mesenchymal stem cells homing to pulmonary metastases using biocompatible magnetic nanoparticles. *Cancer Research* **69**, 8862-7(2009).

77. Loebinger, M.R. et al. Mesenchymal stem cell delivery of TRAIL can eliminate metastatic cancer. *Cancer Research* **69**, 4134-42(2009).

78. Lu, X. et al. ADAMTS1 and MMP1 proteolytically engage EGF-like ligands in an osteolytic signaling cascade for bone metastasis. *Genes & Development* **23**, 1882-94 (2009).

79. Ma, X. et al. The HOXB13:IL17BR expression index is a prognostic factor in early-stage breast cancer. *Journal of Clinical Oncology* **24**, 4611-9(2006).

80. Majumdar, M.K. et al. Human marrow-derived mesenchymal stem cells (MSCs) express hematopoietic cytokines and support long-term hematopoiesis when differentiated toward stromal and osteogenic lineages. *Journal of Hematotherapy & Stem Cell Research* **9**, 841-848(2000).

81. Manders, K. et al. Clinical management of women with metastatic breast cancer: a descriptive study according to age group. *BMC cancer* **6**, 179(2006).

82. Manolagas, S.C. Role of cytokines in bone resorption. *Bone* **17**, 63S-67S(1995).

83. Maroulakou, I.G. et al. Prostate and mammary adenocarcinoma in transgenic mice carrying a rat C3(1) simian virus 40 large tumor antigen fusion gene. *Proceedings of the National Academy of Sciences of the United States of America* **91**, 11236-40(1994).

84. Martin, F.T. et al. Potential role of mesenchymal stem cells (MSCs) in the breast tumour microenvironment: stimulation of epithelial to mesenchymal transition (EMT). *Breast Cancer Research and Treatment* (2010).

85. Mauney, J.R., Volloch, V. & Kaplan, D.L. Matrix-mediated retention of adipogenic differentiation potential by human adult bone marrow-derived mesenchymal stem cells during ex vivo expansion. *Biomaterials* **26**, 6167-75(2005).

86. Miller, F.R., Miller, B.E. & Heppner, G.H. Characterization of metastatic heterogeneity among subpopulations of a single mouse mammary tumor: heterogeneity in phenotypic stability. *Invasion & Metastasis* **3**, 22-31(1983).

87. Minn, A.J. et al. Genes that mediate breast cancer metastasis to lung. *Nature* **436**, 518-524(2005).

88. Molloy, A.P. et al. Mesenchymal stem cell secretion of chemokines during differentiation into osteoblasts, and their potential role in mediating interactions with breast cancer cells. *International Journal of Cancer* **124**, 326-32(2009).

89. Moreau, J.E. et al. Tissue-engineered bone serves as a target for metastasis of human breast cancer in a mouse model. *Cancer Research* **67**, 10304-10308(2007).

90. Mori, N. et al. Preferential induction of mammary tumors in p53 hemizygous BALB/c mice by fractionated irradiation of a sub-lethal dose of X-rays. *Journal of Radiation Research* **44**, 249-54(2003).

91. Mosca, J.D. et al. Mesenchymal stem cells as vehicles for gene delivery. *Clinical Orthopaedics and Related Research* S71-90(2000).

92. Moussad, E.E. & Brigstock, D.R. Connective tissue growth factor: what's in a name? *Molecular Genetics and Metabolism* **71**, 276-92(2000).

93. Mundy, G.R. Metastasis to bone: causes, consequences and therapeutic opportunities. *Nature Reviews Cancer* **2**, 584-93(2002).

94. Müller, A. et al. Involvement of chemokine receptors in breast cancer metastasis. *Nature* **410**, 50-6(2001).

95. Nannuru, K.C. et al. Matrix Metalloproteinase (MMP)-13 Regulates Mammary Tumor–Induced Osteolysis by Activating MMP9 and Transforming Growth Factor-β Signaling at the Tumor-Bone Interface. *Cancer Research* **70**, 3495-3504(2010).

96. Nemeth, J.A. et al. Severe combined immunodeficient-hu model of human prostate cancer metastasis to human bone. *Cancer Research* **59**, 1987-93(1999).

97. Neudert, M. et al. Site-specific human breast cancer (MDA-MB-231) metastases in nude rats: model characterisation and in vivo effects of ibandronate on tumour growth. *International Journal of Cancer* **107**, 468-77(2003).

98. Nielsen, L.L. et al. Histopathology of salivary and mammary gland tumors in transgenic mice expressing a human Ha-ras oncogene. *Cancer Research* **51**, 3762-7 (1991).

99. Noti, J.D. Adherence to osteopontin via alphavbeta3 suppresses phorbol ester-mediated apoptosis in MCF-7 breast cancer cells that overexpress protein kinase C-alpha. *International Journal of Oncology* **17**, 1237-43(2000).

100. O'Neill, K.O. et al. Bioluminescent imaging: a critical tool in pre-clinical oncology research. *The Journal of Pathology* 317-327(2009).

101. Paget, S. The distribution of secondary growths in cancer of the breast. 1889. *Cancer Metastasis Reviews* **8**, 98-101(1989).

102. Pantel, K., Brakenhoff, R.H. & Brandt, B. Detection, clinical relevance and specific biological properties of disseminating tumour cells. *Nature Reviews Cancer* **8**, 329-40 (2008).

103. Parsons, J.T., Zetter, B. & Mohla, S. Shifting paradigms in tumor metastasis: challenges and opportunities. *Cancer Biology & Therapy* **1**, 582-5(2002).

104. Peyruchaud, O. et al. Early detection of bone metastases in a murine model using fluorescent human breast cancer cells: application to the use of the bisphosphonate zoledronic acid in the treatment of osteolytic lesions. *Journal of Bone and Mineral Research* **16**, 2027-34(2001).

105. Price, J.E. et al. Tumorigenicity and metastasis of human breast carcinoma cell lines in nude mice. *Cancer Research* **50**, 717-21(1990).

106. Quaglino, E. et al. ErbB2 transgenic mice: a tool for investigation of the immune prevention and treatment of mammary carcinomas. *Current Protocols in Immunology* **Chapter 20**, Unit 20.9.1-20.9-10(2008).

107. Quintela-Fandino, M. et al. HUNK suppresses metastasis of basal type breast cancers by disrupting the interaction between PP2A and cofilin-1. *Proceedings of the National Academy of Sciences of the United States of America* **107**, 2622-7(2010).

108. Ramasamy, R. et al. Mesenchymal stem cells inhibit proliferation and apoptosis of tumor cells: impact on in vivo tumor growth. *Leukemia* **21**, 304-10(2007).

109. Rhodes, L.V. et al. Adult human mesenchymal stem cells enhance breast tumorigenesis and promote hormone independence. *Breast Cancer Research & Treatment* (2009).

110. Ritter, E. et al. Breast cancer cell-derived fibroblast growth factor 2 and vascular endothelial growth factor are chemoattractants for bone marrow stromal stem cells. *Annals of Surgery* **247**, 310-4(2008).

111. Rodan, G.A. The development and function of the skeleton and bone metastases. *Cancer* **97**, 726-32(2003).

112. Roodman, D. Role of stromal-derived cytokines and growth factors in bone metastasis. *Cancer* **97**, 733-8(2003).

113. Rubens, R. The nature of metastatic bone disease. *Bone Metastases. Diagnosis and Treatment*. 1-10(1992).

114. Rubio, D. et al. Spontaneous human adult stem cell transformation. *Cancer Research* **65**, 3035-9(2005).

115. Sasser, A.K. et al. Interleukin-6 is a potent growth factor for ER-alpha-positive human breast cancer. *The FASEB Journal* **21**, 3763-70(2007).

116. Schedin, P. & Elias, A. Multistep tumorigenesis and the microenvironment. *Breast Cancer Research* **6**, 93-101(2004).

117. Shevde, L.A. et al. Osteopontin: an effector and an effect of tumor metastasis. *Current Molecular Medicine* **10**, 71-81(2010).

118. Shi, Y. et al. A novel cytokine receptor-ligand pair. Identification, molecular characterization, and in vivo immunomodulatory activity. *Journal of Biological Chemistry* **275**, 19167-76(2000).

119. Shore, P. A role for Runx2 in normal mammary gland and breast cancer bone metastasis. *Journal of Cellular Biochemistry* **96**, 484-9(2005).

120. Shtivelman, E. & Namikawa, R. Species-specific metastasis of human tumor cells in the severe combined immunodeficiency mouse engrafted with human tissue. *Proceedings of the National Academy of Sciences of the United States of America* **92**, 4661-4665 (1995).

121. Sinn, E. et al. Coexpression of MMTV/v-Ha-ras and MMTV/c-myc genes in transgenic mice: synergistic action of oncogenes in vivo. *Cell* **49**, 465-75(1987).

122. Siveen, K.S. & Kuttan, G. Role of macrophages in tumour progression. *Immunology Letters* **123**, 97-102(2009).

123. Sloan, E.K. & Anderson, R.L. Genes involved in breast cancer metastasis to bone. *Cellular and Molecular Life Sciences* **59**, 1491- 1502(2002).

124. Spaeth, E.L. et al. Mesenchymal stem cell transition to tumor-associated fibroblasts contributes to fibrovascular network expansion and tumor progression. *PloS One* **4**, e4992(2009).

125. Studeny, M. et al. Mesenchymal stem cells: potential precursors for tumor stroma and targeted-delivery vehicles for anticancer agents. *Journal of the National Cancer Institute* **96**, 1593-603(2004).

126. Sun, Y. et al. p53 down-regulates human matrix metalloproteinase-1 (Collagenase-1) gene expression. *The Journal of Biological Chemistry* **274**, 11535-40(1999).

127. Sun, Y. et al. Wild type and mutant p53 differentially regulate the gene expression of human collagenase-3 (hMMP-13). *The Journal of Biological Chemistry* **275**, 11327-32 (2000).

128. Tang, Y. et al. TGF-β1--induced migration of bone mesenchymal stem cells couples bone resorption with formation. *Nature Medicine* **15**, 757-765(2009).

129. Teicher, B.A. Malignant cells, directors of the malignant process: role of transforming growth factor-beta. *Cancer Metastasis Reviews* **20**, 133-43(2001).

130. van 't Veer, L.J. et al. Gene expression profiling predicts clinical outcome of breast cancer. *Nature* **415**, 530-536(2002).

131. van de Vijver, M.J. et al. A gene-expression signature as a predictor of survival in breast cancer. *New England Journal of Medicine* **347**, 1999-2009(2002).

132. Vogelstein, B. & Kinzler, K.W. Cancer genes and the pathways they control. *Nature Medicine* **10**, 789-99(2004).

133. Waltregny, D. et al. Increased expression of bone sialoprotein in bone metastases compared with visceral metastases in human breast and prostate cancers. *Journal of Bone and Mineral Research* **15**, 834-43(2000).

134. Wang, C.Y. & Chang, Y.W. A model for osseous metastasis of human breast cancer established by intrafemur injection of the MDA-MB-435 cells in nude mice. *Anticancer Research* **17**, 2471-4

135. Weaver, V.M. & Bissell, M.J. Functional culture models to study mechanisms governing apoptosis in normal and malignant mammary epithelial cells. *Journal of Mammary Gland Biology and Neoplasia* **4**, 193-201(1999).

136. Weber, M.H. et al. Mechanisms of tumor metastasis to bone. *Critical Reviews in Eukaryotic Gene Expression* **10**, 281-302(2000).

137. Weigelt, B. & van't Veer, L. Hard-wired genotype in metastatic breast cancer. *Cell Cycle* 756-757(2004).at

138. Wertheim, G.B. et al. The Snf1-related kinase, Hunk, is essential for mammary tumor metastasis. *Proceedings of the National Academy of Sciences of the United States of America* **106**, 15855-60(2009).

139. Xu, F. et al. In vitro interaction between mouse breast cancer cells and mouse mesenchymal stem cells during adipocyte differentiation. *Journal of Tissue Engineering and Regenerative Medicine* **3**, 338-47(2009).

140. Yago, T. et al. IL-17 induces osteoclastogenesis from human monocytes alone in the absence of osteoblasts, which is potently inhibited by anti-TNF-alpha antibody: a novel mechanism of osteoclastogenesis by IL-17. *Journal of Cellular Biochemistry* **108**, 947-55 (2009).

141. Yang, E. et al. Blockade of PAR1 signaling with cell-penetrating pepducins inhibits Akt survival pathways in breast cancer cells and suppresses tumor survival and metastasis. *Cancer Research* **69**, 6223-31(2009).

142. Yang, J. et al. Twist, a master regulator of morphogenesis, plays an essential role in tumor metastasis. *Cell* **117**, 927-39(2004).

143. Yang, W. et al. Breast cancer metastasis in a human bone NOD/SCID mouse model. *Cancer Biology & Therapy* **6**, 1289-94(2007).

144. Yin, J.J., Pollock, C.B. & Kelly, K. Mechanisms of cancer metastasis to the bone. *Cell Research* **15**, 57-62(2005).

145. Yoneda, T. & Hiraga, T. Crosstalk between cancer cells and bone microenvironment in bone metastasis. *Biochemical and Biophysical Research Communications* **328**, 679-87 (2005).

146. Yoneda, T. Cellular and molecular basis of preferential metastasis of breast cancer to bone. *Journal of Orthopaedic Science* **5**, 75-81(2000).

147. Yoneda, T. et al. Inhibition of osteolytic bone metastasis of breast cancer by combined treatment with the bisphosphonate ibandronate and tissue inhibitor of the matrix metalloproteinase-2. *The Journal of Clinical Investigation* **99**, 2509-17(1997).

148. Yonou, H. et al. Establishment of a novel species- and tissue-specific metastasis model of human prostate cancer in humanized non-obese diabetic/severe combined immunodeficient mice engrafted with human adult lung and bone. *Cancer Research* **61**, 2177-82(2001).

149. Yu, Y. et al. Elevated breast cancer risk in irradiated BALB/c mice associates with unique functional polymorphism of the Prkdc (DNA-dependent protein kinase catalytic subunit) gene. *Cancer Research* **61**, 1820 -1824(2001).

150. Zappia, E. et al. Mesenchymal stem cells ameliorate experimental autoimmune encephalomyelitis inducing T-cell anergy. *Blood* **106**, 1755-61(2005).

Appendix A

Up-regulated Genes From Gene Array

Genes that are 1.4 fold up regulated in SUM1315-BP2 vs SUM1315				
Gene ID	**Fold**	**Common Name**	**GenBank**	**Description**
H200002983	8.606	TRUB1	AK026721	Homo sapiens cDNA: FLJ23068 fis, clone LNG05562
H300011355	5.411	ENSG00000165990	NM_145032	AMBIGUOUS
H200013197	4.633	FLJ30213	AK054967	Homo sapiens cDNA FLJ30213 fis, clone BRACE2001673, highly similar to Mus musculus mdgl-1 mRNA
H300005126	4.392	ENSG00000178191	NM_173644	AMBIGUOUS
H300003272	3.932			FIBRONECTIN TYPE III DOMAIN CONTAINING FRAGMENT
H300003450	3.833	ENSG00000179241		DEFENSIN BETA 114 (FRAGMENT). [Source:SPTREMBL;Acc:Q8NES9]
H300002447	3.795	ENSG00000178994		UNKNOWN
H300004039	3.189	ENSG00000176191		PUTATIVE G-PROTEIN COUPLED RECEPTOR. [Source:SPTREMBL;Acc:Q8TDV2]
H300001239	3.18	ENSG00000179323		AMBIGUOUS
H200001036	2.997	CL25022	NM_015702	Hypothetical protein
H300000184	2.924			AMBIGUOUS
H200004439	2.888	MGC15887	BC009447	Homo sapiens, clone MGC:15887 IMAGE:3530481, mRNA, complete cds
H300014862	2.825	ENSG00000174506		FAT CELL-SPECIFIC LOW MOLECULAR WEIGHT PROTEIN (FAT TISSUE-SPECIFIC LOW MW PROTEIN) (B27).
H300003751	2.71			UNKNOWN
H300007811	2.648			AMBIGUOUS
H300012150	2.535	ENSG00000169672		ADENYLATE CYCLASE, TYPE I (EC 4.6.1.1) (ATP PYROPHOSPHATE-LYASE) (CA(2+)/CALMODULIN ACTIVATED ADENYLYL CYCLASE)
H200010936	2.533	CEBPB	NM_005194	CCAAT/enhancer binding protein (C/EBP), beta
H300014944	2.489	FLJ34064	NM_152633	AMBIGUOUS
H200000964	2.416	LOC151162	AK056461	Homo sapiens cDNA FLJ31899 fis, clone NT2RP7004173
H200000637	2.413	CHRNA7	NM_000746	Cholinergic receptor, nicotinic, alpha polypeptide 7
H300009206	2.412	ENSG00000181345		UNKNOWN
H300015698	2.408	ENSG00000161649		AMBIGUOUS
H200009068	2.393		AK023907	Homo sapiens cDNA FLJ13845 fis, clone THYRO1000815

Genes that are 1.4 fold up regulated in SUM1315-BP2 vs SUM1315				
H200007507	2.354	PSIP1	AK024516	Homo sapiens cDNA: FLJ20863 fis, clone ADKA01804
H200003816	2.337	FSD1	NM_024333	Fibronectin type 3 and SPRY domain-containing protein
H200016023	2.307		L33988	Homo sapiens (clone E06) gene from CpG-enriched DNA, partial cds
H200008973	2.306	KIAA0889	AK022023	Homo sapiens cDNA FLJ11961 fis, clone HEMBB1001020, highly similar to Homo sapiens mRNA for KIAA0889
H200001842	2.275	KIAA1040	AB028963	KIAA1040 protein
H300008629	2.272			UNKNOWN
H300017550	2.27			GOLGI
H200001064	2.254	IL17BR	AF208111	Interleukin 17B receptor
H300005744	2.249	ENSG00000178289		TRANSCRIPTION INITIATION FACTOR TFIID 28 KDA SUBUNIT BETA
H200006955	2.243	KIAA0153	NM_015140	KIAA0153 protein
H200008981	2.223	MTBP	AK022122	Mdm2, transformed 3T3 cell double minute 2, p53 binding protein (mouse) binding protein, 104kD
H200000815	2.207	FLJ20209	AK000216	Hypothetical protein FLJ20209
H200018104	2.15		AF132204	Homo sapiens PRO2259 mRNA, complete cds
H200000708	2.148	MMP13	NM_002427	Matrix metalloproteinase 13 (collagenase 3)
H300007339	2.141	ENSG00000181720		UNKNOWN
H200000957	2.122	FLJ12783	NM_031426	Hypothetical protein FLJ12783
H200003650	2.107	B3GAT3	NM_012200	Beta-1,3-glucuronyltransferase 3 (glucuronosyltransferase I)
H300007958	2.104	ENSG00000175598		AMBIGUOUS
H200014761	2.092	HIF1A	NM_001530	Hypoxia-inducible factor 1, alpha subunit (basic helix-loop-helix transcription factor)
H200010300	2.082	DJ511E16.2	AK025442	Hypothetical protein dJ511E16.2
H200011645	2.081	HUNK	NM_014586	Hormonally upregulated Neu-associated kinase
H300005012	2.077	ENSG00000162032		ANKYRIN REPEAT PROFILE/ANKYRIN REPEAT/ANKYRIN REPEAT REGION CIRCULAR PROFILE/YEAST DNA BINDING DOMAIN CONTAINING

Genes that are 1.4 fold up regulated in SUM1315-BP2 vs SUM1315				
H300011186	2.068	ENSG00000173981		VOLTAGE-GATED POTASSIUM CHANNEL BETA-1 SUBUNIT (K+ CHANNEL BETA-1 SUBUNIT) (KV-BETA-1)
H300012331	2.061	ENSG00000163885	NM_152616	TRIPARTITE MOTIF-CONTAINING 42. [Source:RefSeq;Acc:NM_152616]
H200007828	2.049	DMD	NM_004010	Dystrophin (muscular dystrophy, Duchenne and Becker types), includes DXS142, DXS164, DXS206, DXS230,
H200010898	2.046	DMRT1	NM_021951	Doublesex and mab-3 related transcription factor 1
H200007824	2.041	KIAA0489	AB007958	KIAA0489 protein
H200005851	2.033	FLJ32549	AK057111	Homo sapiens cDNA FLJ32549 fis, clone SPLEN1000049
H200000143	2.027	APOBEC1	NM_001644	Apolipoprotein B mRNA editing enzyme, catalytic polypeptide 1
H200000749	2.02	CBLB	NM_004351	Cas-Br-M (murine) ectropic retroviral transforming sequence b
H300006628	2.018	ENSG00000181077		AMBIGUOUS
H200011653	2.015	CORO1A	NM_007074	Coronin, actin binding protein, 1A
H300013215	2.008	ENSG00000167764	NM_145048	AMBIGUOUS
H200000588	2	CHRNB2	NM_000748	Cholinergic receptor, nicotinic, beta polypeptide 2 (neuronal)
H200014146	1.997	UTF1	NM_003577	Undifferentiated embryonic cell transcription factor 1
H300009087	1.991	ENSG00000171967		AMBIGUOUS
H200001420	1.983	DKFZp761N1114	AK057733	Homo sapiens cDNA FLJ25004 fis, clone CBL00608
H200011358	1.982	MGC2647	AK057106	Homo sapiens, clone MGC:14381 IMAGE:4299817, mRNA, complete cds
H200003965	1.982	GS3786	NM_014888	Predicted osteoblast protein
H200001467	1.982	FGB	NM_005141	Fibrinogen, B beta polypeptide
H300011295	1.975	ENSG00000160796		AMBIGUOUS
H200001443	1.975	KIAA0682	NM_014852	KIAA0682 gene product
H200001059	1.966	USP20	NM_006676	Ubiquitin specific protease 20
H300002048	1.957			UNKNOWN
H200000376	1.948	GABRR1	NM_002042	Gamma-aminobutyric acid (GABA) receptor, rho 1
H200000006	1.94	FECH	NM_000140	Ferrochelatase (protoporphyria)
H200004833	1.935		AK024874	Homo sapiens cDNA: FLJ21221 fis, clone COL00570

Genes that are 1.4 fold up regulated in SUM1315-BP2 vs SUM1315				
H200002886	1.932	C17orf31	AB018275	Chromosome 17 open reading frame 31
H200008936	1.928	FLJ11467	AK057042	Hypothetical protein FLJ11467
H200007409	1.923	FOXH1	NM_003923	Forkhead box H1
H200008944	1.912	GRB10	AK021643	Homo sapiens cDNA FLJ11581 fis, clone HEMBA1003598
H300008319	1.909	ENSG00000173250	NM_130387	ANKYRIN REPEAT AND SOCS BOX CONTAINING PROTEIN 14 (ASB-14). [Source:SWISSPROT;Acc:Q8WXK2]
H200010254	1.903	DJ102H19.4	AK021476	Hypothetical protein dJ102H19.4
H200012009	1.902	PRO2198	NM_018621	Hypothetical protein PRO2198
H200013942	1.901	FLJ11585	NM_023075	Hypothetical protein FLJ11585
H300000958	1.897	ENSG00000181955		UNKNOWN
H300010366	1.895	ENSG00000171136		CLEAVAGE AND POLYADENYLATION SPECIFICITY FACTOR, 100 KDA SUBUNIT (CPSF 100 KDA SUBUNIT)
H200017384	1.895	PRO0514	NM_014131	PRO0514 protein
H300007734	1.89	ENSG00000180437		AMBIGUOUS
H200012103	1.889	PAPA-1	NM_031288	PAP-1 binding protein
H300009443	1.887			ZINC FINGER DHHC DOMAIN CONTAINING 2
H200000589	1.882	MBL2	NM_000242	Mannose-binding lectin (protein C) 2, soluble (opsonic defect)
H200002704	1.881	PIGQ	NM_004204	Phosphatidylinositol glycan, class Q
H200000031	1.88	GRIN1	NM_007327	Glutamate receptor, ionotropic, N-methyl D-aspartate 1
H200012751	1.876	LOC58509	AC005175	NY-REN-24 antigen
H300006167	1.873	ENSG00000170628	NM_173497	SMAD UBIQUITINATION REGULATORY FACTOR EC_6.3.2.- UBIQUITIN LIGASE SMAD SPECIFIC E3 UBIQUITIN LIGASE
H200000028	1.872	CYP4F2	NM_001082	Cytochrome P450, subfamily IVF, polypeptide 2
H200009835	1.87		AK021973	Homo sapiens cDNA FLJ11911 fis, clone HEMBB1000141
H200005770	1.869	ADM2	BC012864	Homo sapiens, clone IMAGE: 3882589, mRNA
H200005336	1.864	LOC90321	AK024268	Homo sapiens cDNA FLJ14206 fis, clone NT2RP3003157

Genes that are 1.4 fold up regulated in SUM1315-BP2 vs SUM1315				
H200009702	1.86		AK055324	Homo sapiens cDNA FLJ30762 fis, clone FEBRA2000575
H200004628	1.859	AKL3L	AK001553	Adenylate kinase 3 alpha like
H300015312	1.855	ENSG00000172945		UNKNOWN
H200002135	1.855	NUP133	NM_018230	Nucleoporin 133kD
H300019283	1.851	ENSG00000143940		DELETED IN AZOOSPERMIA DAZ AUTOSOMAL DELETED IN AZOOSPERMIA 1
H200007872	1.847	THBS3	NM_007112	Thrombospondin 3
H200008393	1.846	FLJ10154	NM_018011	Hypothetical protein FLJ10154
H200009696	1.845		AK000893	Homo sapiens cDNA FLJ10031 fis, clone HEMBA1000867
H300006529	1.844	ENSG00000178861	NM_153230	AMBIGUOUS
H300002231	1.839	ENSG00000150051	NM_007350	PLECKSTRIN HOMOLOGY-LIKE DOMAIN, FAMILY A, MEMBER 1; PQ-RICH PROTEIN
H200010315	1.837	ATP5G2	NM_005176	ATP synthase, H+ transporting, mitochondrial F0 complex, subunit c (subunit 9), isoform 2
H200000838	1.837	STMN4	NM_030795	Stathmin-like 4
H200007003	1.836	LOC162427	AK057409	Homo sapiens cDNA FLJ32847 fis, clone TESTI2003376
H200008463	1.83	ARF6	AL117621	Homo sapiens mRNA; cDNA DKFZp564M0264 (from clone DKFZp564M0264)
H200010643	1.824	ADK	NM_006721	Adenosine kinase
H200008392	1.822	KIAA1100	NM_014901	KIAA1100 protein
H200013939	1.814	PLAGL2	NM_002657	Pleiomorphic adenoma gene-like 2
H200016042	1.813		Z98751	Human DNA sequence from PAC 560B9 on chromosome 1q24-1q25. Contains profilin-like pseudogene, 60S ri
H300001543	1.81	ENSG00000161649		AMBIGUOUS
H200008518	1.81	HLA-A	NM_002116	Major histocompatibility complex, class I, A
H200014098	1.803	BNIP2	NM_004330	BCL2/adenovirus E1B 19kD interacting protein 2
H200002862	1.801	P29	NM_015484	GCIP-interacting protein p29
H200001515	1.798	PICALM	NM_007166	Phosphatidylinositol binding clathrin assembly protein
H200002026	1.792	FACVL1	NM_003645	Fatty-acid-Coenzyme A ligase, very long-chain 1
H200000913	1.791	PSMC1	BC013908	Proteasome (prosome, macropain) 26S subunit, ATPase, 1

Genes that are 1.4 fold up regulated in SUM1315-BP2 vs SUM1315				
H200006355	1.787	LILRB5	NM_006840	Leukocyte immunoglobulin-like receptor, subfamily B (with TM and ITIM domains), member 5
H200012058	1.787	NNAT	NM_005386	Neuronatin
H200018144	1.786	MSTP028	NM_031954	MSTP028 protein
H200014532	1.785	FLJ12735	AJ314648	Hypothetical protein FLJ12735
H200002058	1.784	ASGR1	NM_001671	Asialoglycoprotein receptor 1
H300009795	1.781	ENSG00000180438		AMBIGUOUS
H200000149	1.78	AADAC	NM_001086	Arylacetamide deacetylase (esterase)
H200009877	1.776	HTR2A	NM_000621	5-hydroxytryptamine (serotonin) receptor 2A
H300005257	1.772	ENSG00000122795		AMBIGUOUS
H200015866	1.771	DDAH2	NM_013974	Dimethylarginine dimethylaminohydrolase 2
H200003688	1.77	KIAA1091	AL117448	KIAA1091 protein
H200002252	1.769	TRAPPC6B	AK056690	Homo sapiens cDNA: FLJ21784 fis, clone HEP00285
H200003707	1.769	MGC33488	BC005114	Homo sapiens, clone IMAGE: 4053044, mRNA, partial cds
H200008708	1.768	ZFHX1B	AF161345	Homo sapiens HSPC082 mRNA, partial cds
H200017232	1.764	SEC14L2	NM_012429	SEC14-like 2 (S. cerevisiae)
H200000584	1.763	TG737	NM_006531	Probe hTg737 (polycystic kidney disease, autosomal recessive, in)
H200005027	1.762	ITGAX	NM_000887	Integrin, alpha X (antigen CD11C (p150), alpha polypeptide)
H200000226	1.758	FKBP4	NM_002014	FK506 binding protein 4 (59kD)
H200000097	1.758	ZNF134	NM_003435	Zinc finger protein 134 (clone pHZ-15)
H300010796	1.756	ENSG00000105323		HELICASE C TERMINAL DOMAIN/DEAD/DEAH BOX HELICASE CONTAINING
H300002760	1.756	ENSG00000164309		KINESIN
H200000120	1.756	STK19	NM_032454	Serine/threonine kinase 19
H200001907	1.753	ZNF147	AK024597	Homo sapiens cDNA: FLJ20944 fis, clone ADSE01780
H200007543	1.753	KCNK17	NM_031460	Potassium channel, subfamily K, member 17 (TASK-4)
H300002604	1.752	ENSG00000171192		UNKNOWN
H200015032	1.752		AK055008	Homo sapiens cDNA FLJ30446 fis, clone BRACE2009255
H200003652	1.752	LOC92799	BC007653	Homo sapiens clone CDABP0005 mRNA sequence

Genes that are 1.4 fold up regulated in SUM1315-BP2 vs SUM1315				
H300016338	1.746	ENSG00000175107		ZINC FINGER PROTEIN 44 (ZINC FINGER PROTEIN KOX7) (GONADOTROPIN INDUCIBLE TRANSCRIPTION REPRESSOR-2) (GIOT-2)
H200008740	1.743	ANKHZN	NM_016376	ANKHZN protein
H200015400	1.741	ZNF41	X60155	Zinc finger protein 41
H200006332	1.741	DNAJA4	AL133096	Homo sapiens mRNA full length insert cDNA clone EUROIMAGE 730912
H200008972	1.74		AK022016	Homo sapiens cDNA FLJ11954 fis, clone HEMBB1000888
H200008943	1.74		AK021640	Homo sapiens cDNA FLJ11578 fis, clone HEMBA1003571
H300005114	1.739			LOC145053. [Source:SPTREMBL;Acc:Q8N469]
H200007106	1.738	LOC51024	NM_016068	CGI-135 protein
H200010619	1.738	CNGB1	NM_001297	Cyclic nucleotide gated channel beta 1
H200016308	1.736	SLPI	NM_003064	Secretory leukocyte protease inhibitor (antileukoproteinase)
H200005345	1.736	TPK1	AF297710	Thiamin pyrophosphokinase 1
H300015164	1.736	ENSG00000163075	NM_144662	PROTEASOME SUBUNIT ALPHA TYPE 7-LIKE (EC 3.4.25.1). [Source:SWISSPROT;Acc:Q8TAA3]
H200005549	1.736	ATP5H	NM_006356	ATP synthase, H+ transporting, mitochondrial F0 complex, subunit d
H300007756	1.735	ENSG00000180906		60S RIBOSOMAL L21
H200006322	1.732	P4HA1	NM_000917	Procollagen-proline, 2-oxoglutarate 4-dioxygenase (proline 4-hydroxylase), alpha polypeptide I
H200016950	1.73	FLJ20307	AB051490	Hypothetical protein FLJ20307
H200013714	1.73	CYP26A1	NM_057157	Cytochrome P450, subfamily XXVIA, polypeptide 1
H300002264	1.727	ENSG00000180122		UNKNOWN
H200003998	1.725	KIAA1165	AB032991	Hypothetical protein KIAA1165
H200000102	1.725	FLT3	NM_004119	Fms-related tyrosine kinase 3
H200014971	1.72	HELLS	AF155827	Helicase, lymphoid-specific
H200001422	1.72	TSGA2	AK057315	Testes specific A2 homolog (mouse)
H200010654	1.72	BIG1	NM_006421	Brefeldin A-inhibited guanine nucleotide-exchange protein 1
H200001850	1.72	ASB3	NM_016115	Ankyrin repeat and SOCS box-containing 3

Genes that are 1.4 fold up regulated in SUM1315-BP2 vs SUM1315				
H200001817	1.719	IRC1	AJ224864	Leukocyte membrane antigen
H200001088	1.717	DDX15	NM_001358	DEAD/H (Asp-Glu-Ala-Asp/ His) box polypeptide 15
H200008572	1.715	NHP2L1	NM_005008	NHP2 non-histone chromosome protein 2-like 1 (S. cerevisiae)
H300020542	1.715	ENSG00000162753		ADENYLATE KINASE 5 ISOFORM 1; ADENYLATE KINASE 6; ATP-AMP TRANSPHOSPHORYLASE. [Source:RefSeq;Acc:NM_174 858]
H300002519	1.715	ENSG00000162997		UNKNOWN
H200015821	1.714	DKFZp761K1824	NM_017597	Hypothetical protein DKFZp761K1824
H200004385	1.714	MPP3	NM_001932	Membrane protein, palmitoylated 3 (MAGUK p55 subfamily member 3)
H200004116	1.711	PRDX5	NM_012094	Peroxiredoxin 5
H200007371	1.711		BC011940	Homo sapiens, clone MGC: 20802 IMAGE:4329532, mRNA, complete cds
H300019362	1.71	ENSG00000177233		AMBIGUOUS
H300020515	1.709	ENSG00000169046	NM_152756	ARM REPEAT STRUCTURE CONTAINING
H200010611	1.708	PITPNM	NM_004910	Phosphatidylinositol transfer protein, membrane-associated
H200005885	1.706	TCF1	M57732	Transcription factor 1, hepatic; LF-B1, hepatic nuclear factor (HNF1), albumin proximal factor
H300010110	1.704	ENSG00000176394		AMBIGUOUS
H200003631	1.703	FLJ20287	NM_017746	Hypothetical protein FLJ20287
H200009055	1.703	LOC90246	AK023635	Homo sapiens cDNA FLJ13573 fis, clone PLACE1008584
H200011432	1.702	C10orf39	AL137551	Homo sapiens mRNA; cDNA DKFZp434D0720 (from clone DKFZp434D0720)
H200012013	1.699		AK057612	Homo sapiens cDNA FLJ33050 fis, clone TRACH1000057
H200004254	1.697		AP001660	Homo sapiens genomic DNA, chromosome 21q, section 4/105
H200005091	1.695	CD81	NM_004356	CD81 antigen (target of antiproliferative antibody 1)
H200002377	1.693	PROX1	AK025453	Homo sapiens cDNA: FLJ21800 fis, clone HEP00618
H300002107	1.693	ENSG00000178297		UNKNOWN
H200006004	1.692	EBP	NM_006579	Emopamil binding protein (sterol isomerase)

Genes that are 1.4 fold up regulated in SUM1315-BP2 vs SUM1315				
H200009062	1.691	FLJ13769	NM_025012	Hypothetical protein FLJ13769
H200016940	1.69	HBA1	NM_000558	Hemoglobin, alpha 1
H300018137	1.686	ENSG00000174136	NM_152582	SIMILAR TO SARCOMA ANTIGEN TUMOR ANTIGEN
H200004522	1.686	MGC17515	AK056929	Homo sapiens cDNA FLJ32367 fis, clone PUAEN1000239
H200004409	1.685	FLJ12484	NM_022767	Hypothetical protein FLJ12484
H200008457	1.685	SF1	NM_004630	Splicing factor 1
H200016546	1.683	FLJ20731	NM_017946	Hypothetical protein FLJ20731
H200001437	1.683	MT	AL359401	Isoform 1 of a novel human mRNA from chromosome 22
H300000344	1.683	ENSG00000179334		AMBIGUOUS
H200016525	1.681	AKT2	AK054771	Homo sapiens cDNA FLJ30209 fis, clone BRACE2001564, highly similar to RAC-BETA SERINE/THREONINE KINA
H200009394	1.68		AK021525	Homo sapiens cDNA FLJ11463 fis, clone HEMBA1001608
H200003252	1.68	FLJ32810	AK023666	Homo sapiens cDNA FLJ13604 fis, clone PLACE1010401
H200016229	1.68	TPM4	NM_003290	Tropomyosin 4
H200001373	1.679	LOC129607	BC016969	Homo sapiens, clone IMAGE: 4428577, mRNA, partial cds
H200005653	1.679	LOC90701	NM_033280	Similar to signal peptidase complex (18kD)
H200000631	1.677	MYOM1	NM_003803	Myomesin 1 (skelemin) (185kD)
H200000965	1.675	KIAA1089	AB029012	KIAA1089 protein
H200008239	1.674		AL360140	Homo sapiens mRNA full length insert cDNA clone EUROIMAGE 113222
H200001350	1.673	SUCLG1	NM_003849	Succinate-CoA ligase, GDP-forming, alpha subunit
H300002925	1.671	ENSG00000174914		ZINC FINGER
H200001819	1.671	CCNE1	NM_001238	Cyclin E1
H200003718	1.671	EFNB3	NM_001406	Ephrin-B3
H200006734	1.67	PEX7	NM_000288	Peroxisomal biogenesis factor 7
H200016952	1.67	FLJ20340	NM_017773	Hypothetical protein FLJ20340
H200010845	1.669	MGC4766	NM_031451	Hypothetical protein MGC4766 similar to testis specific protein TES101RP
H200004630	1.668	DTNBP1	AL136637	Dystrobrevin binding protein 1
H200006255	1.668	HERC1	NM_003922	Hect (homologous to the E6-AP (UBE3A) carboxyl terminus) domain and RCC1 (CHC1)-like domain (RLD) 1

Genes that are 1.4 fold up regulated in SUM1315-BP2 vs SUM1315				
H200001366	1.666	CPNE4	BC014396	Copine IV
H200009551	1.666	CRR9	AK057095	Homo sapiens cDNA FLJ32533 fis, clone SMINT2000239
H200011589	1.664	SREBF2	NM_004599	Sterol regulatory element binding transcription factor 2
H200000328	1.664	BN51T	NM_001722	BN51 (BHK21) temperature sensitivity complementing
H200013957	1.662	TLL2	AB023149	Tolloid-like 2
H200021220	1.66	KIAA1085	AB029008	KIAA1085 protein
H200015630	1.658	NTKL	AF297709	N-terminal kinase-like
H200010155	1.656		BI831542	ESTs
H200010439	1.655	DKFZp313N0621	AK056593	Homo sapiens cDNA FLJ32031 fis, clone NTONG2000107
H200008990	1.655		AK022220	Homo sapiens cDNA FLJ12158 fis, clone MAMMA1000522
H300000993	1.654	ENSG00000177004		BK2514C3.2.1 (NOVEL PROTEIN, ISOFORM 1) (FRAGMENT). [Source:SPTREMBL;Acc:Q9BWX6]
H200003632	1.653	MGC25181	AK055846	Homo sapiens cDNA: FLJ23449 fis, clone HSI05859
H200009037	1.653	FLJ13215	NM_025004	Hypothetical protein FLJ13215
H200016956	1.653	FLJ20456	NM_017831	Hypothetical protein FLJ20456
H200005526	1.652	TLR2	NM_003264	Toll-like receptor 2
H200010649	1.652	LILRA2	NM_006866	Leukocyte immunoglobulin-like receptor, subfamily A (with TM domain), member 2
H200015186	1.651	KIAA0447	AB007916	KIAA0447 gene product
H200008024	1.65	PDE4D	U02882	Phosphodiesterase 4D, cAMP-specific (phosphodiesterase E3 dunce homolog, Drosophila)
H200009260	1.648	LRRC15	AK022342	Homo sapiens cDNA FLJ12280 fis, clone MAMMA1001744
H200010227	1.647	BBC3	AF332558	Bcl-2 binding component 3
H200009063	1.645		AK023838	Homo sapiens cDNA FLJ13776 fis, clone PLACE4000387
H200009162	1.645		AK026914	Homo sapiens cDNA: FLJ23261 fis, clone COL05862
H200008998	1.643	MCM3AP; GANP; MAP80; KIAA0572	AK022303	Homo sapiens cDNA FLJ12241 fis, clone MAMMA1001274
H200000352	1.642	MCC	NM_002387	Mutated in colorectal cancers
H200007250	1.642	EMK1	NM_017490	ELKL motif kinase

Genes that are 1.4 fold up regulated in SUM1315-BP2 vs SUM1315				
H200000731	1.641	GZMK	NM_002104	Granzyme K (serine protease, granzyme 3; tryptase II)
H200012030	1.641	SIGLEC5	NM_003830	Sialic acid binding Ig-like lectin 5
H200003191	1.639	TMEFF2	AL157430	Transmembrane protein with EGF-like and two follistatin-like domains 2
H200001261	1.638	KIAA1109	AB029032	KIAA1109 protein
H200008728	1.636	KIAA0738	AF119896	Homo sapiens PRO2751 mRNA, complete cds
H200008026	1.635	PORIMIN	NM_052932	Pro-oncosis receptor inducing membrane injury gene
H200010154	1.635	HES6	NM_018645	Likely ortholog of mouse Hes6 neuronal differentiation gene
H200010341	1.634	AKR1A1	NM_006066	Aldo-keto reductase family 1, member A1 (aldehyde reductase)
H300001882	1.633	FLJ35424	NM_173661	AMBIGUOUS
H200001349	1.633	DKFZp762B226	AB033034	Hypothetical protein DKFZp762B226
H200010952	1.632	RGS20	NM_003702	Regulator of G-protein signalling 20
H200003266	1.632	FLJ14681	NM_032824	Hypothetical protein FLJ14681
H200000992	1.631	MRPL16	NM_017840	Mitochondrial ribosomal protein L16
H200003915	1.631	TNFAIP6	NM_007115	Tumor necrosis factor, alpha-induced protein 6
H300004071	1.63			SEVEN TRANSMEMBRANE HELIX RECEPTOR. [Source:SPTREMBL;Acc:Q8NH51]
H200013805	1.63	N143	AJ002572	Transcriptional unit N143
H300002740	1.629	ENSG00000179872		UNKNOWN
H200015857	1.629	FLJ10902	NM_018266	Hypothetical protein FLJ10902
H200009807	1.629		AK024099	Homo sapiens cDNA FLJ14037 fis, clone HEMBA1004860
H200016389	1.629	MY050	NM_032624	Hypothetical brain protein my050
H200018808	1.628	QSCN6L1	AJ420461	Homo sapiens mRNA full length insert cDNA clone EUROIMAGE 1644069
H200002848	1.627		AL109702	Homo sapiens mRNA full length insert cDNA clone EUROIMAGE 42138
H200006712	1.625	RIL	AF153882	LIM domain protein
H200011314	1.625	CHST1	NM_003654	Carbohydrate (keratan sulfate Gal-6) sulfotransferase 1
H200009378	1.625	FLJ12178	NM_025134	Hypothetical protein FLJ12178

Genes that are 1.4 fold up regulated in SUM1315-BP2 vs SUM1315				
H200008371	1.623	MYBL2	NM_002466	V-myb myeloblastosis viral oncogene homolog (avian)-like 2
H200003765	1.622	LOC55893	NM_018660	Papillomavirus regulatory factor PRF-1
H200006014	1.621	POR1	NM_012402	Partner of RAC1 (arfaptin 2)
H200002108	1.621	SLC24A3	NM_020689	Solute carrier family 24 (sodium/potassium/calcium exchanger), member 3
H200014650	1.62	SLC25A14	NM_003951	Solute carrier family 25 (mitochondrial carrier, brain), member 14
H200010088	1.619	SQRDL	AF131859	Homo sapiens clone 24923 mRNA sequence
H200009079	1.619		AK024127	Homo sapiens cDNA FLJ14065 fis, clone HEMBB1000917
H200014478	1.619	MGC12936	NM_032316	Hypothetical protein MGC12936
H200001801	1.619	CPSF5	NM_007006	Cleavage and polyadenylation specific factor 5, 25 kD subunit
H200010112	1.619		AK056351	Homo sapiens cDNA FLJ31789 fis, clone NT2RI2008656
H200014675	1.618	CACNA1G	NM_018896	Calcium channel, voltage-dependent, alpha 1G subunit
H200001129	1.618	LOC51201	NM_016353	Rec
H200015583	1.618	WHIP	NM_020135	Werner helicase interacting protein
H200004080	1.616	IKBKAP	AF153419	Inhibitor of kappa light polypeptide gene enhancer in B-cells, kinase complex-associated protein
H200009711	1.615		AK001151	Homo sapiens cDNA FLJ10289 fis, clone MAMMA1002319
H200006035	1.614	TYRP1	NM_000550	Tyrosinase-related protein 1
H200014471	1.613		AK021987	Homo sapiens cDNA FLJ11925 fis, clone HEMBB1000354
H300001804	1.613	ENSG00000178672		60S RIBOSOMAL L21
H200010130	1.612	MGC45419	BI913611	ESTs, Weakly similar to KCC1_HUMAN CALCIUM/ CALMODULIN-DEPENDENT PROTEIN KINASE TYPE I
H200015502	1.612	HEY1	NM_012258	Hairy/enhancer-of-split related with YRPW motif 1
H200009043	1.61		AK023407	Homo sapiens cDNA FLJ13345 fis, clone OVARC1002082
H200015828	1.61	PAGE-5	BC009230	Homo sapiens, clone MGC: 16481 IMAGE:3955765, mRNA, complete cds
H300008894	1.61	ENSG00000179580		RING FINGER CONTAINING

Genes that are 1.4 fold up regulated in SUM1315-BP2 vs SUM1315				
H200003080	1.605	DKFZp761N0624	NM_032295	Hypothetical protein DKFZp761N0624
H200008001	1.602	POLR2A	NM_000937	Polymerase (RNA) II (DNA directed) polypeptide A (220kD)
H300003528	1.6	ENSG00000167602		HELIX HAIRPIN HELIX MOTIF CLASS 2
H200011734	1.599	FLJ22332	NM_024724	Hypothetical protein FLJ22332
H200006490	1.598	PECAM1	NM_000442	Platelet/endothelial cell adhesion molecule (CD31 antigen)
H200016757	1.598	BPNT1	NM_006085	3'(2'), 5'-bisphosphate nucleotidase 1
H200009071	1.597	FLJ13885	NM_025016	Hypothetical protein FLJ13885
H200011471	1.596	C1orf17	NM_015101	Chromosome 1 open reading frame 17
H200000004	1.595	CEACAM4	NM_001817	Carcinoembryonic antigen-related cell adhesion molecule 4
H200008992	1.594		AK022247	Homo sapiens cDNA FLJ12185 fis, clone MAMMA1000798
H200000816	1.594	KIAA0978	AB023195	KIAA0978 protein
H200001414	1.593	FLJ22316	NM_025080	Hypothetical protein FLJ22316
H200004253	1.593	CGI-02	NM_012123	CGI-02 protein
H200001994	1.592	FLJ14784	NM_032839	Hypothetical protein FLJ14784
H200009067	1.591	DAAM1	AK023892	Homo sapiens cDNA FLJ13830 fis, clone THYRO1000637
H200001468	1.589	MAZ	NM_002383	MYC-associated zinc finger protein (purine-binding transcription factor)
H200008422	1.588	CFL1	NM_005507	Cofilin 1 (non-muscle)
H200004507	1.588	LOC51705	NM_016242	Endomucin-2
H200000685	1.588	OXTR	NM_000916	Oxytocin receptor
H300006346	1.586	ENSG00000180466	NM_153360	AMBIGUOUS
H200010665	1.586	ABCA2	NM_001606	ATP-binding cassette, sub-family A (ABC1), member 2
H200016974	1.585	LOC56997	NM_020247	Hypothetical protein, clone Telethon(Italy_B41) _Strait02270_FL142
H200004394	1.585	PRKCBP1	AF144233	Homo sapiens DNA binding peptide mRNA, partial cds
H200007308	1.584	ZNF230	AK056865	Homo sapiens cDNA FLJ32303 fis, clone PROST2002527
H200000608	1.584	APXL	NM_001649	Apical protein-like (Xenopus laevis)
H200003007	1.583	ARPP-21	AL133109	Homo sapiens mRNA; cDNA DKFZp566N1047 (from clone DKFZp566N1047); partial cds

Genes that are 1.4 fold up regulated in SUM1315-BP2 vs SUM1315				
H200001423	1.582	PITPNB	NM_012399	Phosphotidylinositol transfer protein, beta
H200005604	1.582		AJ001873	Homo Sapiens mRNA, partial cDNA sequence from cDNA selection, DCR1-16.0
H200007551	1.58	KCTD1	AK056805	Homo sapiens cDNA FLJ32243 fis, clone PROST1000039
H200009097	1.58		AK024613	Homo sapiens cDNA: FLJ20960 fis, clone ADSH00709
H300020538	1.58	ENSG00000162636	NM_139284	LEUCINE-RICH REPEAT LGI FAMILY, MEMBER 4; LGI1-LIKE PROTEIN 3; LEUCINE-RICH GLIOMA-INACTIVATED GENE 4
H200012799	1.58	BCAS1	NM_003657	Breast carcinoma amplified sequence 1
H200020967	1.579	YDD19	U82319	YDD19 protein
H300006050	1.578	ENSG00000175819	NM_173503	UNKNOWN
H200004454	1.577	SE70-2	AK027339	Cutaneous T-cell lymphoma tumor antigen se70-2
H200002346	1.577	PROK1	NM_032414	Prokineticin 1 precursor
H200013883	1.576	CDC23	NM_004661	CDC23 (cell division cycle 23, yeast, homolog)
H200013318	1.575	FRAT2	NM_012083	Frequently rearranged in advanced T-cell lymphomas 2
H200008070	1.575	IL3RA	NM_002183	Interleukin 3 receptor, alpha (low affinity)
H200001818	1.575	GNA13	AK026902	Homo sapiens cDNA: FLJ23249 fis, clone COL04196
H200000910	1.574	RPL28	BC011582	Ribosomal protein L28
H200015252	1.574	RASAL2; nGAP	AB007970	Homo sapiens mRNA, chromosome 1 specific transcript KIAA0501
H200015244	1.573	HARS	AK055917	Histidyl-tRNA synthetase
H300021392	1.572	ENSG00000163071		PROTEASOME SUBUNIT ALPHA TYPE 7-LIKE (EC 3.4.25.1)
H200009734	1.572		AK021698	Homo sapiens cDNA FLJ11636 fis, clone HEMBA1004312
H200006605	1.569	BIRC1	NM_004536	Baculoviral IAP repeat-containing 1
H200014152	1.569	FLJ21369	NM_024802	Hypothetical protein FLJ21369
H200015534	1.569	ACACB	BC009753	Homo sapiens, clone IMAGE: 3833472, mRNA
H200002708	1.569	LAD1	NM_005558	Ladinin 1
H200003937	1.569	FLJ90492	AK023165	Homo sapiens cDNA FLJ13103 fis, clone NT2RP3002304
H200011660	1.568	OSBPL8	AB040884	Oxysterol binding protein-like 8

Genes that are 1.4 fold up regulated in SUM1315-BP2 vs SUM1315				
H200002156	1.568	NAP1L5	AK054689	Homo sapiens cDNA FLJ30127 fis, clone BRACE1000115, weakly similar to NUCLEOSOME ASSEMBLY PROTEIN 1-
H200016745	1.567	UPK1B	BC012851	Uroplakin 1B
H200005173	1.567	ZNF165	NM_003447	Zinc finger protein 165
H200007293	1.567	KCNN1	NM_002248	Potassium intermediate/small conductance calcium-activated channel, subfamily N, member 1
H200000662	1.567	GPX2	NM_002083	Glutathione peroxidase 2 (gastrointestinal)
H200006666	1.567	PASK	NM_015148	PAS domain containing serine/threonine kinase
H200005391	1.567	MGC11314	NM_032721	Hypothetical protein MGC11314
H200018668	1.566	FLJ23519	NM_032240	Hypothetical protein FLJ23519
H200000377	1.566	GABRB3	BC010641	Gamma-aminobutyric acid (GABA) A receptor, beta 3
H200010108	1.565	PECI	NM_006117	Peroxisomal D3,D2-enoyl-CoA isomerase
H200006357	1.565	GTF2E2	NM_002095	General transcription factor IIE, polypeptide 2 (beta subunit, 34kD)
H200000250	1.564	GCNT2	NM_001491	Glucosaminyl (N-acetyl) transferase 2, I-branching enzyme
H200012129	1.564	SERPINA10	NM_016186	Serine (or cysteine) proteinase inhibitor, clade A (alpha-1 antiproteinase, antitrypsin), member 10
H200006657	1.562	MEST	NM_002402	Mesoderm specific transcript homolog (mouse)
H200009708	1.561		AK001136	Homo sapiens cDNA FLJ10274 fis, clone HEMBB1001169
H200007323	1.561	KCNH1	NM_002238	Potassium voltage-gated channel, subfamily H (eag-related), member 1
H200004189	1.559	INPP4A	NM_001566	Inositol polyphosphate-4-phosphatase, type I, 107kD
H200005610	1.559	MGC11061	NM_032312	Hypothetical protein MGC11061
H200008368	1.559		U22172	Human DNA damage repair and recombination protein RAD52 pseudogene mRNA, partial cds
H300004454	1.559	ENSG00000179254		GLUTAMATE CARBOXYPEPTIDASE II EC_3.4.17.21

Genes that are 1.4 fold up regulated in SUM1315-BP2 vs SUM1315				
H300007487	1.557	ENSG00000176594		TUMOR REJECTION ANTIGEN. [Source:SPTREMBL;Acc:Q8WYR7]
H200007852	1.557	CRB1	NM_012076	Crumbs homolog 1 (Drosophila)
H200007307	1.557	GPR133	AL162032	Homo sapiens mRNA; cDNA DKFZp434B1272 (from clone DKFZp434B1272); partial cds
H200007740	1.557	MADH5	AK055211	Homo sapiens cDNA FLJ10174 fis, clone HEMBA1003959
H200005136	1.557	HSPC251	NM_016505	Hypothetical protein
H300009589	1.557	ENSG00000160401		HECT DOMAIN CONTAINING 1 FRAGMENT
H200004555	1.556	MGC11102	NM_032325	Hypothetical protein MGC11102
H200015616	1.555	FLJ22479	AK027620	Hypothetical protein FLJ22479
H200002952	1.555	DKFZp547M236	NM_018713	Hypothetical protein DKFZp547M236
H200013885	1.554	NOT56L	NM_005787	Not56 (D. melanogaster)-like protein
H200020012	1.552		AL353132	Human DNA sequence from clone RP11-189G24 on chromosome 20. Contains a cytochrome B5 (CYB5) pseudoge
H200009087	1.552		AK024213	Homo sapiens cDNA FLJ14151 fis, clone MAMMA1003031
H200014723	1.551		AK021785	Homo sapiens cDNA FLJ11723 fis, clone HEMBA1005314
H200015046	1.551	RAI17	AK024490	Homo sapiens mRNA for FLJ00092 protein, partial cds
H200000529	1.551	VDR	NM_000376	Vitamin D (1,25-dihydroxyvitamin D3) receptor
H300006846	1.551	ENSG00000180682		UNKNOWN
H200005310	1.551	NF1	AK026658	Homo sapiens cDNA: FLJ23005 fis, clone LNG00396, highly similar to AF055023 Homo sapiens clone 24723
H200012056	1.551	ARHGEF7	AK055476	Homo sapiens cDNA FLJ30914 fis, clone FEBRA2006368
H200017856	1.551		AL359605	Homo sapiens mRNA; cDNA DKFZp547G036 (from clone DKFZp547G036)
H200014652	1.55	BAZ1B	NM_023005	Bromodomain adjacent to zinc finger domain, 1B

Genes that are 1.4 fold up regulated in SUM1315-BP2 vs SUM1315				
H200012126	1.55	FARSLB	AK001025	Homo sapiens cDNA FLJ10163 fis, clone HEMBA1003568, weakly similar to 52 KD RO PROTEIN
H200000639	1.548	ADRB2	M15169	Adrenergic, beta-2-, receptor, surface
H200000707	1.548	RRM1	NM_001033	Ribonucleotide reductase M1 polypeptide
H200007650	1.547	RUNX1	S76346	AML1
H200010914	1.546	GRTH	NM_013264	Gonadotropin-regulated testicular RNA helicase
H200000784	1.546	ADFP	NM_001122	Adipose differentiation-related protein
H200001538	1.546	LOC51125	NM_016099	HSPC041 protein
H200009514	1.545	DKFZp761G058	AK054678	Homo sapiens cDNA FLJ30116 fis, clone BRACE1000042, weakly similar to PROTEIN PHOSPHATASE 2C ABI2 (E
H200021193	1.545	C7orf32	AK057700	Homo sapiens, clone MGC: 17890 IMAGE:3908757, mRNA, complete cds
H200001105	1.545	RAB14	AL162081	RAB14, member RAS oncogene family
H200002132	1.544	HTMP10	NM_033207	Transmembrane protein HTMP10
H200016771	1.543	EN1	NM_001426	Engrailed homolog 1
H200018635	1.543		AK026699	Homo sapiens cDNA: FLJ23046 fis, clone LNG02491
H200003090	1.543	MGC52057	AK055699	Homo sapiens cDNA FLJ31137 fis, clone IMR322001049
H200007207	1.542	MDM1	NM_020128	Nuclear protein double minute 1
H200006949	1.542	HRIHFB2206	BC012182	HRIHFB2206 protein
H200014411	1.542		AK023629	Homo sapiens cDNA FLJ13567 fis, clone PLACE1008331
H200017152	1.542	GA17	AK001768	Homo sapiens cDNA FLJ10906 fis, clone OVARC1000035
H200009379	1.542	PRO1575	NM_014092	PRO1575 protein
H200009112	1.542		AK025081	Homo sapiens cDNA: FLJ21428 fis, clone COL04203
H200000817	1.542	AGT	NM_000029	Angiotensinogen (serine (or cysteine) proteinase inhibitor, clade A (alpha-1 antiproteinase, antitry
H200021190	1.541	M6PR	AK057556	Homo sapiens cDNA FLJ32994 fis, clone THYMU1000105
H200006806	1.541	NTS	NM_006183	Neurotensin

Genes that are 1.4 fold up regulated in SUM1315-BP2 vs SUM1315				
H200006687	1.541	LMOD1	NM_012134	Leiomodin 1 (smooth muscle)
H200003935	1.541	MY038	NM_032626	Hypothetical brain protein my038
H200008487	1.54	VPS41	NM_014396	Vacuolar protein sorting 41 (yeast)
H200017879	1.54		AK022159	Homo sapiens cDNA FLJ12097 fis, clone HEMBB1002617
H200015056	1.54	LOC91664	BC007307	Homo sapiens, Similar to zinc finger protein 268, clone IMAGE:3352268, mRNA, partial cds
H200004020	1.54	MGC4606	NM_024516	Hypothetical protein MGC4606
H200012608	1.539	CLECSF5	NM_013252	C-type (calcium dependent, carbohydrate-recognition domain) lectin, superfamily member 5
H200009846	1.538		AK021505	Homo sapiens cDNA FLJ11443 fis, clone HEMBA1001330
H200001367	1.538	KIAA0574	AB011146	KIAA0574 protein
H200002750	1.538	ZFP29	AL109959	Homo sapiens mRNA full length insert cDNA clone EUROIMAGE 1019273
H200004912	1.537	GJB6	NM_006783	Gap junction protein, beta 6 (connexin 30)
H200009852	1.537	ZFP93	NM_004234	Zinc finger protein 93 homolog (mouse)
H200005556	1.536	CLIC3	NM_004669	Chloride intracellular channel 3
H200010573	1.536	MYST3	AJ420560	Homo sapiens mRNA full length insert cDNA clone EUROIMAGE 1476475
H200013326	1.535		AK024355	Homo sapiens cDNA FLJ14293 fis, clone PLACE1007866
H200019276	1.534	HSSOX6	NM_033326	Sox-6
H200000122	1.534	FUT7	NM_004479	Fucosyltransferase 7 (alpha (1,3) fucosyltransferase)
H200015268	1.533	COL3A1	AK021531	Homo sapiens cDNA FLJ11469 fis, clone HEMBA1001658
H200012054	1.532	KIAA1320	AB037741	KIAA1320 protein
H300003950	1.531	ENSG00000004872		PAIRED BOX PAX
H200017857	1.531	GRIN3A	AL359651	Homo sapiens mRNA full length insert cDNA clone EUROIMAGE 2190570
H200001342	1.531	LOC147343	AK054755	Homo sapiens cDNA FLJ30193 fis, clone BRACE2001340
H200001824	1.531	KIAA0239	D87076	KIAA0239 protein

Genes that are 1.4 fold up regulated in SUM1315-BP2 vs SUM1315				
H200007143	1.53	CLECSF2	NM_005127	C-type (calcium dependent, carbohydrate-recognition domain) lectin, superfamily member 2 (activation
H200012008	1.53	SECRET	NM_006998	Secretagogin
H200010246	1.53	ALDH3B2	NM_000695	Aldehyde dehydrogenase 3 family, member B2
H200003864	1.53	KIAA1223	AB033049	KIAA1223 protein
H200004412	1.53		AK023572	Homo sapiens cDNA FLJ13510 fis, clone PLACE1005146
H200004771	1.529	LYL1	NM_005583	Lymphoblastic leukemia derived sequence 1
H200006924	1.529	DOCK1	NM_001380	Dedicator of cyto-kinesis 1
H200019748	1.529	PCDHGC5	NM_018929	Protocadherin gamma subfamily C, 5
H200009500	1.529	GAS5	AK025846	Growth arrest-specific 5
H200002273	1.529	LOC93081	AF070559	Homo sapiens, Similar to RIKEN cDNA 1700029F09 gene, clone MGC:26637 IMAGE:4825712, mRNA, complete c
H200008101	1.528	ZFYVE20	AK054598	Homo sapiens cDNA FLJ30036 fis, clone 3NB692001496
H200000386	1.528	HDC	NM_002112	Histidine decarboxylase
H200007388	1.527	LFNG	BC014851	Lunatic fringe homolog (Drosophila)
H200012868	1.527	SPAG9	NM_003971	Sperm associated antigen 9
H200004274	1.526	DCX	NM_000555	Doublecortex; lissencephaly, X-linked (doublecortin)
H200005346	1.526	ZNF175	BC007778	Homo sapiens, Similar to zinc finger protein 175, clone MGC:12651 IMAGE:4301632, mRNA, complete cds
H200008391	1.526	RPL11	NM_000975	Ribosomal protein L11
H200008996	1.525	CRSP8; CRAP34; CRSP34; MGC11274	AK022289	Homo sapiens cDNA FLJ12227 fis, clone MAMMA1001154
H200015451	1.525		AL512727	Homo sapiens mRNA; cDNA DKFZp547P042 (from clone DKFZp547P042)
H300008502	1.524	ENSG00000166359		KERATIN TYPE II CYTOSKELETAL
H200007692	1.524	TEAD2	BC007556	Homo sapiens, Similar to TEA domain family member 2, clone MGC:15481 IMAGE: 2967735, mRNA, complete c
H200009056	1.524	FLJ13621	NM_025009	Hypothetical protein FLJ13621
H200003415	1.523	EFS2	NM_005864	Signal transduction protein (SH3 containing)
H200018281	1.523		AL117475	Homo sapiens mRNA; cDNA DKFZp727C211 (from clone DKFZp727C211)

Genes that are 1.4 fold up regulated in SUM1315-BP2 vs SUM1315				
H300015437	1.523	ENSG00000173273		CYTIDINE MONOPHOSPHATE-N-ACETYLNEURAMINIC ACID HYDROXYLASE (CMP-N-ACETYLNEURAMINATE MONOOXYGENASE)
H200004329	1.522	FLJ22418	NM_024626	Hypothetical protein FLJ22418
H200009976	1.522		AK021513	Homo sapiens cDNA FLJ11451 fis, clone HEMBA1001433
H200005689	1.522	HCGII-7	X81001	HCGII-7 protein
H200014754	1.522	ZNF14	NM_021030	Zinc finger protein 14 (KOX 6)
H300004506	1.521	ENSG00000179341		60S RIBOSOMAL L21
H200012613	1.521	LOC148066	BC017592	Homo sapiens, clone MGC: 27006 IMAGE:4828408, mRNA, complete cds
H200006679	1.521	RBL2	X76061	Retinoblastoma-like 2 (p130)
H200010939	1.521		AK054999	Homo sapiens cDNA FLJ30437 fis, clone BRACE2009045
H200005746	1.521	IKIP	AK055613	Homo sapiens cDNA FLJ31051 fis, clone HSYRA2000605, weakly similar to MYOSIN HEAVY CHAIN, CLONE 203
H200006757	1.521	SMCY	NM_004653	Smcy homolog, Y chromosome (mouse)
H200012914	1.521	ADCK4	BC013114	Homo sapiens, clone MGC: 16884 IMAGE:4342891, mRNA, complete cds
H200004424	1.521	SULT1C1	NM_001056	Sulfotransferase family, cytosolic, 1C, member 1
H200002001	1.52	DKFZp566O084	NM_015510	DKFZP566O084 protein
H200018902	1.52		AK000357	Homo sapiens cDNA FLJ20350 fis, clone HEP13972, highly similar to Z184_HUMAN ZINC FINGER PROTEIN 184
H300006428	1.52	ENSG00000175051		OLFACTORY RECEPTOR (FRAGMENT). [Source:SPTREMBL;Acc:Q96 R28]
H200006339	1.52	KIAA0254	NM_014758	KIAA0254 gene product
H200010671	1.519	FLJ22729	NM_024683	Hypothetical protein FLJ22729
H200018515	1.518		AK024907	Homo sapiens cDNA: FLJ21254 fis, clone COL01317
H200015100	1.518	RPIB9	AK055233	Homo sapiens cDNA FLJ30671 fis, clone FCBBF1000687, moderately similar to Mus musculus Rap2 interact

Genes that are 1.4 fold up regulated in SUM1315-BP2 vs SUM1315				
H200004792	1.518	TMPRSS5	NM_030770	Transmembrane protease, serine 5 (spinesin)
H200014906	1.517	LOC121838	AK001938	Homo sapiens cDNA FLJ11079 fis, clone PLACE1005111
H200001398	1.517	MAN1	NM_014319	Integral inner nuclear membrane protein
H200015214	1.517	FBXL11	NM_012308	F-box and leucine-rich repeat protein 11
H200003893	1.516	ZNF75	S67970	Zinc finger protein 75 (D8C6)
H200013295	1.516		AK001829	Homo sapiens cDNA FLJ10967 fis, clone PLACE1000798
H200009869	1.515	BTN2A3	AK056871	Homo sapiens cDNA FLJ32309 fis, clone PROST2002960, highly similar to Human butyrophilin (BTF1) mRNA
H200012541	1.515	KIAA1172	AF023142	Pre-mRNA splicing SR protein rA4
H200001754	1.515	PRKAA1	NM_006251	Protein kinase, AMP-activated, alpha 1 catalytic subunit
H200001374	1.514	DKFZP566H073	NM_015528	DKFZP566H073 protein
H200009875	1.514	KIAA1720	AK056382	KIAA1720 protein
H200016849	1.514	LOC221814	AL122087	Homo sapiens mRNA; cDNA DKFZp564C0371 (from clone DKFZp564C0371)
H200003987	1.513	KIAA0854	NM_014943	KIAA0854 protein
H200017329	1.513	KIAA0146	D63480	KIAA0146 protein
H300002466	1.513	ENSG00000173727	NM_030970	UNKNOWN
H200007282	1.513	HMCS	NM_017947	Molybdenum cofactor sulfurase
H200003945	1.513	FLJ20094	NM_017665	Hypothetical protein FLJ20094
H200009540	1.512	USP31	AK057491	Homo sapiens cDNA FLJ32929 fis, clone TESTI2007407
H200010317	1.512	CXCR4	NM_003467	Chemokine (C-X-C motif), receptor 4 (fusin)
H200002224	1.512	FLJ13920	NM_024558	Hypothetical protein FLJ13920
H200007514	1.512	ZNF501	BC013762	Homo sapiens, Similar to hypothetical protein MGC10520, clone MGC: 21738 IMAGE:4521303, mRNA, complet
H200001746	1.512	RAPGEF1; C3G; GRF2	AK023760	Homo sapiens mRNA full length insert cDNA clone EUROIMAGE 1288997
H300020265	1.511	ENSG00000154240		RAB-LIKE PROTEIN 2A. [Source:SWISSPROT;Acc:Q9 UBK7]
H300009582	1.511	ENSG00000173348		AMBIGUOUS
H200009941	1.511	KIAA0565	AB011137	KIAA0565 gene product

Genes that are 1.4 fold up regulated in SUM1315-BP2 vs SUM1315				
H200009175	1.51	dJ23O21.1	AL137181	Human DNA sequence from clone RP1-23O21 on chromosome 6. Contains an acidic calponin 3 (CNN3) pseudo
H300004000	1.51	ENSG00000156162		HGC6.4 PROTEIN. [Source:SPTREMBL;Acc:Q9Y6Z5]
H200004229	1.51	LOC286075	AK055198	Homo sapiens, Similar to zinc finger protein 30, clone MGC:10201 IMAGE:3910185, mRNA, complete cds
H200001509	1.51	FLJ20312	NM_017761	Hypothetical protein FLJ20312
H200000281	1.509	TACR1	NM_001058	Tachykinin receptor 1
H200003941	1.508	COL21A1	NM_030820	Collagen, type XXI, alpha 1
H200007934	1.508	HNRPDL	NM_005463	Heterogeneous nuclear ribonucleoprotein D-like
H200018816	1.508	VPS13D	AK022477	Homo sapiens cDNA FLJ12415 fis, clone MAMMA1003015
H200012831	1.508	TNFSF14	NM_003807	Tumor necrosis factor (ligand) superfamily, member 14
H200002697	1.508		AK025902	Homo sapiens mRNA; cDNA DKFZp586H0324 (from clone DKFZp586H0324)
H200006352	1.507	SP2	D28588	Sp2 transcription factor
H200010438	1.507	SPTLC1	NM_006415	Serine palmitoyltransferase, long chain base subunit 1
H200004389	1.507	KCNJ3	NM_002239	Potassium inwardly-rectifying channel, subfamily J, member 3
H200015863	1.506	SUCLG2	BC007716	Succinate-CoA ligase, GDP-forming, beta subunit
H200007227	1.506	KIAA1763	AB051550	KIAA1763 protein
H200005239	1.506	MCM2	NM_004526	MCM2 minichromosome maintenance deficient 2, mitotin (S. cerevisiae)
H200000099	1.506		U05589	Human ribosomal S1 protein mRNA, partial cds
H200001264	1.506		AK000789	Homo sapiens cDNA FLJ20782 fis, clone COL03841
H200017464	1.506	ALDH2	AK021975	Homo sapiens, clone MGC:9645 IMAGE:3922910, mRNA, complete cds
H200019350	1.505	FLJ10376	NM_018076	Hypothetical protein FLJ10376
H200009405	1.505	FLJ22670	NM_025144	Hypothetical protein FLJ22670
H200005222	1.505	FLJ32384	AK056946	Homo sapiens cDNA FLJ32384 fis, clone SKMUS1000104, weakly similar to Homo sapiens mRNA for HEXIM1 p

Genes that are 1.4 fold up regulated in SUM1315-BP2 vs SUM1315				
H200001794	1.505	ABCF1	NM_001090	ATP-binding cassette, sub-family F (GCN20), member 1
H200010636	1.505	RRM2B	AB036063	Ribonucleotide reductase M2 B (TP53 inducible)
H200004958	1.504	NYD-SP15	NM_030911	Protein kinase NYD-SP15
H200013146	1.504	PRDM6	AF272898	Homo sapiens PR-domain zinc finger protein 6 isoform A (PRDM6) mRNA, partial cds; alternatively spli
H200008349	1.503		AF131741	Homo sapiens clone 25058 mRNA sequence
H200008997	1.503	JAZ	AK022292	Homo sapiens cDNA FLJ12230 fis, clone MAMMA1001186
H200004205	1.503	GNG4	NM_004485	Guanine nucleotide binding protein 4
H200004182	1.503	LOC51020	NM_016063	CGI-130 protein
H200011579	1.503	PP1057	NM_031285	Hypothetical protein PP1057
H200008410	1.503		AK001279	Homo sapiens cDNA FLJ10417 fis, clone NT2RP1000112
H200019684	1.503	FLJ20897	NM_032378	Hypothetical protein FLJ20897
H200009086	1.502		AK024171	Homo sapiens cDNA FLJ14109 fis, clone MAMMA1001322, moderately similar to B-CELL GROWTH FACTOR PRECU
H200007802	1.502	NPY1R	NM_000909	Neuropeptide Y receptor Y1
H200010347	1.502	EPOR	NM_000121	Erythropoietin receptor
H200021031	1.502	RPL23AP7; RPL23AL1; bA395L14.9	X92108	H.sapiens mRNA for subtelomeric repeat sequence
H200012071	1.502	LOC132241	BC014110	Homo sapiens, clone MGC: 20842 IMAGE:4542449, mRNA, complete cds
H200016378	1.502	DKFZp761P211	AL137507	Homo sapiens mRNA; cDNA DKFZp761P211 (from clone DKFZp761P211)
H200003278	1.501	KIAA1273	AB033099	KIAA1273 protein
H200004984	1.501	MGC12928	NM_032891	Hypothetical protein MGC12928
H200009688	1.5	HSPC052	BC016914	HSPC052 protein
H200000305	1.5	E2F3	NM_001949	E2F transcription factor 3
H200011470	1.5	ATP2C1	AF189723	ATPase, Ca++ transporting, type 2C, member 1
H200000804	1.499	FLJ22555	NM_024520	Hypothetical protein FLJ22555
H200015391	1.499	C22orf2	NM_015373	Chromosome 22 open reading frame 2
H200011473	1.498	KLHL1	NM_020866	Kelch-like 1 (Drosophila)
H200012057	1.497		AK056080	Homo sapiens cDNA FLJ31518 fis, clone NT2RI2000064

Genes that are 1.4 fold up regulated in SUM1315-BP2 vs SUM1315				
H200006794	1.496	PCCA	NM_000282	Propionyl Coenzyme A carboxylase, alpha polypeptide
H200013656	1.496	PIP5K1A	NM_003557	Phosphatidylinositol-4-phosphate 5-kinase, type I, alpha
H200005262	1.496	H105E3	NM_015922	NAD(P) dependent steroid dehydrogenase-like; H105e3
H200002870	1.496	ZNFN2A1	AB046809	Zinc finger protein, subfamily 2A (FYVE domain containing), 1
H200010642	1.496	PCSK5	NM_006200	Proprotein convertase subtilisin/kexin type 5
H200008711	1.496		AF161365	Homo sapiens HSPC102 mRNA, partial cds
H200019472	1.496	DSS1	NM_006304	Deleted in split-hand/split-foot 1 region
H200002376	1.495	CSL4	NM_016046	Homolog of yeast exosomal core protein CSL4
H200000933	1.494	OPCML	AF070577	Homo sapiens clone 24461 mRNA sequence
H200015834	1.494	MGC3113	NM_024035	Hypothetical protein MGC3113
H200007452	1.493	SACS	NM_014363	Spastic ataxia of Charlevoix-Saguenay (sacsin)
H200000329	1.493	C1R	AK024951	Complement component 1, r subcomponent
H200002106	1.493	FLJ11608	NM_024557	Hypothetical protein FLJ11608
H200003766	1.493	HSU79275	U79275	Hypothetical protein
H200015101	1.493	LOC81501	NM_030788	DC-specific transmembrane protein
H300009091	1.492	ENSG00000165606		AMBIGUOUS
H200006686	1.492		U90905	Human clone 23574 mRNA sequence
H200009109	1.492		AK025037	Homo sapiens cDNA: FLJ21384 fis, clone COL03354
H200005440	1.491	USP6NL	BC010351	Homo sapiens, clone IMAGE: 4047207, mRNA, partial cds
H200008951	1.491	TMF1	AK021741	Homo sapiens cDNA FLJ11679 fis, clone HEMBA1004807
H200018484	1.49		AK024561	Homo sapiens cDNA: FLJ20908 fis, clone ADSE00417
H200005019	1.49	FLJ13842	NM_024645	Hypothetical protein FLJ13842
H200004428	1.49	GPR146	BC014241	Homo sapiens, Similar to hypothetical protein, MGC: 7035, clone MGC:20737 IMAGE:4563636, mRNA, comple
H200002119	1.49	ADCY6	NM_015270	Adenylate cyclase 6

Genes that are 1.4 fold up regulated in SUM1315-BP2 vs SUM1315				
H200002916	1.49	FLJ20203	AB046826	Hypothetical protein FLJ20203
H200000036	1.488	MGAT3	NM_002409	Mannosyl (beta-1,4-)-glycoprotein beta-1,4-N-acetylglucosaminyltransferase
H200008465	1.486	S164	L40392	S164 protein
H200009188	1.486	C20orf118	AL079335	Chromosome 20 open reading frame 118
H200016360	1.486	BXMAS2-10	BC016789	Homo sapiens, clone MGC: 24011 IMAGE:4091916, mRNA, complete cds
H200007259	1.485	KIAA1365	NM_020794	Densin-180
H200003405	1.485	LOC339229	AY007126	Homo sapiens clone CDABP0028 mRNA sequence
H200010138	1.485	APPL	NM_012096	Adaptor protein containing pH domain, PTB domain and leucine zipper motif
H200006459	1.484	ADORA1	NM_000674	Adenosine A1 receptor
H200010843	1.484	CHM-I	NM_007015	Chondromodulin I precursor
H200004590	1.484	MSH3	NM_002439	MutS homolog 3 (E. coli)
H200005573	1.484	CALB1	NM_004929	Calbindin 1, (28kD)
H200013126	1.484	FLJ20542	AK022675	Homo sapiens cDNA FLJ12613 fis, clone NT2RM4001594
H200001378	1.484	DDX35	NM_021931	DEAD/H (Asp-Glu-Ala-Asp/His) box polypeptide 35
H200013835	1.484	TMEM1	AL050119	Homo sapiens mRNA; cDNA DKFZp586C091 (from clone DKFZp586C091)
H300020135	1.484	ENSG00000151743		A DISINTEGRIN-LIKE AND METALLOPROTEASE (REPROLYSIN TYPE) WITH THROMBOSPONDIN TYPE 1 MOTIF, 17 PREPROPROTEIN.
H200008885	1.484	JAM1	AF172398	Junctional adhesion molecule 1
H200001348	1.483	NAGK	NM_017567	N-acetylglucosamine kinase
H200009588	1.483	AFG3L1	AK056488	Homo sapiens cDNA FLJ31926 fis, clone NT2RP7005502, moderately similar to Homo sapiens mRNA for para
H200008020	1.483	C16orf34	AK023154	Homo sapiens cDNA FLJ13092 fis, clone NT2RP3002147
H200005665	1.483	MGC20533	BC004398	Similar to RIKEN cDNA 2410004L22 gene (M. musculus)
H200012615	1.483	FLJ25323	AK058052	Homo sapiens cDNA FLJ25323 fis, clone TST00323

Genes that are 1.4 fold up regulated in SUM1315-BP2 vs SUM1315				
H200002239	1.483	B4GALT4	NM_003778	UDP-Gal:betaGlcNAc beta 1,4- galactosyltransferase, polypeptide 4
H200001748	1.483	LOC51005	NM_015944	CGI-14 protein
H200008022	1.482	DKFZP434C212	AB040954	DKFZP434C212 protein
H200011780	1.482	SLC30A3	NM_003459	Solute carrier family 30 (zinc transporter), member 3
H200015769	1.481	ARIH2	NM_006321	Ariadne homolog 2 (Drosophila)
H200000027	1.481	PMAIP1	NM_021127	Phorbol-12-myristate-13-acetate-induced protein 1
H200005571	1.481	DDX20	NM_007204	DEAD/H (Asp-Glu-Ala-Asp/ His) box polypeptide 20, 103kD
H200016402	1.481		AF116715	Homo sapiens PRO2829 mRNA, complete cds
H200008571	1.48	SQSTM1	NM_003900	Sequestosome 1
H200008426	1.48	DUSP6	NM_001946	Dual specificity phosphatase 6
H200011801	1.48	KBTBD6	BC000560	Homo sapiens mRNA; cDNA DKFZp547M073 (from clone DKFZp547M073)
H200008881	1.48	C20orf177	AL137442	Chromosome 20 open reading frame 177
H200002015	1.48	CTSF	NM_003793	Cathepsin F
H200001440	1.48	BLP1	NM_031940	BBP-like protein 1
H200009121	1.48	LOC91948	AK025311	Homo sapiens cDNA: FLJ21658 fis, clone COL08688
H200004489	1.48	UCP4	NM_004277	Uncoupling protein 4
H200019831	1.479	LOC284017	AK021878	Homo sapiens cDNA FLJ11816 fis, clone HEMBA1006416
H300009831	1.479	ENSG00000177207		UNKNOWN
H300004504	1.479	ENSG00000177581		UNKNOWN
H200014311	1.478	TCEB1	AK057889	Transcription elongation factor B (SIII), polypeptide 1 (15kD, elongin C)
H200010920	1.478		AK022219	Homo sapiens cDNA FLJ12157 fis, clone MAMMA1000500
H200004181	1.478	SLC39A10	AK055670	Homo sapiens cDNA FLJ31108 fis, clone IMR322000164
H200007571	1.478	FLJ12606	NM_024804	Hypothetical protein FLJ12606
H200004137	1.477	POT1	NM_015450	Protection of telomeres 1
H200015456	1.477	ALS2CR13	AB053315	Homo sapiens ALS2CR13 mRNA, partial cds
H200013645	1.477	DKFZP434N1235	NM_031291	Hypothetical protein DKFZp434N1235
H200010113	1.476	FLJ10851	NM_018245	Hypothetical protein FLJ10851
H200002935	1.476	KNSL2	BC000712	Kinesin-like 2
H200002223	1.476	TXNRD1	NM_003330	Thioredoxin reductase 1

Genes that are 1.4 fold up regulated in SUM1315-BP2 vs SUM1315				
H200009575	1.476	LOC116064	AK056809	Homo sapiens cDNA FLJ32247 fis, clone PROST1000120
H200014660	1.476	AP4M1	NM_004722	Adaptor-related protein complex 4, mu 1 subunit
H200013938	1.476	LIM	NM_006457	LIM protein (similar to rat protein kinase C-binding enigma)
H200010114	1.476	DKFZP434H132	BC011379	DKFZP434H132 protein
H200001844	1.475	LOC81558	NM_030802	C/EBP-induced protein
H200005464	1.475	DKFZP586N2124	NM_015424	DKFZP586N2124 protein
H200017235	1.475		AK024106	Homo sapiens cDNA FLJ14044 fis, clone HEMBA1006124
H300001519	1.475	ENSG00000178751		BETA 1 3 GALACTOSYLTRANSFERASE
H200004235	1.475	PDI2	AB023211	Peptidyl arginine deiminase, type II
H300003034	1.474	ENSG00000181147		UNKNOWN
H200003670	1.474	C20orf44	NM_018244	Chromosome 20 open reading frame 44
H200003073	1.474	IL20RA	NM_014432	Interleukin 20 receptor, alpha
H200015179	1.474		AL110169	Homo sapiens mRNA; cDNA DKFZp586N2224 (from clone DKFZp586N2224)
H300002799	1.474	ENSG00000179305		PLATELET RECEPTOR FOR TYPE III COLLAGEN (FRAGMENT). [Source:SPTREMBL;Acc:Q8NFD8]
H300020608	1.473	ENSG00000164049		LEUCINE RICH REGION CONTAINING
H200001285	1.472	DKFZP564O1664	NM_030800	Hypothetical protein DKFZp564O1664
H200006027	1.472	BAT8	NM_006709	HLA-B associated transcript 8
H200001444	1.471	YF13H12	NM_014297	Protein expressed in thyroid
H200005950	1.471	ARNTL	NM_001178	Aryl hydrocarbon receptor nuclear translocator-like
H200010641	1.471	TITF1	AK027147	Homo sapiens cDNA: FLJ23494 fis, clone LNG01885
H200017327	1.47	PCL1	AB020715	Prenylcysteine lyase
H200000168	1.47	CYP4B1	NM_000779	Cytochrome P450, subfamily IVB, polypeptide 1
H200004301	1.469	BBX	AL136769	Bobby sox homolog (Drosophila)
H200005553	1.469	MDS009	NM_020234	X 009 protein
H200011792	1.468	GLP	NM_018652	Golgin-like protein
H200012356	1.468		AK022033	Homo sapiens cDNA FLJ11971 fis, clone HEMBB1001208
H200012083	1.468	BST2	NM_004335	Bone marrow stromal cell antigen 2

Genes that are 1.4 fold up regulated in SUM1315-BP2 vs SUM1315				
H200008504	1.468	TNFSF4	NM_003326	Tumor necrosis factor (ligand) superfamily, member 4 (tax-transcriptionally activated glycoprotein 1
H300010310	1.467	ENSG00000171920		UNKNOWN
H200014884	1.467	EPPK1	NM_031308	Epiplakin 1
H200020716	1.467		AK057203	Homo sapiens cDNA FLJ32641 fis, clone SYNOV2001035
H300006102	1.467	ENSG00000180588		UNKNOWN
H200005578	1.466	C20orf114	NM_033197	Chromosome 20 open reading frame 114
H200015074	1.466	KIAA1766	AB051553	KIAA1766 protein
H200002864	1.466	HFE	NM_000410	Hemochromatosis
H200005909	1.466	ETFB	NM_001985	Electron-transfer-flavoprotein, beta polypeptide
H200008254	1.466	HSD-3.1	AK055864	Hypothetical protein
H200004234	1.466		AK026459	Homo sapiens cDNA: FLJ22806 fis, clone KAIA2845
H200007156	1.465		AK054652	Homo sapiens cDNA FLJ30090 fis, clone BNGH41000015
H300005024	1.465	ENSG00000177571		LINE 1 REVERSE TRANSCRIPTASE HOMOLOG
H200003046	1.465	DXYS155E	NM_005088	DNA segment on chromosome X and Y (unique) 155 expressed sequence
H200009407	1.465		AK021454	Homo sapiens cDNA FLJ11392 fis, clone HEMBA1000575
H200001131	1.464	MEL	NM_005370	Mel transforming oncogene (derived from cell line NK14)-RAB8 homolog
H200000043	1.464	RPL7	NM_000971	Ribosomal protein L7
H200010245	1.463	BTN3A2	NM_007047	Butyrophilin, subfamily 3, member A2
H200005629	1.463	DNCI2	AK055491	Dynein, cytoplasmic, intermediate polypeptide 2
H200011705	1.463	MGC3133	NM_031287	Hypothetical protein MGC3133
H200010291	1.462	CBR1	NM_001757	Carbonyl reductase 1
H200011289	1.462	RAGE	NM_014226	Renal tumor antigen
H200014310	1.462	RAB3C	BC013033	Homo sapiens, clone MGC: 4711 IMAGE:3534915, mRNA, complete cds
H200008613	1.462		AK056555	Homo sapiens cDNA FLJ31993 fis, clone NT2RP7009168
H200019425	1.462		AK021970	Homo sapiens cDNA FLJ11908 fis, clone HEMBB1000089

Genes that are 1.4 fold up regulated in SUM1315-BP2 vs SUM1315				
H200000938	1.461	DKFZP566A1524	AK055334	Hypothetical protein DKFZp566A1524
H200004881	1.461		AF007131	Homo sapiens clone 23963 mRNA sequence
H200005817	1.461	MKRN3	NM_005664	Makorin, ring finger protein, 3
H200013729	1.461	BCS1L	NM_004328	BCS1-like (yeast)
H200013876	1.46	STAM	NM_003473	Signal transducing adaptor molecule (SH3 domain and ITAM motif) 1
H200007215	1.46	MUSK	NM_005592	Muscle, skeletal, receptor tyrosine kinase
H200003985	1.46	C21orf63	NM_058187	Homo sapiens chromosome 21 open reading frame 63 (C21orf63), mRNA
H200006557	1.459	GSK3B	NM_002093	Glycogen synthase kinase 3 beta
H200006282	1.459	SERPINA5	BC008915	Serine (or cysteine) proteinase inhibitor, clade A (alpha-1 antiproteinase, antitrypsin), member 5
H200003391	1.459	LOC51071	NM_015954	CGI-26 protein
H200011242	1.458	LOC285458	BC008921	Homo sapiens, Similar to RIKEN cDNA 1700010L19 gene, clone MGC:16214 IMAGE:3659061, mRNA, complete c
H200001112	1.458	MRPS23	NM_016070	Mitochondrial ribosomal protein S23
H200000262	1.458	PPARA	NM_005036	Peroxisome proliferative activated receptor, alpha
H200003860	1.458	SSR3	NM_007107	Signal sequence receptor, gamma (translocon-associated protein gamma)
H200007185	1.458	GRM8	NM_000845	Glutamate receptor, metabotropic 8
H200004027	1.458	FLJ13409	AB051498	Hypothetical protein FLJ13409
H200009027	1.458	HELLS	AK022928	Homo sapiens cDNA FLJ12866 fis, clone NT2RP2003691
H200011612	1.457	KIAA0515	AB011087	KIAA0515 protein
H200017381	1.457	PRO0255	NM_014124	PRO0255 protein
H200001980	1.456	KCNJ6	NM_002240	Potassium inwardly-rectifying channel, subfamily J, member 6
H200001416	1.456	MAD1L1	NM_003550	MAD1 mitotic arrest deficient-like 1 (yeast)
H200017671	1.456	PRO0800	NM_018592	Hypothetical protein PRO0800
H200007221	1.456	FLJ22800	NM_024795	Hypothetical protein FLJ22800
H200012500	1.456	DKFZp434H2111	AK026776	Homo sapiens cDNA: FLJ23123 fis, clone LNG08039

Genes that are 1.4 fold up regulated in SUM1315-BP2 vs SUM1315				
H200018972	1.456		AK000786	Homo sapiens cDNA FLJ20779 fis, clone COL05077
H200006456	1.455	RGN	NM_004683	Regucalcin (senescence marker protein-30)
H200011582	1.455	THBS2	NM_003247	Thrombospondin 2
H200006326	1.455	ADH6	NM_000672	Alcohol dehydrogenase 6 (class V)
H200003409	1.455	CSPG6	NM_005445	Chondroitin sulfate proteoglycan 6 (bamacan)
H200020445	1.455	PC4	NM_006713	Activated RNA polymerase II transcription cofactor 4
H200003763	1.454		AL110139	Homo sapiens mRNA; cDNA DKFZp564O1763 (from clone DKFZp564O1763)
H200001800	1.454	SLC25A13	NM_014251	Solute carrier family 25, member 13 (citrin)
H200003249	1.454	FTSJ1	NM_012280	FtsJ homolog 1 (E. coli)
H200007897	1.454	WASL	AK023554	Homo sapiens cDNA FLJ13492 fis, clone PLACE1004284
H200008111	1.454	SLC24A1	NM_004727	Solute carrier family 24 (sodium/potassium/calcium exchanger), member 1
H200009384	1.454	PFDN5	NM_002624	Prefoldin 5
H200015401	1.453	PTP4A1	NM_003463	Protein tyrosine phosphatase type IVA, member 1
H200009298	1.453		AK024152	Homo sapiens cDNA FLJ14090 fis, clone MAMMA1000264
H200015955	1.453		AJ242956	Homo sapiens partial N-myc (exon 3), HPV45 L2, HPV45 L1, HPV45 E6, HPV45 E7 and HPV45 E1 genes isola
H200005528	1.453	PCCB	NM_000532	Propionyl Coenzyme A carboxylase, beta polypeptide
H200001011	1.453	HSPC150	NM_014176	HSPC150 protein similar to ubiquitin-conjugating enzyme
H200011386	1.452	FLJ21125	AK026924	Homo sapiens cDNA: FLJ23271 fis, clone HEP00174
H200011678	1.452	IL17B	NM_014443	Interleukin 17B
H200007158	1.451	FLJ10458	NM_018096	Hypothetical protein similar to beta-transducin family
H200017303	1.451	ACAT2	NM_005891	Acetyl-Coenzyme A acetyltransferase 2 (acetoacetyl Coenzyme A thiolase)
H300007564	1.45	ENSG00000172150		PROLIFERATING CELL NUCLEAR ANTIGEN PCNA
H200017362	1.45	FIL1(EPSILON)	NM_014440	Interleukin 1, epsilon
H200004183	1.45	NXPH2	AF043467	Neurexophilin 2
H200009324	1.45		AK022059	Homo sapiens cDNA FLJ11997 fis, clone HEMBB1001458

Genes that are 1.4 fold up regulated in SUM1315-BP2 vs SUM1315				
H200016338	1.449	PGF	AK023843	Homo sapiens cDNA FLJ13781 fis, clone PLACE4000465
H200001556	1.449	FLJ31434	AK055996	Homo sapiens, Similar to hypothetical protein FLJ12838, clone IMAGE: 4130879, mRNA, partial cds
H200015559	1.449	NUP107	NM_020401	Nuclear pore complex protein
H200003174	1.449	KIAA0664	AB014564	KIAA0664 protein
H200012101	1.448	UNKL	BC011924	Homo sapiens, clone MGC: 20510 IMAGE:4542472, mRNA, complete cds
H200012182	1.448	SMURF1	AB046845	E3 ubiquitin ligase SMURF1
H200002863	1.448	C22orf4	AK000851	Chromosome 22 open reading frame 4
H200010157	1.447	PIGCP1	AL543108	Phosphatidylinositol glycan, class C, pseudogene 1
H200005322	1.447	NESHBP	NM_015429	DKFZP586L2024 protein
H200013753	1.447	SERPING1	NM_000062	Serine (or cysteine) proteinase inhibitor, clade G (C1 inhibitor), member 1, (angioedema, hereditary
H200005626	1.447	LOC221061	AL050367	Homo sapiens mRNA; cDNA DKFZp564A026 (from clone DKFZp564A026)
H200018587	1.446		AK025325	Homo sapiens cDNA: FLJ21672 fis, clone COL09025
H200004905	1.446	FLJ30726	AK055288	Homo sapiens cDNA FLJ30726 fis, clone FCBBF5000261, moderately similar to ZINC FINGER PROTEIN 35
H200004579	1.446	FLJ10618	AL049246	Hypothetical protein FLJ10618
H200009477	1.446	PTEN; BZS; MHAM; TEP1; MMAC1; PTEN1; MGC11227	AK021619	Homo sapiens cDNA FLJ11557 fis, clone HEMBA1003083
H200007975	1.446	SCML2	NM_006089	Sex comb on midleg-like 2 (Drosophila)
H200014632	1.446		AK054919	Homo sapiens cDNA FLJ30357 fis, clone BRACE2007727
H300011592	1.445	ENSG00000125995		UNKNOWN
H200015588	1.445	IGSF4	AK023357	Homo sapiens cDNA FLJ13295 fis, clone OVARC1001240
H200003501	1.444	LOC57209	AL049341	Kruppel-type zinc finger protein
H200003925	1.444	NID67	AK027847	Putative small membrane protein NID67
H200012055	1.444	RES4-25	AF040965	Gene near HD on 4p16.3 with homology to hypothetical S. pombe gene
H300021075	1.443	ENSG00000171858	NM_145054	AMBIGUOUS

Genes that are 1.4 fold up regulated in SUM1315-BP2 vs SUM1315				
H200015227	1.443	HBS1L	AB028961	HBS1-like (S. cerevisiae)
H200017321	1.443	DNAJB11	NM_016306	DnaJ (Hsp40) homolog, subfamily B, member 11
H200008949	1.443		AK021724	Homo sapiens cDNA FLJ11662 fis, clone HEMBA1004629
H200003737	1.443	LOC113444	BC011880	Homo sapiens, Similar to hypothetical protein, MGC: 7764, clone MGC:20548 IMAGE:3607345, mRNA, comple
H200004995	1.443	JAK1	NM_002227	Janus kinase 1 (a protein tyrosine kinase)
H200001415	1.442	FLJ10936	BC008596	Hypothetical protein FLJ10936
H200017911	1.442	AASS	AK023446	Homo sapiens cDNA FLJ13384 fis, clone PLACE1001062, highly similar to Homo sapiens mRNA for lysine-k
H200007601	1.442	DKFZp434H247	AL137304	Hypothetical protein DKFZp434H247
H200010917	1.442	LOC283248	BC010608	Homo sapiens, clone IMAGE: 4157757, mRNA, partial cds
H200000809	1.442	MAP4K4	NM_004834	Mitogen-activated protein kinase kinase kinase kinase 4
H200000323	1.442	ARSB	NM_000046	Arylsulfatase B
H200005001	1.442	FLJ11175	AK026984	Homo sapiens cDNA: FLJ23331 fis, clone HEP12664
H200004280	1.442	ZFHX1B	NM_014795	Zinc finger homeobox 1b
H200015759	1.442	PEF	NM_012392	PEF protein with a long N-terminal hydrophobic domain (peflin)
H200013556	1.441	LOC51028	AK023182	CGI-145 protein
H200004236	1.441		AK057721	Homo sapiens cDNA FLJ33159 fis, clone UTERU2000465
H200003549	1.44	TNFRSF5	NM_001250	Tumor necrosis factor receptor superfamily, member 5
H200002910	1.44	FLJ13942	NM_024581	Hypothetical protein FLJ13942
H300006281	1.44	ENSG00000180240		UNKNOWN
H200002893	1.44	WRCH-1	AK001478	Wnt-1 responsive Cdc42 homolog
H300005514	1.44	ENSG00000179386		VOLTAGE DEPENDENT TYPE CALCIUM CHANNEL ALPHA SUBUNIT CALCIUM CHANNEL L TYPE ALPHA 1 POLYPEPTIDE
H200002627	1.44	DYRK4	AF263541	Dual-specificity tyrosine-(Y)-phosphorylation regulated kinase 4

Genes that are 1.4 fold up regulated in SUM1315-BP2 vs SUM1315				
H200007600	1.44	FGF7	NM_002009	Fibroblast growth factor 7 (keratinocyte growth factor)
H200009003	1.439	RYR3	AK022386	Homo sapiens cDNA FLJ12324 fis, clone MAMMA1002118
H200002117	1.439	SYT13	AB037848	Synaptotagmin XIII
H200017207	1.439	RPS18	NM_022551	Ribosomal protein S18
H200005216	1.439	ICOS	NM_012092	Inducible T-cell co-stimulator
H200011644	1.439	ABT1	NM_013375	TATA-binding protein-binding protein
H200019725	1.439		BC009051	Homo sapiens, clone MGC: 9852 IMAGE:3865825, mRNA, complete cds
H200011534	1.439	DKFZP566C243	NM_015388	DKFZP566C243 protein
H200013920	1.439	NT5	NM_002526	5' nucleotidase (CD73)
H200010516	1.438	BTN2A2	NM_006995	Butyrophilin, subfamily 2, member A2
H200009371	1.438	HNRPM	AK022050	Homo sapiens cDNA FLJ11988 fis, clone HEMBB1001367
H200011199	1.438	IL1RL2	NM_003854	Interleukin 1 receptor-like 2
H200000778	1.437	FLJ10743	NM_018201	Hypothetical protein FLJ10743
H200007273	1.437	LOC170394	BC011630	Homo sapiens, clone IMAGE: 3957606, mRNA, partial cds
H200019861	1.437	PRO2730	AB019571	Homo sapiens mRNA expressed only in placental villi, clone SMAP5
H300000191	1.437	ENSG00000178287		UNKNOWN
H200004929	1.437	BACE	NM_012104	Beta-site APP-cleaving enzyme
H200009466	1.437		AK022396	Homo sapiens cDNA FLJ12334 fis, clone MAMMA1002209
H200005285	1.437	SCYA21	NM_002989	Small inducible cytokine subfamily A (Cys-Cys), member 21
H200019085	1.436	H63	AK022565	Homo sapiens clone H63 unknown mRNA
H300005814	1.436	ENSG00000170217		FIBROBLAST GROWTH FACTOR FGF
H200017306	1.436		AK021942	Homo sapiens cDNA FLJ11880 fis, clone HEMBA1007129
H200004121	1.436	ACYP2	BC012290	Homo sapiens, Similar to acylphosphatase 2, muscle type, clone MGC:9009 IMAGE:3864319, mRNA, complet
H200013933	1.436	LBP	NM_004139	Lipopolysaccharide binding protein
H200003863	1.436	FLJ23614	AK002078	Homo sapiens cDNA FLJ11216 fis, clone PLACE1008002

Genes that are 1.4 fold up regulated in SUM1315-BP2 vs SUM1315				
H200005191	1.435	LGP2	NM_024119	Likely ortholog of mouse D11lgp2
H200001545	1.435	KIAA0871	NM_014961	KIAA0871 protein
H200008752	1.435	MYOD1	NM_002478	Myogenic factor 3
H200016602	1.435	FLJ20371	NM_017791	Hypothetical protein FLJ20371
H300005845	1.435	ENSG00000155066		UNKNOWN
H200001574	1.435	HS3ST4	AF105378	Heparan sulfate (glucosamine) 3-O-sulfotransferase 4
H200003653	1.435	VPS33B	NM_018668	Vacuolar protein sorting 33B (yeast)
H200012453	1.435	PLSCR2	NM_020359	Phospholipid scramblase 2
H200001051	1.434	MYO1A	NM_005379	Myosin IA
H200008782	1.434	KIAA1340	AK002197	Homo sapiens cDNA FLJ11335 fis, clone PLACE1010630
H200015907	1.434	OR5G1P	AF045576	Olfactory receptor, family 5, subfamily G, member 1 pseudogene
H200003146	1.434	KIAA1898	AB067485	KIAA1898 protein
H200004086	1.434	SYNPO2	AK021484	Homo sapiens cDNA FLJ11422 fis, clone HEMBA1001008
H300000725	1.433	ENSG00000178527	NM_152578	AMBIGUOUS
H200002111	1.433	ENTPD6	NM_001247	Ectonucleoside triphosphate diphosphohydrolase 6 (putative function)
H200017352	1.433	STIM2	AB040915	Stromal interaction molecule 2
H200002720	1.433	MRPL15	NM_014175	Mitochondrial ribosomal protein L15
H200002160	1.433	NAPB	AK022817	N-ethylmaleimide-sensitive factor attachment protein, beta
H200012971	1.432	BRI3BP	AK025766	BRI3 binding protein
H300020807	1.432	ENSG00000166630		UNKNOWN
H200004407	1.432	C14orf73	AK000671	Homo sapiens cDNA FLJ20664 fis, clone KAIA795
H300004843	1.431	ENSG00000177694	NM_173792	AMBIGUOUS
H200021178	1.431		AK055649	Homo sapiens cDNA FLJ31087 fis, clone IMR321000074
H200013284	1.431	PRO2834	NM_018542	Hypothetical protein PRO2834
H300002377	1.431	ENSG00000172335		AMBIGUOUS
H200006581	1.431	XK	NM_021083	Kell blood group precursor (McLeod phenotype)
H200016162	1.431	TNFRSF10A	NM_003844	Tumor necrosis factor receptor superfamily, member 10a
H200017322	1.431	GSA7	AL122075	Ubiquitin activating enzyme E1-like protein
H200005143	1.43	MAPK12	NM_002969	Mitogen-activated protein kinase 12

Genes that are 1.4 fold up regulated in SUM1315-BP2 vs SUM1315				
H200017519	1.43	TPT	NM_014317	Trans-prenyltransferase
H200012012	1.43	CD72	NM_001782	CD72 antigen
H200018216	1.43	PDL-108	AB019409	Periodontal ligament fibroblast protein
H300018340	1.43	ENSG00000163936		AMBIGUOUS
H200003368	1.43	NEK7	AL080111	Homo sapiens mRNA; cDNA DKFZp586G2222 (from clone DKFZp586G2222)
H300021223	1.429	ENSG00000174937		AMBIGUOUS
H200017620	1.429	HPS3	AY033141	Hermansky-Pudlak syndrome 3
H300007877	1.429			MYOSIN-REACTIVE IMMUNOGLOBULIN HEAVY CHAIN VARIABLE REGION (FRAGMENT). [Source:SPTREMBL;Acc:Q9UL88]
H200011635	1.429	LXN	NM_020169	Latexin protein
H200000465	1.429	CD1D	NM_001766	CD1D antigen, d polypeptide
H200004195	1.429	FUT6	NM_000150	Fucosyltransferase 6 (alpha (1,3) fucosyltransferase)
H200003036	1.429	KIAA1035	NM_015239	KIAA1035 protein
H200015813	1.429	ZNF582	AK055489	Homo sapiens cDNA FLJ30927 fis, clone FEBRA2006736
H200004230	1.429	NFIB	NM_005596	Nuclear factor I/B
H200020030	1.428	LOC135270	AL138731	Human DNA sequence from clone RP1-23E21 on chromosome 6 Contains a pseudogene similar to JAB1, an ST
H200010969	1.428	FLJ13044	NM_024698	Hypothetical protein FLJ13044
H200016811	1.428	FLJ10932	NM_018277	Hypothetical protein FLJ10932
H200008361	1.428	FLJ10058	NM_017985	Hypothetical protein FLJ10058
H200003531	1.427	MNT	NM_020310	MAX binding protein
H200007555	1.427	FLJ21665	NM_024803	Hypothetical protein FLJ21665
H200006380	1.427	BTG3	AL049332	BTG family, member 3
H200019259	1.427	TTY9	NM_031927	Testis transcript Y 9
H200005028	1.427	CAMP	NM_004345	Cathelicidin antimicrobial peptide
H200001493	1.427	Ubc6p	NM_058167	Ubiquitin conjugating enzyme 6
H200011628	1.426	CYP2U1	AK026498	Homo sapiens cDNA: FLJ22845 fis, clone KAIA5195
H200005625	1.426	SCYA17	NM_002987	Small inducible cytokine subfamily A (Cys-Cys), member 17
H200010143	1.425	OATL1	BG330197	ESTs, Moderately similar to located at OATL1 [H.sapiens]
H200006813	1.425	BLVRA	NM_000712	Biliverdin reductase A

Genes that are 1.4 fold up regulated in SUM1315-BP2 vs SUM1315				
H200009798	1.425		AK023556	Homo sapiens cDNA FLJ13494 fis, clone PLACE1004384
H300007061	1.424	ENSG00000170507	NM_030970	UNKNOWN
H200013290	1.424	CG030	U50531	Hypothetical gene CG030
H200015930	1.424	H2BFA	BC001131	H2B histone family, member A
H200002221	1.424	DKFZP727A071	BC011758	DKFZP727A071 protein
H200012222	1.423	KCTD7	AK055201	Homo sapiens cDNA FLJ30639 fis, clone CTONG2002803
H200016729	1.423	CNNM2	NM_017649	Cyclin M2
H200007835	1.423	RHAG	NM_000324	Rhesus blood group-associated glycoprotein
H200001369	1.423	LOC57862	NM_021188	Clones 23667 and 23775 zinc finger protein
H200015246	1.423	KIAA1718	AB051505	KIAA1718 protein
H200015595	1.423	MGC20781	NM_052935	Hypothetical protein MGC20781
H200000244	1.423	CRYM	NM_001888	Crystallin, mu
H200002158	1.422	PER3	NM_016831	Period homolog 3 (Drosophila)
H200010629	1.422		AK023696	Homo sapiens cDNA FLJ13634 fis, clone PLACE1011133
H200000276	1.422	GZMB	NM_004131	Granzyme B (granzyme 2, cytotoxic T-lymphocyte-associated serine esterase 1)
H200009675	1.421	DLST	S72422	Dihydrolipoamide S-succinyltransferase (E2 component of 2-oxo-glutarate complex)
H200018140	1.421	SLC26A2	AK025078	Homo sapiens cDNA: FLJ21425 fis, clone COL04162
H200016955	1.421	FLJ20433	NM_017820	Hypothetical protein FLJ20433
H200011008	1.421	LDHC	NM_002301	Lactate dehydrogenase C
H200000227	1.421	IMPDH1	NM_000883	IMP (inosine monophosphate) dehydrogenase 1
H200011271	1.42	DKFZP434B0335	AB037779	DKFZP434B0335 protein
H200013908	1.42	LOC158402	AK056358	Homo sapiens cDNA FLJ31796 fis, clone NT2RI2008841
H200002016	1.42	FLJ32205	AK056767	Homo sapiens, clone MGC: 16395 IMAGE:3939387, mRNA, complete cds
H200010340	1.42	HDGF	NM_004494	Hepatoma-derived growth factor (high-mobility group protein 1-like)
H200002756	1.42	KIAA1233	AB033059	KIAA1233 protein
H200013320	1.42	D6S2654E	NM_012135	DNA segment on chromosome 6(unique) 2654 expressed sequence

Genes that are 1.4 fold up regulated in SUM1315-BP2 vs SUM1315				
H200010661	1.419	TGIF2	BC012816	TGFB-induced factor 2 (TALE family homeobox)
H200009425	1.419		AK026687	Homo sapiens cDNA: FLJ23034 fis, clone LNG02018
H200011650	1.418	SPUF	NM_013349	Secreted protein of unknown function
H200001671	1.418	KIAA1301	AB037722	KIAA1301 protein
H200009039	1.418		AK023302	Homo sapiens cDNA FLJ13240 fis, clone OVARC1000496
H200001522	1.418	RYBP	AB029551	RING1 and YY1 binding protein
H200003338	1.418	SAMHD1	NM_015474	SAM domain and HD domain, 1
H200008285	1.418	MGC4161	NM_024303	Hypothetical protein MGC4161
H300007259	1.418	ENSG00000173236	NM_030970	UNKNOWN
H200000388	1.418	RARG	NM_000966	Retinoic acid receptor, gamma
H300008325	1.418	ENSG00000176122		60S RIBOSOMAL L30
H200012156	1.418	LOC51101	NM_016010	CGI-62 protein
H200003071	1.417	PRDM4	NM_012406	PR domain containing 4
H200004440	1.417	HSD3B1	NM_000862	Hydroxy-delta-5-steroid dehydrogenase, 3 beta- and steroid delta-isomerase 1
H200017217	1.417	KCNMB3	NM_014407	Potassium large conductance calcium-activated channel, subfamily M beta member 3
H200018490	1.417		AK024585	Homo sapiens cDNA: FLJ20932 fis, clone ADSE01312
H200014638	1.416	CDH1	NM_004360	Cadherin 1, type 1, E-cadherin (epithelial)
H200012622	1.416	GUCY1B2	NM_004129	Guanylate cyclase 1, soluble, beta 2
H200002051	1.416	RODH	NM_003725	Oxidative 3 alpha hydroxysteroid dehydrogenase; retinol dehydrogenase; 3-hydroxysteroid epimerase
H300006831	1.416	ENSG00000176462		60S RIBOSOMAL L21
H200012120	1.415	FLJ20539	NM_017870	Hypothetical protein FLJ20539
H200008749	1.415	SNX13; RGS-PX1; KIAA0713	AL353943	Homo sapiens mRNA; cDNA DKFZp761E0611 (from clone DKFZp761E0611)
H200003703	1.415	KIAA0285	NM_014807	KIAA0285 gene product
H200015279	1.414		AK022264	Homo sapiens cDNA FLJ12202 fis, clone MAMMA1000908
H200003671	1.414	CAPS	NM_004058	Calcyphosine
H200004304	1.414	C8orf13	AJ301564	Reserved
H200013343	1.414	MTMR4	AB014547	Myotubularin related protein 4

Genes that are 1.4 fold up regulated in SUM1315-BP2 vs SUM1315				
H200007102	1.414	KCNB1	L02840	Potassium voltage-gated channel, Shab-related subfamily, member 1
H200010916	1.414	KSP37	NM_031950	Ksp37 protein
H200019624	1.414	dJ383J4.3	BC007923	Homo sapiens cDNA FLJ31786 fis, clone NT2RI2008526
H200007395	1.414	KIAA0754	AB018297	KIAA0754 protein
H200007998	1.413	CYorf15A	AF332224	Homo sapiens testis protein mRNA, partial cds
H200009964	1.413		AK021743	Homo sapiens cDNA FLJ11681 fis, clone HEMBA1004865
H200010001	1.413	CGA	AK023644	Homo sapiens cDNA FLJ13582 fis, clone PLACE1009048
H200003695	1.413	GRIN3A	AL137422	Homo sapiens mRNA; cDNA DKFZp761A1623 (from clone DKFZp761A1623); partial cds
H200004887	1.413	ZNF228	NM_013380	Zinc finger protein 228
H200005160	1.413	FLJ14437	NM_032578	Myopalladin
H200009382	1.413	PHLDA1	AK026181	Homo sapiens cDNA: FLJ22528 fis, clone HRC12825
H200009164	1.413	FLJ23305	NM_025059	Hypothetical protein FLJ23305
H300004779	1.412	ENSG00000178683		UNKNOWN
H200020980	1.412		AF118079	Homo sapiens PRO1854 mRNA, complete cds
H200000471	1.412	NPY	NM_000905	Neuropeptide Y
H200012858	1.412	FLJ11160	NM_018344	Hypothetical protein FLJ11160
H300003586	1.412	ENSG00000173464	NM_172005	PROBABLE PROTEASE INHIBITOR WAP13. [Source:RefSeq;Acc:NM_172005]
H200003268	1.412	ARV1	NM_022786	Likely ortholog of yeast ARV1
H200010328	1.411	KCNMA1	U11058	Potassium large conductance calcium-activated channel, subfamily M, alpha member 1
H200011482	1.411	LOC201191	AF035306	Homo sapiens clone 23771 mRNA sequence
H200013889	1.411	RPGR	NM_000328	Retinitis pigmentosa GTPase regulator
H200003242	1.411	PIST	AY033606	PDZ/coiled-coil domain binding partner for the rho-family GTPase TC10
H200003812	1.411	GMPPB	AB058754	GDP-mannose pyrophosphorylase B
H200011318	1.411	AGRP	NM_001138	Agouti related protein homolog (mouse)
H200016009	1.411	MC4R	NM_005912	Melanocortin 4 receptor
H200013953	1.41	BACH1	NM_001186	BTB and CNC homology 1, basic leucine zipper transcription factor 1

Genes that are 1.4 fold up regulated in SUM1315-BP2 vs SUM1315				
H200000275	1.41	PSCD1	NM_004762	Pleckstrin homology, Sec7 and coiled/coil domains 1 (cytohesin 1)
H200018619	1.41		AK026385	Homo sapiens cDNA: FLJ22732 fis, clone HSI15880
H200000073	1.41	GALC	NM_000153	Galactosylceramidase (Krabbe disease)
H200005230	1.409	GDI2	NM_001494	GDP dissociation inhibitor 2
H200020817	1.409	LOC284898	AK055980	Homo sapiens cDNA FLJ31418 fis, clone NT2NE2000353
H200010867	1.409	KIAA1862	AB058765	KIAA1862 protein
H200015023	1.409		BC015907	Homo sapiens, clone IMAGE: 3922927, mRNA
H200004638	1.409	MBC3205	NM_033408	Hypothetical protein MBC3205
H200013379	1.409	KIAA1602	AB046822	KIAA1602 protein
H200000453	1.409	INHA	NM_002191	Inhibin, alpha
H200020714	1.409	TRIM31	AK057215	Homo sapiens cDNA FLJ32653 fis, clone TESTI1000018
H300012255	1.408	ENSG00000170090		BRAIN AND ACUTE LEUKEMIA, CYTOPLASMIC. [Source:RefSeq;Acc:NM_024812]
H200013700	1.408	DDC	NM_000790	Dopa decarboxylase (aromatic L-amino acid decarboxylase)
H200009906	1.408	LOC51312	AY032628	Mitochondrial solute carrier
H300016489	1.408	ENSG00000176527		ATP DEPENDENT HELICASE
H200001749	1.408	CASP7	NM_033339	Caspase 7, apoptosis-related cysteine protease
H200000470	1.408	NGFR	NM_002507	Nerve growth factor receptor (TNFR superfamily, member 16)
H200011569	1.408	UBE2D2	AK001428	Ubiquitin-conjugating enzyme E2D 2 (UBC4/5 homolog, yeast)
H200013730	1.408	FPGT	NM_003838	Fucose-1-phosphate guanylyltransferase
H200009898	1.408	SLC22A1LS	NM_007105	Solute carrier family 22 (organic cation transporter), member 1-like antisense
H200004228	1.408	MTR	BC015894	Homo sapiens, clone IMAGE: 3909623, mRNA, partial cds
H200004496	1.408	TERE1	NM_013319	Transitional epithelia response protein
H200003433	1.407	MAP-1	AK024029	Modulator of apoptosis 1
H200003506	1.407	PI4KII	AJ303098	Phosphatidylinositol 4-kinase type II
H200003170	1.407	FLJ10637	NM_018164	Hypothetical protein FLJ10637
H200010854	1.407	NYD-SP14	NM_031956	NYD-SP14 protein

Genes that are 1.4 fold up regulated in SUM1315-BP2 vs SUM1315				
H300007218	1.407	ENSG00000168275	NM_030970	UNKNOWN
H200005261	1.407	HAS1	NM_001523	Hyaluronan synthase 1
H200008230	1.407	KIAA1198	AB033024	KIAA1198 protein
H200001587	1.406	DJ465N24.2.1	AF267856	Hypothetical protein dJ465N24.2.1
H200016928	1.406		AC005587	Homo sapiens PAC clone RP5-988G15 from 7q33-q35
H200009759	1.406		AK022139	Homo sapiens cDNA FLJ12077 fis, clone HEMBB1002453
H200013706	1.406	FKBP6	NM_003602	FK506 binding protein 6 (36kD)
H200003963	1.406	TXK	NM_003328	TXK tyrosine kinase
H200004485	1.406	HOXC9	AK000445	Homeo box C9
H200006890	1.406	MYD88	U70451	Myeloid differentiation primary response gene (88)
H200018514	1.406		AK024897	Homo sapiens cDNA: FLJ21244 fis, clone COL01174
H200005444	1.406	KIAA1677	AB051464	KIAA1677
H200017374	1.405	PRO1880	NM_014104	PRO1880 protein
H200018540	1.405	HRASLS2	AK025029	Homo sapiens cDNA: FLJ21376 fis, clone COL03231
H200010387	1.405	MS4A1	NM_021950	Membrane-spanning 4-domains, subfamily A, member 2 (Fc fragment of IgE, high affinity I, receptor fo
H200003292	1.405	CG005	NM_014887	Hypothetical protein from BCRA2 region
H200017481	1.405	BRD7	NM_013263	Bromodomain-containing 7
H200011163	1.405		AF009267	Homo sapiens clone FBA1 Cri-du-chat region mRNA
H200000797	1.405	NLK	NM_016231	Nemo-like kinase
H200005145	1.405	MGC40214	AK023339	Homo sapiens cDNA FLJ13277 fis, clone OVARC1001044
H200010993	1.405	USP16	NM_006447	Ubiquitin specific protease 16
H200014977	1.405	KIAA1030	AB028953	KIAA1030 protein
H200018282	1.404		AL117486	Homo sapiens mRNA; cDNA DKFZp434K211 (from clone DKFZp434K211)
H200015934	1.404	RPL23AL1	AK055264	Ribosomal protein L23a-like 1
H200019718	1.404	GTPBG3	NM_032620	Mitochondrial GTP binding protein
H200014651	1.404	CH25H	NM_003956	Cholesterol 25-hydroxylase
H200010362	1.404	MUC1	J05582	Mucin 1, transmembrane
H200007251	1.404		AK057045	Homo sapiens cDNA FLJ32483 fis, clone SKNMC2001503, weakly similar to P-SELECTIN GLYCOPROTEIN LIGAND
H200018032	1.404		AL049244	Homo sapiens mRNA; cDNA DKFZp564C163 (from clone DKFZp564C163)

Genes that are 1.4 fold up regulated in SUM1315-BP2 vs SUM1315				
H200004961	1.404	MGC10871	NM_031492	Hypothetical protein similar to RNA-binding protein lark
H200010207	1.403	IFNAR2	L41944	Interferon (alpha, beta and omega) receptor 2
H200009015	1.403		AK022455	Homo sapiens cDNA FLJ12393 fis, clone MAMMA1002711
H200007061	1.403	DHFR	NM_000791	Dihydrofolate reductase
H200017190	1.403		AK022410	Homo sapiens cDNA FLJ12348 fis, clone MAMMA1002299
H200007168	1.403	MGC3169	NM_024074	Hypothetical protein MGC3169
H200001580	1.403	HPIP	NM_020524	Hematopoietic PBX-interacting protein
H200004283	1.403	FLJ21941	AK023547	Homo sapiens cDNA FLJ13485 fis, clone PLACE1003892
H200007572	1.402	KIAA1952	BC012922	Homo sapiens, clone IMAGE: 4449401, mRNA, partial cds
H200005596	1.402	CD38	NM_001775	CD38 antigen (p45)
H200000283	1.402	STK2	NM_003157	Serine/threonine kinase 2
H200001758	1.402	CGI-152	NM_020410	CGI-152 protein
H200007072	1.402	AMPD3	NM_000480	Adenosine monophosphate deaminase (isoform E)
H200012039	1.402	LOC283537	AK026720	Homo sapiens cDNA: FLJ23067 fis, clone LNG04993

Appendix B

Down-regulated Genes From Gene Array

Genes that are 1.4 fold down regulated in SUM1315-BP2 vs. SUM1315					
Gene ID	**Normalized Data**	**Fold**	**Common Name**	**GenBank**	**Description**
H200018596	0.714	-1.4006	FLJ21777	NM_032209	Hypothetical protein FLJ21777
H200008502	0.714	-1.4006	MGC14288	NM_032901	Hypothetical protein MGC14288
H200003639	0.714	-1.4006	DPAGT1	NM_001382	Dolichyl-phosphate (UDP-N-acetylglucosamine) N-acetylglucosaminephospho transferase 1 (GlcNAc-1-P tra
H200020589	0.714	-1.4006	MGC16044	BC016154	Homo sapiens, clone MGC: 13247 IMAGE:4040497, mRNA, complete cds
H200012696	0.714	-1.4006	KIAA1349	AB037770	KIAA1349 protein
H200016803	0.714	-1.4006	FLJ20019	NM_017624	Hypothetical protein FLJ20019
H200013348	0.714	-1.4006	ZK1	NM_005815	Kruppel-type zinc finger (C2H2)
H200009857	0.714	-1.4006		AK056762	Homo sapiens cDNA FLJ32200 fis, clone PLACE6002871
H200009694	0.713	-1.4025	PEX26	AK000085	Homo sapiens cDNA FLJ20078 fis, clone COL02974
H200009156	0.713	-1.4025		AK026820	Homo sapiens cDNA: FLJ23167 fis, clone LNG09902
H300005836	0.713	-1.4025	ENSG0000017 8804		SEVEN TRANSMEMBRANE HELIX RECEPTOR. [Source:SPTREMBL;Acc:Q 8NG83]
H200008876	0.713	-1.4025	MN7	AF041080	D15F37 (pseudogene)
H300002804	0.713	-1.4025	ENSG0000017 8651		AMBIGUOUS
H200005782	0.713	-1.4025	AND-1	NM_007086	AND-1 protein
H300008731	0.713	-1.4025	ENSG0000017 9167		UNKNOWN
H200001339	0.713	-1.4025	AKR7A2	NM_003689	Aldo-keto reductase family 7, member A2 (aflatoxin aldehyde reductase)
H200020193	0.713	-1.4025	SLC1A7	BC000651	Homo sapiens, Similar to solute carrier family 1 (glutamate transporter), member 7, clone MGC: 2078 I
H200015322	0.713	-1.4025		AL050145	Homo sapiens mRNA; cDNA DKFZp586C2020 (from clone DKFZp586C2020)
H200000926	0.713	-1.4025	P66	AB032976	Transcription repressor p66 component of the MeCP1 complex
H200019184	0.713	-1.4025	DGUOK	BC001121	Deoxyguanosine kinase

Genes that are 1.4 fold down regulated in SUM1315-BP2 vs. SUM1315					
H200020873	0.713	-1.4025		AK055419	Homo sapiens cDNA FLJ30857 fis, clone FEBRA2003275
H200015845	0.713	-1.4025	COL9A2	AK021682	Homo sapiens cDNA FLJ11620 fis, clone HEMBA1004138
H200016106	0.713	-1.4025	H4FB	NM_003539	H4 histone family, member B
H200015254	0.713	-1.4025	MGC2742	NM_023938	Hypothetical protein MGC2742
H200004625	0.713	-1.4025		AK026189	Homo sapiens cDNA: FLJ22536 fis, clone HRC13155
H200011601	0.713	-1.4025	MGC2749	NM_024069	Hypothetical protein MGC2749
H200010605	0.712	-1.4045	DKFZP586D2223	NM_018561	DKFZP586D2223 protein
H200015923	0.712	-1.4045		AL030997	Human DNA sequence from clone 1189K21 on chromosome Xq26.3-27.3. Contains two pseudogenes similar to
H200003538	0.712	-1.4045	FLJ10315	NM_018056	Hypothetical protein FLJ10315
H200009742	0.712	-1.4045		AK021985	Homo sapiens cDNA FLJ11923 fis, clone HEMBB1000341
H200020246	0.712	-1.4045	PIGF	NM_002643	Phosphatidylinositol glycan, class F
H200015922	0.712	-1.4045		AL030997	Human DNA sequence from clone 1189K21 on chromosome Xq26.3-27.3. Contains two pseudogenes similar to
H300022791	0.712	-1.4045	ENSG00000176154		AMBIGUOUS
H200009701	0.712	-1.4045	ASB7; FLJ22551	AK000966	Homo sapiens cDNA FLJ10104 fis, clone HEMBA1002515
H200008861	0.712	-1.4045	LASS2	NM_013384	LAG1 longevity assurance homolog 2 (S. cerevisiae)
H200017786	0.712	-1.4045	CTHRC1	BC014245	Homo sapiens, Similar to RIKEN cDNA 1110014B07 gene, clone MGC:20766 IMAGE:4586039, mRNA, complete c
H200020503	0.712	-1.4045	RAB6B	AK055102	RAB6B, member RAS oncogene family
H200018011	0.712	-1.4045	PWCR1	AF241255	Prader-Willi syndrome chromosome region 1
H200003229	0.712	-1.4045	ZNF16	NM_006958	Zinc finger protein 16 (KOX 9)
H200020623	0.712	-1.4045	LOC286090	AK057888	Homo sapiens cDNA FLJ25159 fis, clone CBR08036

Genes that are 1.4 fold down regulated in SUM1315-BP2 vs. SUM1315					
H200000166	0.712	-1.4045	IL12A	NM_000882	Interleukin 12A (natural killer cell stimulatory factor 1, cytotoxic lymphocyte maturation factor 1,
H200020769	0.711	-1.4065	FLJ32011	AK056573	Homo sapiens cDNA FLJ32011 fis, clone NT2RP7009507
H200007638	0.711	-1.4065	FLJ20079	NM_017656	Hypothetical protein FLJ20079
H300008893	0.711	-1.4065	ENSG00000180409		PRECURSOR MATRIX METALLOPROTEINASE MMP
H200008265	0.711	-1.4065	ATP5E	NM_006886	ATP synthase, H+ transporting, mitochondrial F1 complex, epsilon subunit
H200015912	0.711	-1.4065		AJ012680	Homo sapiens gene encoding hypothetical protein with HTH motif
H300021538	0.711	-1.4065			AMBIGUOUS
H200009266	0.711	-1.4065		AX015323	Sequence 17 from Patent WO9951740
H200014213	0.711	-1.4065	FLJ11752	AK057661	Homo sapiens cDNA FLJ11752 fis, clone HEMBA1005582, weakly similar to TROPOMYOSIN 1, NON-MUSCLE ISOF
H300021569	0.711	-1.4065	ENSG00000179250		AMBIGUOUS
H200010412	0.711	-1.4065	NCALD	NM_032041	Neurocalcin delta
H200020727	0.711	-1.4065		AK057127	Homo sapiens cDNA FLJ32565 fis, clone SPLEN2000020
H200016301	0.711	-1.4065	WIT-1	NM_015855	Wilms tumor associated protein
H200014757	0.711	-1.4065	PGCP	NM_006102	Plasma glutamate carboxypeptidase
H200011174	0.71	-1.4085	THG-1	NM_030935	TSC-22-like
H200017251	0.71	-1.4085	CHRNE	NM_000080	Cholinergic receptor, nicotinic, epsilon polypeptide
H200020622	0.71	-1.4085		AK057907	Homo sapiens cDNA FLJ25178 fis, clone CBR09176
H200005112	0.71	-1.4085	NCK1	NM_006153	NCK adaptor protein 1
H200007376	0.71	-1.4085	ZNF568	BC016334	Homo sapiens, clone IMAGE:4052822, mRNA, partial cds
H200017614	0.71	-1.4085	DKFZP564C186	BC009786	Homo sapiens, clone IMAGE:4274902, mRNA, partial cds
H200013506	0.71	-1.4085	LOC58512	AF131778	Similar to PSD-95/SAP90-associated protein-3 (R. norvegicus) from clone 24861

Genes that are 1.4 fold down regulated in SUM1315-BP2 vs. SUM1315					
H200003020	0.71	-1.4085	MGC39820	AL161983	Homo sapiens mRNA; cDNA DKFZp761K2024 (from clone DKFZp761K2024)
H200016464	0.71	-1.4085	EDG7	NM_012152	Endothelial differentiation, lysophosphatidic acid G-protein-coupled receptor, 7
H200005041	0.71	-1.4085	MONDOA	NM_014938	Mlx interactor
H200013330	0.71	-1.4085		AK024136	Homo sapiens cDNA FLJ14074 fis, clone HEMBB1001869
H200019286	0.709	-1.4104	CRYZL1	NM_005111	Crystallin, zeta (quinone reductase)-like 1
H200016985	0.709	-1.4104	MDS027	BC013687	Uncharacterized hematopoietic stem/ progenitor cells protein MDS027
H300003648	0.709	-1.4104			UNKNOWN
H200018582	0.709	-1.4104		AK025295	Homo sapiens cDNA: FLJ21642 fis, clone COL08374
H200001258	0.709	-1.4104	ARHGEF12	NM_015313	Rho guanine nucleotide exchange factor (GEF) 12
H200015786	0.709	-1.4104	LOC51213	NM_016383	HOM-TES-85 tumor antigen
H200003910	0.709	-1.4104	FLJ21865	AL110283	Hypothetical protein FLJ21865
H200006942	0.709	-1.4104	KIAA0247	NM_014734	KIAA0247 gene product
H200002073	0.709	-1.4104	HCA112	NM_018487	Hepatocellular carcinoma-associated antigen 112
H200003612	0.709	-1.4104	gm117	AK024939	Homo sapiens cDNA: FLJ21286 fis, clone COL01915
H200001128	0.709	-1.4104	MUC13	NM_033049	Mucin 13, epithelial transmembrane
H200003936	0.709	-1.4104	RECK	NM_021111	Reversion-inducing-cysteine-rich protein with kazal motifs
H200013686	0.709	-1.4104	LAMP1	NM_005561	Lysosomal-associated membrane protein 1
H200016790	0.709	-1.4104	FLJ20802	NM_017959	Hypothetical protein FLJ20802
H200000748	0.709	-1.4104	PRKAG1	NM_002733	Protein kinase, AMP-activated, gamma 1 non-catalytic subunit
H200019024	0.709	-1.4104	FLJ12847	AK057995	Homo sapiens cDNA FLJ25266 fis, clone STM05361
H200013903	0.709	-1.4104	MOB	AK026683	Homo sapiens mRNA for Hmob33 protein, 3' untranslated region
H200006850	0.709	-1.4104	UNC119	NM_054035	Unc-119 homolog (C. elegans)
H200009363	0.709	-1.4104	FLJ22688	NM_025129	Hypothetical protein FLJ22688

Genes that are 1.4 fold down regulated in SUM1315-BP2 vs. SUM1315					
H200017173	0.708	-1.4124		AL137542	Homo sapiens mRNA; cDNA DKFZp434P1019 (from clone DKFZp434P1019)
H200006349	0.708	-1.4124	MAML1	NM_014757	Mastermind-like 1 (Drosophila)
H300009128	0.708	-1.4124	ENSG00000180625		GENE SUPPORTED BY
H200010107	0.708	-1.4124	APTX	NM_017692	Aprataxin
H200017612	0.708	-1.4124	FLJ21034	NM_024940	Hypothetical protein FLJ21034
H300002551	0.708	-1.4124			PEPTIDYL PROLYL CIS TRANS ISOMERASE EC_5.2.1.8 PPIASE ROTAMASE CYCLOPHILIN
H200013926	0.708	-1.4124	KIAA0573	AB011145	KIAA0573 protein
H200017669	0.708	-1.4124	PRO1318	NM_018581	Hypothetical protein PRO1318
H200017470	0.708	-1.4124	PRO1483	NM_018582	Hypothetical protein PRO1483
H200002955	0.707	-1.4144	SETDB1	NM_012432	SET domain, bifurcated 1
H200001638	0.707	-1.4144	FLJ20366	NM_017786	Hypothetical protein FLJ20366
H200012359	0.707	-1.4144	RUNX2	NM_004348	Runt-related transcription factor 2
H200014196	0.707	-1.4144	ZNF124	NM_003431	Zinc finger protein 124 (HZF-16)
H200013606	0.707	-1.4144		AK021839	Homo sapiens cDNA FLJ11777 fis, clone HEMBA1005909
H200006202	0.707	-1.4144	PDLIM1	NM_020992	PDZ and LIM domain 1 (elfin)
H200018899	0.707	-1.4144	PLDN	AK057545	Pallidin homolog (mouse)
H200006470	0.707	-1.4144	MEF2D	AK027180	Homo sapiens cDNA: FLJ23527 fis, clone LNG05966
H300008886	0.707	-1.4144	ENSG00000181734		SEVEN TRANSMEMBRANE HELIX RECEPTOR. [Source:SPTREMBL;Acc:Q8NH06]
H200017622	0.707	-1.4144	FLJ13611	NM_024941	Hypothetical protein FLJ13611
H200010602	0.707	-1.4144	H4FH	NM_003543	H4 histone family, member H
H200013976	0.707	-1.4144	KIAA1076	AB028999	KIAA1076 protein
H200004497	0.707	-1.4144	KCNQ3	NM_004519	Potassium voltage-gated channel, KQT-like subfamily, member 3
H200015307	0.707	-1.4144	UGT2A1	NM_006798	UDP glycosyltransferase 2 family, polypeptide A1
H300005801	0.707	-1.4144			UNKNOWN
H200004987	0.707	-1.4144	RAB27A	U38654	RAB27A, member RAS oncogene family

Genes that are 1.4 fold down regulated in SUM1315-BP2 vs. SUM1315					
H200003358	0.707	-1.4144	KCNK3	NM_002246	Potassium channel, subfamily K, member 3 (TASK-1)
H200002090	0.706	-1.4164	RELN	NM_005045	Reelin
H200016191	0.706	-1.4164	CALN1	NM_031468	Calneuron 1
H200010164	0.706	-1.4164	ZNF37A	BC015858	Zinc finger protein 37a (KOX 21)
H200003581	0.706	-1.4164	MYCN	BC002712	V-myc myelocytomatosis viral related oncogene, neuroblastoma derived (avian)
H200004571	0.706	-1.4164	MYST1	NM_032188	Histone acetyltransferase MYST1
H200007006	0.706	-1.4164	TAF11	NM_005643	TAF11 RNA polymerase II, TATA box binding protein (TBP)-associated factor, 28 kD
H200006162	0.706	-1.4164	GSTM5	NM_000851	Glutathione S-transferase M5
H200019736	0.706	-1.4164		BC008359	Homo sapiens, clone MGC: 16021 IMAGE:3606756, mRNA, complete cds
H300003468	0.706	-1.4164	ENSG00000178008		UNKNOWN
H200018017	0.706	-1.4164	LOC64180	NM_022357	Putative metallopeptidase (family M19)
H200013078	0.706	-1.4164	RPS15	BC000085	Ribosomal protein S15
H200005102	0.706	-1.4164	AQP6	NM_053286	Aquaporin 6, kidney specific
H200013862	0.706	-1.4164	SH3KBP1	NM_031892	SH3-domain kinase binding protein 1
H200007030	0.706	-1.4164	GRM7	NM_000844	Glutamate receptor, metabotropic 7
H200015692	0.706	-1.4164	CGI-96	NM_015703	CGI-96 protein
H200004225	0.705	-1.4184	UNC5A	BC009333	Homo sapiens, Similar to transmembrane receptor Unc5H1, clone IMAGE: 4126760, mRNA, partial cds
H200004945	0.705	-1.4184	M160	NM_033330	Scavenger receptor cysteine-rich type 1 protein M160 precursor
H200011085	0.705	-1.4184	CTSG	NM_001911	Cathepsin G
H200014730	0.705	-1.4184	PHKG2	NM_000294	Phosphorylase kinase, gamma 2 (testis)
H200005843	0.705	-1.4184	FLJ10901	NM_018265	Hypothetical protein FLJ10901
H200021185	0.705	-1.4184	ZFYVE26	AK055455	Homo sapiens cDNA FLJ30893 fis, clone FEBRA2005380
H200010545	0.705	-1.4184	PRKWNK3	AB046786	Protein kinase, lysine deficient 3

Genes that are 1.4 fold down regulated in SUM1315-BP2 vs. SUM1315					
H200004803	0.705	-1.4184	FLJ23878	AL157461	Homo sapiens mRNA; cDNA DKFZp434K152 (from clone DKFZp434K152)
H200012779	0.705	-1.4184	TSA1902	NM_021797	Eosinophil chemotactic cytokine
H200010610	0.705	-1.4184	DKFZP434N014	AB040959	DKFZP434N014 protein
H200014342	0.705	-1.4184	D2LIC	BC016324	Homo sapiens, clone MGC:23709 IMAGE:4093010, mRNA, complete cds
H200003360	0.705	-1.4184	GL009	NM_032492	Hypothetical protein GL009
H200020551	0.705	-1.4184		AK021893	Homo sapiens cDNA FLJ11831 fis, clone HEMBA1006562
H200007024	0.705	-1.4184	LOXL2	NM_002318	Lysyl oxidase-like 2
H200014617	0.704	-1.4205	Spir-2	AB058735	Spir-2 protein
H200019162	0.704	-1.4205	LRRFIP1	NM_004735	Leucine rich repeat (in FLII) interacting protein 1
H200004755	0.704	-1.4205	SCN4A	NM_000334	Sodium channel, voltage-gated, type IV, alpha polypeptide
H200003201	0.704	-1.4205		AK055007	Homo sapiens mRNA full length insert cDNA clone EUROIMAGE 34988
H200001306	0.704	-1.4205	PAFAH1B3	NM_002573	Platelet-activating factor acetylhydrolase, isoform Ib, gamma subunit (29kD)
H200001389	0.704	-1.4205	ACAS2L	AK024396	Acetyl-Coenzyme A synthetase 2 (AMP forming)-like
H300009860	0.704	-1.4205	ENSG00000181168		UNKNOWN
H200017529	0.704	-1.4205	AIPL1	NM_014336	Aryl hydrocarbon receptor interacting protein-like 1
H200020430	0.704	-1.4205	DKFZp434K1323	AK024481	Homo sapiens cDNA FLJ31670 fis, clone NT2RI2004984
H200014490	0.704	-1.4205		AK024541	Homo sapiens cDNA: FLJ20888 fis, clone ADKA03289
H200017993	0.704	-1.4205		AK055657	Homo sapiens cDNA FLJ31598 fis, clone NT2RI2002549
H200003808	0.704	-1.4205	KIAA0766	NM_014805	KIAA0766 gene product
H200021066	0.704	-1.4205	FLJ31031	AK054818	Homo sapiens cDNA FLJ30256 fis, clone BRACE2002458
H200007492	0.704	-1.4205	SMARCB1	NM_003073	SWI/SNF related, matrix associated, actin dependent regulator of chromatin, subfamily b, member 1
H200016328	0.704	-1.4205	TOR1B	NM_014506	Torsin family 1, member B (torsin B)

Genes that are 1.4 fold down regulated in SUM1315-BP2 vs. SUM1315					
H200002945	0.704	-1.4205	RBMS2	NM_002898	RNA binding motif, single stranded interacting protein 2
H200007722	0.704	-1.4205	VMD2	AF052095	Homo sapiens clone 23911 mRNA sequence
H200004541	0.703	-1.4225	PDE1A	NM_005019	Phosphodiesterase 1A, calmodulin-dependent
H200014048	0.703	-1.4225	E1B-AP5	NM_007040	E1B-55kDa-associated protein 5
H300005578	0.703	-1.4225	ENSG00000136974	NM_000978	60S RIBOSOMAL PROTEIN L23 (L17). [Source:SWISSPROT;Acc: P23131]
H200006442	0.703	-1.4225	FLJ11618	NM_022452	Hypothetical protein FLJ11618
H200018129	0.703	-1.4225	NAP1L1	AL162068	Nucleosome assembly protein 1-like 1
H200020403	0.703	-1.4225	PRKWNK1	U00946	Human clone A9A2BRB5 (CAC)n/(GTG)n repeat-containing mRNA
H200004577	0.703	-1.4225	TEAD1	AL133574	Homo sapiens mRNA; cDNA DKFZp586C1817 (from clone DKFZp586C1817)
H200009142	0.703	-1.4225	FLJ22692	NM_025049	Hypothetical protein FLJ22692
H200006370	0.703	-1.4225	CBX1	NM_006807	Chromobox homolog 1 (HP1 beta homolog Drosophila)
H200013965	0.703	-1.4225	ELF1	M82882	E74-like factor 1 (ets domain transcription factor)
H200018916	0.703	-1.4225	C14orf9	BC002867	Homo sapiens, clone IMAGE:3940519, mRNA, partial cds
H200010389	0.702	-1.4245	FMR1	NM_002024	Fragile X mental retardation 1
H200007542	0.702	-1.4245	LOC134285	BC018083	Homo sapiens, clone IMAGE:4797244, mRNA, partial cds
H200020733	0.702	-1.4245	LOC154860	AK057037	Homo sapiens cDNA FLJ32475 fis, clone SKNMC2000612
H200021108	0.702	-1.4245		AF131844	Homo sapiens clone 25015 mRNA sequence
H200020003	0.702	-1.4245	DHRS6	AK023323	Homo sapiens cDNA FLJ13261 fis, clone OVARC1000885, weakly similar to OXIDOREDUCTASE UCPA (EC 1.-.-.
H200018860	0.702	-1.4245	PRDM15	AL355710	Homo sapiens EST from clone 112590, full insert
H200016066	0.702	-1.4245	GPR10	NM_004248	G protein-coupled receptor 10

Genes that are 1.4 fold down regulated in SUM1315-BP2 vs. SUM1315					
H200020685	0.702	-1.4245		AK057398	Homo sapiens cDNA FLJ32836 fis, clone TESTI2003258
H200020273	0.702	-1.4245	SOS2	L13858	Son of sevenless homolog 2 (Drosophila)
H200017972	0.702	-1.4245	SLC37A1	NM_018964	Solute carrier family 37 (glycerol-3-phosphate transporter), member 1
H200017670	0.702	-1.4245	PRO1617	NM_018587	Hypothetical protein PRO1617
H200004542	0.702	-1.4245	PDE1C	NM_005020	Phosphodiesterase 1C, calmodulin-dependent (70kD)
H200019985	0.702	-1.4245	GYPB	NM_002100	Glycophorin B (includes Ss blood group)
H200000855	0.701	-1.4265	KPNA3	NM_002267	Karyopherin alpha 3 (importin alpha 4)
H200012819	0.701	-1.4265	HNRPK	NM_002140	Heterogeneous nuclear ribonucleoprotein K
H200019001	0.701	-1.4265	PRO1900	NM_016344	PRO1900 protein
H200012618	0.701	-1.4265	SKD1	NM_004869	Suppressor of K+ transport defect 1
H200014980	0.701	-1.4265	ARHB	NM_004040	Ras homolog gene family, member B
H200000890	0.701	-1.4265	DKFZp761H039	AL359592	Hypothetical protein DKFZp761H039
H200007469	0.701	-1.4265	CDON	NM_016952	Cell adhesion molecule-related/down-regulated by oncogenes
H200019902	0.701	-1.4265	ARL5	NM_012097	ADP-ribosylation factor-like 5
H200020095	0.701	-1.4265		AK057240	Homo sapiens cDNA FLJ32678 fis, clone TESTI1000183
H200018431	0.701	-1.4265	RIPX	AK022074	Homo sapiens cDNA FLJ12012 fis, clone HEMBB1001668
H200007704	0.701	-1.4265	SFRS5	NM_006925	Splicing factor, arginine/serine-rich 5
H200010452	0.701	-1.4265	LOC284018	AK026583	Homo sapiens cDNA: FLJ22930 fis, clone KAT07255
H200001218	0.7	-1.4286		AF130048	Homo sapiens clone FLB3344 PRO0845 mRNA, complete cds
H300009816	0.7	-1.4286	ENSG00000176445		AMBIGUOUS
H200018020	0.7	-1.4286	ZNFN1A4	AB058685	Zinc finger protein, subfamily 1A, 4 (Eos)
H200018131	0.7	-1.4286	FLJ20626	AK055359	Homo sapiens cDNA FLJ30797 fis, clone FEBRA2001146, weakly similar to ZINC FINGER PROTEIN 174

Genes that are 1.4 fold down regulated in SUM1315-BP2 vs. SUM1315					
H200010060	0.7	-1.4286	ADCY1	AK055343	Homo sapiens cDNA FLJ30781 fis, clone FEBRA2000874
H300005201	0.7	-1.4286	ENSG00000177766		UNKNOWN
H200011726	0.7	-1.4286	GTR2	NM_022157	Rag C protein
H200003566	0.7	-1.4286	FAF1	NM_007051	Fas (TNFRSF6) associated factor 1
H200019990	0.7	-1.4286	CAM-KIIN	NM_033259	CaM-KII inhibitory protein
H200020646	0.7	-1.4286	MGC37245	AK057650	Homo sapiens cDNA FLJ33088 fis, clone TRACH2000496, highly similar to Rattus norvegicus kidney-speci
H300004441	0.7	-1.4286	ENSG00000181355		UNKNOWN
H200007736	0.7	-1.4286	C6orf89	AK058086	Homo sapiens mRNA full length insert cDNA clone EUROIMAGE 1916903
H300005066	0.7	-1.4286	ENSG00000181079		PREPRO-NEUROPEPTIDE W POLYPEPTIDE (FRAGMENT). [Source:SPTREMBL;Acc:Q8N729]
H200004927	0.699	-1.4306	FLJ11006	NM_018298	Hypothetical protein FLJ11006
H200017919	0.699	-1.4306		AK021911	Homo sapiens cDNA FLJ11849 fis, clone HEMBA1006709
H200019759	0.699	-1.4306	LOC85415	NM_033103	Rhophilin-like protein
H200005064	0.699	-1.4306	LIP1	AK026289	Likely ortholog of mouse lipoic acid synthase
H200006411	0.699	-1.4306	COX10	NM_001303	COX10 homolog, cytochrome c oxidase assembly protein, heme A: farnesyltransferase (yeast)
H200014162	0.699	-1.4306	MUCDHL	NM_021924	Mucin and cadherin-like
H200018881	0.699	-1.4306	LOC56965	NM_020213	Hypothetical protein from EUROIMAGE 1977056
H200003876	0.699	-1.4306	LOC90110	AL117623	Homo sapiens mRNA; cDNA DKFZp564O2364 (from clone DKFZp564O2364)
H200020266	0.699	-1.4306	LOC92771	NM_033424	Similar to MYOSIN HEAVY CHAIN, CARDIAC MUSCLE ALPHA ISOFORM (MYHC-ALPHA) (M. musculus)
H200013432	0.699	-1.4306	AK7	AK057426	Homo sapiens cDNA FLJ32864 fis, clone TESTI2003625
H200001204	0.699	-1.4306	KIAA0672	NM_014859	KIAA0672 gene product
H200015459	0.699	-1.4306	HNRPA2B1	NM_031243	Heterogeneous nuclear ribonucleoprotein A2/B1

Genes that are 1.4 fold down regulated in SUM1315-BP2 vs. SUM1315					
H300003531	0.699	-1.4306	ENSG00000173922		XAGE-4 PROTEIN (FRAGMENT). [Source:SPTREMBL;Acc:Q8WWM0]
H200010402	0.699	-1.4306	PC	NM_000920	Pyruvate carboxylase
H200004399	0.699	-1.4306	FLJ11149	BC007069	Hypothetical protein FLJ11149
H200016585	0.699	-1.4306	HBG1	AF130098	Hemoglobin, gamma A
H200020965	0.698	-1.4327	DRD5	NM_000798	Dopamine receptor D5
H200007642	0.698	-1.4327	PAI-RBP1	NM_015640	PAI-1 mRNA-binding protein
H200014060	0.698	-1.4327	PRKCD	NM_006254	Protein kinase C, delta
H200011501	0.698	-1.4327	LOC56932	AL365412	Hypothetical protein from EUROIMAGE 1759349
H200011661	0.698	-1.4327	UBL5	NM_024292	Ubiquitin-like 5
H200011172	0.698	-1.4327	EMCN	AL133118	Homo sapiens mRNA; cDNA DKFZp586N0121 (from clone DKFZp586N0121)
H200016392	0.698	-1.4327	FLJ13262	NM_024914	Hypothetical protein FLJ13262
H200001673	0.698	-1.4327	MGC3232	NM_032313	Hypothetical protein MGC3232
H200019584	0.698	-1.4327	C12orf14	AK027736	Homo sapiens cDNA FLJ14830 fis, clone OVARC1001011
H200005270	0.698	-1.4327	GIT2	NM_057169	G protein-coupled receptor kinase-interactor 2
H300006939	0.698	-1.4327	ENSG00000178653		UNKNOWN
H300002521	0.698	-1.4327			UNKNOWN
H200019142	0.698	-1.4327	C14orf52	AK057626	Homo sapiens cDNA FLJ33064 fis, clone TRACH2000079, moderately similar to Xenopus laevis Churchill p
H200018197	0.698	-1.4327	ZNF83	NM_018300	Zinc finger protein 83 (HPF1)
H300006233	0.698	-1.4327	ENSG00000099288		ATRIAL NATRIURETIC PEPTIDE CLEARANCE RECEPTOR PRECURSOR ANP C ANPRC NPR C ATRIAL NATRIURETIC PEPTIDE C TYPE RECEPTOR
H300004461	0.698	-1.4327	MRPL41	NM_032477	MITOCHONDRIAL RIBOSOMAL PROTEIN L41. [Source:RefSeq;Acc:NM_032477]
H200019940	0.697	-1.4347	FLJ13639	BC009825	Hypothetical protein FLJ13639
H200014223	0.697	-1.4347	GOLGA4	NM_002078	Golgi autoantigen, golgin subfamily a, 4

Genes that are 1.4 fold down regulated in SUM1315-BP2 vs. SUM1315					
H200015764	0.697	-1.4347		AF131779	Homo sapiens clone 25074 mRNA sequence
H200008918	0.697	-1.4347	PRDM12	NM_021619	PR domain containing 12
H200001331	0.697	-1.4347		AK057771	Homo sapiens cDNA FLJ25042 fis, clone CBL03351
H200019882	0.697	-1.4347	CLK3	BC009857	Homo sapiens, clone MGC: 16360 IMAGE:3927645, mRNA, complete cds
H200018217	0.697	-1.4347	DKFZP434F1735	NM_015590	DKFZP434F1735 protein
H200002321	0.697	-1.4347	DO	NM_021071	Dombrock blood group
H300010287	0.697	-1.4347			UNKNOWN
H200001627	0.697	-1.4347	DKFZP434D1335	AK027643	DKFZP434D1335 protein
H200006965	0.697	-1.4347	DNAJB1	NM_006145	DnaJ (Hsp40) homolog, subfmaily B, member 1
H200013003	0.696	-1.4368	MGC13138	NM_033410	Hypothetical protein MGC13138
H200006252	0.696	-1.4368	DAG1	NM_004393	Dystroglycan 1 (dystrophin-associated glycoprotein 1)
H200019083	0.696	-1.4368	KAI1	NM_002231	Kangai 1 (suppression of tumorigenicity 6, prostate; CD82 antigen (R2 leukocyte antigen, antigen det
H200020787	0.696	-1.4368		AK056289	Homo sapiens cDNA FLJ31727 fis, clone NT2RI2006762, weakly similar to Human B219/OB receptor isoform
H200010818	0.696	-1.4368	SH3GL1	NM_003025	SH3-domain GRB2-like 1
H200000095	0.696	-1.4368	TCP10	NM_004610	T-complex 10 (mouse)
H200002831	0.696	-1.4368	FXYD2	NM_021603	FXYD domain-containing ion transport regulator 2
H200016153	0.696	-1.4368	FAAH	NM_024306	Fatty acid hydroxylase
H200014576	0.696	-1.4368	HCAP-G	NM_022346	Chromosome condensation protein G
H300008486	0.696	-1.4368	ENSG00000177664		UNKNOWN
H200019160	0.695	-1.4388	MRS3/4	AF327403	Putative mitochondrial solute carrier
H200015033	0.695	-1.4388	FLJ21162	NM_024873	Hypothetical protein FLJ21162
H200020655	0.695	-1.4388	1500005N04Rik	AK057615	Homo sapiens cDNA FLJ33053 fis, clone TRACH1000100, moderately similar to Oryctolagus cuniculus PiUS
H200005065	0.695	-1.4388	CHAC	NM_033305	Chorea acanthocytosis
H200017951	0.695	-1.4388	STK11	NM_000455	Serine/threonine kinase 11 (Peutz-Jeghers syndrome)
H200013051	0.695	-1.4388	PCDH20	NM_022843	Protocadherin 20

Genes that are 1.4 fold down regulated in SUM1315-BP2 vs. SUM1315					
H200020709	0.695	-1.4388	NIFU	AK057251	Homo sapiens cDNA FLJ32689 fis, clone TESTI2000207, moderately similar to NIFU-LIKE PROTEIN
H300001061	0.695	-1.4388			UNKNOWN
H200004312	0.695	-1.4388	MYF6	NM_002469	Myogenic factor 6 (herculin)
H200008607	0.695	-1.4388	RASGRP1	NM_005739	RAS guanyl releasing protein 1 (calcium and DAG-regulated)
H200017467	0.695	-1.4388	DKFZP564A033	AL050006	DKFZP564A033 protein
H200001624	0.695	-1.4388	NDUFS1	NM_005006	NADH dehydrogenase (ubiquinone) Fe-S protein 1 (75kD) (NADH-coenzyme Q reductase)
H200009498	0.694	-1.4409	CYC1	NM_001916	Cytochrome c-1
H200006644	0.694	-1.4409	CXADR	NM_001338	Coxsackie virus and adenovirus receptor
H200004750	0.694	-1.4409	LDOC1	NM_012317	Leucine zipper, down-regulated in cancer 1
H200016399	0.694	-1.4409	NY-REN-41	BC008496	NY-REN-41 antigen
H200003663	0.694	-1.4409	HDAC10	AF426160	Histone deacetylase 10
H200013038	0.694	-1.4409		AK055220	Homo sapiens cDNA FLJ30658 fis, clone DFNES2000432
H200002778	0.694	-1.4409	LOC51185	NM_016302	Protein x 0001
H200003592	0.694	-1.4409	TNRC4	NM_007185	Trinucleotide repeat containing 4
H200001999	0.694	-1.4409	RAD51C	NM_058216	RAD51 homolog C (S. cerevisiae)
H200014613	0.694	-1.4409	MAP1A	NM_002373	Microtubule-associated protein 1A
H200020577	0.694	-1.4409	MRGX2	NM_054030	Homo sapiens G protein-coupled receptor MRGX2 (MRGX2), mRNA
H200015223	0.693	-1.443	ARL8	AK027275	Homo sapiens cDNA FLJ14369 fis, clone HEMBA1001174, highly similar to ADP-RIBOSYLATION FACTOR-LIKE P
H300014208	0.693	-1.443	ENSG00000078403		MITOCHONDRIAL RIBOSOMAL PROTEIN L43. [Source:RefSeq;Acc:NM_032112]
H200020174	0.693	-1.443	MGC20235	U25750	Human chromosome 17q21 mRNA clone 1046:1-1
H200010258	0.693	-1.443	PTPN22	NM_015967	Protein tyrosine phosphatase, non-receptor type 22 (lymphoid)

Genes that are 1.4 fold down regulated in SUM1315-BP2 vs. SUM1315					
H200021032	0.693	-1.443	FAM31B	BC016588	Homo sapiens, clone IMAGE:4499339, mRNA, partial cds
H200014718	0.693	-1.443	KRT5	NM_000424	Keratin 5 (epidermolysis bullosa simplex, Dowling-Meara/Kobner/Weber-Cockayne types)
H200005106	0.693	-1.443		AK056401	Homo sapiens cDNA FLJ31839 fis, clone NT2RP7000086
H200016989	0.693	-1.443	KIAA0710	NM_014871	KIAA0710 gene product
H200004263	0.693	-1.443	LOC152485	AL117519	Homo sapiens mRNA; cDNA DKFZp434P0235 (from clone DKFZp434P0235)
H200016137	0.693	-1.443	MGC16943	BC010503	Similar to RIKEN cDNA 4933424N09 gene
H200020695	0.693	-1.443	C9orf84	AK057341	Homo sapiens cDNA FLJ32779 fis, clone TESTI2002090
H200016049	0.693	-1.443	FGF22	NM_020637	Fibroblast growth factor 22
H200009779	0.693	-1.443		AK022411	Homo sapiens cDNA FLJ12349 fis, clone MAMMA1002308
H300018459	0.692	-1.4451	ENSG00000070086		DJ126A5.2.1 (NOVEL PROTEIN) (ISOFORM 1). [Source:SPTREMBL;Acc:Q9Y3H2]
H200012177	0.692	-1.4451	RAB4	BC004309	RAB4, member RAS oncogene family
H200007335	0.692	-1.4451	HB-1	NM_021182	Minor histocompatibility antigen HB-1
H200006706	0.692	-1.4451	LOC126208	AF000560	Homo sapiens TTF-I interacting peptide 20 mRNA, partial cds
H200016533	0.692	-1.4451	NUDC	NM_006600	Nuclear distribution gene C homolog (A. nidulans)
H200018809	0.692	-1.4451	MGC10960	NM_032653	Hypothetical protein MGC10960
H200004664	0.692	-1.4451	DKFZp547D2210	AK056295	Homo sapiens cDNA FLJ31733 fis, clone NT2RI2006943
H200001989	0.692	-1.4451	C20orf4	NM_015511	Chromosome 20 open reading frame 4
H200012201	0.692	-1.4451	ACTL7B	NM_006686	Actin-like 7B
H200005195	0.692	-1.4451	SELM	AY043487	Homo sapiens selenoprotein SelM mRNA, complete cds
H200018504	0.692	-1.4451		AK024862	Homo sapiens cDNA: FLJ21209 fis, clone COL00396
H200011363	0.692	-1.4451	C20orf40	NM_014054	Chromosome 20 open reading frame 40

Genes that are 1.4 fold down regulated in SUM1315-BP2 vs. SUM1315					
H200000456	0.692	-1.4451	IQGAP1	NM_003870	IQ motif containing GTPase activating protein 1
H200003177	0.692	-1.4451	SCN1A	AF225985	Sodium channel, voltage-gated, type I, alpha polypeptide
H200020285	0.692	-1.4451	KCNE4	BC014429	Homo sapiens, Similar to potassium voltage-gated channel, Isk-related subfamily, gene 4, clone MGC:2
H200005682	0.691	-1.4472	HSPC132	NM_016399	Hypothetical protein
H300008483	0.691	-1.4472	ENSG00000177888		AMBIGUOUS
H200018736	0.691	-1.4472	HXCP2	NM_032579	Colon and small intestine-specific cysteine-rich protein precursor similar to FIZZ2/resistin-like pr
H200003980	0.691	-1.4472	FLJ23186	NM_024616	Hypothetical protein FLJ23186
H200006164	0.691	-1.4472	P4HB	NM_000918	Procollagen-proline, 2-oxoglutarate 4-dioxygenase (proline 4-hydroxylase), beta polypeptide (protein
H300021617	0.691	-1.4472	ENSG00000179158		METHYL-CPG BINDING DOMAIN PROTEIN 3-LIKE 2. [Source:RefSeq;Acc:NM_144614]
H200013841	0.691	-1.4472	LOH11CR2A	NM_014622	Loss of heterozygosity, 11, chromosomal region 2, gene A
H200018358	0.691	-1.4472		AL157456	Homo sapiens mRNA; cDNA DKFZp761K1112 (from clone DKFZp761K1112)
H200015829	0.691	-1.4472		AK022801	Homo sapiens cDNA FLJ12739 fis, clone NT2RP2000498
H200017313	0.691	-1.4472	FGFR2	NM_023028	Fibroblast growth factor receptor 2 (bacteria-expressed kinase, keratinocyte growth factor receptor,
H200017557	0.691	-1.4472	OPN3	NM_014322	Opsin 3 (encephalopsin, panopsin)
H200020573	0.691	-1.4472		BC016876	Homo sapiens, clone IMAGE:3891207, mRNA
H300004942	0.691	-1.4472			UNKNOWN
H300011550	0.691	-1.4472	ENSG00000151989		MYOCARDIN. [Source:RefSeq;Acc:NM_153604]
H200004358	0.691	-1.4472	ALPI	NM_001631	Alkaline phosphatase, intestinal

Genes that are 1.4 fold down regulated in SUM1315-BP2 vs. SUM1315					
H200020953	0.691	-1.4472	ODF3	AB067774	Homo sapiens mRNA for h-SHIPPO 1, complete cds
H200020639	0.691	-1.4472	PPP1R12A	AK057712	Homo sapiens cDNA FLJ33150 fis, clone UTERU2000260
H200000908	0.691	-1.4472	EIF1A	NM_001412	Eukaryotic translation initiation factor 1A
H200018513	0.691	-1.4472	IFIX	AK024890	Homo sapiens cDNA: FLJ21237 fis, clone COL01114
H200021078	0.691	-1.4472	PGPL	NM_012227	Pseudoautosomal GTP-binding protein-like
H300013055	0.69	-1.4493	ENSG00000004848	NM_004322	BCL2-ANTAGONIST OF CELL DEATH (BAD) (BCL-2 BINDING COMPONENT 6) (BCL-XL/BCL-2 ASSOCIATED DEATH PROMOTER) (BCL2-LIKE 8 PROTEIN). [Source:SWISSPROT;Acc: Q92934]
H300020497	0.69	-1.4493	ENSG00000161847	NM_152408	AMBIGUOUS
H200003176	0.69	-1.4493	KIAA0844	NM_014951	KIAA0844 protein
H200019176	0.69	-1.4493	MGC4549	NM_032377	Hypothetical protein MGC4549
H200017569	0.69	-1.4493	LOC51064	NM_015917	Glutathione S-transferase subunit 13 homolog
H200010865	0.69	-1.4493	LOC51231	NM_016440	VRK3 for vaccinia related kinase 3
H200004589	0.69	-1.4493		AK054729	Homo sapiens cDNA FLJ30167 fis, clone BRACE2000743
H200002665	0.69	-1.4493	DKFZP434E2135	NM_030804	Hypothetical protein DKFZp434E2135
H200010396	0.69	-1.4493	TRADD	NM_003789	TNFRSF1A-associated via death domain
H200016136	0.69	-1.4493	MEGF11	NM_032445	MEGF11 protein
H200002695	0.69	-1.4493	MGC1203	NM_024296	Hypothetical protein MGC1203
H200017586	0.689	-1.4514	FLJ10895	NM_019084	Hypothetical protein FLJ10895
H200003829	0.689	-1.4514	UGDH	NM_003359	UDP-glucose dehydrogenase
H200005947	0.689	-1.4514	GJA1	NM_000165	Gap junction protein, alpha 1, 43kD (connexin 43)
H200020164	0.689	-1.4514	ANXA2P1	M62896	Annexin A2 pseudogene 1
H200006499	0.689	-1.4514	RAB2	NM_002865	RAB2, member RAS oncogene family
H200014686	0.689	-1.4514	ADAM5	AJ132820	A disintegrin and metalloproteinase domain 5
H200014948	0.689	-1.4514	KCNK2	NM_014217	Potassium channel, subfamily K, member 2 (TREK-1)

Genes that are 1.4 fold down regulated in SUM1315-BP2 vs. SUM1315					
H200007728	0.689	-1.4514	SFRS3	AF107405	Splicing factor, arginine/ serine-rich 3
H200005040	0.689	-1.4514	CD5L	NM_005894	CD5 antigen-like (scavenger receptor cysteine rich family)
H200005913	0.689	-1.4514	CD163	Z22970	CD163 antigen
H200007338	0.689	-1.4514	CCR3	NM_001837	Chemokine (C-C motif) receptor 3
H200010355	0.688	-1.4535	CD79B	NM_000626	CD79B antigen (immunoglobulin-associated beta)
H200007778	0.688	-1.4535	PTCRA	U36759	Human pre TCR alpha mRNA, partial cds
H200017855	0.688	-1.4535		AL359599	Homo sapiens mRNA; cDNA DKFZp547C126 (from clone DKFZp547C126)
H200000599	0.688	-1.4535	BAGE	NM_001187	B melanoma antigen
H300003016	0.688	-1.4535	ENSG0000018 0940		UNKNOWN
H200018384	0.688	-1.4535		AL390150	Homo sapiens mRNA; cDNA DKFZp547L156 (from clone DKFZp547L156)
H200010527	0.688	-1.4535	ILKAP	AK055417	Integrin-linked kinase-associated serine/threonine phosphatase 2C
H200006816	0.688	-1.4535	FETUB	NM_014375	Fetuin B
H200004565	0.688	-1.4535	ZNF85; HPF4; HTF1	BC008688	Homo sapiens, clone MGC: 9010 IMAGE:3873712, mRNA, complete cds
H200011685	0.688	-1.4535	NICE-1	NM_019060	NICE-1 protein
H200016500	0.688	-1.4535	KIAA1841	AB058744	KIAA1841 protein
H200019181	0.688	-1.4535	FLJ20030	NM_017627	Hypothetical protein FLJ20030
H200021225	0.688	-1.4535	ZNF513	AK056765	Homo sapiens cDNA FLJ32203 fis, clone PLACE6003038, weakly similar to ZINC FINGER PROTEIN 84
H200004298	0.688	-1.4535	FLB6421	NM_020119	Hypothetical protein FLB6421
H200020522	0.688	-1.4535		BC006361	Homo sapiens, clone MGC: 13137 IMAGE:4129277, mRNA, complete cds
H200003544	0.688	-1.4535	DAPK3	NM_001348	Death-associated protein kinase 3
H200020223	0.687	-1.4556	KCNMA1	U02632	Human calcium-activated potassium channel mRNA, partial cds
H200001318	0.687	-1.4556	FLJ22167	NM_024533	Hypothetical protein FLJ22167
H200003539	0.687	-1.4556	FLJ20898	NM_024600	Hypothetical protein FLJ20898

Genes that are 1.4 fold down regulated in SUM1315-BP2 vs. SUM1315					
H200018101	0.687	-1.4556		AF130114	Homo sapiens clone FLB9131 PRO2459 mRNA, complete cds
H200007343	0.687	-1.4556	NPY5R	NM_006174	Neuropeptide Y receptor Y5
H200016853	0.687	-1.4556	EPHB1	AL133099	Homo sapiens mRNA; cDNA DKFZp434B1521 (from clone DKFZp434B1521)
H200006483	0.687	-1.4556	TCF21	NM_003206	Transcription factor 21
H200016911	0.687	-1.4556	LOC51301	NM_016591	Core 2 beta-1,6-N-acetylglucosaminyltransferase 3
H200004779	0.687	-1.4556	DKFZP434P0714	NM_032131	Hypothetical protein DKFZp434P0714
H200020523	0.687	-1.4556	SYNCOILIN	AK056550	Homo sapiens cDNA FLJ31988 fis, clone NT2RP7008863
H2NC000011	0.687	-1.4556			Randomized negative control
H200005565	0.687	-1.4556	KIAA0661	NM_014771	95 kDa retinoblastoma protein binding protein
H200020620	0.687	-1.4556	NAG	AK057915	Homo sapiens cDNA FLJ25186 fis, clone CBR09457, highly similar to Neuroblastoma-amplified protein
H200018714	0.686	-1.4577	ZAN	NM_003386	Zonadhesin
H200020309	0.686	-1.4577	TECTB	NM_058222	Homo sapiens tectorin beta (TECTB) mRNA, complete cds
H300007672	0.686	-1.4577			UNKNOWN
H200003503	0.686	-1.4577	CDK8	NM_001260	Cyclin-dependent kinase 8
H200002826	0.686	-1.4577	LOC59346	AK024498	PDZ-LIM protein mystique
H200016992	0.686	-1.4577	PCYT1A	NM_005017	Phosphate cytidylyltransferase 1, choline, alpha isoform
H200008722	0.686	-1.4577		AF244571	Homo sapiens clone L49 HERV-K-T47-like long terminal repeat sequence
H200009903	0.686	-1.4577	MGC3032	BC000572	Hypothetical protein MGC3032
H200017735	0.686	-1.4577	PRO2900	NM_018635	Hypothetical protein PRO2900
H200009268	0.686	-1.4577		AK021583	Homo sapiens cDNA FLJ11521 fis, clone HEMBA1002486
H300008144	0.685	-1.4599	ENSG00000177186	NM_152365	AMBIGUOUS
H200017544	0.685	-1.4599	PPP2R2C	AF086924	Protein phosphatase 2 (formerly 2A), regulatory subunit B (PR 52), gamma isoform
H200019711	0.685	-1.4599	MGC16279	NM_032916	Hypothetical protein MGC16279

Genes that are 1.4 fold down regulated in SUM1315-BP2 vs. SUM1315					
H200013490	0.685	-1.4599	LOC84663	NM_032576	Lipopolysaccaride-specific response 5-like protein
H200004203	0.685	-1.4599	PIK3C3	NM_002647	Phosphoinositide-3-kinase, class 3
H200003140	0.685	-1.4599	C20orf3	AB033767	Chromosome 20 open reading frame 3
H200008177	0.685	-1.4599	IL1RAP	NM_002182	Interleukin 1 receptor accessory protein
H200014189	0.685	-1.4599	HTN3	NM_000200	Histatin 3
H200012290	0.685	-1.4599	HNF4G	AK025222	Homo sapiens cDNA: FLJ21569 fis, clone COL06508
H200018367	0.685	-1.4599	C2orf22; MGC33602	AL161956	Homo sapiens mRNA; cDNA DKFZp761A17121 (from clone DKFZp761A17121)
H300006329	0.685	-1.4599			UNKNOWN
H200003922	0.685	-1.4599	ZF	NM_021212	HCF-binding transcription factor Zhangfei
H200009914	0.685	-1.4599	KIAA1204	AB033030	KIAA1204 protein
H200007386	0.684	-1.462		AL157504	Homo sapiens mRNA; cDNA DKFZp586O0724 (from clone DKFZp586O0724)
H300009623	0.684	-1.462	ENSG0000018 0621		AMBIGUOUS
H200003668	0.684	-1.462	LOC51191	NM_016323	Cyclin-E binding protein 1
H200007176	0.684	-1.462		AK023620	Homo sapiens cDNA FLJ13558 fis, clone PLACE1007743
H200010035	0.684	-1.462	NUMA1	NM_006185	Nuclear mitotic apparatus protein 1
H200020419	0.684	-1.462	LOC286334	AJ420454	Homo sapiens mRNA full length insert cDNA clone EUROIMAGE 1517766
H200006375	0.684	-1.462	PRKACA	NM_002730	Protein kinase, cAMP-dependent, catalytic, alpha
H300001133	0.684	-1.462	ENSG0000017 1985		AMBIGUOUS
H200003498	0.684	-1.462	MAN1A1	NM_005907	Mannosidase, alpha, class 1A, member 1
H200015109	0.684	-1.462	EIF4G1	NM_004953	Eukaryotic translation initiation factor 4 gamma, 1
H200010529	0.684	-1.462	LCCP	NM_016201	Leman coiled-coil protein
H200009426	0.684	-1.462		AK025953	Homo sapiens cDNA: FLJ22300 fis, clone HRC04759
H200011956	0.684	-1.462	CDH16	NM_004062	Cadherin 16, KSP-cadherin
H200002398	0.684	-1.462	HCLS1	NM_005335	Hematopoietic cell-specific Lyn substrate 1
H200005872	0.683	-1.4641	PTPN4	NM_002830	Protein tyrosine phosphatase, non-receptor type 4 (megakaryocyte)
H200019237	0.683	-1.4641		AF334589	Homo sapiens P41 mRNA, complete cds

Genes that are 1.4 fold down regulated in SUM1315-BP2 vs. SUM1315					
H200013775	0.683	-1.4641	PPP3CB	NM_021132	Protein phosphatase 3 (formerly 2B), catalytic subunit, beta isoform (calcineurin A beta)
H200010521	0.683	-1.4641	CAMP-GEFII	NM_007023	CAMP-regulated guanine nucleotide exchange factor II
H200017117	0.683	-1.4641		AL049349	Homo sapiens mRNA; cDNA DKFZp566C133 (from clone DKFZp566C133)
H200011293	0.683	-1.4641	CLTA	NM_007096	Clathrin, light polypeptide (Lca)
H300006448	0.683	-1.4641	USH1G	NM_173477	AMBIGUOUS
H200006038	0.683	-1.4641	SEC14L1	NM_003003	SEC14-like 1 (S. cerevisiae)
H200003265	0.683	-1.4641	KIAA0367	AB002365	KIAA0367 protein
H200011629	0.683	-1.4641	SH3BP5	AL133111	SH3-domain binding protein 5 (BTK-associated)
H200019136	0.683	-1.4641		AK057428	Homo sapiens cDNA FLJ32866 fis, clone TESTI2003718
H200007563	0.683	-1.4641		AK024204	Homo sapiens cDNA FLJ14142 fis, clone MAMMA1002880
H200007390	0.683	-1.4641	TUBB4	NM_006086	Tubulin, beta, 4
H200009543	0.683	-1.4641	VPS13C	AK056744	Homo sapiens cDNA FLJ32182 fis, clone PLACE6001823
H200001548	0.683	-1.4641	SRGAP3	AB007871	KIAA0411 gene product
H200019527	0.682	-1.4663	CASKIN1	AB037727	Cask-interacting protein 1
H200006815	0.682	-1.4663	ECM1	NM_004425	Extracellular matrix protein 1
H200005680	0.682	-1.4663	FAM33A	AK056473	Homo sapiens cDNA FLJ31911 fis, clone NT2RP7004751
H200003068	0.682	-1.4663	GC20	NM_005875	Translation factor sui1 homolog
H200009051	0.682	-1.4663	FLJ13501	NM_025007	Hypothetical protein FLJ13501
H200005132	0.682	-1.4663	SEMA6C	AB058772	Sema domain, transmembrane domain (TM), and cytoplasmic domain, (semaphorin) 6C
H200011491	0.682	-1.4663	CED-6	NM_016315	CED-6 protein
H200019484	0.682	-1.4663	DNCH1	AK023747	Homo sapiens cDNA FLJ13685 fis, clone PLACE2000039, highly similar to DYNEIN HEAVY CHAIN, CYTOSOLIC
H200006996	0.682	-1.4663	DKFZp451J0118	AF070546	Homo sapiens clone 24607 mRNA sequence
H200021087	0.682	-1.4663	RSU1	AK055596	Homo sapiens cDNA FLJ31034 fis, clone HSYRA1000178

Genes that are 1.4 fold down regulated in SUM1315-BP2 vs. SUM1315					
H200005925	0.682	-1.4663	TMP21	NM_006827	Transmembrane trafficking protein
H200014119	0.682	-1.4663	C3AR1	NM_004054	Complement component 3a receptor 1
H200007082	0.682	-1.4663	LOC51604	NM_015937	CGI-06 protein
H200003195	0.682	-1.4663	TMOD3	AL137543	Tropomodulin 3 (ubiquitous)
H200003425	0.682	-1.4663	MDS018	AK027491	Hypothetical protein MDS018
H200002771	0.682	-1.4663	C12orf22	NM_030809	Chromosome 12 open reading frame 22
H200009105	0.682	-1.4663	FLJ21290	NM_025034	Hypothetical protein FLJ21290
H200008131	0.681	-1.4684	ELL2	NM_012081	ELL-RELATED RNA POLYMERASE II, ELONGATION FACTOR
H200013878	0.681	-1.4684	C18orf1	NM_004338	Chromosome 18 open reading frame 1
H200012070	0.681	-1.4684	FLJ43654	AK056215	Homo sapiens cDNA FLJ31653 fis, clone NT2RI2004190
H300009342	0.681	-1.4684	ENSG00000167716		AMBIGUOUS
H200017711	0.681	-1.4684	C20orf32	NM_020356	Chromosome 20 open reading frame 32
H200020268	0.681	-1.4684	FLJ21617	NM_030897	Hypothetical protein FLJ21617
H200003590	0.681	-1.4684		AK023999	Homo sapiens cDNA FLJ13937 fis, clone Y79AA1000805
H200001353	0.681	-1.4684		AK056198	Homo sapiens Cri-du-chat region mRNA, clone NIBB11
H200005361	0.68	-1.4706	FLJ10514	NM_018122	Hypothetical protein FLJ10514
H200000178	0.68	-1.4706	THRA	NM_003250	Thyroid hormone receptor, alpha (erythroblastic leukemia viral (v-erb-a) oncogene homolog, avian)
H200005043	0.68	-1.4706	FLJ20618	NM_017903	Hypothetical protein FLJ20618
H200008181	0.68	-1.4706	EIF4A2	NM_001967	Eukaryotic translation initiation factor 4A, isoform 2
H200020334	0.68	-1.4706	SYNCRIP	AY034482	Homo sapiens hnRNP Q2 mRNA, complete cds
H200005058	0.68	-1.4706	PFC	NM_002621	Properdin P factor, complement
H200020647	0.68	-1.4706	HPS4	AK057648	Homo sapiens cDNA FLJ33086 fis, clone TRACH2000461
H200020151	0.68	-1.4706	LIP8	AL137669	LYST-interacting protein LIP8

Genes that are 1.4 fold down regulated in SUM1315-BP2 vs. SUM1315					
H200018382	0.68	-1.4706		AL390157	Homo sapiens mRNA; cDNA DKFZp434D179 (from clone DKFZp434D179)
H300005217	0.68	-1.4706	ENSG00000177825		TYROSINE PHOSPHATASE NON RECEPTOR TYPE 13 EC_3.1.3.48 TYROSINE PHOSPHATASE 1E PTP E1 HPTPE1 PTP BAS TYROSINE PHOSPHATASE PTPL1 FAS ASSOCIATED TYROSINE PHOSPHATASE 1 FAP 1
H200012902	0.68	-1.4706	KIAA1542	AB040975	KIAA1542 protein
H200010270	0.68	-1.4706	DKFZp434D177	AK055895	Hypothetical protein DKFZp434D177
H200004364	0.68	-1.4706	HLXB9	NM_005515	Homeo box HB9
H200011142	0.679	-1.4728	KIAA1350	AB037771	KIAA1350 protein
H300009256	0.679	-1.4728	ENSG00000181553		AMBIGUOUS
H200013472	0.679	-1.4728	CPA5	AF384667	Homo sapiens carboxypeptidase A5 mRNA, complete cds
H300006859	0.679	-1.4728	ENSG00000177095		PUTATIVE G-PROTEIN COUPLED RECEPTOR (SEVEN TRANSMEMBRANE HELIX RECEPTOR). [Source:SPTREMBL;Acc:Q8TDT2]
H200017806	0.679	-1.4728	PCTAIRE2BP	AB025254	Tudor repeat associator with PCTAIRE 2
H200019635	0.679	-1.4728	PIP5K1A	BC007005	Homo sapiens, clone IMAGE:3680651, mRNA
H200010451	0.678	-1.4749	ABCC3	NM_020038	ATP-binding cassette, sub-family C (CFTR/MRP), member 3
H200007712	0.678	-1.4749	KIAA0830	AB020637	KIAA0830 protein
H200007540	0.678	-1.4749	CLDN8	AK022269	Claudin 8
H200007843	0.678	-1.4749	FLJ20989	NM_023080	Hypothetical protein FLJ20989
H200016856	0.678	-1.4749	TEX15	NM_031271	Testis expressed sequence 15
H200015698	0.678	-1.4749	PCDHA7	NM_018910	Protocadherin alpha 7
H200018258	0.678	-1.4749		AL050132	Homo sapiens mRNA; cDNA DKFZp586I041 (from clone DKFZp586I041)
H200017260	0.678	-1.4749	KIAA0904	AB020711	KIAA0904 protein
H200014590	0.678	-1.4749		AL110204	Homo sapiens mRNA; cDNA DKFZp586K1922 (from clone DKFZp586K1922)

Genes that are 1.4 fold down regulated in SUM1315-BP2 vs. SUM1315					
H200011524	0.678	-1.4749	DDIT4L	BC013592	Homo sapiens, Similar to RIKEN cDNA 1700037B15 gene, clone MGC:9960 IMAGE:3877854, mRNA, complete cd
H200013138	0.678	-1.4749	EN2	NM_001427	Engrailed homolog 2
H200017250	0.678	-1.4749	GPR27	NM_018971	G protein-coupled receptor 27
H200003664	0.678	-1.4749	C20orf100	NM_032883	Chromosome 20 open reading frame 100
H200003768	0.678	-1.4749	KIAA1615	AK025110	KIAA1615 protein
H200005949	0.678	-1.4749	CTRB1	NM_001906	Chymotrypsinogen B1
H200013232	0.677	-1.4771		AK056355	Homo sapiens mRNA; cDNA DKFZp547P134 (from clone DKFZp547P134)
H200004342	0.677	-1.4771	CHD2	NM_001271	Chromodomain helicase DNA binding protein 2
H200012652	0.677	-1.4771	TEKT2	NM_014466	Tektin 2 (testicular)
H200021004	0.677	-1.4771	FLJ36166	AL049437	Homo sapiens mRNA; cDNA DKFZp586E1120 (from clone DKFZp586E1120)
H200008412	0.677	-1.4771		AK024399	Homo sapiens cDNA FLJ14337 fis, clone PLACE4000494
H300009954	0.677	-1.4771			UNKNOWN
H200000516	0.677	-1.4771	TRD@	X73617	T cell receptor delta locus
H200020340	0.677	-1.4771		AY003854	Homo sapiens isolate sy-4M/12-H1 immunoglobulin heavy chain variable region mRNA, partial cds
H200005355	0.677	-1.4771	PACE	NM_002569	Paired basic amino acid cleaving enzyme (furin, membrane associated receptor protein)
H200007795	0.677	-1.4771	DLK1	NM_003836	Delta-like 1 homolog (Drosophila)
H200020306	0.676	-1.4793	PPP1R14BP1	AF030942	Protein phosphatase 1, regulatory (inhibitor) subunit 14B pseudogene 1
H200010242	0.676	-1.4793	CTSW	NM_001335	Cathepsin W (lymphopain)
H200001603	0.676	-1.4793	KIAA0144	NM_014847	KIAA0144 gene product
H200002861	0.676	-1.4793	3'HEXO	AL137679	Homo sapiens mRNA; cDNA DKFZp434D2426 (from clone DKFZp434D2426); partial cds
H300010339	0.676	-1.4793	ENSG00000170909		SSX5 PROTEIN. [Source:SWISSPROT;Acc:O60225]
H300003841	0.676	-1.4793	ENSG00000179228		FKSG89

Genes that are 1.4 fold down regulated in SUM1315-BP2 vs. SUM1315					
H200020751	0.676	-1.4793		AK056856	Homo sapiens cDNA FLJ32294 fis, clone PROST2001796
H200008544	0.676	-1.4793	FLJ25005	AK056653	Homo sapiens cDNA FLJ25005 fis, clone CBL00905
H200018880	0.676	-1.4793	D10S170	NM_005436	DNA segment, single copy, probe pH4 (transforming sequence, thyroid-1,
H200001666	0.676	-1.4793	STAB2	AK024503	Stabilin-2
H200010701	0.676	-1.4793	CDK4	NM_000075	Cyclin-dependent kinase 4
H200011316	0.676	-1.4793	AQP9	NM_020980	Aquaporin 9
H200004293	0.676	-1.4793	RFC4	NM_002916	Replication factor C (activator 1) 4 (37kD)
H300006924	0.676	-1.4793	ENSG00000105705	NM_006623	D-3-PHOSPHOGLYCERATE DEHYDROGENASE (EC 1.1.1.95) (3-PGDH). [Source:SWISSPROT;Acc:O43175]
H200004759	0.675	-1.4815	NHLH2	AB007959	Nescient helix loop helix 2
H200013627	0.675	-1.4815		AK055856	Homo sapiens cDNA FLJ31294 fis, clone KIDNE2007810, weakly similar to DEOXYURIDINE 5'-TRIPHOSPHATE N
H200002084	0.675	-1.4815	FLJ11320	BC001427	GDP-fucose transporter 1
H200001226	0.675	-1.4815	SYN2	NM_003178	Synapsin II
H200020732	0.675	-1.4815		AK057064	Homo sapiens cDNA FLJ32502 fis, clone SKNSH2000550
H200019195	0.675	-1.4815	MGC2780	NM_025266	Hypothetical protein MGC2780
H200017342	0.675	-1.4815	LOC85414	NM_033102	Prostein protein
H200008550	0.675	-1.4815		AK057858	Homo sapiens cDNA FLJ25129 fis, clone CBR06594
H200011154	0.674	-1.4837	KBTBD3	AK055247	Homo sapiens cDNA FLJ30685 fis, clone FCBBF2000276
H200010984	0.674	-1.4837		BC014230	Homo sapiens, clone IMAGE:3607242, mRNA, partial cds
H200007410	0.674	-1.4837	COL6A2	NM_001849	Collagen, type VI, alpha 2
H300011609	0.674	-1.4837	ENSG00000103275		CD209 ANTIGEN; DENDRITIC CELL-SPECIFIC ICAM3-GRABBING NONINTEGRIN. [Source:RefSeq;Acc:NM_021155]
H200010442	0.674	-1.4837	STXBP2	NM_006949	Syntaxin binding protein 2
H200020609	0.674	-1.4837		AK058066	Homo sapiens cDNA FLJ25337 fis, clone TST00714

Genes that are 1.4 fold down regulated in SUM1315-BP2 vs. SUM1315					
H200006235	0.674	-1.4837	PSMF1	NM_006814	Proteasome (prosome, macropain) inhibitor subunit 1 (PI31)
H200014309	0.674	-1.4837	ZNF144	NM_007144	Zinc finger protein 144 (Mel-18)
H200018911	0.674	-1.4837	FLJ12661	NM_025138	Hypothetical protein FLJ12661
H200011126	0.674	-1.4837	MAST205	NM_015112	KIAA0807 protein
H200005023	0.674	-1.4837	SAS	NM_005981	Sarcoma amplified sequence
H200020973	0.673	-1.4859	UCHL1	AK055249	Homo sapiens cDNA FLJ30687 fis, clone FCBBF2000379
H200016571	0.673	-1.4859	LOC51143	NM_016141	Dynein light chain-A
H200004925	0.673	-1.4859	BMP2K	AK021725	Homo sapiens cDNA FLJ11663 fis, clone HEMBA1004631
H200003330	0.673	-1.4859	CACNA1D	NM_000720	Calcium channel, voltage-dependent, L type, alpha 1D subunit
H200010889	0.673	-1.4859	FLJ11116	NM_019045	Similar to rab11-binding protein
H200008648	0.673	-1.4859	ARF4L	NM_001661	ADP-ribosylation factor 4-like
H200017183	0.673	-1.4859	H2AFE	NM_021066	H2A histone family, member E
H300022095	0.673	-1.4859	ENSG00000101639	NM_080426	GUANINE NUCLEOTIDE-BINDING PROTEIN G(S), ALPHA SUBUNIT (ADENYLATE CYCLASE-STIMULATING G ALPHA PROTEIN). [Source:SWISSPROT;Acc: P04895]
H200020283	0.673	-1.4859		BC014487	Homo sapiens, clone IMAGE:4873952, mRNA
H200008045	0.673	-1.4859	CDC27	NM_001256	Cell division cycle 27
H300006654	0.673	-1.4859	ENSG00000178984		UNKNOWN
H200015685	0.673	-1.4859	SCRIB	D63481	Scribble
H200019599	0.673	-1.4859		BC005846	Homo sapiens, clone IMAGE:2822887, mRNA
H200013420	0.673	-1.4859	CARM1	AF055027	Coactivator-associated arginine methyltransferase-1
H200003867	0.673	-1.4859	C10orf46	AK057742	Homo sapiens cDNA: FLJ23332 fis, clone HEP12754
H200000896	0.673	-1.4859	VAV2	NM_003371	Vav 2 oncogene
H200020292	0.672	-1.4881	LOC116123	BC014341	Homo sapiens, clone MGC: 23941 IMAGE:3997249, mRNA, complete cds
H200010289	0.672	-1.4881	FLJ10545	NM_018132	Hypothetical protein FLJ10545

Genes that are 1.4 fold down regulated in SUM1315-BP2 vs. SUM1315					
H200007111	0.672	-1.4881	FLJ31842	AK056404	Homo sapiens cDNA FLJ31842 fis, clone NT2RP7000259
H200017973	0.672	-1.4881	MGC4840	AK027666	Hypothetical protein MGC4840
H200019117	0.672	-1.4881	GAD1	NM_000817	Glutamate decarboxylase 1 (brain, 67kD)
H200018317	0.672	-1.4881		AK000834	Homo sapiens cDNA FLJ20827 fis, clone ADKA03543
H200014416	0.672	-1.4881		AK055002	Homo sapiens cDNA FLJ30440 fis, clone BRACE2009185
H300004312	0.671	-1.4903			RECEPTOR
H200008308	0.671	-1.4903	KIAA0626	NM_021647	KIAA0626 gene product
H200015805	0.671	-1.4903	LYRIC	AK000745	Homo sapiens mRNA; cDNA DKFZp564C1563 (from clone DKFZp564C1563)
H200006923	0.671	-1.4903	RGS3	NM_021106	Regulator of G-protein signalling 3
H200016096	0.671	-1.4903	OSM	BC011589	Oncostatin M
H200003189	0.671	-1.4903	CA11	NM_001217	Carbonic anhydrase XI
H200019509	0.671	-1.4903	BEX1	NM_018476	Brain expressed, X-linked 1
H200017606	0.67	-1.4925	NSBP1	NM_030763	Nucleosomal binding protein 1
H200015935	0.67	-1.4925	MYLC2PL	BC002778	Homo sapiens, Similar to myosin light chain 2, precursor lymphocyte-specific, clone MGC:3479 IMAGE:3
H200013570	0.67	-1.4925	CRYBA2	NM_057093	Crystallin, beta A2
H200011233	0.67	-1.4925	LOC51299	NM_016588	Neuritin
H200003502	0.67	-1.4925	ARAP3	AK001579	ARF-GAP, RHO-GAP, ankyrin repeat and plekstrin homology domains-containing protein 3
H200018403	0.67	-1.4925	VENTX2P1; NA88A	AF164963	Homo sapiens tumor antigen NA88-A pseudogene, complete sequence
H200011946	0.67	-1.4925	MSH4	NM_002440	MutS homolog 4 (E. coli)
H200006204	0.67	-1.4925	PCK2	NM_004563	Phosphoenolpyruvate carboxykinase 2 (mitochondrial)
H200019948	0.669	-1.4948	FLJ12242	BC009961	Homo sapiens, Similar to hypothetical protein FLJ12242, clone MGC: 15311 IMAGE:4300199, mRNA, complet
H200009321	0.669	-1.4948	ZNF35	NM_003420	Zinc finger protein 35 (clone HF.10)

Genes that are 1.4 fold down regulated in SUM1315-BP2 vs. SUM1315					
H200021290	0.669	-1.4948	RAB9B	BC018033	Homo sapiens, clone IMAGE:4800052, mRNA, partial cds
H300000942	0.669	-1.4948	ENSG00000177617		AMBIGUOUS
H200009530	0.669	-1.4948	FLJ31818	AK056380	Homo sapiens cDNA FLJ31818 fis, clone NT2RP6000017
H200007201	0.669	-1.4948	GYLTL1B	AK055829	Homo sapiens cDNA FLJ31267 fis, clone KIDNE2006053, moderately similar to Mus musculus mRNA for acet
H200004993	0.669	-1.4948	SSI-1	NM_003745	JAK binding protein
H200012242	0.669	-1.4948	KIAA0749	AB018292	KIAA0749 protein
H200020211	0.669	-1.4948	MGC15937	BC013929	Homo sapiens, clone IMAGE:3839841, mRNA
H200014209	0.669	-1.4948	KIAA1271	AB033097	KIAA1271 protein
H200004336	0.669	-1.4948	WFDC1	NM_021197	WAP four-disulfide core domain 1
H200019546	0.669	-1.4948	MGC16121	NM_032762	Hypothetical protein MGC16121
H200008100	0.669	-1.4948	FLJ13964	AB033047	Hypothetical protein FLJ13964
H300000220	0.669	-1.4948	ENSG00000177204		AMBIGUOUS
H200009232	0.668	-1.497	ECE1	NM_001397	Endothelin converting enzyme 1
H200008388	0.668	-1.497	CDW92	AJ420812	CDw92 antigen
H200007342	0.668	-1.497	GPR50	NM_004224	G protein-coupled receptor 50
H200005389	0.668	-1.497	LOC285535	AK021540	Homo sapiens cDNA FLJ11478 fis, clone HEMBA1001781
H200005426	0.668	-1.497		AK057710	Homo sapiens cDNA FLJ33148 fis, clone UTERU2000238
H200002860	0.668	-1.497	DKFZP566K023	NM_015485	DKFZP566K023 protein
H200021172	0.668	-1.497	THRAP1	AK054894	Homo sapiens cDNA FLJ30332 fis, clone BRACE2007254
H200007994	0.668	-1.497	BHLHB2	NM_003670	Basic helix-loop-helix domain containing, class B, 2
H200014843	0.668	-1.497	FLJ30681	AK055243	Homo sapiens cDNA FLJ30681 fis, clone FCBBF2000195
H200005608	0.668	-1.497	FLJ31528	AK056090	Homo sapiens cDNA FLJ31528 fis, clone NT2RI2000412
H200019359	0.668	-1.497	REPS1	AL049259	Homo sapiens mRNA; cDNA DKFZp564E193 (from clone DKFZp564E193)

Genes that are 1.4 fold down regulated in SUM1315-BP2 vs. SUM1315					
H200012020	0.668	-1.497	LOC145786	AK023283	Homo sapiens cDNA FLJ13221 fis, clone NT2RP4002075
H200013758	0.668	-1.497	DKFZp667B1218	AK001526	Homo sapiens cDNA FLJ10664 fis, clone NT2RP2006196
H200008775	0.668	-1.497	FLJ14033	NM_022462	Hypothetical protein FLJ14033 similar to hypoxia inducible factor 3, alpha subunit
H200010600	0.668	-1.497	DKFZP434M098	AL117587	DKFZP434M098 protein
H200006987	0.668	-1.497	SLC35A1	NM_006416	Solute carrier family 35 (CMP-sialic acid transporter), member 1
H300003595	0.668	-1.497	ENSG00000179044		UNKNOWN
H200008174	0.667	-1.4993	KIAA0561	AB011133	KIAA0561 protein
H200008793	0.667	-1.4993	HSPC051	NM_013387	Ubiquinol-cytochrome c reductase complex (7.2 kD)
H200021118	0.667	-1.4993		AK054588	Homo sapiens cDNA FLJ30026 fis, clone 3NB692001123
H200016838	0.667	-1.4993	OR12D3	NM_030959	Olfactory receptor, family 12, subfamily D, member 3
H200013763	0.667	-1.4993	ULK2	NM_014683	Unc-51-like kinase 2 (C. elegans)
H200004671	0.667	-1.4993	KIAA0974	AB023191	DnaJ protein SB73
H200003924	0.667	-1.4993	CRSP6; CRSP77; DRIP80; TRAP80; FLJ10812	AK022156	Homo sapiens cDNA FLJ12094 fis, clone HEMBB1002607, highly similar to Homo sapiens vitamin D3 recept
H200006603	0.667	-1.4993	MOX2	NM_005944	Antigen identified by monoclonal antibody MRC OX-2
H200019118	0.667	-1.4993	SLC5A3	NM_006933	Solute carrier family 5 (inositol transporters), member 3
H200012391	0.667	-1.4993	ZNF224	AK025777	Homo sapiens cDNA: FLJ22124 fis, clone HEP19352
H200016577	0.667	-1.4993		AK022085	Homo sapiens cDNA FLJ12023 fis, clone HEMBB1001785
H200019393	0.667	-1.4993	EXOSC6; p11; EAP4; MTR3; Mtr3p; hMtr3p	AK024276	Homo sapiens clone TA40 untranslated mRNA, complete sequence
H200011757	0.666	-1.5015	LOC139886	AK021705	Homo sapiens cDNA FLJ11643 fis, clone HEMBA1004366
H200001662	0.666	-1.5015	ZNF91	NM_003430	Zinc finger protein 91 (HPF7, HTF10)
H200017276	0.666	-1.5015	LOC51759	NM_016520	Hepatocellular carcinoma-associated antigen 59

Genes that are 1.4 fold down regulated in SUM1315-BP2 vs. SUM1315					
H200009957	0.666	-1.5015	FLJ12488	NM_031218	Hypothetical protein FLJ12488
H200011973	0.666	-1.5015	KIAA1138	AB032964	KIAA1138 protein
H200014285	0.666	-1.5015	LOC51249	NM_016486	Hypothetical protein
H200019492	0.666	-1.5015	DGAT2	NM_032564	Diacylglycerol O-acyltransferase homolog 2 (mouse)
H200001691	0.666	-1.5015	PARVB	NM_013327	Parvin, beta
H200004761	0.666	-1.5015	SPRR1A	S73288	Small proline-rich protein SPRK [human, odontogenic keratocysts, mRNA Partial, 317 nt]
H200008109	0.666	-1.5015	FLJ32356	AK056918	Homo sapiens cDNA FLJ32356 fis, clone PROST2007974, weakly similar to ANTER-SPECIFIC PROLINE-RICH PR
H200005590	0.666	-1.5015	DKFZp761O132	NM_032298	Hypothetical protein DKFZp761O132
H300020662	0.666	-1.5015	ENSG00000164627		AMBIGUOUS
H200006297	0.666	-1.5015	LCP1	NM_002298	Lymphocyte cytosolic protein 1 (L-plastin)
H200016941	0.666	-1.5015	ATP6M	NM_015994	ATPase, H+ transporting, lysosomal (vacuolar proton pump)
H200016233	0.666	-1.5015	HRY	NM_005524	Hairy homolog (Drosophila)
H200003164	0.666	-1.5015		AK056052	Homo sapiens clone CDABP0036 mRNA sequence
H200012385	0.666	-1.5015	EDG4	NM_004720	Endothelial differentiation, lysophosphatidic acid G-protein-coupled receptor, 4
H200010040	0.666	-1.5015		AK023065	Homo sapiens cDNA FLJ13003 fis, clone NT2RP3000418
H200013840	0.666	-1.5015	BBX	AF052174	Homo sapiens clone 24630 mRNA sequence
H200018311	0.665	-1.5038	RANBP10	AK000686	Homo sapiens cDNA FLJ20679 fis, clone KAIA414
H200001808	0.665	-1.5038	KIAA1741	AB051528	KIAA1741 protein
H200001188	0.665	-1.5038	PIK3R1	M61906	Phosphoinositide-3-kinase, regulatory subunit, polypeptide 1 (p85 alpha)
H200012682	0.665	-1.5038	HOXA9	BC010023	Homeo box A9
H200015841	0.665	-1.5038	GALNT7	NM_017423	UDP-N-acetyl-alpha-D-galactosamine:polypeptide N-acetylgalactosaminyltransferase 7 (GalNAc-T7)
H300008061	0.665	-1.5038	ENSG00000166159		KERATIN TYPE I

Genes that are 1.4 fold down regulated in SUM1315-BP2 vs. SUM1315					
H200011863	0.665	-1.5038		M20919	Human DNA with a hepatitis B virus surface antigen (HBsAg) gene (complete cds) insertion
H200021179	0.665	-1.5038	PYGM	AK057547	Homo sapiens cDNA FLJ32985 fis, clone THYMU1000025, moderately similar to GLYCOGEN PHOSPHORYLASE, MU
H300002345	0.665	-1.5038			UNKNOWN
H200006519	0.664	-1.506	PALM	NM_002579	Paralemmin
H200018082	0.664	-1.506		AF248270	Homo sapiens gag-pro-pol precursor protein gene, partial cds
H200018246	0.664	-1.506		AL049263	Homo sapiens mRNA; cDNA DKFZp564F133 (from clone DKFZp564F133)
H200016179	0.664	-1.506		NM_018611	Homo sapiens hypothetical protein PRO1966 (PRO1966), mRNA
H200005924	0.664	-1.506	ARSE	NM_000047	Arylsulfatase E (chondrodysplasia punctata 1)
H200021041	0.664	-1.506	FLJ30934	AK055496	Homo sapiens cDNA FLJ30934 fis, clone FEBRA2007017, moderately similar to Homo sapiens TRAF4-associa
H200013377	0.664	-1.506	FLJ14871	NM_032854	Hypothetical protein FLJ14871
H200001858	0.664	-1.506	ALTE	NM_004729	Ac-like transposable element
H200005989	0.664	-1.506	AP3D1	NM_003938	Adaptor-related protein complex 3, delta 1 subunit
H200017914	0.664	-1.506	FLJ10595	NM_020117	Hypothetical protein FLJ10595
H200005092	0.663	-1.5083	SCYA11	NM_002986	Small inducible cytokine subfamily A (Cys-Cys), member 11 (eotaxin)
H200010360	0.663	-1.5083	INSM1	NM_002196	Insulinoma-associated 1
H200000882	0.663	-1.5083		AK026922	Homo sapiens cDNA: FLJ23269 fis, clone COL09533
H200004672	0.663	-1.5083	PB1	AF197569	Polybromo 1
H200003568	0.663	-1.5083	ZMPSTE24	NM_005857	Zinc metalloproteinase (STE24 homolog, yeast)
H200018905	0.663	-1.5083	DKFZP564D1378	NM_032124	Hypothetical protein DKFZp564D1378
H200017876	0.663	-1.5083	FLJ22686	AF418290	Hypothetical protein FLJ22686
H200002802	0.663	-1.5083	CDK2	NM_001798	Cyclin-dependent kinase 2
H200007509	0.662	-1.5106	P53AIP1	NM_022112	P53-regulated apoptosis-inducing protein 1

Genes that are 1.4 fold down regulated in SUM1315-BP2 vs. SUM1315					
H200020118	0.662	-1.5106	FLJ22427	NM_032223	Hypothetical protein FLJ22427
H200016945	0.662	-1.5106	KIAA1457	AB040890	KIAA1457 protein
H200017598	0.662	-1.5106	MRG	NM_052967	Mas-related G protein-coupled MRG
H200003977	0.662	-1.5106	F5	NM_000130	Coagulation factor V (proaccelerin, labile factor)
H200019944	0.662	-1.5106	KPNA1	NM_002264	Karyopherin alpha 1 (importin alpha 5)
H200003906	0.662	-1.5106	MAP3K3	NM_002401	Mitogen-activated protein kinase kinase kinase 3
H200009974	0.662	-1.5106		AK001225	Homo sapiens cDNA FLJ10363 fis, clone NT2RM2001312
H200007362	0.662	-1.5106	NESG1	NM_012337	Nasopharyngeal epithelium specific protein 1
H200004457	0.661	-1.5129		AL137270	Homo sapiens mRNA; cDNA DKFZp434G0614 (from clone DKFZp434G0614)
H200009296	0.661	-1.5129	FLJ22170	NM_025099	Hypothetical protein FLJ22170
H200016037	0.661	-1.5129		AF017336	Homo sapiens genomic clone X17/P1-68 encoding RNA which may be differentially expressed in individua
H300010248	0.661	-1.5129	ENSG00000181425		UNKNOWN
H200003307	0.661	-1.5129	MST4	NM_016542	Serine/threonine protein kinase MASK
H200001181	0.661	-1.5129	KIAA0731	AB018274	KIAA0731 protein
H200003655	0.661	-1.5129	TM4SF7	NM_003271	Transmembrane 4 superfamily member 7
H200020693	0.66	-1.5152		AK057352	Homo sapiens cDNA FLJ32790 fis, clone TESTI2002361
H200004921	0.66	-1.5152	KIAA1634	AB046854	KIAA1634 protein
H200013837	0.66	-1.5152	KIAA1268	AB033094	KIAA1268 protein
H200007058	0.66	-1.5152	CKS2	NM_001827	CDC28 protein kinase 2
H200020330	0.66	-1.5152	ODC-p	AY050638	Homo sapiens ornithine decarboxylase-like protein variant 6 mRNA, complete cds, alternatively splice
H200012893	0.66	-1.5152	MGC10772	NM_030567	Hypothetical protein MGC10772
H200004245	0.659	-1.5175		AL359654	Homo sapiens mRNA full length insert cDNA clone EUROIMAGE 196784
H200018575	0.659	-1.5175		AK025218	Homo sapiens cDNA: FLJ21565 fis, clone COL06463
H200015880	0.659	-1.5175	S100A14	NM_021039	S100 calcium binding protein A14 (calgizzarin)

Genes that are 1.4 fold down regulated in SUM1315-BP2 vs. SUM1315					
H200021068	0.659	-1.5175	PSIP1	NM_021144	PC4 and SFRS1 interacting protein 1
H200001227	0.659	-1.5175	TIMP2	AL110197	Homo sapiens mRNA; cDNA DKFZp586J021 (from clone DKFZp586J021)
H300015573	0.659	-1.5175	ENSG00000118526	NM_080805	ALPHA 1 TYPE XIII COLLAGEN ISOFORM 12. [Source:RefSeq;Acc:NM_080808]
H200016772	0.659	-1.5175	MAPK6	NM_002748	Mitogen-activated protein kinase 6
H200018495	0.659	-1.5175		AK024662	Homo sapiens cDNA: FLJ21009 fis, clone CAE04083
H200019665	0.659	-1.5175	MGC16179	NM_032766	Hypothetical protein MGC16179
H200005589	0.658	-1.5198	KIAA1511	AB040944	KIAA1511 protein
H200008796	0.658	-1.5198	SURF4	AK026646	Surfeit 4
H200020860	0.658	-1.5198	NNMT	AK055557	Homo sapiens cDNA FLJ30995 fis, clone HLUNG1000084
H200010010	0.658	-1.5198	FLJ20753	AB046860	Hypothetical protein FLJ20753
H200009642	0.658	-1.5198	ITGAV	NM_002210	Integrin, alpha V (vitronectin receptor, alpha polypeptide, antigen CD51)
H200010286	0.658	-1.5198		AK023489	Homo sapiens cDNA FLJ13427 fis, clone PLACE1002477
H200018135	0.658	-1.5198		AK022441	Homo sapiens cDNA FLJ12379 fis, clone MAMMA1002554
H200017958	0.657	-1.5221	KIAA1494	AB040927	KIAA1494 protein
H200020128	0.657	-1.5221	WASF2	NM_006990	WAS protein family, member 2
H200003206	0.657	-1.5221	FLJ11749	NM_024591	Hypothetical protein FLJ11749
H200020264	0.657	-1.5221	KIAA1887	AB067474	KIAA1887 protein
H200001157	0.657	-1.5221	MANBAL	AK026708	Mannosidase, beta A, lysosomal-like
H200006393	0.657	-1.5221	PLP2	NM_002668	Proteolipid protein 2 (colonic epithelium-enriched)
H200018624	0.657	-1.5221	BCL2L14; BCLG	AK026440	Homo sapiens cDNA: FLJ22787 fis, clone KAIA2156
H200007059	0.657	-1.5221	TNNI2	NM_003282	Troponin I, skeletal, fast
H200011672	0.657	-1.5221	ARHH	NM_004310	Ras homolog gene family, member H
H200000136	0.656	-1.5244	AFM	NM_001133	Afamin
H200019967	0.656	-1.5244	LOC91151	NM_033208	Similar to jerky (mouse) homolog-like

Genes that are 1.4 fold down regulated in SUM1315-BP2 vs. SUM1315					
H200020947	0.656	-1.5244	ZNF335; NIF1	AK054694	Homo sapiens cDNA FLJ30132 fis, clone BRACE1000166
H200016239	0.656	-1.5244	KDELR3	NM_006855	KDEL (Lys-Asp-Glu-Leu) endoplasmic reticulum protein retention receptor 3
H200010420	0.656	-1.5244	KIAA0552	NM_014731	KIAA0552 gene product
H200006299	0.656	-1.5244	F2	NM_000506	Coagulation factor II (thrombin)
H200002137	0.656	-1.5244	LCHN	AB032973	LCHN protein
H200019399	0.656	-1.5244	MGC39325	AK023658	Homo sapiens cDNA FLJ13596 fis, clone PLACE1009637
H200001634	0.656	-1.5244	FHL2	NM_001450	Four and a half LIM domains 2
H200009773	0.655	-1.5267		AK022343	Homo sapiens cDNA FLJ12281 fis, clone MAMMA1001745
H200009660	0.655	-1.5267	YKT6	BC007319	SNARE protein
H200000409	0.655	-1.5267	FGD1	NM_004463	Faciogenital dysplasia (Aarskog-Scott syndrome)
H200007249	0.655	-1.5267	PYY2	NM_021093	Peptide YY, 2 (seminalplasmin)
H200014211	0.655	-1.5267	EIF4G2	NM_001418	Eukaryotic translation initiation factor 4 gamma, 2
H200000225	0.655	-1.5267	IL8RB	NM_001557	Interleukin 8 receptor, beta
H200008787	0.655	-1.5267	BTN3A1	U90552	Butyrophilin, subfamily 3, member A1
H200000112	0.655	-1.5267	DLX2	NM_004405	Distal-less homeo box 2
H200000142	0.655	-1.5267	ADRA1D	NM_000678	Adrenergic, alpha-1D-, receptor
H200004989	0.655	-1.5267	FLJ20718	NM_017939	Hypothetical protein FLJ20718
H200004600	0.655	-1.5267	FLJ10718	NM_018192	Hypothetical protein FLJ10718
H200005581	0.654	-1.5291		AF339776	Homo sapiens clone IMAGE:1542282, mRNA sequence
H200021046	0.654	-1.5291	C14orf32	AK054650	Homo sapiens cDNA FLJ30088 fis, clone BNGH41000010
H200008628	0.654	-1.5291	KIAA0116	BC012831	KIAA0116 protein
H200012313	0.654	-1.5291	SPAM1	NM_003117	Sperm adhesion molecule 1 (PH-20 hyaluronidase, zona pellucida binding)
H300007567	0.654	-1.5291	ENSG00000180841		UNKNOWN
H200008882	0.654	-1.5291	FLJ20940	NM_032192	Hypothetical protein FLJ20940
H200002796	0.654	-1.5291	EIF4EL3	NM_004846	Eukaryotic translation initiation factor 4E-like 3
H200013100	0.654	-1.5291		AK023264	Homo sapiens cDNA FLJ13202 fis, clone NT2RP3004503

Genes that are 1.4 fold down regulated in SUM1315-BP2 vs. SUM1315					
H200001625	0.654	-1.5291	TDE2L	BC017085	Homo sapiens, clone MGC: 9709 IMAGE:3850147, mRNA, complete cds
H200020318	0.654	-1.5291	RNF32	BC015416	Homo sapiens, Similar to hypothetical protein DKFZp434C135, clone MGC:21976 IMAGE: 4395421, mRNA, com
H300007947	0.654	-1.5291	ENSG00000180741		ENVELOPE
H200020358	0.654	-1.5291	ALS2CR15	AB053316	Homo sapiens ALS2CR14 mRNA, complete cds
H200018552	0.654	-1.5291	HBLD2	AK025086	Homo sapiens cDNA: FLJ21433 fis, clone COL04232
H200003873	0.653	-1.5314	CDC7L1	NM_003503	CDC7 cell division cycle 7-like 1 (S. cerevisiae)
H200017325	0.653	-1.5314	IFI27	NM_005532	Interferon, alpha-inducible protein 27
H200001195	0.653	-1.5314	FLJ20886	BC016142	Hypothetical protein FLJ20886
H200000065	0.653	-1.5314	MPHOSPH1	NM_016195	M-phase phosphoprotein 1
H200006818	0.653	-1.5314	COX8	NM_004074	Cytochrome c oxidase subunit VIII
H200019515	0.653	-1.5314	IRF5	NM_002200	Interferon regulatory factor 5
H200007375	0.653	-1.5314		AK055022	Homo sapiens cDNA FLJ30460 fis, clone BRACE2009434
H300000461	0.653	-1.5314			UNKNOWN
H200018957	0.653	-1.5314	NBR2	NM_005821	NBR2
H300012121	0.653	-1.5314	ENSG00000148341		MAJOR HISTOCOMPATIBILITY COMPLEX, CLASS I, A PRECURSOR; HLA-A1 CLASS I ANTIGEN. [Source:RefSeq;Acc:NM_002116]
H300000268	0.653	-1.5314	ENSG00000178059		G90
H200008584	0.653	-1.5314	ASB2	AB056723	Ankyrin repeat and SOCS box-containing 2
H200013436	0.652	-1.5337	TBX4	NM_018488	T-box 4
H200004233	0.652	-1.5337	FLJ11175	NM_018349	Hypothetical protein FLJ11175
H200014206	0.652	-1.5337	CRABP2	NM_001878	Cellular retinoic acid binding protein 2
H200012686	0.652	-1.5337	KLHL10	AK057224	Homo sapiens cDNA FLJ32662 fis, clone TESTI1000064, weakly similar to Fugu rubripes sex comb on midl
H200003580	0.652	-1.5337	DKFZP564D206	BC008484	DKFZP564D206 protein
H200020244	0.652	-1.5337	ELA1	NM_001971	Elastase 1, pancreatic

Genes that are 1.4 fold down regulated in SUM1315-BP2 vs. SUM1315					
H200020869	0.652	-1.5337	FLJ11588	AK055449	Homo sapiens cDNA FLJ30887 fis, clone FEBRA2005036
H200002791	0.651	-1.5361	DKFZp667O2416	AK056427	Hypothetical protein DKFZp667O2416
H200003972	0.651	-1.5361	SLC26A2	NM_000112	Solute carrier family 26 (sulfate transporter), member 2
H300007874	0.651	-1.5361	ENSG00000176421		AMBIGUOUS
H200020845	0.651	-1.5361		AK055761	Homo sapiens cDNA FLJ31199 fis, clone KIDNE2000555
H200012769	0.65	-1.5385	TUB	AK022297	Homo sapiens cDNA FLJ12235 fis, clone MAMMA1001243
H200018709	0.65	-1.5385	MGC5457	NM_032633	Hypothetical protein MGC5457
H200011369	0.65	-1.5385	GFRA1	NM_005264	GDNF family receptor alpha 1
H200018430	0.65	-1.5385		AK022061	Homo sapiens cDNA FLJ11999 fis, clone HEMBB1001527
H300007810	0.65	-1.5385	ENSG00000181736		UNKNOWN
H200019787	0.65	-1.5385		BC009038	Homo sapiens, clone IMAGE:4179482, mRNA
H200015353	0.65	-1.5385	MGC4643	NM_032715	Hypothetical protein MGC4643
H200006242	0.65	-1.5385	USP14	NM_005151	Ubiquitin specific protease 14 (tRNA-guanine transglycosylase)
H200017413	0.65	-1.5385	SIX4	NM_017420	Sine oculis homeobox homolog 4 (Drosophila)
H200019451	0.65	-1.5385		AK023174	Homo sapiens cDNA FLJ13112 fis, clone NT2RP3002587
H200013353	0.65	-1.5385	LOC51135	NM_016123	Putative protein kinase NY-REN-64 antigen
H200001720	0.65	-1.5385	FLJ13868	NM_022744	Hypothetical protein FLJ13868
H200002066	0.649	-1.5408	LOC51242	NM_016471	Hypothetical protein
H200008149	0.649	-1.5408	ZFR	NM_016107	Zinc finger RNA binding protein
H200019017	0.649	-1.5408	KIAA0184	D80006	KIAA0184 protein
H200002760	0.649	-1.5408	C21orf108	AF231919	Chromosome 21 open reading frame 108
H200003801	0.649	-1.5408	CEP2	NM_007186	Centrosomal protein 2
H200002832	0.649	-1.5408	PRO2849	NM_022335	Hypothetical protein PRO2849
H200008140	0.649	-1.5408	KIAA1564	AB046784	KIAA1564 protein
H200007017	0.649	-1.5408	GK003	AF226046	GK003 protein
H200015811	0.648	-1.5432	LEP16	NM_032563	Epidermal differentiation complex protein like protein

Genes that are 1.4 fold down regulated in SUM1315-BP2 vs. SUM1315					
H200000492	0.648	-1.5432	FOLH1	NM_004476	Folate hydrolase (prostate-specific membrane antigen) 1
H200008629	0.648	-1.5432	HSPCB	BC016839	Homo sapiens, clone IMAGE:3888869, mRNA, partial cds
H200008575	0.648	-1.5432	MEF2A	NM_005587	MADS box transcription enhancer factor 2, polypeptide A (myocyte enhancer factor 2A)
H200001282	0.647	-1.5456	SLC7A11	NM_014331	Solute carrier family 7, (cationic amino acid transporter, y+ system) member 11
H200001216	0.647	-1.5456	HT010	NM_018471	Uncharacterized hypothalamus protein HT010
H200014808	0.647	-1.5456	WRB	NM_004627	Tryptophan rich basic protein
H200003313	0.647	-1.5456		AF070632	Homo sapiens clone 24405 mRNA sequence
H300009855	0.647	-1.5456	MGC30156	NM_152639	SIMILAR TO CAPICUA DROSOPHILA HOMOLOG
H200018326	0.646	-1.548	IBTK	AB037838	Homo sapiens mRNA for KIAA1417 protein, partial cds
H200011429	0.646	-1.548	KIAA1327	AB037748	KIAA1327 protein
H200019344	0.646	-1.548	ARD1	NM_003491	N-acetyltransferase, homolog of S. cerevisiae ARD1
H200018715	0.646	-1.548	P143	NM_032555	P143 protein
H200020478	0.645	-1.5504		AK057529	Homo sapiens cDNA FLJ32769 fis, clone TESTI2001894
H200020690	0.645	-1.5504	MGC33889	AK057361	Homo sapiens cDNA FLJ32799 fis, clone TESTI2002516, moderately similar to MELANOMA-ASSOCIATED ANTIGE
H200006626	0.645	-1.5504	p100	NM_014390	EBNA-2 co-activator (100kD)
H200014187	0.645	-1.5504	TCF7L2	BG681433	ESTs
H200005977	0.645	-1.5504	PRNP	NM_000311	Prion protein (p27-30) (Creutzfeld-Jakob disease, Gerstmann-Strausler-Scheinker syndrome, fatal fami
H200014950	0.645	-1.5504	KIAA1102	AB029025	KIAA1102 protein
H200017106	0.645	-1.5504	DIA1	NM_007326	Diaphorase (NADH) (cytochrome b-5 reductase)
H200004001	0.644	-1.5528	SENP7	AL136599	Sentrin/SUMO-specific protease
H200010139	0.644	-1.5528	AP4B1	NM_006594	Adaptor-related protein complex 4, beta 1 subunit

Genes that are 1.4 fold down regulated in SUM1315-BP2 vs. SUM1315					
H200004981	0.644	-1.5528	SCYA25	NM_005624	Small inducible cytokine subfamily A (Cys-Cys), member 25
H200012812	0.644	-1.5528	KIAA1388	AB037809	KIAA1388 protein
H300007286	0.644	-1.5528			UNKNOWN
H200005995	0.644	-1.5528	MAPKAPK2	NM_004759	Mitogen-activated protein kinase-activated protein kinase 2
H200020337	0.644	-1.5528	ACTRT1	BC014597	Homo sapiens, Similar to RIKEN cDNA 1700052K15 gene, clone MGC:26590 IMAGE:4825563, mRNA, complete c
H200001971	0.644	-1.5528	C20orf110	AL137597	Chromosome 20 open reading frame 110
H200005591	0.644	-1.5528		BC010635	Homo sapiens, clone IMAGE:3867347, mRNA, partial cds
H200019889	0.644	-1.5528	DKFZP434A0131	NM_018991	DKFZp434A0131 protein
H200017578	0.644	-1.5528	FLJ12387	NM_022822	Hypothetical protein FLJ12387 similar to kinesin light chain
H200019412	0.644	-1.5528		AK054947	Homo sapiens cDNA FLJ11527 fis, clone HEMBA1002558
H200010100	0.644	-1.5528	KIAA0935	AB023152	KIAA0935 protein
H200018697	0.643	-1.5552	LOC284912	BC001801	Homo sapiens, clone MGC:3170 IMAGE:3355513, mRNA, complete cds
H200016006	0.643	-1.5552	PMCHL1	AY008411	Pro-melanin-concentrating hormone-like 1
H200003063	0.643	-1.5552	FLJ25476	AK021842	Homo sapiens cDNA FLJ11780 fis, clone HEMBA1005931, weakly similar to ZINC FINGER PROTEIN 83
H200017715	0.643	-1.5552	LDLB	AB037802	Low density lipoprotein receptor defect B complementing
H200016595	0.643	-1.5552	POLA	NM_016937	Polymerase (DNA directed), alpha
H200020955	0.643	-1.5552	SYMPK	BC015979	Homo sapiens, clone IMAGE:3684744, mRNA, partial cds
H200005189	0.643	-1.5552	ATF7	NM_006856	Activating transcription factor 7
H200012217	0.642	-1.5576	AP2S1	NM_004069	Adaptor-related protein complex 2, sigma 1 subunit
H200018772	0.642	-1.5576		AL136306	Human DNA sequence from clone RP3-334F4 on chromosome 6 Contains ESTs, STSs and GSSs. Contains a LAM

Genes that are 1.4 fold down regulated in SUM1315-BP2 vs. SUM1315					
H200018026	0.642	-1.5576		AC004755	Homo sapiens chromosome 19, fosmid 37502
H200011857	0.642	-1.5576	RNAC	NM_005772	RNA cyclase homolog
H200001591	0.642	-1.5576	RPS20	AF113008	Ribosomal protein S20
H200008110	0.642	-1.5576	UBL3	NM_007106	Ubiquitin-like 3
H200018409	0.641	-1.5601		AK021461	Homo sapiens cDNA FLJ11399 fis, clone HEMBA1000655
H200020009	0.641	-1.5601	FLJ20699	AK025188	Homo sapiens cDNA: FLJ21535 fis, clone COL06131
H200019025	0.641	-1.5601	RPL17	AK027111	Homo sapiens cDNA: FLJ23458 fis, clone HSI07327
H200006501	0.641	-1.5601	MYH11	NM_022844	Myosin, heavy polypeptide 11, smooth muscle
H200019789	0.641	-1.5601	TUBB	NM_001069	Tubulin, beta polypeptide
H200004049	0.641	-1.5601	FLJ10199	NM_018022	Hypothetical protein FLJ10199
H200019004	0.641	-1.5601	CROC4	NM_006365	Transcriptional activator of the c-fos promoter
H200006323	0.641	-1.5601	PPP1R1A	NM_006741	Protein phosphatase 1, regulatory (inhibitor) subunit 1A
H300001873	0.641	-1.5601	ENSG00000174739		AMBIGUOUS
H200016342	0.641	-1.5601	FLJ14356	NM_030824	Hypothetical protein FLJ14356
H200004922	0.641	-1.5601	FBXO4	NM_018007	F-box only protein 4
H300007816	0.641	-1.5601			60S RIBOSOMAL L13
H200008478	0.641	-1.5601	CPB1	NM_001871	Carboxypeptidase B1 (tissue)
H200001769	0.64	-1.5625	RGS14	NM_006480	Regulator of G-protein signalling 14
H200019926	0.64	-1.5625	KDELR3	AL080113	Homo sapiens mRNA; cDNA DKFZp586K2322 (from clone DKFZp586K2322)
H200020571	0.64	-1.5625	BPAG1	BC016991	Homo sapiens, clone IMAGE:4400287, mRNA, partial cds
H200005786	0.64	-1.5625	KIAA1322	AB037743	KIAA1322 protein
H200016518	0.64	-1.5625	CYCL	NM_021031	Cytochrome c-like antigen
H200020744	0.64	-1.5625	LOC151234	AK056906	Homo sapiens cDNA FLJ32344 fis, clone PROST2006450, moderately similar to N-HYDROXYARYLAMINE SULFOTR
H200012857	0.64	-1.5625	GAS2	NM_005256	Growth arrest-specific 2
H200005325	0.639	-1.5649	LOC115509	BC014000	Homo sapiens, clone MGC:20208 IMAGE:3936339, mRNA, complete cds

Genes that are 1.4 fold down regulated in SUM1315-BP2 vs. SUM1315					
H200020104	0.639	-1.5649	RPL22	AF113701	Homo sapiens mRNA; cDNA DKFZp586E0524 (from clone DKFZp586E0524)
H200005633	0.639	-1.5649		AK021837	Homo sapiens cDNA FLJ11775 fis, clone HEMBA1005891
H200007077	0.638	-1.5674	HPS	NM_000195	Hermansky-Pudlak syndrome
H200021070	0.638	-1.5674		AK055394	Homo sapiens cDNA FLJ30832 fis, clone FEBRA2002009
H200011590	0.638	-1.5674	GYPA	NM_002099	Glycophorin A (includes MN blood group)
H200020531	0.638	-1.5674	DKFZP547L112	AL512723	Hypothetical protein DKFZp547L112
H200014275	0.638	-1.5674	FLJ12517	AK026908	Hypothetical protein FLJ12517
H300008556	0.638	-1.5674	ENSG00000126746	NM_138425	PUTATIVE C10 PROTEIN. [Source:SWISSPROT;Acc:Q99622]
H200017600	0.637	-1.5699	FLJ31265	AK055827	Homo sapiens cDNA FLJ31265 fis, clone KIDNE2006030, moderately similar to Gallus gallus syndesmos mR
H200019896	0.637	-1.5699	AAT1	AK055558	AAT1-alpha
H200007920	0.637	-1.5699	HSPC213	AK056145	Hypothetical protein
H200008496	0.637	-1.5699	LOC51068	NM_015938	CGI-07 protein
H200002943	0.637	-1.5699	PCBP4	NM_020418	Poly(rC) binding protein 4
H300021579	0.637	-1.5699	ENSG00000177286		TATA BINDING PROTEIN INTERACTING PROTEIN 49 KDA; RUVB (E COLI HOMOLOG)-LIKE 1. [Source:RefSeq;Acc:NM_003707]
H200010424	0.637	-1.5699	SNCB	NM_003085	Synuclein, beta
H300007478	0.637	-1.5699	ENSG00000181731		AMBIGUOUS
H200002855	0.637	-1.5699	CTH	NM_001902	Cystathionase (cystathionine gamma-lyase)
H200003681	0.637	-1.5699	KIAA0546	AB011118	KIAA0546 protein
H200014778	0.637	-1.5699	SARDH	AF095735	Sarcosine dehydrogenase
H300001770	0.637	-1.5699	ENSG00000178914	NM_173687	AMBIGUOUS
H300002846	0.637	-1.5699	ENSG00000167598		SIMILAR TO P14 GENE
H300002796	0.636	-1.5723	DEFB119	NM_153323	BETA-DEFENSIN 120 PRECURSOR (BETA-DEFENSIN 20) (DEFB-20). [Source:SWISSPROT;Acc:Q8N689]

Genes that are 1.4 fold down regulated in SUM1315-BP2 vs. SUM1315					
H200020267	0.636	-1.5723	MAX	BC013669	Homo sapiens, clone MGC: 18164 IMAGE:4155088, mRNA, complete cds
H200003604	0.636	-1.5723	FLJ10782	NM_018216	Hypothetical protein FLJ10782
H200020222	0.636	-1.5723	MAG	AF041410	Malignancy-associated protein
H200019414	0.636	-1.5723	8D6A	AK056039	Homo sapiens cDNA FLJ11573 fis, clone HEMBA1003376
H200008520	0.635	-1.5748	LOC51644	NM_016057	CGI-120 protein
H200019564	0.635	-1.5748	KAP4.2	NM_033062	Keratin associated protein 4.2
H200014540	0.635	-1.5748	LOC58525	AC007059	Hypothetical protein DKFZp547M136 similar to widely-interspaced zinc finger motifs
H200014089	0.635	-1.5748	CRADD	NM_003805	CASP2 and RIPK1 domain containing adaptor with death domain
H200002784	0.634	-1.5773	SRGAP1	AB037725	KIAA1304 protein
H200014186	0.634	-1.5773	PSG4	AK056754	Pregnancy specific beta-1-glycoprotein 4
H200019523	0.634	-1.5773	GHRL	NM_016362	Ghrelin precursor
H200002060	0.634	-1.5773	EML4	AK021782	Homo sapiens cDNA FLJ11720 fis, clone HEMBA1005293
H200019555	0.633	-1.5798	FLJ14816	NM_032845	Hypothetical protein FLJ14816
H200011839	0.633	-1.5798	KIAA0892	AB020699	KIAA0892 protein
H200021113	0.633	-1.5798		AK055547	Homo sapiens cDNA FLJ30985 fis, clone HHDPC2000462
H200004077	0.632	-1.5823	FLJ23462	AL136693	Duodenal cytochrome b
H200002713	0.632	-1.5823	DXS9879E	NM_006014	DNA segment on chromosome X (unique) 9879 expressed sequence
H200011606	0.632	-1.5823	COL6A1	NM_001848	Collagen, type VI, alpha 1
H200019011	0.632	-1.5823	RPL23	AK025200	Homo sapiens cDNA: FLJ21547 fis, clone COL06206
H200005943	0.631	-1.5848	ORC3L	NM_012381	Origin recognition complex, subunit 3-like (yeast)
H200000417	0.631	-1.5848	ABAT	NM_000663	4-aminobutyrate aminotransferase
H200019111	0.631	-1.5848	MGC2663	NM_024106	Hypothetical protein MGC2663
H200002997	0.631	-1.5848	FLJ11011	NM_018299	Hypothetical protein FLJ11011
H200000249	0.631	-1.5848	MYH2	NM_017534	Myosin, heavy polypeptide 2, skeletal muscle, adult
H200006013	0.631	-1.5848	KIAA0193	NM_014766	KIAA0193 gene product
H200008336	0.631	-1.5848	CLTC	NM_004859	Clathrin, heavy polypeptide (Hc)

Genes that are 1.4 fold down regulated in SUM1315-BP2 vs. SUM1315					
H200017759	0.631	-1.5848	C2orf9	NM_032309	Chromosome 2 open reading frame 9
H200005584	0.631	-1.5848	KIAA0318	AB002316	KIAA0318 protein
H200013864	0.631	-1.5848		AK024380	Homo sapiens cDNA FLJ14318 fis, clone PLACE3000402
H200020928	0.63	-1.5873		AK054825	Homo sapiens cDNA FLJ30263 fis, clone BRACE2002606
H200003018	0.63	-1.5873	SUGT1	AK054932	Homo sapiens cDNA FLJ30370 fis, clone BRACE2007832
H200008134	0.63	-1.5873	KIAA0931	AB023148	KIAA0931 protein
H200019552	0.63	-1.5873	FLJ14549	NM_032805	Hypothetical protein FLJ14549
H200018068	0.629	-1.5898	TSPYL3	AL121897	TSPY-like 3
H200018097	0.629	-1.5898	C21orf116	AF130090	Homo sapiens clone FLB9530 PRO2574 mRNA, complete cds
H200020721	0.629	-1.5898	WDR10	AK057162	Homo sapiens cDNA FLJ32600 fis, clone STOMA1000052
H200015370	0.629	-1.5898	CDIPT	NM_006319	CDP-diacylglycerol--inositol 3-phosphatidyltransferase (phosphatidylinositol synthase)
H200004453	0.629	-1.5898	MGC11115	AK057716	Hypothetical protein MGC11115
H200001995	0.628	-1.5924	SCYA13	NM_005408	Small inducible cytokine subfamily A (Cys-Cys), member 13
H200000878	0.628	-1.5924	TRAM	BC000687	Translocating chain-associating membrane protein
H200018277	0.628	-1.5924		AL110230	Homo sapiens mRNA; cDNA DKFZp564A0769 (from clone DKFZp564A0769)
H200016482	0.628	-1.5924	LOC153684	AK002146	Homo sapiens cDNA FLJ11284 fis, clone PLACE1009542
H200003638	0.628	-1.5924	ZNF26	NM_019591	Zinc finger protein 26 (KOX 20)
H200001219	0.628	-1.5924	JTB	NM_006694	Jumping translocation breakpoint
H200001631	0.628	-1.5924	PTGDS	NM_000954	Prostaglandin D2 synthase (21kD, brain)
H200017390	0.628	-1.5924	FLJ23024	NM_024936	Hypothetical protein FLJ23024
H200001703	0.627	-1.5949	SIRT5	NM_031244	Sirtuin silent mating type information regulation 2 homolog 5 (S. cerevisiae)
H200016475	0.627	-1.5949	KLRC3	NM_002261	Killer cell lectin-like receptor subfamily C, member 3

Genes that are 1.4 fold down regulated in SUM1315-BP2 vs. SUM1315					
H200020322	0.627	-1.5949		BC015216	Homo sapiens, clone IMAGE:3849975, mRNA, partial cds
H200016043	0.627	-1.5949		AL021327	Human DNA sequence from PAC 124O9 on chromosome 6q21. Contains DNAJ2 (HDJ1) like pseudogene, ESTs, S
H200014733	0.627	-1.5949	KIAA0240	D87077	KIAA0240 protein
H300004229	0.627	-1.5949	ENSG00000181775		AMBIGUOUS
H200019534	0.627	-1.5949	HEIL2	NM_032363	HEIL2 protein
H200019899	0.626	-1.5974	PPIA	NM_021130	Peptidylprolyl isomerase A (cyclophilin A)
H200020762	0.626	-1.5974		AK056720	Homo sapiens cDNA FLJ32158 fis, clone PLACE6000231
H200011281	0.626	-1.5974	Igk-V8	S65921	Anti-colorectal carcinoma light chain
H200001905	0.626	-1.5974	FLJ20154	NM_017787	Hypothetical protein FLJ20154
H200003400	0.626	-1.5974	FLJ13612	AF218006	Hypothetical protein FLJ13612
H200003556	0.626	-1.5974	SSSCA1	NM_006396	Sjogren's syndrome/ scleroderma autoantigen 1
H200018788	0.625	-1.6	LOC146489	X69637	H.sapiens mRNA sequence (16p11.2)
H200007404	0.625	-1.6	HK3	NM_002115	Hexokinase 3 (white cell)
H200008343	0.625	-1.6	VIAAT	AK055051	Homo sapiens cDNA FLJ30489 fis, clone BRAWH2000142, highly similar to Rattus norvegicus vesicular GA
H200001098	0.625	-1.6	KIAA0475	NM_014864	KIAA0475 gene product
H200013066	0.625	-1.6		AK055347	Homo sapiens cDNA FLJ30785 fis, clone FEBRA2000901
H200005504	0.625	-1.6	SNFT	NM_018664	Jun dimerization protein p21SNFT
H200008078	0.625	-1.6	BIRC4	NM_001167	Baculoviral IAP repeat-containing 4
H200015989	0.625	-1.6	<epsilon> IgE	S71435	Epsilon , IgE
H200016423	0.624	-1.6026	FLJ20837	NM_017964	Hypothetical protein FLJ20837
H200016564	0.624	-1.6026		AK024177	Homo sapiens cDNA FLJ14115 fis, clone MAMMA1001760
H200006940	0.624	-1.6026	CAPG	NM_001747	Capping protein (actin filament), gelsolin-like
H200018915	0.624	-1.6026	KIAA1133	AB051436	Novel C3HC4 type Zinc finger (ring finger)
H200005438	0.624	-1.6026	FLJ20330	NM_018988	Hypothetical protein

Genes that are 1.4 fold down regulated in SUM1315-BP2 vs. SUM1315					
H200000430	0.624	-1.6026	COL7A1	NM_000094	Collagen, type VII, alpha 1 (epidermolysis bullosa, dystrophic, dominant and recessive)
H200011918	0.624	-1.6026	TSC22	AK027071	Transforming growth factor beta-stimulated protein TSC-22
H200006462	0.623	-1.6051	LMNA	NM_005572	Lamin A/C
H200008631	0.623	-1.6051	KPNA5	NM_002269	Karyopherin alpha 5 (importin alpha 6)
H200017925	0.623	-1.6051		AK024198	Homo sapiens cDNA FLJ14136 fis, clone MAMMA1002744
H200021065	0.622	-1.6077		BC016831	Homo sapiens, clone IMAGE:4696935, mRNA
H200013283	0.622	-1.6077		AL390163	Homo sapiens mRNA; cDNA DKFZp761M1216 (from clone DKFZp761M1216)
H200005302	0.622	-1.6077	MGC14136	NM_032910	Hypothetical protein MGC14136
H200006630	0.622	-1.6077	MAPK14	NM_001315	Mitogen-activated protein kinase 14
H200004491	0.622	-1.6077	C8orf1	NM_004337	Chromosome 8 open reading frame 1
H200001502	0.621	-1.6103	C8FW	NM_025195	Phosphoprotein regulated by mitogenic pathways
H200010464	0.621	-1.6103	C11orf10	NM_014206	Chromosome 11 open reading frame 10
H200013068	0.621	-1.6103		AK025924	Homo sapiens cDNA: FLJ22271 fis, clone HRC03191
H200013921	0.621	-1.6103	KIAA0057	NM_012288	TRAM-like protein
H200013466	0.621	-1.6103	FLJ14721	NM_032829	Hypothetical protein FLJ14721
H200020816	0.62	-1.6129	PCCA	AK055982	Homo sapiens cDNA FLJ31420 fis, clone NT2NE2000369, moderately similar to PROPIONYL-COA CARBOXYLASE
H200021131	0.62	-1.6129	KIAA1908	AB067495	KIAA1908 protein
H200018786	0.62	-1.6129		AL356954	Human DNA sequence from clone RP11-520F24 on chromosome 13 Contains ESTs, STSs and GSSs. Contains an
H200013463	0.62	-1.6129	MGC15397	BC008043	Similar to RIKEN cDNA 5730578N08 gene
H200020704	0.62	-1.6129	FLJ32742	AK057304	Homo sapiens cDNA FLJ32742 fis, clone TESTI2001352
H200003923	0.62	-1.6129	COLEC12	NM_030781	Collectin sub-family member 12

Genes that are 1.4 fold down regulated in SUM1315-BP2 vs. SUM1315					
H200018738	0.62	-1.6129	FKSG29	AY014273	Homo sapiens FKSG29 (FKSG29) mRNA, complete cds
H200017551	0.62	-1.6129	HSPC111	NM_016391	Hypothetical protein
H200018667	0.619	-1.6155		AK027170	Homo sapiens cDNA: FLJ23517 fis, clone LNG04851
H200004346	0.619	-1.6155	PIP5K1B	BC013062	Homo sapiens, Similar to RIKEN cDNA 2900009I07 gene, clone MGC:17347 IMAGE:2901027, mRNA, complete c
H200004422	0.619	-1.6155	C8B	NM_000066	Complement component 8, beta polypeptide
H200001407	0.619	-1.6155	GPS2	NM_032442	G protein pathway suppressor 2
H300004609	0.619	-1.6155	ENSG00000181824	NM_153044	AMBIGUOUS
H200014562	0.618	-1.6181	FGFRL1	NM_021923	Fibroblast growth factor receptor-like 1
H300006471	0.618	-1.6181	ENSG00000176055	NM_005947	METALLOTHIONEIN-IB (MT-1B). [Source:SWISSPROT;Acc: P07438]
H200021098	0.618	-1.6181		AK057805	Homo sapiens cDNA FLJ25076 fis, clone CBL06117
H200013404	0.618	-1.6181	MGC11303	NM_032513	Hypothetical protein MGC11303 similar to Zink transporter 2
H200003224	0.618	-1.6181	UGCGL2	NM_020121	UDP-glucose ceramide glucosyltransferase-like 2
H200002214	0.617	-1.6207	TR	NM_006440	Thioredoxin reductase beta
H200003788	0.617	-1.6207	PPIL1	NM_016059	Peptidylprolyl isomerase (cyclophilin)-like 1
H200003970	0.617	-1.6207	KIAA0460	AK056707	KIAA0460 protein
H200001686	0.617	-1.6207	BCMP1	NM_031442	Brain cell membrane protein 1
H200006622	0.616	-1.6234	RCN2	NM_002902	Reticulocalbin 2, EF-hand calcium binding domain
H200020763	0.616	-1.6234	RHBDF1	AK056708	Homo sapiens cDNA FLJ32146 fis, clone PLACE5000115
H200016102	0.616	-1.6234	WNT1	NM_005430	Wingless-type MMTV integration site family, member 1
H200008483	0.616	-1.6234	RPS4Y	NM_001008	Ribosomal protein S4, Y-linked
H200017650	0.616	-1.6234	PRO2130	NM_018513	Hypothetical protein PRO2130
H200002439	0.616	-1.6234	CCT8	NM_006585	Chaperonin containing TCP1, subunit 8 (theta)
H200006401	0.616	-1.6234	HNRPA0	NM_006805	Heterogeneous nuclear ribonucleoprotein A0
H200012015	0.615	-1.626	KIAA0756	AB018299	KIAA0756 protein

Genes that are 1.4 fold down regulated in SUM1315-BP2 vs. SUM1315					
H200019955	0.615	-1.626	NXPH1	AB047362	Neurexophilin 1
H300007983	0.615	-1.626			UNKNOWN
H300003420	0.615	-1.626	ENSG00000174980		ADULT MALE TESTIS CDNA PRODUCT:
H200018406	0.614	-1.6287		AK021418	Homo sapiens cDNA FLJ11356 fis, clone HEMBA1000150, highly similar to Homo sapiens putative RNA heli
H200005929	0.614	-1.6287	CLIC1	NM_001288	Chloride intracellular channel 1
H200003003	0.614	-1.6287	MTPN	AK055660	Homo sapiens cDNA FLJ31098 fis, clone IMR321000219
H200007532	0.614	-1.6287		AK022141	Homo sapiens cDNA FLJ12079 fis, clone HEMBB1002458

Appendix C

Statistics From Gene Array

Genes that have a significant p-value and fold change						
Gene ID	**P-value**	**Fold Over .**	**Fold Under .**	**Common Name**	**GenBank ID**	**Description**
H200016940	7.22E-08	1.69		HBA1	NM_000558	Hemoglobin, alpha 1
H200004987	3.03E-06	0.71	-1.414	RAB27A	U38654	RAB27A, member RAS oncogene family
H300022783	5.86E-06	0.58	-1.739			HLA CLASS I HISTOCOMPATIBILITY ANTIGEN, ALPHA CHAIN G PRECURSOR (HLA G ANTIGEN). [Source:SWISSPROT;Acc:P 17693]
H300012121	1.05E-05	0.65	-1.531	ENSG00000 148341		MAJOR HISTOCOMPATIBILITY COMPLEX, CLASS I, A PRECURSOR; HLA-A1 CLASS I ANTIGEN. [Source:RefSeq;Acc:NM_00 2116]
H200010164	1.85E-05	0.71	-1.416	ZNF37A	BC015858	Zinc finger protein 37a (KOX 21)
H200009068	2.14E-05	2.39			AK023907	Homo sapiens cDNA FLJ13845 fis, clone THYRO1000815
H200010936	3.61E-05	2.53		CEBPB	NM_005194	CCAAT/enhancer binding protein (C/EBP), beta
H200007704	5.19E-05	0.70	-1.427	SFRS5	NM_006925	Splicing factor, arginine/ serine-rich 5
H200016941	6.72E-05	0.67	-1.502	ATP6M	NM_015994	ATPase, H+ transporting, lysosomal (vacuolar proton pump)
H200015989	0.0001	0.63	-1.6	<epsilon> IgE	S71435	Epsilon , IgE
H200010286	0.00013	0.66	-1.52		AK023489	Homo sapiens cDNA FLJ13427 fis, clone PLACE1002477
H200013377	0.00013	0.66	-1.506	FLJ14871	NM_032854	Hypothetical protein FLJ14871
H200006333	0.00016	0.54	-1.838	HYAL2	NM_033158	Hyaluronoglucosaminidase 2
H200008981	0.00017	2.22		MTBP	AK022122	Mdm2, transformed 3T3 cell double minute 2, p53 binding protein (mouse) binding protein, 104kD
H200003650	0.00017	2.11		B3GAT3	NM_012200	Beta-1,3-glucuronyltransferase 3 (glucuronosyltransferase I)
H200007507	0.00018	2.35		PSIP1	AK024516	Homo sapiens cDNA: FLJ20863 fis, clone ADKA01804
H200007824	0.00021	2.04		KIAA0489	AB007958	KIAA0489 protein
H200006115	0.00035	0.55	-1.828	OAT	NM_000274	Ornithine aminotransferase (gyrate atrophy)
H300007756	0.00036	1.74		ENSG00000 180906		60S RIBOSOMAL L21

Genes that have a significant p-value and fold change						
H200003604	0.00036	0.64	-1.572	FLJ10782	NM_018216	Hypothetical protein FLJ10782
H200008943	0.00038	1.74			AK021640	Homo sapiens cDNA FLJ11578 fis, clone HEMBA1003571
H200008973	0.00039	2.31		KIAA0889	AK022023	Homo sapiens cDNA FLJ11961 fis, clone HEMBB1001020, highly similar to Homo sapiens mRNA for KIAA0889
H200007409	0.0004	1.92		FOXH1	NM_003923	Forkhead box H1
H200008483	0.00043	0.62	-1.623	RPS4Y	NM_001008	Ribosomal protein S4, Y-linked
H200004833	0.00044	1.94			AK024874	Homo sapiens cDNA: FLJ21221 fis, clone COL00570
H300002231	0.00046	1.84		ENSG00000150051	NM_007350	PLECKSTRIN HOMOLOGY-LIKE DOMAIN, FAMILY A, MEMBER 1; PQ-RICH PROTEIN. [Source:RefSeq;Acc:NM_007350]
H200012058	0.00049	1.79		NNAT	NM_005386	Neuronatin
H200001414	0.00053	1.59		FLJ22316	NM_025080	Hypothetical protein FLJ22316
H300002466	0.00059	1.51		ENSG00000173727	NM_030970	UNKNOWN
H300022095	0.00061	0.67	-1.486	ENSG00000101639	NM_080426	GUANINE NUCLEOTIDE-BINDING PROTEIN G(S), ALPHA SUBUNIT (ADENYLATE CYCLASE-STIMULATING G ALPHA PROTEIN). [Source:SWISSPROT;Acc:P04895]
H200009162	0.00061	1.65			AK026914	Homo sapiens cDNA: FLJ23261 fis, clone COL05862
H200010939	0.00062	1.52			AK054999	Homo sapiens cDNA FLJ30437 fis, clone BRACE2009045
H200013938	0.00067	1.48		LIM	NM_006457	LIM protein (similar to rat protein kinase C-binding enigma)
H200017106	0.0007	0.65	-1.55	DIA1	NM_007326	Diaphorase (NADH) (cytochrome b-5 reductase)
H200010227	0.00071	1.65		BBC3	AF332558	Bcl-2 binding component 3
H200002346	0.00081	1.58		PROK1	NM_032414	Prokineticin 1 precursor
H200008936	0.00082	1.93		FLJ11467	AK057042	Hypothetical protein FLJ11467
H300007259	0.00086	1.42		ENSG00000173236	NM_030970	UNKNOWN
H300007061	0.00093	1.42		ENSG00000170507	NM_030970	UNKNOWN
H200000043	0.00095	1.46		RPL7	NM_000971	Ribosomal protein L7

Genes that have a significant p-value and fold change						
H200001794	0.00097	1.51		ABCF1	NM_001090	ATP-binding cassette, sub-family F (GCN20), member 1
H200004590	0.00106	1.48		MSH3	NM_002439	MutS homolog 3 (E. coli)
H200008111	0.00106	1.45		SLC24A1	NM_004727	Solute carrier family 24 (sodium/potassium/calcium exchanger), member 1
H200012165	0.00108	0.61	-1.639	SENP3	NM_015670	Sentrin/SUMO-specific protease 3
H200000588	0.0011	2.00		CHRNB2	NM_000748	Cholinergic receptor, nicotinic, beta polypeptide 2 (neuronal)
H200020358	0.00111	0.65	-1.529	ALS2CR15	AB053316	Homo sapiens ALS2CR14 mRNA, complete cds
H200010611	0.00111	1.71		PITPNM	NM_004910	Phosphatidylinositol transfer protein, membrane-associated
H200011653	0.00111	2.02		CORO1A	NM_007074	Coronin, actin binding protein, 1A
H200001758	0.00112	1.40		CGI-152	NM_020410	CGI-152 protein
H200021220	0.00114	1.66		KIAA1085	AB029008	KIAA1085 protein
H300019362	0.0012	1.71		ENSG00000177233		AMBIGUOUS
H200000707	0.00125	1.55		RRM1	NM_001033	Ribonucleotide reductase M1 polypeptide
H200009941	0.00125	1.51		KIAA0565	AB011137	KIAA0565 gene product
H200015857	0.00134	1.63		FLJ10902	NM_018266	Hypothetical protein FLJ10902
H200017250	0.00135	0.68	-1.475	GPR27	NM_018971	G protein-coupled receptor 27
H200003801	0.0015	0.65	-1.541	CEP2	NM_007186	Centrosomal protein 2
H300003154	0.00152	0.59	-1.684	ENSG00000149635		N27C7-4 PROTEIN. [Source:SPTREMBL;Acc:Q8WYQ3]
H200009067	0.00153	1.59		DAAM1	AK023892	Homo sapiens cDNA FLJ13830 fis, clone THYRO1000637
H300005257	0.00156	1.77		ENSG00000122795		AMBIGUOUS
H200000376	0.00159	1.95		GABRR1	NM_002042	Gamma-aminobutyric acid (GABA) receptor, rho 1
H200014471	0.00163	1.61			AK021987	Homo sapiens cDNA FLJ11925 fis, clone HEMBB1000354
H200009852	0.00167	1.54		ZFP93	NM_004234	Zinc finger protein 93 homolog (mouse)
H200011590	0.00169	0.64	-1.567	GYPA	NM_002099	Glycophorin A (includes MN blood group)
H300001804	0.00169	1.61		ENSG00000178672		60S RIBOSOMAL L21
H200002862	0.00172	1.80		P29	NM_015484	GCIP-interacting protein p29
H200014675	0.00181	1.62		CACNA1G	NM_018896	Calcium channel, voltage-dependent, alpha 1G subunit
H200007975	0.00185	1.45		SCML2	NM_006089	Sex comb on midleg-like 2 (Drosophila)

Genes that have a significant p-value and fold change						
H200007452	0.00186	1.49		SACS	NM_014363	Spastic ataxia of Charlevoix-Saguenay (sacsin)
H200009734	0.0019	1.57			AK021698	Homo sapiens cDNA FLJ11636 fis, clone HEMBA1004312
H200018135	0.00193	0.66	-1.52		AK022441	Homo sapiens cDNA FLJ12379 fis, clone MAMMA1002554
H200015400	0.00199	1.74		ZNF41	X60155	Zinc finger protein 41
H200004628	0.002	1.86		AKL3L	AK001553	Adenylate kinase 3 alpha like
H200002704	0.00201	1.88		PIGQ	NM_004204	Phosphatidylinositol glycan, class Q
H200012868	0.00201	1.53		SPAG9	NM_003971	Sperm associated antigen 9
H200010529	0.00205	0.68	-1.462	LCCP	NM_016201	Leman coiled-coil protein
H200000142	0.00217	0.66	-1.527	ADRA1D	NM_000678	Adrenergic, alpha-1D-, receptor
H200009835	0.00223	1.87			AK021973	Homo sapiens cDNA FLJ11911 fis, clone HEMBB1000141
H200015923	0.00225	0.71	-1.404		AL030997	Human DNA sequence from clone 1189K21 on chromosome Xq26.3-27.3. Contains two pseudogenes similar to
H200003922	0.00226	0.69	-1.46	ZF	NM_021212	HCF-binding transcription factor Zhangfei
H200007395	0.00226	1.41		KIAA0754	AB018297	KIAA0754 protein
H200000910	0.00231	1.57		RPL28	BC011582	Ribosomal protein L28
H200005553	0.00231	1.47		MDS009	NM_020234	X 009 protein
H300005024	0.00232	1.47		ENSG00000177571		LINE 1 REVERSE TRANSCRIPTASE HOMOLOG
H200003906	0.00233	0.66	-1.511	MAP3K3	NM_002401	Mitogen-activated protein kinase kinase kinase 3
H200006093	0.00235	0.54	-1.866	HSPA5	NM_005347	Heat shock 70kD protein 5 (glucose-regulated protein, 78kD)
H200015502	0.00236	1.61		HEY1	NM_012258	Hairy/enhancer-of-split related with YRPW motif 1
H200004555	0.00241	1.56		MGC11102	NM_032325	Hypothetical protein MGC11102
H200011432	0.00245	1.70		C10orf39	AL137551	Homo sapiens mRNA; cDNA DKFZp434D0720 (from clone DKFZp434D0720)
H200018104	0.00246	2.15			AF132204	Homo sapiens PRO2259 mRNA, complete cds
H200009055	0.00249	1.70		LOC90246	AK023635	Homo sapiens cDNA FLJ13573 fis, clone PLACE1008584
H200020623	0.0025	0.71	-1.404	LOC286090	AK057888	Homo sapiens cDNA FLJ25159 fis, clone CBR08036

Genes that have a significant p-value and fold change						
H300020265	0.00252	1.51		ENSG00000154240		RAB-LIKE PROTEIN 2A. [Source:SWISSPROT;Acc:Q9UBK7]
H200005851	0.00257	2.03		FLJ32549	AK057111	Homo sapiens cDNA FLJ32549 fis, clone SPLEN1000049
H200015630	0.00258	1.66		NTKL	AF297709	N-terminal kinase-like
H200010914	0.0026	1.55		GRTH	NM_013264	Gonadotropin-regulated testicular RNA helicase
H200008998	0.00269	1.64		MCM3AP; GANP; MAP80; KIAA0572	AK022303	Homo sapiens cDNA FLJ12241 fis, clone MAMMA1001274
H200015930	0.00273	1.42		H2BFA	BC001131	H2B histone family, member A
H200006955	0.00286	2.24		KIAA0153	NM_015140	KIAA0153 protein
H300007218	0.00286	1.41		ENSG00000168275	NM_030970	UNKNOWN
H200017464	0.00306	1.51		ALDH2	AK021975	Homo sapiens, clone MGC:9645 IMAGE:3922910, mRNA, complete cds
H200000244	0.00319	1.42		CRYM	NM_001888	Crystallin, mu
H200000992	0.00325	1.63		MRPL16	NM_017840	Mitochondrial ribosomal protein L16
H200012103	0.00359	1.89		PAPA-1	NM_031288	PAP-1 binding protein
H200010138	0.00373	1.49		APPL	NM_012096	Adaptor protein containing pH domain, PTB domain and leucine zipper motif
H200014562	0.00376	0.62	-1.618	FGFRL1	NM_021923	Fibroblast growth factor receptor-like 1
H200008972	0.00387	1.74			AK022016	Homo sapiens cDNA FLJ11954 fis, clone HEMBB1000888
H200017329	0.00393	1.51		KIAA0146	D63480	KIAA0146 protein
H200020980	0.00406	1.41			AF118079	Homo sapiens PRO1854 mRNA, complete cds
H200004078	0.00434	0.59	-1.689	KIAA1547	AB046767	KIAA1547 protein
H200000276	0.00435	1.42		GZMB	NM_004131	Granzyme B (granzyme 2, cytotoxic T-lymphocyte-associated serine esterase 1)
H200015692	0.00441	0.71	-1.416	CGI-96	NM_015703	CGI-96 protein
H200007003	0.00445	1.84		LOC162427	AK057409	Homo sapiens cDNA FLJ32847 fis, clone TESTI2003376
H200005885	0.00447	1.71		TCF1	M57732	Transcription factor 1, hepatic; LF-B1, hepatic nuclear factor (HNF1), albumin proximal factor
H200010654	0.00456	1.72		BIG1	NM_006421	Brefeldin A-inhibited guanine nucleotide-exchange protein 1
H200008391	0.00458	1.53		RPL11	NM_000975	Ribosomal protein L11

Genes that have a significant p-value and fold change						
H200009175	0.00464	1.51		dJ23O21.1	AL137181	Human DNA sequence from clone RP1-23O21 on chromosome 6. Contains an acidic calponin 3 (CNN3) pseudo
H300010310	0.00469	1.47		ENSG00000 171920		UNKNOWN
H200002223	0.0047	1.48		TXNRD1	NM_003330	Thioredoxin reductase 1
H200018619	0.00472	1.41			AK026385	Homo sapiens cDNA: FLJ22732 fis, clone HSI15880
H200000226	0.00475	1.76		FKBP4	NM_002014	FK506 binding protein 4 (59kD)
H300004506	0.00475	1.52		ENSG00000 179341		60S RIBOSOMAL L21
H200012056	0.00494	1.55		ARHGEF7	AK055476	Homo sapiens cDNA FLJ30914 fis, clone FEBRA2006368
H200001420	0.00495	1.98		DKFZp761N 1114	AK057733	Homo sapiens cDNA FLJ25004 fis, clone CBL00608
H200002708	0.00498	1.57		LAD1	NM_005558	Ladinin 1
H200011678	0.00501	1.45		IL17B	NM_014443	Interleukin 17B
H200019504	0.00506	0.61	-1.65		BC006119	Homo sapiens, clone IMAGE:3505629, mRNA, partial cds
H200001746	0.00514	1.51		RAPGEF1; C3G; GRF2	AK023760	Homo sapiens mRNA full length insert cDNA clone EUROIMAGE 1288997
H200007273	0.00515	1.44		LOC170394	BC011630	Homo sapiens, clone IMAGE:3957606, mRNA, partial cds
H200009063	0.00533	1.65			AK023838	Homo sapiens cDNA FLJ13776 fis, clone PLACE4000387
H200019276	0.00541	1.53		HSSOX6	NM_033326	Sox-6
H200008944	0.00542	1.91		GRB10	AK021643	Homo sapiens cDNA FLJ11581 fis, clone HEMBA1003598
H200012914	0.00552	1.52		ADCK4	BC013114	Homo sapiens, clone MGC: 16884 IMAGE:4342891, mRNA, complete cds
H200008024	0.00554	1.65		PDE4D	U02882	Phosphodiesterase 4D, cAMP-specific (phosphodiesterase E3 dunce homolog, Drosophila)
H200002760	0.00576	0.65	-1.541	C21orf108	AF231919	Chromosome 21 open reading frame 108
H200019725	0.00588	1.44			BC009051	Homo sapiens, clone MGC: 9852 IMAGE:3865825, mRNA, complete cds
H200001818	0.00637	1.58		GNA13	AK026902	Homo sapiens cDNA: FLJ23249 fis, clone COL04196

Genes that have a significant p-value and fold change						
H200009232	0.00673	0.67	-1.497	ECE1	NM_001397	Endothelin converting enzyme 1
H200007227	0.00682	1.51		KIAA1763	AB051550	KIAA1763 protein
H200000817	0.00684	1.54		AGT	NM_000029	Angiotensinogen (serine (or cysteine) proteinase inhibitor, clade A (alpha-1 antiproteinase, antitry
H200004630	0.00697	1.67		DTNBP1	AL136637	Dystrobrevin binding protein 1
H200016546	0.00699	1.68		FLJ20731	NM_017946	Hypothetical protein FLJ20731
H200020668	0.00704	0.60	-1.664		AK057513	Homo sapiens cDNA FLJ32951 fis, clone TESTI2008033
H200012126	0.0073	1.55		FARSLB	AK001025	Homo sapiens cDNA FLJ10163 fis, clone HEMBA1003568, weakly similar to 52 KD RO PROTEIN
H300008325	0.00734	1.42		ENSG00000 176122		60S RIBOSOMAL L30
H200011918	0.0074	0.62	-1.603	TSC22	AK027071	Transforming growth factor beta-stimulated protein TSC-22
H200015595	0.00744	1.42		MGC20781	NM_052935	Hypothetical protein MGC20781
H300005845	0.00753	1.44		ENSG00000 155066		UNKNOWN
H200008571	0.00755	1.48		SQSTM1	NM_003900	Sequestosome 1
H200003987	0.00767	1.51		KIAA0854	NM_014943	KIAA0854 protein
H200010245	0.00776	1.46		BTN3A2	NM_007047	Butyrophilin, subfamily 3, member A2
H200006987	0.00788	0.67	-1.497	SLC35A1	NM_006416	Solute carrier family 35 (CMP-sialic acid transporter), member 1
H200005112	0.00793	0.71	-1.408	NCK1	NM_006153	NCK adaptor protein 1
H200013957	0.00796	1.66		TLL2	AB023149	Tolloid-like 2
H200012008	0.0081	1.53		SECRET	NM_006998	Secretagogin
H200018281	0.0081	1.52			AL117475	Homo sapiens mRNA; cDNA DKFZp727C211 (from clone DKFZp727C211)
H200019552	0.0082	0.63	-1.587	FLJ14549	NM_032805	Hypothetical protein FLJ14549
H200015863	0.00823	1.51		SUCLG2	BC007716	Succinate-CoA ligase, GDP-forming, beta subunit
H200019259	0.00829	1.43		TTY9	NM_031927	Testis transcript Y 9
H200007106	0.00832	1.74		LOC51024	NM_016068	CGI-135 protein
H200021243	0.00833	0.60	-1.675	FLJ20244	BC018302	Homo sapiens, Similar to hypothetical protein FLJ20244, clone MGC: 17561 IMAGE:3463518, mRNA, complet
H200016301	0.00848	0.71	-1.406	WIT-1	NM_015855	Wilms tumor associated protein
H200006352	0.00848	1.51		SP2	D28588	Sp2 transcription factor

Genes that have a significant p-value and fold change						
H200020704	0.00853	0.62	-1.613	FLJ32742	AK057304	Homo sapiens cDNA FLJ32742 fis, clone TESTI2001352
H200009551	0.00858	1.67		CRR9	AK057095	Homo sapiens cDNA FLJ32533 fis, clone SMINT2000239
H200019748	0.00859	1.53		PCDHGC5	NM_018929	Protocadherin gamma subfamily C, 5
H200002119	0.00861	1.49		ADCY6	NM_015270	Adenylate cyclase 6
H200004358	0.00881	0.69	-1.447	ALPI	NM_001631	Alkaline phosphatase, intestinal
H200002983	0.00884	8.61		TRUB1	AK026721	Homo sapiens cDNA: FLJ23068 fis, clone LNG05562
H300006831	0.0089	1.42		ENSG00000176462		60S RIBOSOMAL L21
H200001011	0.00894	1.45		HSPC150	NM_014176	HSPC150 protein similar to ubiquitin-conjugating enzyme
H200001398	0.00898	1.52		MAN1	NM_014319	Integral inner nuclear membrane protein
H200018011	0.00904	0.71	-1.404	PWCR1	AF241255	Prader-Willi syndrome chromosome region 1
H200001373	0.00904	1.68		LOC129607	BC016969	Homo sapiens, clone IMAGE:4428577, mRNA, partial cds
H200000933	0.00907	1.49		OPCML	AF070577	Homo sapiens clone 24461 mRNA sequence
H200013078	0.00908	0.71	-1.416	RPS15	BC000085	Ribosomal protein S15
H200003924	0.00923	0.67	-1.499	CRSP6; CRSP77; DRIP80; TRAP80; FLJ10812	AK022156	Homo sapiens cDNA FLJ12094 fis, clone HEMBB1002607, highly similar to Homo sapiens vitamin D3 recept
H200008711	0.00937	1.50			AF161365	Homo sapiens HSPC102 mRNA, partial cds
H200020860	0.00941	0.66	-1.52	NNMT	AK055557	Homo sapiens cDNA FLJ30995 fis, clone HLUNG1000084
H200002695	0.00945	0.69	-1.449	MGC1203	NM_024296	Hypothetical protein MGC1203
H200012054	0.00945	1.53		KIAA1320	AB037741	KIAA1320 protein
H200012751	0.00963	1.88		LOC58509	AC005175	NY-REN-24 antigen
H200016229	0.00965	1.68		TPM4	NM_003290	Tropomyosin 4
H200000809	0.00975	1.44		MAP4K4	NM_004834	Mitogen-activated protein kinase kinase kinase kinase 4
H200002440	0.00995	0.49	-2.062	DKFZP434E2216	BC001043	Hypothetical protein DKFZp434E2216
H200009405	0.00995	1.51		FLJ22670	NM_025144	Hypothetical protein FLJ22670
H200008254	0.0101	1.47		HSD-3.1	AK055864	Hypothetical protein
H200002084	0.0102	0.68	-1.481	FLJ11320	BC001427	GDP-fucose transporter 1
H200005989	0.0102	0.66	-1.506	AP3D1	NM_003938	Adaptor-related protein complex 3, delta 1 subunit

Genes that have a significant p-value and fold change						
H200009711	0.0102	1.62			AK001151	Homo sapiens cDNA FLJ10289 fis, clone MAMMA1002319
H200015845	0.0104	0.71	-1.403	COL9A2	AK021682	Homo sapiens cDNA FLJ11620 fis, clone HEMBA1004138
H200004116	0.0104	1.71		PRDX5	NM_012094	Peroxiredoxin 5
H200005027	0.0104	1.76		ITGAX	NM_000887	Integrin, alpha X (antigen CD11C (p150), alpha polypeptide)
H200011364	0.0105	0.60	-1.669	KIAA0809	AK023824	KIAA0809 protein
H200003506	0.0105	1.41		PI4KII	AJ303098	Phosphatidylinositol 4-kinase type II
H200010993	0.0105	1.41		USP16	NM_006447	Ubiquitin specific protease 16
H200013876	0.0105	1.46		STAM	NM_003473	Signal transducing adaptor molecule (SH3 domain and ITAM motif) 1
H200000328	0.0107	1.66		BN51T	NM_001722	BN51 (BHK21) temperature sensitivity complementing
H200002252	0.0107	1.77		TRAPPC6B	AK056690	Homo sapiens cDNA: FLJ21784 fis, clone HEP00285
H200001366	0.011	1.67		CPNE4	BC014396	Copine IV
H200006483	0.0112	0.69	-1.456	TCF21	NM_003206	Transcription factor 21
H200000352	0.0112	1.64		MCC	NM_002387	Mutated in colorectal cancers
H200018406	0.0113	0.61	-1.629		AK021418	Homo sapiens cDNA FLJ11356 fis, clone HEMBA1000150, highly similar to Homo sapiens putative RNA heli
H200017413	0.0114	0.65	-1.538	SIX4	NM_017420	Sine oculis homeobox homolog 4 (Drosophila)
H200010917	0.0115	1.44		LOC283248	BC010608	Homo sapiens, clone IMAGE:4157757, mRNA, partial cds
H200007897	0.0116	1.45		WASL	AK023554	Homo sapiens cDNA FLJ13492 fis, clone PLACE1004284
H200014532	0.0116	1.79		FLJ12735	AJ314648	Hypothetical protein FLJ12735
H200007006	0.0117	0.71	-1.416	TAF11	NM_005643	TAF11 RNA polymerase II, TATA box binding protein (TBP)-associated factor, 28 kD
H200001994	0.0117	1.59		FLJ14784	NM_032839	Hypothetical protein FLJ14784
H200005995	0.0118	0.64	-1.553	MAPKAPK2	NM_004759	Mitogen-activated protein kinase-activated protein kinase 2
H200003893	0.0118	1.52		ZNF75	S67970	Zinc finger protein 75 (D8C6)
H200006712	0.012	1.63		RIL	AF153882	LIM domain protein

Genes that have a significant p-value and fold change						
H200021031	0.0122	1.50		RPL23AP7; RPL23AL1; bA395L14.9	X92108	H.sapiens mRNA for subtelomeric repeat sequence
H200012055	0.0123	1.44		RES4-25	AF040965	Gene near HD on 4p16.3 with homology to hypothetical S. pombe gene
H200010337	0.0124	0.60	-1.658	PAX6	NM_001604	Paired box gene 6 (aniridia, keratitis)
H200005526	0.0124	1.65		TLR2	NM_003264	Toll-like receptor 2
H300008319	0.0126	1.91		ENSG00000173250	NM_130387	ANKYRIN REPEAT AND SOCS BOX CONTAINING PROTEIN 14 (ASB-14). [Source:SWISSPROT;Acc:Q8WXK2]
H200019393	0.013	0.67	-1.499	EXOSC6; p11; EAP4; MTR3; Mtr3p; hMtr3p	AK024276	Homo sapiens clone TA40 untranslated mRNA, complete sequence
H200003829	0.0131	0.69	-1.451	UGDH	NM_003359	UDP-glucose dehydrogenase
H200015834	0.0131	1.49		MGC3113	NM_024035	Hypothetical protein MGC3113
H200013284	0.0132	1.43		PRO2834	NM_018542	Hypothetical protein PRO2834
H200001131	0.0134	1.46		MEL	NM_005370	Mel transforming oncogene (derived from cell line NK14)-RAB8 homolog
H200013953	0.0134	1.41		BACH1	NM_001186	BTB and CNC homology 1, basic leucine zipper transcription factor 1
H200001367	0.0136	1.54		KIAA0574	AB011146	KIAA0574 protein
H200010439	0.0136	1.66		DKFZp313N0621	AK056593	Homo sapiens cDNA FLJ32031 fis, clone NTONG2000107
H200012608	0.0136	1.54		CLECSF5	NM_013252	C-type (calcium dependent, carbohydrate-recognition domain) lectin, superfamily member 5
H200016856	0.0137	0.68	-1.475	TEX15	NM_031271	Testis expressed sequence 15
H200005239	0.0139	1.51		MCM2	NM_004526	MCM2 minichromosome maintenance deficient 2, mitotin (S. cerevisiae)
H200009407	0.0139	1.47			AK021454	Homo sapiens cDNA FLJ11392 fis, clone HEMBA1000575
H200005770	0.014	1.87		ADM2	BC012864	Homo sapiens, clone IMAGE:3882589, mRNA
H200001999	0.0141	0.69	-1.441	RAD51C	NM_058216	RAD51 homolog C (S. cerevisiae)
H200003670	0.0142	1.47		C20orf44	NM_018244	Chromosome 20 open reading frame 44
H200005262	0.0142	1.50		H105E3	NM_015922	NAD(P) dependent steroid dehydrogenase-like; H105e3

Genes that have a significant p-value and fold change						
H200001036	0.0143	3.00		CL25022	NM_015702	Hypothetical protein
H200007259	0.0143	1.49		KIAA1365	NM_020794	Densin-180
H200004589	0.0144	0.69	-1.449		AK054729	Homo sapiens cDNA FLJ30167 fis, clone BRACE2000743
H200007977	0.0144	0.49	-2.041	UCH37	NM_015984	Ubiquitin C-terminal hydrolase UCH37
H200003998	0.0144	1.73		KIAA1165	AB032991	Hypothetical protein KIAA1165
H200005573	0.0144	1.48		CALB1	NM_004929	Calbindin 1, (28kD)
H200005222	0.0145	1.51		FLJ32384	AK056946	Homo sapiens cDNA FLJ32384 fis, clone SKMUS1000104, weakly similar to Homo sapiens mRNA for HEXIM1 p
H200006459	0.0145	1.48		ADORA1	NM_000674	Adenosine A1 receptor
H200015880	0.0146	0.66	-1.517	S100A14	NM_021039	S100 calcium binding protein A14 (calgizzarin)
H200003816	0.0146	2.34		FSD1	NM_024333	Fibronectin type 3 and SPRY domain-containing protein
H200001468	0.0148	1.59		MAZ	NM_002383	MYC-associated zinc finger protein (purine-binding transcription factor)
H200020445	0.0148	1.46		PC4	NM_006713	Activated RNA polymerase II transcription cofactor 4
H200015401	0.0151	1.45		PTP4A1	NM_003463	Protein tyrosine phosphatase type IVA, member 1
H200000006	0.0154	1.94		FECH	NM_000140	Ferrochelatase (protoporphyria)
H200010315	0.0154	1.84		ATP5G2	NM_005176	ATP synthase, H+ transporting, mitochondrial F0 complex, subunit c (subunit 9), isoform 2
H200017325	0.0155	0.65	-1.531	IFI27	NM_005532	Interferon, alpha-inducible protein 27
H200010242	0.0156	0.68	-1.479	CTSW	NM_001335	Cathepsin W (lymphopain)
H200001749	0.0156	1.41		CASP7	NM_033339	Caspase 7, apoptosis-related cysteine protease
H300007816	0.0157	0.64	-1.56			60S RIBOSOMAL L13
H200004945	0.0158	0.71	-1.418	M160	NM_033330	Scavenger receptor cysteine-rich type 1 protein M160 precursor
H200010402	0.0158	0.70	-1.431	PC	NM_000920	Pyruvate carboxylase
H200005586	0.0161	0.53	-1.89	RGS11	NM_003834	Regulator of G-protein signalling 11
H200005346	0.0162	1.53		ZNF175	BC007778	Homo sapiens, Similar to zinc finger protein 175, clone MGC:12651 IMAGE: 4301632, mRNA, complete cds
H300008132	0.0164	0.52	-1.927	ENSG00000180898		PEPTIDYL PROLYL CIS TRANS ISOMERASE EC_5.2.1.8 PPIASE ROTAMASE CYCLOPHILIN

Genes that have a significant p-value and fold change						
H200009296	0.0166	0.66	-1.513	FLJ22170	NM_025099	Hypothetical protein FLJ22170
H200005549	0.0167	1.74		ATP5H	NM_006356	ATP synthase, H+ transporting, mitochondrial F0 complex, subunit d
H200007571	0.0171	1.48		FLJ12606	NM_024804	Hypothetical protein FLJ12606
H200005653	0.0175	1.68		LOC90701	NM_033280	Similar to signal peptidase complex (18kD)
H200011358	0.0177	1.98		MGC2647	AK057106	Homo sapiens, clone MGC: 14381 IMAGE:4299817, mRNA, complete cds
H200004229	0.0178	1.51		LOC286075	AK055198	Homo sapiens, Similar to zinc finger protein 30, clone MGC:10201 IMAGE: 3910185, mRNA, complete cds
H200002111	0.0179	1.43		ENTPD6	NM_001247	Ectonucleoside triphosphate diphosphohydrolase 6 (putative function)
H200002416	0.0181	0.57	-1.742	FLJ10773	NM_018212	Likely ortholog of mouse NPC derived proline rich protein 1
H200004927	0.0181	0.70	-1.431	FLJ11006	NM_018298	Hypothetical protein FLJ11006
H200007082	0.0181	0.68	-1.466	LOC51604	NM_015937	CGI-06 protein
H200009500	0.0181	1.53		GAS5	AK025846	Growth arrest-specific 5
H200015616	0.0181	1.56		FLJ22479	AK027620	Hypothetical protein FLJ22479
H200000281	0.0182	1.51		TACR1	NM_001058	Tachykinin receptor 1
H200015214	0.0182	1.52		FBXL11	NM_012308	F-box and leucine-rich repeat protein 11
H200018635	0.0182	1.54			AK026699	Homo sapiens cDNA: FLJ23046 fis, clone LNG02491
H200001907	0.0183	1.75		ZNF147	AK024597	Homo sapiens cDNA: FLJ20944 fis, clone ADSE01780
H200004254	0.0186	1.70			AP001660	Homo sapiens genomic DNA, chromosome 21q, section 4/105
H200015698	0.0188	0.68	-1.475	PCDHA7	NM_018910	Protocadherin alpha 7
H200018624	0.0189	0.66	-1.522	BCL2L14; BCLG	AK026440	Homo sapiens cDNA: FLJ22787 fis, clone KAIA2156
H200002015	0.0192	1.48		CTSF	NM_003793	Cathepsin F
H200002878	0.0193	0.59	-1.698	CXorf6	NM_005491	Chromosome X open reading frame 6
H200011612	0.0193	1.46		KIAA0515	AB011087	KIAA0515 protein
H200019759	0.0194	0.70	-1.431	LOC85415	NM_033103	Rhophilin-like protein
H200003252	0.0194	1.68		FLJ32810	AK023666	Homo sapiens cDNA FLJ13604 fis, clone PLACE1010401
H200019789	0.0195	0.64	-1.56	TUBB	NM_001069	Tubulin, beta polypeptide

Genes that have a significant p-value and fold change						
H200016928	0.0196	1.41			AC005587	Homo sapiens PAC clone RP5-988G15 from 7q33-q35
H200007024	0.0197	0.71	-1.418	LOXL2	NM_002318	Lysyl oxidase-like 2
H200010347	0.0197	1.50		EPOR	NM_000121	Erythropoietin receptor
H200012799	0.0197	1.58		BCAS1	NM_003657	Breast carcinoma amplified sequence 1
H200004439	0.0198	2.89		MGC15887	BC009447	Homo sapiens, clone MGC: 15887 IMAGE:3530481, mRNA, complete cds
H200003191	0.0199	1.64		TMEFF2	AL157430	Transmembrane protein with EGF-like and two follistatin-like domains 2
H200010619	0.0199	1.74		CNGB1	NM_001297	Cyclic nucleotide gated channel beta 1
H200012030	0.0199	1.64		SIGLEC5	NM_003830	Sialic acid binding Ig-like lectin 5
H200010396	0.0201	0.69	-1.449	TRADD	NM_003789	TNFRSF1A-associated via death domain
H200009121	0.0201	1.48		LOC91948	AK025311	Homo sapiens cDNA: FLJ21658 fis, clone COL08688
H200009071	0.0202	1.60		FLJ13885	NM_025016	Hypothetical protein FLJ13885
H200013561	0.0203	0.58	-1.727	ABL1	NM_005157	V-abl Abelson murine leukemia viral oncogene homolog 1
H200002886	0.0204	1.93		C17orf31	AB018275	Chromosome 17 open reading frame 31
H200008728	0.0204	1.64		KIAA0738	AF119896	Homo sapiens PRO2751 mRNA, complete cds
H200000708	0.0206	2.15		MMP13	NM_002427	Matrix metalloproteinase 13 (collagenase 3)
H200004385	0.0209	1.71		MPP3	NM_001932	Membrane protein, palmitoylated 3 (MAGUK p55 subfamily member 3)
H200015866	0.0209	1.77		DDAH2	NM_013974	Dimethylarginine dimethylaminohydrolase 2
H300006167	0.0212	1.87		ENSG00000 170628	NM_173497	SMAD UBIQUITINATION REGULATORY FACTOR EC_6.3.2.- UBIQUITIN LIGASE SMAD SPECIFIC E3 UBIQUITIN LIGASE
H200009877	0.0214	1.78		HTR2A	NM_000621	5-hydroxytryptamine (serotonin) receptor 2A
H200003765	0.0217	1.62		LOC55893	NM_018660	Papillomavirus regulatory factor PRF-1
H200017232	0.0217	1.76		SEC14L2	NM_012429	SEC14-like 2 (S. cerevisiae)
H200002997	0.022	0.63	-1.585	FLJ11011	NM_018299	Hypothetical protein FLJ11011
H200001059	0.0221	1.97		USP20	NM_006676	Ubiquitin specific protease 20
H200011650	0.0221	1.42		SPUF	NM_013349	Secreted protein of unknown function
H200011646	0.0222	0.49	-2.062	KCTD12	BC013764	Homo sapiens clone 24775 mRNA sequence

Genes that have a significant p-value and fold change						
H200008368	0.0225	1.56			U22172	Human DNA damage repair and recombination protein RAD52 pseudogene mRNA, partial cds
H200011172	0.0226	0.70	-1.433	EMCN	AL133118	Homo sapiens mRNA; cDNA DKFZp586N0121 (from clone DKFZp586N0121)
H200006806	0.0228	1.54		NTS	NM_006183	Neurotensin
H200009298	0.0228	1.45			AK024152	Homo sapiens cDNA FLJ14090 fis, clone MAMMA1000264
H200001515	0.0229	1.80		PICALM	NM_007166	Phosphatidylinositol binding clathrin assembly protein
H200009207	0.0231	1.40		CD58	AK026834	Homo sapiens cDNA: FLJ23181 fis, clone LNG11094
H200010362	0.0232	1.40		MUC1	J05582	Mucin 1, transmembrane
H200018587	0.0232	1.45			AK025325	Homo sapiens cDNA: FLJ21672 fis, clone COL09025
H200006370	0.0233	0.70	-1.422	CBX1	NM_006807	Chromobox homolog 1 (HP1 beta homolog Drosophila)
H200000118	0.0234	0.43	-2.32	TCF15	NM_004609	Transcription factor 15 (basic helix-loop-helix)
H200002214	0.0234	0.62	-1.621	TR	NM_006440	Thioredoxin reductase beta
H200001423	0.0234	1.58		PITPNB	NM_012399	Phosphotidylinositol transfer protein, beta
H200018140	0.0234	1.42		SLC26A2	AK025078	Homo sapiens cDNA: FLJ21425 fis, clone COL04162
H200005629	0.0235	1.46		DNCI2	AK055491	Dynein, cytoplasmic, intermediate polypeptide 2
H200007722	0.0237	0.70	-1.42	VMD2	AF052095	Homo sapiens clone 23911 mRNA sequence
H200007156	0.0238	1.47			AK054652	Homo sapiens cDNA FLJ30090 fis, clone BNGH41000015
H200016602	0.0238	1.44		FLJ20371	NM_017791	Hypothetical protein FLJ20371
H200008158	0.024	0.55	-1.808	FLJ12619	NM_030939	Hypothetical protein FLJ12619
H200018317	0.0243	0.67	-1.488		AK000834	Homo sapiens cDNA FLJ20827 fis, clone ADKA03543
H200005590	0.0244	0.67	-1.502	DKFZp761O 132	NM_032298	Hypothetical protein DKFZp761O132
H200010845	0.0245	1.67		MGC4766	NM_031451	Hypothetical protein MGC4766 similar to testis specific protein TES101RP
H200000896	0.0246	0.67	-1.486	VAV2	NM_003371	Vav 2 oncogene
H200016102	0.0247	0.62	-1.623	WNT1	NM_005430	Wingless-type MMTV integration site family, member 1

Genes that have a significant p-value and fold change						
H200008940	0.0249	0.53	-1.873	FLJ11556	NM_024964	Hypothetical protein FLJ11556
H200013472	0.025	0.68	-1.473	CPA5	AF384667	Homo sapiens carboxypeptidase A5 mRNA, complete cds
H200011008	0.025	1.42		LDHC	NM_002301	Lactate dehydrogenase C
H200020244	0.0251	0.65	-1.534	ELA1	NM_001971	Elastase 1, pancreatic
H200007250	0.0255	1.64		EMK1	NM_017490	ELKL motif kinase
H200016992	0.0257	0.69	-1.458	PCYT1A	NM_005017	Phosphate cytidylyltransferase 1, choline, alpha isoform
H200002273	0.0263	1.53		LOC93081	AF070559	Homo sapiens, Similar to RIKEN cDNA 1700029F09 gene, clone MGC:26637 IMAGE:4825712, mRNA, complete c
H200008881	0.0264	1.48		C20orf177	AL137442	Chromosome 20 open reading frame 177
H200010641	0.0264	1.47		TITF1	AK027147	Homo sapiens cDNA: FLJ23494 fis, clone LNG01885
H200002890	0.0265	0.61	-1.647	TIP39	NM_012143	Tuftelin-interacting protein
H200003556	0.0267	0.63	-1.597	SSSCA1	NM_006396	Sjogren's syndrome/ scleroderma autoantigen 1
H200012613	0.027	1.52		LOC148066	BC017592	Homo sapiens, clone MGC: 27006 IMAGE:4828408, mRNA, complete cds
H200020953	0.0271	0.69	-1.447	ODF3	AB067774	Homo sapiens mRNA for h-SHIPPO 1, complete cds
H200003915	0.0273	1.63		TNFAIP6	NM_007115	Tumor necrosis factor, alpha-induced protein 6
H200014214	0.0275	0.44	-2.257	UBC	M26880	Ubiquitin C
H200004205	0.0276	1.50		GNG4	NM_004485	Guanine nucleotide binding protein 4
H200013908	0.0277	1.42		LOC158402	AK056358	Homo sapiens cDNA FLJ31796 fis, clone NT2RI2008841
H200006204	0.028	0.67	-1.493	PCK2	NM_004563	Phosphoenolpyruvate carboxykinase 2 (mitochondrial)
H200016162	0.0281	1.43		TNFRSF10A	NM_003844	Tumor necrosis factor receptor superfamily, member 10a
H200019711	0.0282	0.69	-1.46	MGC16279	NM_032916	Hypothetical protein MGC16279
H200017381	0.0284	1.46		PRO0255	NM_014124	PRO0255 protein
H200020164	0.0285	0.69	-1.451	ANXA2P1	M62896	Annexin A2 pseudogene 1
H200001842	0.0285	2.28		KIAA1040	AB028963	KIAA1040 protein
H200013379	0.0285	1.41		KIAA1602	AB046822	KIAA1602 protein
H200003080	0.0286	1.61		DKFZp761N 0624	NM_032295	Hypothetical protein DKFZp761N0624

Genes that have a significant p-value and fold change						
H200018786	0.0294	0.62	-1.613		AL356954	Human DNA sequence from clone RP11-520F24 on chromosome 13 Contains ESTs, STSs and GSSs. Contains an
H200018514	0.0294	1.41			AK024897	Homo sapiens cDNA: FLJ21244 fis, clone COL01174
H200002158	0.0295	1.42		PER3	NM_016831	Period homolog 3 (Drosophila)
H200010671	0.0295	1.52		FLJ22729	NM_024683	Hypothetical protein FLJ22729
H200015100	0.0297	1.52		RPIB9	AK055233	Homo sapiens cDNA FLJ30671 fis, clone FCBBF1000687, moderately similar to Mus musculus Rap2 interact
H200016392	0.0299	0.70	-1.433	FLJ13262	NM_024914	Hypothetical protein FLJ13262
H200000797	0.0299	1.41		NLK	NM_016231	Nemo-like kinase
H200005626	0.03	1.45		LOC221061	AL050367	Homo sapiens mRNA; cDNA DKFZp564A026 (from clone DKFZp564A026)
H200000492	0.0302	0.65	-1.543	FOLH1	NM_004476	Folate hydrolase (prostate-specific membrane antigen) 1
H200001098	0.0302	0.63	-1.6	KIAA0475	NM_014864	KIAA0475 gene product
H200020577	0.0303	0.69	-1.441	MRGX2	NM_054030	Homo sapiens G protein-coupled receptor MRGX2 (MRGX2), mRNA
H200003368	0.0304	1.43		NEK7	AL080111	Homo sapiens mRNA; cDNA DKFZp586G2222 (from clone DKFZp586G2222)
H300006428	0.0305	1.52		ENSG00000175051		OLFACTORY RECEPTOR (FRAGMENT). [Source:SPTREMBL;Acc:Q96R28]
H200003980	0.0306	0.69	-1.447	FLJ23186	NM_024616	Hypothetical protein FLJ23186
H200006198	0.0307	0.60	-1.669	PIGC	NM_002642	Phosphatidylinositol glycan, class C
H200001467	0.0307	1.98		FGB	NM_005141	Fibrinogen, B beta polypeptide
H200008110	0.0309	0.64	-1.558	UBL3	NM_007106	Ubiquitin-like 3
H200020419	0.0309	0.68	-1.462	LOC286334	AJ420454	Homo sapiens mRNA full length insert cDNA clone EUROIMAGE 1517766
H200001416	0.0309	1.46		MAD1L1	NM_003550	MAD1 mitotic arrest deficient-like 1 (yeast)
H200006654	0.0312	0.39	-2.584	ST5	NM_005418	Suppression of tumorigenicity 5
H200003268	0.0313	1.41		ARV1	NM_022786	Likely ortholog of yeast ARV1

Genes that have a significant p-value and fold change						
H200017759	0.0314	0.63	-1.585	C2orf9	NM_032309	Chromosome 2 open reading frame 9
H200000465	0.0314	1.43		CD1D	NM_001766	CD1D antigen, d polypeptide
H200020012	0.0314	1.55			AL353132	Human DNA sequence from clone RP11-189G24 on chromosome 20. Contains a cytochrome B5 (CYB5) pseudoge
H200014980	0.0317	0.70	-1.427	ARHB	NM_004040	Ras homolog gene family, member B
H200007307	0.0319	1.56		GPR133	AL162032	Homo sapiens mRNA; cDNA DKFZp434B1272 (from clone DKFZp434B1272); partial cds
H200014098	0.032	1.80		BNIP2	NM_004330	BCL2/adenovirus E1B 19kD interacting protein 2
H200004929	0.0322	1.44		BACE	NM_012104	Beta-site APP-cleaving enzyme
H200009575	0.0324	1.48		LOC116064	AK056809	Homo sapiens cDNA FLJ32247 fis, clone PROST1000120
H200012313	0.0328	0.65	-1.529	SPAM1	NM_003117	Sperm adhesion molecule 1 (PH-20 hyaluronidase, zona pellucida binding)
H200000685	0.0329	1.59		OXTR	NM_000916	Oxytocin receptor
H200004422	0.0333	0.62	-1.616	C8B	NM_000066	Complement component 8, beta polypeptide
H200008134	0.0336	0.63	-1.587	KIAA0931	AB023148	KIAA0931 protein
H200011524	0.0336	0.68	-1.475	DDIT4L	BC013592	Homo sapiens, Similar to RIKEN cDNA 1700037B15 gene, clone MGC:9960 IMAGE:3877854, mRNA, complete cd
H200003140	0.034	0.69	-1.46	C20orf3	AB033767	Chromosome 20 open reading frame 3
H200004497	0.0341	0.71	-1.414	KCNQ3	NM_004519	Potassium voltage-gated channel, KQT-like subfamily, member 3
H200010100	0.0341	0.64	-1.553	KIAA0935	AB023152	KIAA0935 protein
H200010112	0.0343	1.62			AK056351	Homo sapiens cDNA FLJ31789 fis, clone NT2RI2008656
H200001415	0.0344	1.44		FLJ10936	BC008596	Hypothetical protein FLJ10936
H200003502	0.0345	0.67	-1.493	ARAP3	AK001579	ARF-GAP, RHO-GAP, ankyrin repeat and plekstrin homology domains-containing protein 3
H200004496	0.0349	1.41		TERE1	NM_013319	Transitional epithelia response protein
H200002132	0.0351	1.54		HTMP10	NM_033207	Transmembrane protein HTMP10
H200006734	0.0351	1.67		PEX7	NM_000288	Peroxisomal biogenesis factor 7

Genes that have a significant p-value and fold change						
H200011645	0.0351	2.08		HUNK	NM_014586	Hormonally upregulated Neu-associated kinase
H200001064	0.0352	2.25		IL17BR	AF208111	Interleukin 17B receptor
H200013353	0.0353	0.65	-1.538	LOC51135	NM_016123	Putative protein kinase NY-REN-64 antigen
H200006339	0.0353	1.52		KIAA0254	NM_014758	KIAA0254 gene product
H200002016	0.0356	1.42		FLJ32205	AK056767	Homo sapiens, clone MGC: 16395 IMAGE:3939387, mRNA, complete cds
H200016389	0.0356	1.63		MY050	NM_032624	Hypothetical brain protein my050
H200017217	0.0358	1.42		KCNMB3	NM_014407	Potassium large conductance calcium-activated channel, subfamily M beta member 3
H200001801	0.0359	1.62		CPSF5	NM_007006	Cleavage and polyadenylation specific factor 5, 25 kD subunit
H200007572	0.0359	1.40		KIAA1952	BC012922	Homo sapiens, clone IMAGE:4449401, mRNA, partial cds
H300007958	0.0361	2.10		ENSG00000 175598		AMBIGUOUS
H200003090	0.0363	1.54		MGC52057	AK055699	Homo sapiens cDNA FLJ31137 fis, clone IMR322001049
H200003860	0.0366	1.46		SSR3	NM_007107	Signal sequence receptor, gamma (translocon-associated protein gamma)
H200016308	0.0366	1.74		SLPI	NM_003064	Secretory leukocyte protease inhibitor (antileukoproteinase)
H200000965	0.0368	1.68		KIAA1089	AB029012	KIAA1089 protein
H200017557	0.0369	0.69	-1.447	OPN3	NM_014322	Opsin 3 (encephalopsin, panopsin)
H200012500	0.0369	1.46		DKFZp434H 2111	AK026776	Homo sapiens cDNA: FLJ23123 fis, clone LNG08039
H200017856	0.0369	1.55			AL359605	Homo sapiens mRNA; cDNA DKFZp547G036 (from clone DKFZp547G036)
H200009136	0.0377	1.40		FLJ22595	NM_025047	Hypothetical protein FLJ22595
H200014652	0.0379	1.55		BAZ1B	NM_023005	Bromodomain adjacent to zinc finger domain, 1B
H200012201	0.038	0.69	-1.445	ACTL7B	NM_006686	Actin-like 7B
H200000149	0.0381	1.78		AADAC	NM_001086	Arylacetamide deacetylase (esterase)
H200003737	0.0383	1.44		LOC113444	BC011880	Homo sapiens, Similar to hypothetical protein, MGC: 7764, clone MGC:20548 IMAGE:3607345, mRNA, comple

Genes that have a significant p-value and fold change						
H200005604	0.0383	1.58			AJ001873	Homo Sapiens mRNA, partial cDNA sequence from cDNA selection, DCR1-16.0
H200009846	0.0383	1.54			AK021505	Homo sapiens cDNA FLJ11443 fis, clone HEMBA1001330
H200000227	0.0384	1.42		IMPDH1	NM_000883	IMP (inosine monophosphate) dehydrogenase 1
H200013320	0.0384	1.42		D6S2654E	NM_012135	DNA segment on chromosome 6(unique) 2654 expressed sequence
H200001538	0.0385	1.55		LOC51125	NM_016099	HSPC041 protein
H300002604	0.0386	1.75		ENSG00000 171192		UNKNOWN
H200020003	0.0388	0.70	-1.425	DHRS6	AK023323	Homo sapiens cDNA FLJ13261 fis, clone OVARC1000885, weakly similar to OXIDOREDUCTASE UCPA (EC 1.-.-.
H200000631	0.0392	1.68		MYOM1	NM_003803	Myomesin 1 (skelemin) (185kD)
H200004409	0.0392	1.69		FLJ12484	NM_022767	Hypothetical protein FLJ12484
H200008951	0.0392	1.49		TMF1	AK021741	Homo sapiens cDNA FLJ11679 fis, clone HEMBA1004807
H200006686	0.0395	1.49			U90905	Human clone 23574 mRNA sequence
H200018515	0.0396	1.52			AK024907	Homo sapiens cDNA: FLJ21254 fis, clone COL01317
H200010516	0.0399	1.44		BTN2A2	NM_006995	Butyrophilin, subfamily 2, member A2
H200018816	0.04	1.51		VPS13D	AK022477	Homo sapiens cDNA FLJ12415 fis, clone MAMMA1003015
H200013921	0.0402	0.62	-1.61	KIAA0057	NM_012288	TRAM-like protein
H200017207	0.0403	1.44		RPS18	NM_022551	Ribosomal protein S18
H200007343	0.0405	0.69	-1.456	NPY5R	NM_006174	Neuropeptide Y receptor Y5
H200000778	0.0405	1.44		FLJ10743	NM_018201	Hypothetical protein FLJ10743
H200018216	0.0406	1.43		PDL-108	AB019409	Periodontal ligament fibroblast protein
H200020174	0.0413	0.69	-1.443	MGC20235	U25750	Human chromosome 17q21 mRNA clone 1046:1-1
H200001817	0.0414	1.72		IRC1	AJ224864	Leukocyte membrane antigen
H200013871	0.0417	0.61	-1.653	MGC5509	NM_024093	Hypothetical protein MGC5509
H200009097	0.0417	1.58			AK024613	Homo sapiens cDNA: FLJ20960 fis, clone ADSH00709
H200003278	0.0418	1.50		KIAA1273	AB033099	KIAA1273 protein

Genes that have a significant p-value and fold change						
H200001342	0.0421	1.53		LOC147343	AK054755	Homo sapiens cDNA FLJ30193 fis, clone BRACE2001340
H200003653	0.0423	1.44		VPS33B	NM_018668	Vacuolar protein sorting 33B (yeast)
H200000323	0.0424	1.44		ARSB	NM_000046	Arylsulfatase B
H200009426	0.0426	0.68	-1.462		AK025953	Homo sapiens cDNA: FLJ22300 fis, clone HRC04759
H200006355	0.0426	1.79		LILRB5	NM_006840	Leukocyte immunoglobulin-like receptor, subfamily B (with TM and ITIM domains), member 5
H200010412	0.0432	0.71	-1.406	NCALD	NM_032041	Neurocalcin delta
H200007795	0.0435	0.68	-1.477	DLK1	NM_003836	Delta-like 1 homolog (Drosophila)
H200015534	0.0436	1.57		ACACB	BC009753	Homo sapiens, clone IMAGE:3833472, mRNA
H200009062	0.0438	1.69		FLJ13769	NM_025012	Hypothetical protein FLJ13769
H200001624	0.0439	0.70	-1.439	NDUFS1	NM_005006	NADH dehydrogenase (ubiquinone) Fe-S protein 1 (75kD) (NADH-coenzyme Q reductase)
H200004381	0.0439	0.48	-2.07	LBX1	NM_006562	Transcription factor similar to D. melanogaster homeodomain protein lady bird late
H200008782	0.0439	1.43		KIAA1340	AK002197	Homo sapiens cDNA FLJ11335 fis, clone PLACE1010630
H200009869	0.0439	1.52		BTN2A3	AK056871	Homo sapiens cDNA FLJ32309 fis, clone PROST2002960, highly similar to Human butyrophilin (BTF1) mRNA
H200013003	0.0442	0.70	-1.437	MGC13138	NM_033410	Hypothetical protein MGC13138
H200000589	0.0443	1.88		MBL2	NM_000242	Mannose-binding lectin (protein C) 2, soluble (opsonic defect)
H200008885	0.0444	1.48		JAM1	AF172398	Junctional adhesion molecule 1
H200006456	0.0446	1.46		RGN	NM_004683	Regucalcin (senescence marker protein-30)
H200020845	0.0447	0.65	-1.536		AK055761	Homo sapiens cDNA FLJ31199 fis, clone KIDNE2000555
H200008722	0.0448	0.69	-1.458		AF244571	Homo sapiens clone L49 HERV-K-T47-like long terminal repeat sequence
H200019409	0.045	0.60	-1.658		AK000949	Homo sapiens cDNA FLJ10087 fis, clone HEMBA1002191

Genes that have a significant p-value and fold change						
H300011186	0.045	2.07		ENSG00000173981		VOLTAGE-GATED POTASSIUM CHANNEL BETA-1 SUBUNIT (K+ CHANNEL BETA-1 SUBUNIT) (KV-BETA-1). [Source:SWISSPROT;Acc:Q14722]
H200004322	0.0452	0.60	-1.658	FTCD	NM_006657	Formiminotransferase cyclodeaminase
H200007778	0.0453	0.69	-1.453	PTCRA	U36759	Human pre TCR alpha mRNA, partial cds
H200016950	0.0457	1.73		FLJ20307	AB051490	Hypothetical protein FLJ20307
H200008740	0.0461	1.74		ANKHZN	NM_016376	ANKHZN protein
H200005504	0.0463	0.63	-1.6	SNFT	NM_018664	Jun dimerization protein p21SNFT
H200017303	0.0463	1.45		ACAT2	NM_005891	Acetyl-Coenzyme A acetyltransferase 2 (acetoacetyl Coenzyme A thiolase)
H200011672	0.0472	0.66	-1.522	ARHH	NM_004310	Ras homolog gene family, member H
H200016974	0.0472	1.59		LOC56997	NM_020247	Hypothetical protein, clone Telethon(Italy_B41) _Strait02270_FL142
H200007201	0.0475	0.67	-1.495	GYLTL1B	AK055829	Homo sapiens cDNA FLJ31267 fis, clone KIDNE2006053, moderately similar to Mus musculus mRNA for acet
H200004912	0.0475	1.54		GJB6	NM_006783	Gap junction protein, beta 6 (connexin 30)
H200019736	0.0476	0.71	-1.416		BC008359	Homo sapiens, clone MGC:16021 IMAGE:3606756, mRNA, complete cds
H200000305	0.0476	1.50		E2F3	NM_001949	E2F transcription factor 3
H200007852	0.0477	1.56		CRB1	NM_012076	Crumbs homolog 1 (Drosophila)
H200009708	0.0477	1.56			AK001136	Homo sapiens cDNA FLJ10274 fis, clone HEMBB1001169
H200001369	0.0478	1.42		LOC57862	NM_021188	Clones 23667 and 23775 zinc finger protein
H200004638	0.0478	1.41		MBC3205	NM_033408	Hypothetical protein MBC3205
H200018736	0.0479	0.69	-1.447	HXCP2	NM_032579	Colon and small intestine-specific cysteine-rich protein precursor similar to FIZZ2/ resistin-like pr
H200001502	0.048	0.62	-1.61	C8FW	NM_025195	Phosphoprotein regulated by mitogenic pathways
H200000731	0.048	1.64		GZMK	NM_002104	Granzyme K (serine protease, granzyme 3; tryptase II)
H200007872	0.048	1.85		THBS3	NM_007112	Thrombospondin 3

Genes that have a significant p-value and fold change						
H200002933	0.0481	0.56	-1.776	MAEA	NM_005882	Macrophage erythroblast attacher
H200001440	0.0482	1.48		BLP1	NM_031940	BBP-like protein 1
H200007802	0.0482	1.50		NPY1R	NM_000909	Neuropeptide Y receptor Y1
H200001980	0.0484	1.46		KCNJ6	NM_002240	Potassium inwardly-rectifying channel, subfamily J, member 6
H200008613	0.0486	1.46			AK056555	Homo sapiens cDNA FLJ31993 fis, clone NT2RP7009168
H300009582	0.0486	1.51		ENSG00000173348		AMBIGUOUS
H200018282	0.0492	1.40			AL117486	Homo sapiens mRNA; cDNA DKFZp434K211 (from clone DKFZp434K211)
H200009266	0.0493	0.71	-1.406		AX015323	Sequence 17 from Patent WO9951740
H200002073	0.0495	0.71	-1.41	HCA112	NM_018487	Hepatocellular carcinoma-associated antigen 112
H200007059	0.0498	0.66	-1.522	TNNI2	NM_003282	Troponin I, skeletal, fast
H200008357	0.0498	0.52	-1.942	COL1A2	NM_000089	Collagen, type I, alpha 2
H200019659	0.0498	0.61	-1.631	RBM17	AK021863	Homo sapiens cDNA FLJ11801 fis, clone HEMBA1006253, weakly similar to DNA-DAMAGE-REPAIR/TOLERATION P
H200009056	0.0499	1.52		FLJ13621	NM_025009	Hypothetical protein FLJ13621